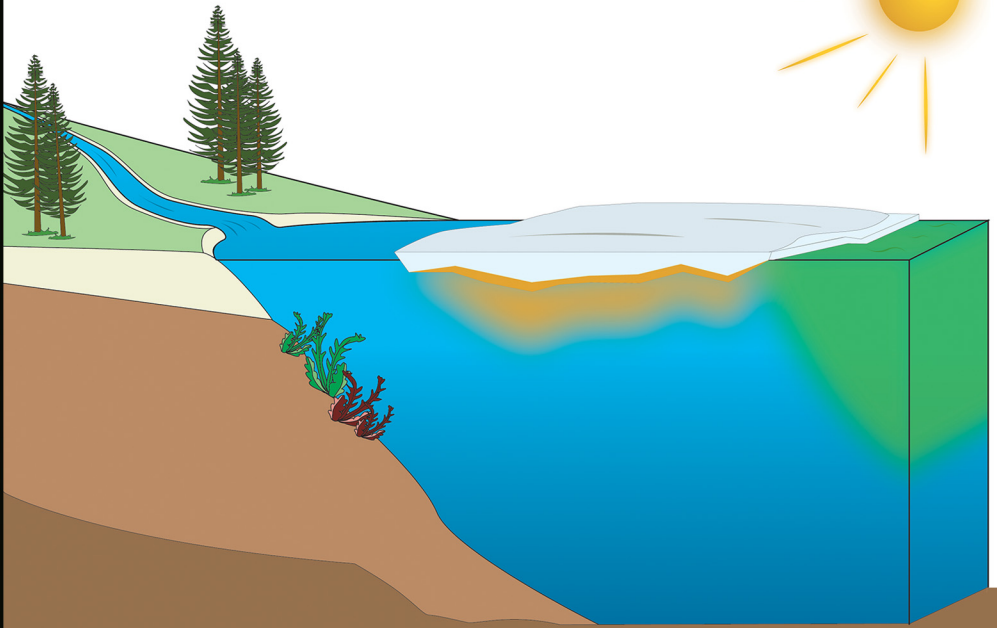
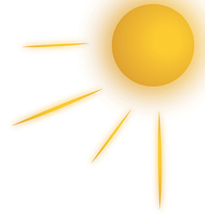


Lipid Oxidation Products



Useful Tools for Monitoring Photo-
and Autoxidation in Phototrophs

Jean-François Rontani

Lipid Oxidation Products

Lipid Oxidation Products:

*Useful Tools for Monitoring
Photo-and Autoxidation
in Phototrophs*

By

Jean-François Rontani

**Cambridge
Scholars
Publishing**



Lipid Oxidation Products:
Useful Tools for Monitoring Photo- and Autoxidation in Phototrophs

By Jean-François Rontani

This book first published 2021

Cambridge Scholars Publishing

Lady Stephenson Library, Newcastle upon Tyne, NE6 2PA, UK

British Library Cataloguing in Publication Data
A catalogue record for this book is available from the British Library

Copyright © 2021 by Jean-François Rontani

All rights for this book reserved. No part of this book may be reproduced, stored in a retrieval system, or transmitted, in any form or by any means, electronic, mechanical, photocopying, recording or otherwise, without the prior permission of the copyright owner.

ISBN (10): 1-5275-7304-4

ISBN (13): 978-1-5275-7304-8

CONTENTS

Preface	vii
Acknowledgements	ix
Introduction	x
Chapter One.....	1
Photooxidative Reactions	
Chapter Two	4
Induction of Type-II Photosensitized Oxidation Processes in the Membranes of Phototrophic Organisms	
Chapter Three	8
Reaction of Singlet Oxygen with Olefins	
Chapter Four	12
Degradation and Rearrangement of Allylic Hydroperoxides Under Environmental Conditions	
Chapter Five	15
Type-II Photosensitized Oxidation of the Main Unsaturated Lipids of Autotrophic Organisms: Selection of Process Specific Tracers	
Chapter Six	34
Induction of Type-II Photosensitized Oxidation in Non-Phototrophic Organisms	
Chapter Seven.....	40
Effect of Temperature and Irradiance on the Efficiency of Type-II Photosensitized Oxidation Processes	
Chapter Eight.....	43
Free Radical Oxidation (Autoxidation) Processes	

Chapter Nine.....	48
Induction of Autoxidation Processes in Membranes of Phototrophic Organisms	
Chapter Ten	51
Autoxidation of the Main Unsaturated Lipids of Autotrophic Organisms: Selection of Process Specific Tracers	
Chapter Eleven	71
Gas Chromatography-Mass Spectrometry Characterization of Selected Tracers of Lipid Photo- and Autoxidation	
Chapter Twelve	95
Quantification of Selected Tracers of Lipid Photo- and Autoxidation in Environmental Samples	
Chapter Thirteen	106
Environmental Hotspots of Photo- and Autoxidation of Phototrophic Organisms	
Chapter Fourteen	112
Potential Applications of Lipid Oxidation Tracers	
Chapter Fifteen	126
Interactions between Biotic and Abiotic Degradation Processes	
Chapter Sixteen	137
Enzymatic Oxidation: A Potential Source of Biases in Lipid Oxidation Estimates	
Bibliography	143

PREFACE

The organic matter preserved in aquatic sediments provides an abundance of evidence for the environmental conditions prevailing at the time of deposition. Understanding the sources of organic matter and the processes that modify its composition is the foundation of the field of organic geochemistry. Many lipid biomarkers (compounds that can be related to specific organisms) have been identified that allow different sources (e.g., bacteria, archaea, vascular plants, microalgae, macroalgae, zooplankton, benthic animals etc) to be differentiated. However, only a small proportion of compounds biologically produced in the water column reach the sediment intact and many of the chemical structures are modified by chemical and biological processes in the water column and by processing through aquatic food webs.

Much attention has been paid to the microbial degradation of lipids, but abiotic processes can be particularly important in the surface layers of aquatic environments, where sunlight can penetrate, and also in oxic surface sediments. Through decades of research, Dr. J.-F. Rontani has shown that photooxidative degradation can destroy much of the unsaturated lipids in the water column and hence can strongly alter the lipid signature of organic matter reaching the seafloor. It is thus essential to take into account the potential effects of abiotic degradation when making palaeoenvironmental reconstructions from sedimentary organic matter. In this book, the main types of oxidation are examined in detail and specific degradation products have been identified as biomarkers for such reactions. These results are contrasted with the compounds produced by microbial degradation of lipids thus allowing a comprehensive understanding of the cycling of organic compounds in aquatic environments.

As an example of this approach, Dr. Rontani and his team incubated the geochemically important haptophyte *Emiliania huxleyi* and showed that free radical-mediated processes (autoxidation) were extensive and altered monounsaturated fatty acids, sterols and the chlorophyll phytyl side-chain giving rise to specific oxidation products. These included 11-hydroxyoctadec-*cis*-9-enoic and 8-hydroxyoctadec-*cis*-9-enoic acids, *Z*- and *E*-3,7,11,15-tetramethylhexadec-3-ene-1,2-diols and 3,7,11,15-tetramethylhexadec-2-ene-1,4-diols. Autoxidation also affects the composition of unusual very long-chain alkenones (unsaturated methyl and ethyl

ketones) produced by this species which can lead to small changes in the paleotemperature proxy values derived from alkenone abundances.

Photo- and autoxidation of lipids specific of terrestrial phototrophs are also covered in this book and several tracers for monitoring the abiotic degradation of these organisms on land and in the oceans are proposed.

Interactions between biotic and abiotic degradation processes are also discussed. Although complex, these interactions need to be taken into account during estimates of the balance between degradation and preservation of phototrophic organisms in the natural environment. Lipoxygenase (LOX)-induced autoxidative degradation of terrestrial particulate organic matter constitutes a nice example of such interactions. This process is shown to be widespread in estuaries and that this varies with latitude. At high latitudes, lower temperatures and irradiance favour photooxidative damage to higher plant debris and, consequently, hydroperoxide production. High hydroperoxide content strongly contributes to LOX activation in mixed waters. The high resulting LOX activity enhances alkoxy radical production and thus autoxidation. At low latitudes, photooxidative effects are limited, but riverine autoxidation is enhanced by the high temperatures. This process affords high levels of hydroperoxides also inducing intensive LOX activity and autoxidation in estuaries.

In summary, this book provides, up-to-date and detailed information on oxidation of lipids and how carbon is cycled in aquatic environments which has until now been rather neglected in the literature. The analytical work is meticulous, and inferences are backed up by laboratory studies of geochemically relevant organisms. Multiple examples are provided drawn from scientific papers published over many decades spanning a variety of environments. The book should appeal to those new to the field and to experts alike.

John K. Volkman BSc(Hons), PhD (U. Melb.), Dhc (U. Méd), FAA,
FRACI, C.Chem
CSIRO Oceans and Atmosphere, Hobart, Tasmania, Australia

ACKNOWLEDGEMENTS

Ever since my childhood, it was my dream to do research in chemistry. If this dream has come true, it is thanks to the unwavering support of my parents Louis and Marie-Rose, who were never given the opportunity to get a real education but did everything they could to make it happen for me. The support of my wife Patricia and my two daughters Pauline and Mélanie has also been essential throughout my career.

Special thanks to my friend Claude Aubert, who allowed me to enjoy unfettered access to his facilities in my periods of scarcity and very limited equipment, and who enabled me to immerse myself in the fascinating study of the mechanisms of fragmentation of lipid compounds in mass spectrometry.

I would like to salute the memory of Professor François Blanc (ex director of the Marseilles Centre of Oceanology) who enabled me to join the CNRS and engage the world of research in organic geochemistry.

All these studies concerning lipid oxidation processes could not have been carried out without numerous fertile national and international collaborations. I especially want to thank Drs. John K. Volkman, Simon T. Belt, Thomas Brown, Lukas Smik, Stuart G. Wakeham, Frederick G. Prahl, Michal Koblizek, Ronald J. A. Wanders, Thomas Bianchi, Nicolas Ward, Patricia Medeiros, Patricia Bonin, Jean-Claude Marty, Juan-Carlos Miquel, Franck Pinot and Vincent Méjean (the list is not exhaustive)—it really was a joy working with you all.

The many PhD students that I have supervised during my career have also played a role in developing this sphere of research, and their contributions should not be overlooked.

I am also very grateful for all the financial support from the CNRS (EC2CO-microbien and LEFE-Cyber programs) and the University of Aix-Marseille throughout these years, and most recently the LabEx OT-Med (Objectif Terre: Bassin Méditerranéen) and the FEDER Oceanomed grant (No. 1166-39417), which allowed us to acquire PhD funding and invaluable GC-QTOF, LC-QTOF and GC-MS/MS systems, respectively.

Last but not least, the MALINA and GREENEDGE international projects (P.I. Marcel Babin) have enabled us to study our processes of interest in the fascinating but hard-to-reach areas of the Arctic.

INTRODUCTION

Lipids—from hydrocarbons, pigments and terpenoids to free fatty acids, acylglycerides, phospholipids, galactolipids, cutins, suberins and waxes; Harwood and Russell, 1984)—are important components of phototrophic organisms. To illustrate, lipids account for 16-26% of the organic content of phytoplankton (Jónasdóttir, 2019). Their relative stability (preservation in sediments for millions and even billions of years; Huang et al., 1995; Brocks et al., 1999) and specificity (restricted origins from individual or groups of organisms; Huang et al., 2004) means that lipids are often used as tracers of the origin of organic matter in terrestrial and marine environments (Volkman, 2006; Waterson and Canuel, 2008; Parrish, 2013; Nguyen Tu et al., 2017; Guo et al., 2020).

Compounds resulting from abiotic oxidation of unsaturated lipids can also prove very useful for discerning individual degradation processes such as photooxidation or autoxidation in specific phototrophic organisms. Unfortunately, most studies of the degradation of these organisms to date have focused on biotic degradation processes (Afi et al., 1996; Sun et al., 1999; Mäkinen et al., 2017), and investigations have only recently turned to the role played by photochemical and free radical-mediated processes in the degradation of lipid components during the senescence of phototrophic organisms (*e.g.* Walker et al., 2002; Ramel et al., 2012; Rontani et al., 2012a, 2014c, 2017; Amiraux et al., 2016). This book sets out to provide an instructive overview of: (i) the reactions involved during these abiotic degradation processes, (ii) the characterization and quantification of suitable lipid tracers of these processes, and (iii) the potential applications of such compounds.

Although complex lipids (such as acylglycerides, phospholipids, galactolipids and steryl esters) can be analyzed by high-performance liquid chromatography-mass spectrometry (HPLC-MS; Roces et al., 2016; Pham et al., 2019) or by Iatroscan thin-layer chromatography-flame ionization detection (TLC-FID; Volkman et al., 1986; Parrish and Ackman, 1983), monitoring of lipids and their oxidation products is often carried out by gas chromatography-mass spectrometry (GC-MS) after NaBH₄ reduction and alkaline hydrolysis steps. Even though sample preparation for GC-MS analyses is relatively time-consuming, the technique is mostly used in electron ionization (EI) mode, which provides more structural information

than the soft ionization methods (such as ESI, APCI) utilized during HPLC-MS analyses (Xia and Budge, 2017). It is notably very useful to determine the position of functional groups of lipid oxidation products (Koek et al., 2011). The NaBH_4 reduction step serves to convert thermolabile hydroperoxides arising from lipid oxidation to the corresponding alcohols that are more amenable to analysis by GC-MS (Marchand and Rontani, 2001). The subsequent alkaline hydrolysis step then serves to (i) break complex lipids down into their constituent fatty acids, plus glycerol, phosphate, sterol or sugar groups, and (ii) separate fatty acids from 'neutral' lipid components such as hydrocarbons, sterols, alcohols and ketones (Volkman, 2006).

The first chapters of this book explain in detail the mechanisms (mainly involving singlet oxygen) and timing (during senescence or in response to a high stress) of type-II photosensitized oxidation processes in phototrophic organisms. We then go on to describe photooxidation of the main simple unsaturated lipid components of phototrophs (fatty acids, chlorophyll, carotenoids, sterols, triterpenoids, alkenones, *n*-alkenes, HBI alkenes, cuticular waxes, and more). In this part, we focus on the specificity of the photooxidation products formed and on their potential application as tracers of these processes.

The next chapters then discuss the transfer of photooxidative damage in non-phototrophic material (heterotrophic bacteria and zooplanktonic fecal pellets) and the effect of temperature and solar irradiance on the efficiency of type-II photooxidation processes.

We then explain the different steps (initiation, propagation and termination) of the free-radical oxidation (autoxidation) processes and look in detail at the autoxidation mechanisms of the main lipids of phototrophs, which can be affected by these processes, with a focus again on the selection of specific tracers of these processes.

The following chapters pay special attention to the characterization and quantification of the main photo- and autoxidation products of lipids selected as tracers. Mass spectrometry fragmentations of trimethylsilyl derivatives of these compounds are described, and selected fragment ions are proposed for monitoring abiotic degradation of specific phototrophic organisms in environmental samples. We anticipate that this part should be particularly useful for future users of lipid oxidation products. We also list published quantitative estimates of the degradation state of the main lipids of different phototrophic organisms (phytoplankton, phototrophic bacteria, terrestrial and aquatic higher plants) and in a variety of environmental samples (sinking and suspended particulate matter, sediments, sea ice and microbial mats).

We then describe some of the environmental hotspots of phototrophic organism photo- and autoxidation (e.g. polar and more particularly under-ice areas for type-II photosensitized oxidation and polar and equatorial estuaries for autoxidation).

The next chapter proposes several potential applications for lipid oxidation products (i.e. organism-specific indicators of stress, new proxies of paleoenvironmental changes, indicators of abiotic alterations of paleoproxies, ozone depletion and permafrost abiotic degradation, and use for determining the double bond position of monounsaturated fatty acids or *n*-alkenols).

The penultimate chapter uses several examples to discuss the very complex interactions between biotic and abiotic degradation processes that can substantially reshape the balance between degradation and preservation of phototrophic organisms in the natural environment.

The final chapter inventories and discusses the enzymatic oxidation processes liable to bias photo- and autoxidation estimates.

CHAPTER ONE

PHOTOOXIDATIVE REACTIONS

Direct photooxidative reactions

In the natural environment, direct photooxidation occurs when sunlight is absorbed by the chemical of interest to form excited or radical species, which then react with oxygen or water. These processes involve light-absorbing entities called chromophores (defined as a region in a molecule where the energy difference between two different molecular orbitals falls within the range of the solar spectrum; Shukla et al., 2016) that can undergo oxidative change as a direct consequence of absorbing photons (Zafiriou et al., 1984). In autotrophic organisms, only pigments (e.g. chlorophylls and carotenoids; Nelson, 1993), some polyunsaturated fatty acids (Collins et al., 2018), vitamins (e.g. thiamine and riboflavin; Ahmad et al., 2018, Golbach et al., 2014) and some amino acids (e.g. tryptophan, tyrosine, and histidine; Pattison et al., 2012) have absorption peaks in the UV and visible region of solar light (Zafiriou et al., 1984) and can thus be directly photooxidized under environmental conditions.

Indirect photooxidative reactions

Indirect photooxidative reactions are common in the natural environment. They are crucial processes as they can alter molecules that resist photolysis, such as transparent species or chromophores whose reactive states are inefficiently populated by absorption (Zafiriou et al., 1984). The first step of these reactions involves the absorption of light by a substance called a 'photosensitizer', which is a molecule capable of producing a chemical change by transferring energy to an excited neighbouring molecule. These compounds have two systems of electronically excited states: singlet (1S) and triplet (3S) (Foote, 1976). The triplet state is usually longer-lived than the singlet, even though the singlet is the initial product of light absorption (Foote, 1976). Most of the photosensitized oxidation reactions in nature start from the photosensitizer in its triplet state (Gollnick, 1968). To be efficient under environmental conditions, sensitizers

need to: (i) absorb visible or near-UV light, (ii) afford a long-lived triplet state in high quantum yield, and (iii) be sufficiently stable. All photosensitizers contain chromophores, which are usually cyclic compounds with resonating conjugated double bond systems that enable them to absorb visible and UV-A light. However, some chromophores are bicyclic, some are tricyclic, and some, like tetrapyrroles (chlorophylls and hematoporphyrin), are polycyclic (Giese, 1980).

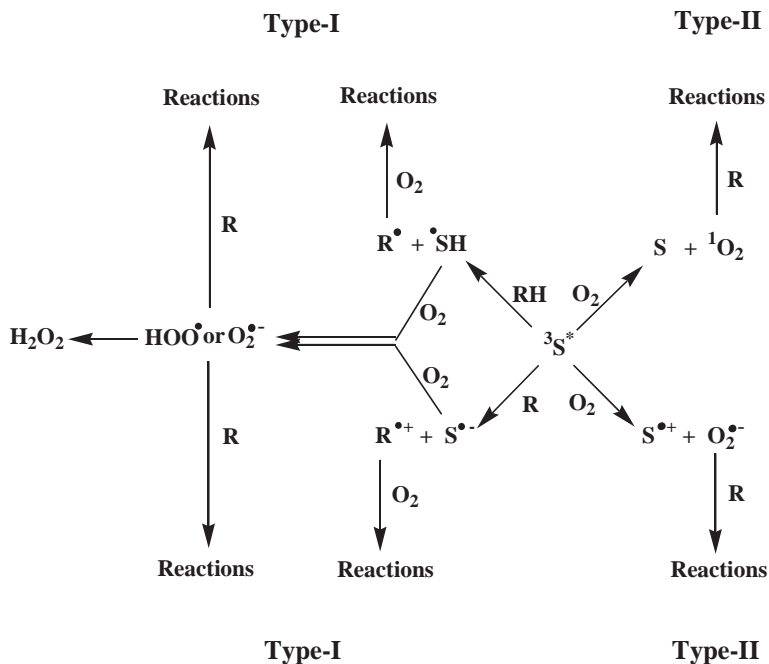


Figure 1. Reactions of a triplet sensitizer (Adapted from Rontani and Belt, 2020). (R or RH = reduced substrate, $^3\text{S}^*$ = triplet sensitizer, $^1\text{O}_2$ = singlet oxygen, $^3\text{O}_2$ = ground-state oxygen, $\text{O}_2^{\cdot-}$ = superoxide ion, $\text{HOO}\cdot$ = hydroperoxide radical, H_2O_2 = hydrogen peroxide)

In the presence of oxygen, triplet sensitizers can follow two main types of reactions (Fig. 1):

– In a type-I reaction, the excited triplet sensitizer reacts directly with a reducing substrate (RH or R) to afford free radicals (after hydrogen atom transfer) or radical ions (after electron transfer) (Schenck and Koch, 1960; Gollnick, 1968). These radicals can then: (i) abstract an electron or

a hydrogen atom to other molecules, (ii) react with oxygen to initiate free-radical chain autoxidation, or (iii) react with the reduced sensitizers (back-reactions). Reduced sensitizers ($\text{SH}\cdot$ and $\text{S}^{\cdot-}$) can also react with oxygen to afford superoxide ion ($\text{O}_2^{\cdot-}$) or hydroperoxide radical ($\text{HOO}\cdot$), which can then disproportionate to H_2O_2 or react with the substrate (Fig. 1) (Foote, 1976).

– In a type-II reaction, the triplet sensitizer transfers its excitation energy to oxygen, forming an electronically excited singlet state of oxygen ($^1\text{O}_2$) (Fig. 1). Given the exceptionally high speed of this energy transfer, it is generally considered to account for most quenching of triplet sensitizers by oxygen (Foote, 1976). The $^1\text{O}_2$ thus formed is strongly electrophilic and can therefore only react with compounds that possess substituted double bonds or other electron-rich functionalities (Frimer, 1979). Less efficient electron transport from triplet sensitizer to oxygen can also occur, affording $\text{O}_2^{\cdot-}$ (Fig. 1) (Kasche and Lindqvist, 1964).

The mechanisms of (type-I or type-II) photosensitized oxidation depend on: (i) type of sensitizer and substrate, and (ii) concentrations of substrate and oxygen. Type-I photoprocesses are generally favoured in the case of readily-reduced sensitizers (e.g. quinones) and readily-oxidized substrates (e.g. phenols or amines; Saito et al., 1975), whereas less readily-reduced sensitizers (e.g. dyes or aromatics) and high oxygen concentrations will favour $^1\text{O}_2$ reactions (Nilson et al., 1972).

CHAPTER TWO

INDUCTION OF TYPE-II PHOTOSENSITIZED OXIDATION PROCESSES IN THE MEMBRANES OF PHOTOTROPHIC ORGANISMS

The photoprotective system of healthy cells

When a chlorophyll molecule absorbs a quantum of light energy, it forms an excited singlet state (^1Chl) which, in healthy cells, is mainly used in the characteristically fast photosynthesis reactions (Foote, 1976). The energy of this excited state gets transferred to the photosynthesis reaction centre where it drives photochemical reactions. However, a small proportion of ^1Chl ($<0.1\%$) undergoes intersystem crossing (ISC) to form the longer-lived triplet state ^3Chl (Knox and Dodge, 1985; Fig. 2). ^3Chl is not only potentially damaging per se in type-I reactions (Knox and Dodge, 1985; Fig. 1), it can also generate damaging $^1\text{O}_2$ and $\text{O}_2^{\cdot-}$ by reaction with ground-state oxygen ($^3\text{O}_2$) via type-II photoprocesses (Fig. 1). $\text{O}_2^{\cdot-}$ may subsequently: (i) disproportionate to $^1\text{O}_2$ and H_2O_2 in the presence of a proton donor (Foote, 1976), and (ii) interact with H_2O_2 in the presence of non-heme Fe^{+3} to generate hydroxyl radicals (HO^{\cdot}) via the Haber–Weiss reaction (Leshem, 1988). Despite the production of these reactive oxygen species (ROS), the photoproduction of $^1\text{O}_2$ is mainly considered to be responsible for light-dependent reactions that damage plant cells (Triantaphylides et al., 2008).

As chloroplasts are susceptible to oxidative damage, they possess an array of antioxidant-protective mechanisms. Carotenoids quench ^3Chl and $^1\text{O}_2$ by energy transfer mechanisms at very high rates (Fig. 2). These compounds have a dual role: preventing $^1\text{O}_2$ formation and helping to remove any $^1\text{O}_2$ that does manage to form (Foote, 1976). Tocopherols and ascorbic acid are also efficient quenchers of $^1\text{O}_2$ (Halliwell, 1987). Tocopherols can also remove $^1\text{O}_2$, $\text{O}_2^{\cdot-}$, HOO^{\cdot} and HO^{\cdot} by acting as sacrificial scavengers, i.e. in processes that induce irreversible oxidation of the tocopherol molecule (Halliwell, 1987). Superoxide dismutase (SOD) enzyme and ascorbic acid can scavenge $\text{O}_2^{\cdot-}$, while catalase

activity can decrease H_2O_2 levels, thus providing less substrate for $\text{HO}\cdot$ formation in the Haber–Weiss reaction (Leshem, 1988).

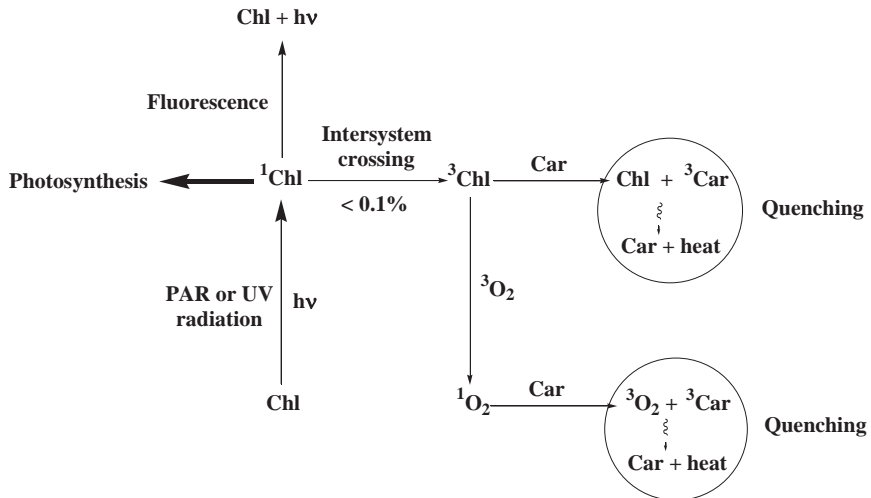


Figure 2. Potential pathways for chlorophyll excitation energy in healthy cells of autotrophic organisms (simplified scheme limited to the formation of $^1\text{O}_2$ and the photoprotective role of carotenoids).

The photodynamic effect in senescent cells

In senescent phototrophic organisms, the cessation of photosynthetic reactions results in an accelerated rate of formation of ^3Chl and ROS (mainly $^1\text{O}_2$) (Nelson, 1993). The rate of formation of these potentially damaging species can then exceed the quenching capacity of the photoprotective system, enabling the photodegradation of cell components to occur (photodynamic effect; Merzlyak and Hendry, 1994) (Fig. 3). Three sites in the photosynthetic apparatus are the major sources for generation of ROS: the photosystem II (PSII) reaction centre, the photosystem I (PSI), and the light-harvesting complex (LHC) of PSII (Pinnola and Bassi, 2018). The direct irreversible reaction of ^3Chl with ground-state triplet oxygen ($^3\text{O}_2$), i.e. direct photobleaching, gives photooxidation products (Harbour and Bolton, 1978) (Fig. 3). $^1\text{O}_2$ reacts very quickly with any nearby biomolecules at near-diffusion-controlled rates (Knox and Dodge, 1985; Cadenas, 1989). The very high reactivity of $^1\text{O}_2$ with numerous cell components such as unsaturated lipids, nucleic acids and some amino acids (Rontani, 2012; Devasagayam and Kamat,

2002) is a consequence of the loss of the spin restriction that normally prevents $^3\text{O}_2$ reaction with these biomolecules (Zolla and Rinalducci, 2002). $^1\text{O}_2$ also reacts with the sensitizer (chlorophyll), causing it to photobleach (Nelson, 1993; Rontani, 2012) (Fig. 3). Photobleaching of the sensitizer reduces $^1\text{O}_2$ production, and thus competes with the photodynamic effect.

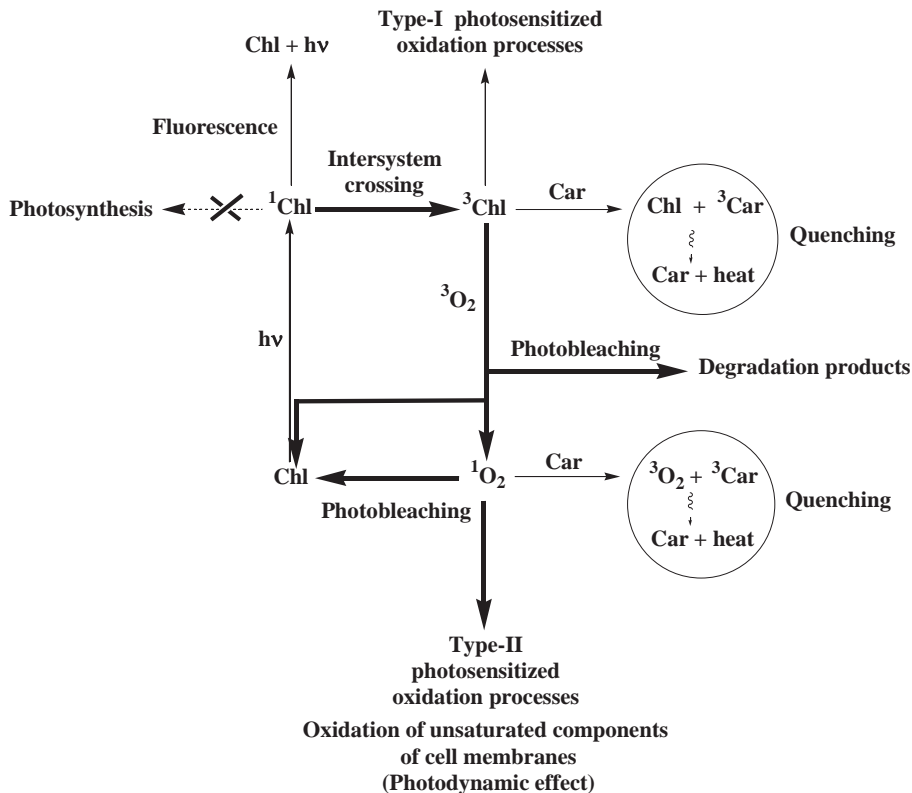


Figure 3. Potential pathways for chlorophyll excitation energy in senescent cells of autotrophic organisms (simplified scheme limited to the formation of $^1\text{O}_2$ and the photoprotective role of carotenoids). Adapted from Rontani et al. (2021b).

Due to its high reactivity and short lifetime, it is generally thought that $^1\text{O}_2$ can mostly interact with molecules in its closest environment (Krasnovsky, 1998). However, $^1\text{O}_2$ produced from sensitizers in a lipid-rich hydrophobic environment could have a longer lifetime and greater

potential diffusive distance than its behaviour in aqueous solution (Suwa et al., 1977). In biological membranes, the lifetime of $^1\text{O}_2$ ranges between 13 and 35 μs (Ehrenberg et al., 1998; Sokolov and Pohl, 2009), which equates to a calculated diffusion length of about 400 nm (Baier et al., 2005). It has been observed in the photosynthetic apparatus of *Chlamydomonas reinhardtii* that $^1\text{O}_2$ produced in thylakoid membranes under high light conditions is able to reach the cytoplasm or even the nucleus (Fisher et al., 2007). It is not surprising, therefore, that type-II photosensitized oxidation of the majority of unsaturated lipid components has been observed in numerous senescent autotrophic organisms ranging from phytoplankton, cyanobacteria and purple sulphur bacteria to terrestrial and aquatic higher plants (Marchand and Rontani, 2003; Rontani et al., 1996a; 2005a; Rontani, 2012; 2019).

Note that in autotrophic organisms, the physiological state of the cells plays a key role in the induction of type-II photosensitized oxidation processes. Indeed, $^1\text{O}_2$ production can only exceed the quenching capacities of the photoprotective system (and thus induce cell damage) when the photosynthetic pathways are inoperative, as is the case in senescent or highly-stressed cells (Nelson, 1993).

The problem of stratospheric ozone depletion has prompted numerous studies to examine the degradative effects of enhanced UV-B doses on lipids in autotrophic organisms (e.g. He and Häder, 2002; Nawkar et al., 2013). However, UV radiation does not hold a monopoly on photochemical damage in autotrophs. In fact, the presence of chlorophylls, which are very efficient photosensitizers (Foote, 1976; Knox and Dodge, 1985), means that numerous organic components of senescing autotrophs are susceptible to photodegradation by visible photosynthetically active radiation (PAR).

CHAPTER THREE

REACTION OF SINGLET OXYGEN WITH OLEFINS

Different types of reactions

Due to its strong electrophilic character and the lack of spin restriction (Dmitrieva et al., 2020), $^1\text{O}_2$ readily reacts with molecules containing double bonds. The reactions of $^1\text{O}_2$ with olefins can be collapsed into three classes, which are outlined in Fig. 4. The first class involves a [2 + 2] cycloaddition to the double bond affording a dioxetane. This reaction mainly takes place in the case of electron-rich or sterically-hindered double bonds (Frimer, 1979). The dioxetane thus formed, which is not very stable, is generally cleaved into two carbonyl fragments under the action of temperature or light. In the presence of allylic hydrogen atoms, a direct reaction of $^1\text{O}_2$ with the carbon-carbon double bond by a concerted “ene”, also named Schenk-ene reaction addition, results in the formation of allylic hydroperoxides at each end of the original double bond while shifting it to the adjacent position (Frimer, 1979) (Fig. 4). In the case of conjugated dienes, the addition of $^1\text{O}_2$ produces cyclic peroxides (endoperoxides) (Clennan, 1991).

Numerous theoretical and experimental studies have investigated the mechanism involved in $^1\text{O}_2$ -mediated allylic oxidation (e.g. Alberti and Orfanopoulos, 2008; Sheppard and Acevedo, 2009). It now seems likely that a perepoxide is a viable intermediate in the $^1\text{O}_2$ addition to simple alkenes (Alberti and Orfanopoulos, 2010). Note, however, that this is not a free radical process.

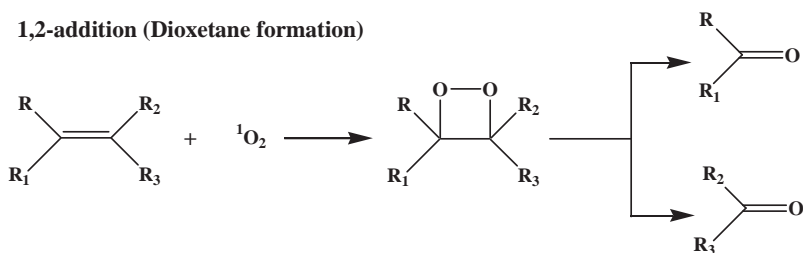
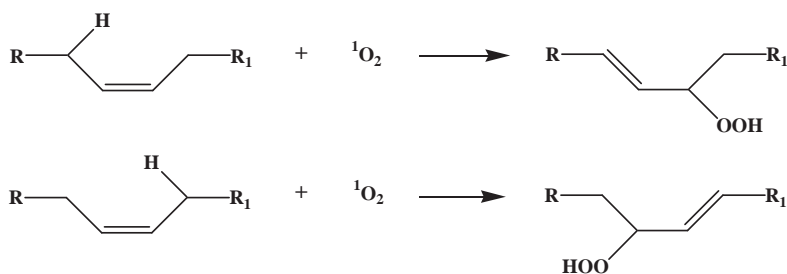
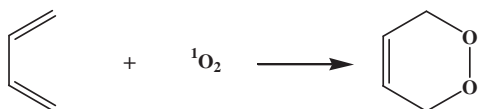
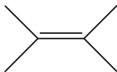
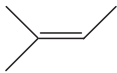
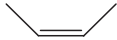
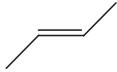
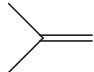
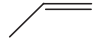
1,2-addition (Dioxetane formation)**1,3-addition (Ene reaction)****1,4-addition (Endoperoxide formation)**

Figure 4. Main classes of ¹O₂ reactions with olefins. Adapted from Frimer (1979).

It was previously observed that the rate of reaction of ¹O₂ with olefins is controlled by entropy (ΔS) and thus by the degree of substitution and the configuration (*cis*- or *trans*-) of the double bond (Table 1) (Hurst et al., 1985). This means that terminal and *trans* olefins are weakly reactive to ¹O₂.

Substrate	ΔS (e.u.)*	k ($\text{mol}^{-1} \text{s}^{-1}$)	References
	-23	2.2×10^7	Hurst et al. (1985)
	-30	7.2×10^5	Hurst et al. (1985)
	-32	4.8×10^4	Hurst et al. (1985)
	-42	7.2×10^3	Hurst et al. (1985)
	-43	4.0×10^3	Hurst et al. (1985)
		2.3×10^2	Kopecky and Reich, 1965

* Entropy units

Table 1. Relative rate constants for the reaction of $^1\text{O}_2$ with isolated acyclic double bonds in solvents.

Features of the “ene” reaction

As seen in Chapter 5, the “ene” reaction plays a key role in the photosensitized oxidation of natural unsaturated lipids bearing allylic hydrogen atoms. A special feature of this reaction is its remarkable side specificity (named *cis* effect), where the more substituted side of trisubstituted double bonds is also the most highly reactive (Stratakis and Orfanopoulos, 2000; Griesbeck et al., 2003) (Fig. 5). Houk et al. (1981) attributed this specificity to lower rotational barriers in the more highly congested environment.

The “ene” reaction appears to be particularly sensitive to electronic effects and to a lesser extent to the steric hindrance when bulky substituents are present (Morales et al., 2012). Indeed, in some cases, the presence of a

bulky substituent may diminish reactivity by partially blocking the singlet oxygen attack on the double bond. This is notably the case in some polycyclic structures such as Δ^5 -sterols and pentacyclic triterpenes (Beutner et al., 2000; Galeron et al., 2016a; 2016b).

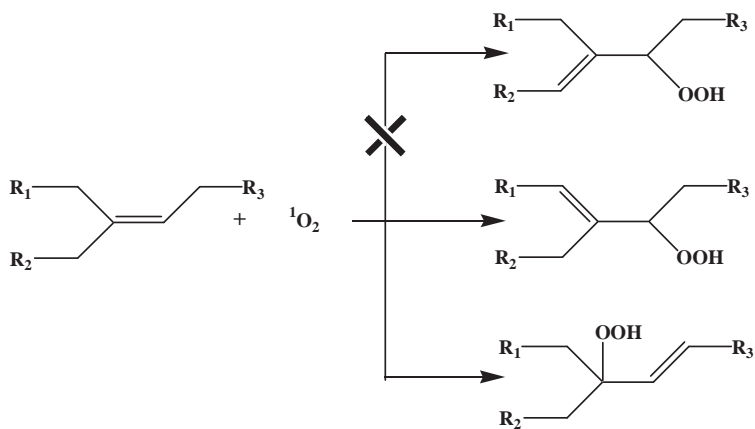


Figure 5. *Cis* effect in the reaction of $^1\text{O}_2$ with trisubstituted alkenes.

CHAPTER FOUR

DEGRADATION AND REARRANGEMENT OF ALLYLIC HYDROPEROXIDES UNDER ENVIRONMENTAL CONDITIONS

Allylic rearrangement

The rearrangement of allylic hydroperoxides (Fig. 6), which produces exclusively *trans* allyl products, has been extensively studied over the years (for reviews, see Porter et al., 1995; 2013). It is known to act on allylperoxy radicals (Frimer, 1979), but the mechanism involved is still open to debate. The latest studies now seem to indicate that it proceeds through an oxygen-allyl radical complex (Porter, 2013). The intensity of this rearrangement is very sensitive to the hydrogen donor properties of the surrounding molecules (Porter et al., 1995). The rearrangement should be slow in biological membranes that are rich in polyunsaturated fatty acids (PUFAs), which are good hydrogen donors, but fast in membranes that are rich in monounsaturated fatty acids (MUFAs) or saturated fatty acids, which are poor hydrogen donors (Rontani et al., 2021a). The extent of the allylic rearrangement of the hydroperoxides present in environmental samples could therefore reflect the composition and ageing of the organisms present (Rontani et al., 2021a).

Heterolytic cleavage

Heterolysis of the hydroperoxide O–O bond leads to the formation of two carbonyl fragments (Hock cleavage). This proton-catalyzed cleavage is initiated by the migration of groups to positive oxygen, which then induces a series of skeletal changes (Fig. 6; Frimer, 1979). The migratory aptitude follows the order: cyclobutyl > aryl > vinyl > hydrogen > cyclopentyl or cyclohexyl >> alkyl (Frimer, 1979). In the particular case of allylic hydroperoxides, the migrating group will be the vinyl group and the resulting fragments will be two aldehydes (Fig. 6). These cleavages are

generally acid-catalyzed, but several of them have been reported to occur in the absence of any added acid (Turner and Herz, 1977; Frimer, 1979), and notably in senescent phytoplanktonic cells (Rontani, 1998) and seawater (Rontani et al., 2007c).

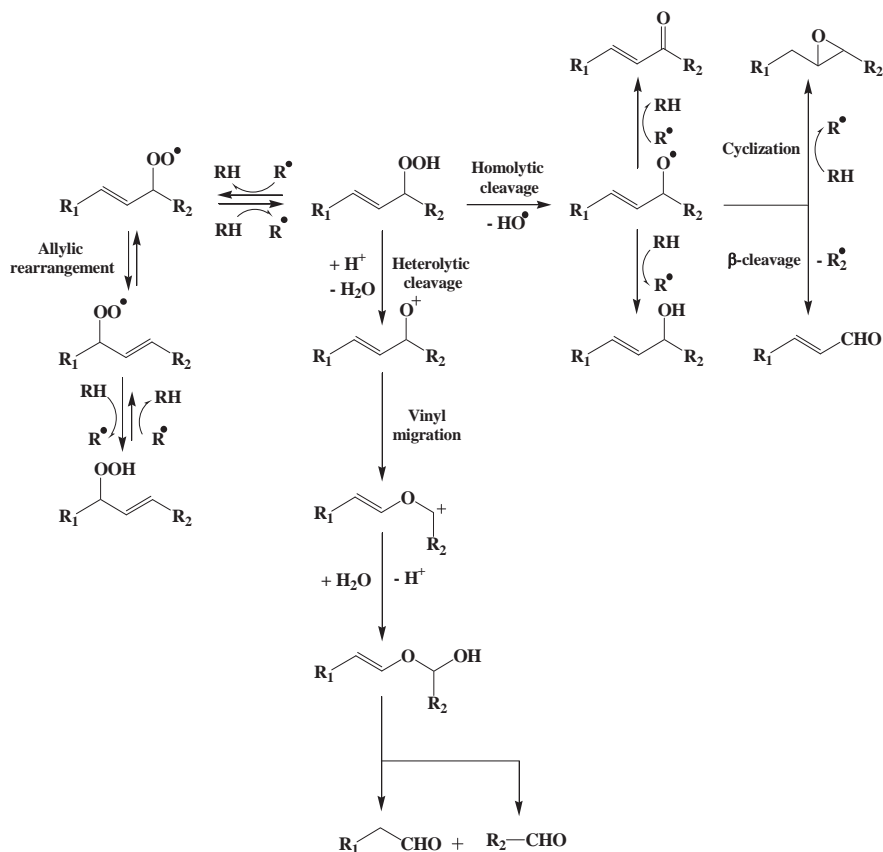


Figure 6. Rearrangement process and main degradation pathways of allylic hydroperoxides.

Homolytic cleavage

Homolysis of the O–O bond of hydroperoxides is induced by enzymes (e.g. lipoxygenases), redox-active metal ions undergoing one-electron

transfer, heat, or light (Schaich, 2005) (see Chapter 8 for further details). It leads to carbonyl (dehydration), alcohol (reduction), fragmentation (β -scission) or oxirane (radical cyclization) products (Fig. 6; Frimer, 1979). Note that β -scission acts mainly on the side of the hydroperoxy group affording an alkyl radical, since cleavage on the other side leads to the formation of an unstable and unlikely vinyl radical. Homolytic cleavage also produces several radicals, and notably the very reactive hydroxyl radical (HO^{\bullet}), which may be at the origin of the initiation of free-radical-mediated oxidation chain-reactions (See Chapter 8).

Further oxidation or condensation

Lipid hydroperoxides can also be oxidized to epoxyhydroperoxides, oxohydroperoxides, bihydroperoxides, cyclic peroxides, and bicyclic endoperoxides (Frankel, 1984), or else undergo condensation reactions forming dimers and polymers cross-linked through either peroxide or ether linkages and containing hydroperoxy, oxo- or hydroxy groups (Neff et al., 1988; Frankel, 1998; Pignitter and Somoza, 2012). These condensation reactions mainly act in the case of polyunsaturated substrates (Frankel, 1998).

Occurrence under natural environmental conditions

Despite these various degradation processes, literature nevertheless features several reports of intact allylic hydroperoxides in environmental samples or organisms, including phytoplankton (Orefice et al., 2015), bacteria (Petit et al., 2013), marine and terrestrial angiosperms (Rontani et al., 2014a; Rontani, 2019), particulate matter (Rontani et al., 2012; Galeron et al., 2015) and marine sediments (Rontani and Marchand, 2000). The unexpected stability of allylic hydroperoxides in sediments (where the residence time of organic matter may be relatively long) could result from protection of these compounds in well-silicified diatoms or higher plant debris (Rontani and Marchand, 2000).

CHAPTER FIVE

TYPE-II PHOTOSENSITIZED OXIDATION OF THE MAIN UNSATURATED LIPIDS OF AUTOTROPHIC ORGANISMS: SELECTION OF PROCESS SPECIFIC TRACERS

Chlorophylls

$^1\text{O}_2$ produced by chlorophyll photosensitization may act directly on the sensitizer, inducing chlorophyll degradation (photobleaching) (Fig. 3). In the literature, the photodegradation of chlorophylls has mainly been studied with respect to the tetrapyrrolic moiety of the molecule (Fig. 7), which is the more reactive. Although promising intermediate photoproducts were identified (Engel et al., 1991; Iturraspe et al., 1994), they are not sufficiently stable and specific to serve as specific tracers for the chlorophyll macrocycle photodegradation in the natural environment.

The trisubstituted double bond of the phytol side-chain of chlorophyll-*a* or -*b* (Fig. 7) can also react with $^1\text{O}_2$. The rate of this reaction is 3–5 times slower than that of the tetrapyrrolic structure (Cuny et al., 1999; Christodoulou et al., 2010). Due to the well-known *Syn* selectivity of the “ene” reaction (*cis* effect) (Alberti and Orfanopoulos, 2006), this reaction affords photoproducts of structures **a** and **b** (Fig. 8), which are quantifiable after reduction and alkaline hydrolysis, respectively, in the form of 6,10,14-trimethylpentadecan-2-ol and 3-methylidene-7,11,15-trimethylhexadecan-1,2-diol (more concisely named ‘phytyldiol’; Fig. 8; Rontani et al., 1994).

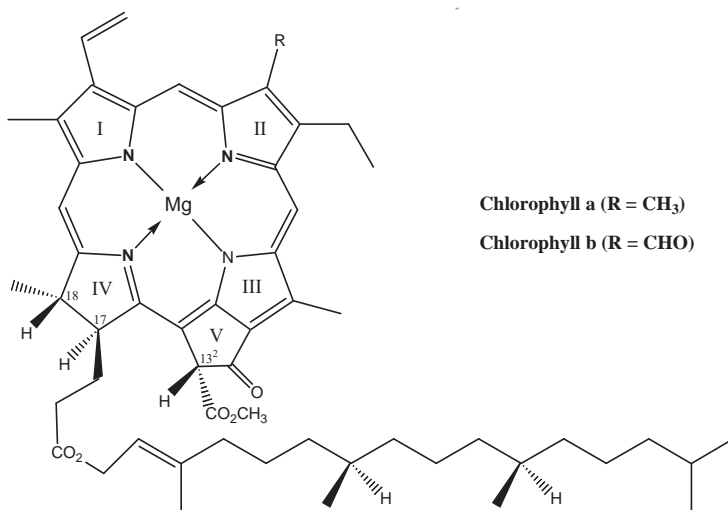


Figure 7. Structures of chlorophyll-a and chlorophyll-b.

Phytyldiol appeared to be relatively stable under environmental conditions (Rontani et al., 1996b) and yet highly specific. This specificity results from the strong preference for *Syn* ene addition of ¹O₂ at the disubstituted side of the double bond (*cis* effect; Alberti and Orfanopoulos, 2006; Fig. 8). Phytyldiol compound was thus proposed as biogeochemical marker of chlorophyll photodegradation in the natural environment (Cuny and Rontani, 1999).

The molar ratio phytyldiol:phytol (defined as chlorophyll phytyl side-chain photodegradation index, or 'CPPI') was proposed as an estimator of the extent of photooxidation of chlorophylls possessing a phytyl side-chain in natural samples, using the empirical Eq. 1 (Cuny et al., 1999).

$$(\text{chlorophyll photooxidation } \% = (1 - [\text{CPPI}+1]^{-18.5}) \times 100 \quad (1)$$

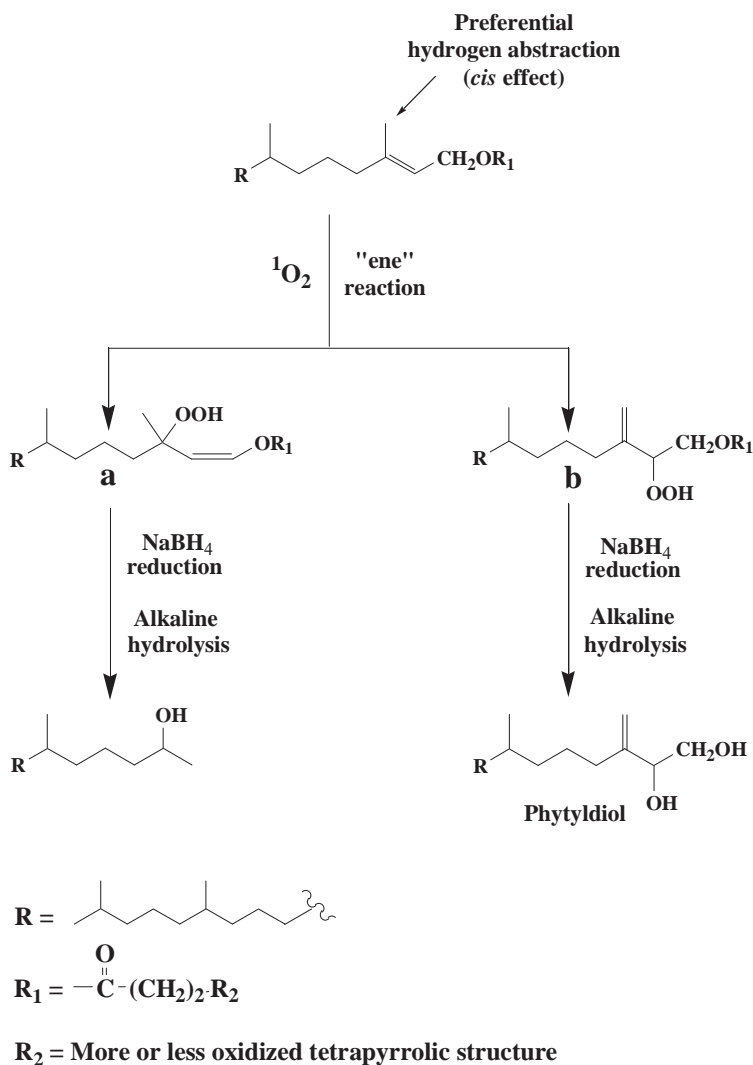
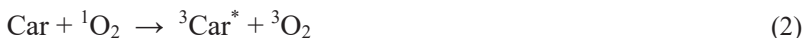


Figure 8. Type-II photosensitized oxidation of the chlorophyll phytol side-chain and subsequent reduction and alkaline hydrolysis of the resulting hydroperoxides. Adapted from Rontani and Belt (2020).

Carotenoids

Carotenoids are tetraterpenes containing a conjugated system of double bonds with delocalized π -electrons (Fig. 9). As seen in Chapter 2, these constituents of thylakoid membranes play special roles in the protection of tissues against damage caused by light and oxygen (Britton, 1995). The physical quenching pathway described in Eqs. 2 and 3 is thought to be the most favoured mechanism for carotenoid and $^1\text{O}_2$ interactions (Boon et al, 2010), but carotenoids can also quench $^1\text{O}_2$ by chemical reaction (scavenging) (Eq. 4).



The reaction of $^1\text{O}_2$ with carotenoids in biological membranes is not well understood (Boon et al., 2010). In the case of β -carotene, which appeared to be a preferred *in vivo* target of $^1\text{O}_2$ compared to xanthophylls (Ramel et al., 2012), it seems that β -carotene-5,8-endoperoxide (Fig. 9) was the primary oxidation product formed (Fiedor et al., 2005). Further degradation of this compound affords several aldehydes and ketones (β -ionone, β -apo-14'-carotenal, β -apo-10'-carotenal, β -apo-8'-carotenal, and more; Stratton et al., 1993; Yamauchi et al., 1998; Ramel et al., 2012). While β -carotene-5,8-endoperoxide makes a useful early signal of $^1\text{O}_2$ production in plant leaves (Ramel et al., 2012), it is clearly not stable enough to serve as a viable environmental tracer. Unfortunately, most of the shorter oxidation products resulting from the degradation of this endoperoxide can be also produced by enzymatic and autoxidative degradation of β -carotene (Boon et al., 2010) and thus do not make unequivocal indicators of type-II photosensitized oxidation of carotenoids in phototrophic organisms.

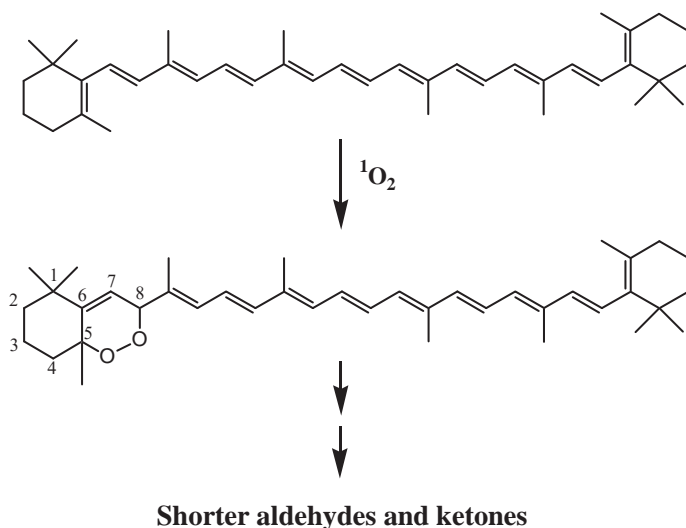


Figure 9. Oxidation of β -carotene by $^1\text{O}_2$.

Unsaturated fatty acids

Unsaturated fatty acid carbon chains contain one or more (methylene-interrupted) double bonds with a terminal carboxylic group ($-\text{COOH}$). These fatty acids fall into two groups depending on number of double bonds: (i) monounsaturated fatty acids (MUFAs), which contain a single double bond, and (ii) polyunsaturated fatty acids (PUFAs), which contain more than one double bond. The fatty acids in eukaryote membranes are mainly esterified with glycerol in phospholipid molecules, which are the building blocks of biological membranes (Mansy, 2010).

Note that most natural unsaturated fatty acids are *cis*-configured, and therefore reactive to $^1\text{O}_2$ (Table 1). The reaction rates of $^1\text{O}_2$ with oleic ($\text{C}_{18:1}$), linoleic ($\text{C}_{18:2}$), linolenic ($\text{C}_{18:3}$) and arachidonic ($\text{C}_{20:4}$) acid in biological membranes are 0.74, 1.3, 1.9, and 2.4 $\text{mole}^{-1}\text{s}^{-1}$, respectively (Min and Boff, 2002), and thus practically proportional to number of double bonds in the molecules. Even if PUFAs are particularly reactive with $^1\text{O}_2$, the resulting oxidation products cannot serve as tracers of type-II photooxidation processes in the environment, due to (i) the instability of the primary oxidation products formed, and (ii) the involvement of cross-linking reactions. Indeed, some allylic hydroperoxides resulting from photosensitized oxidation of PUFAs may quickly cyclize to hydroperoxy

epidioxides while others undergo addition of $^1\text{O}_2$ to the conjugated diene systems resulting from the “ene reaction” after *cis-trans* isomerization, affording hydroperoxide endoperoxides (Fig. 10) (Frankel, 1998). The decomposition of these different multi-oxidized compounds results in the production of several nonspecific volatile products (Frankel, 1998). Allylic hydroperoxides of PUFAs also dimerize and oligomerize, leading to the formation of macromolecular structures containing peroxide or ether linkages and hydroperoxy, hydroxy and oxo groups (Neff et al., 1988) that are not amenable to gas chromatography.

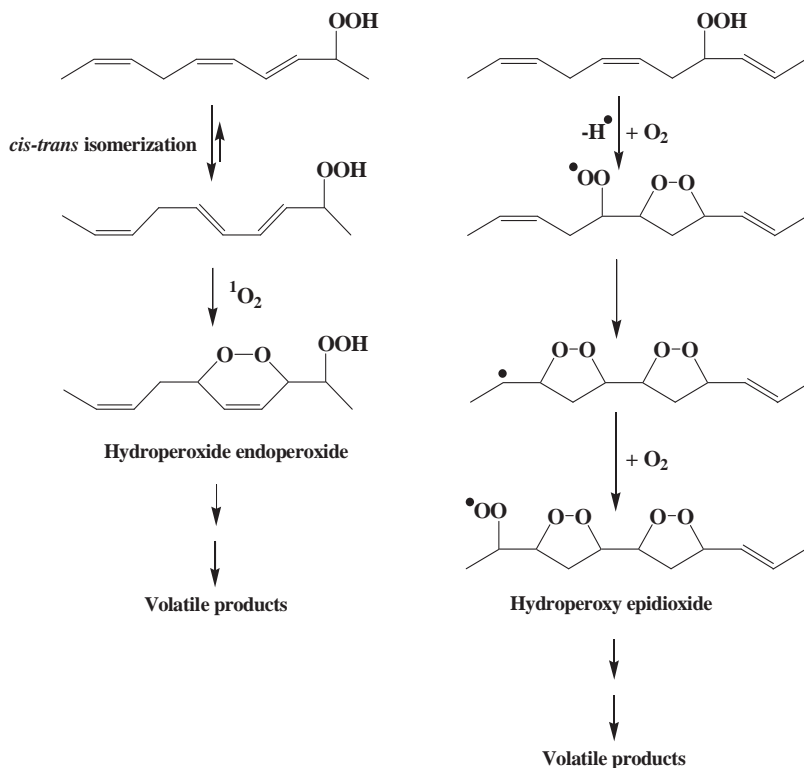


Figure 10. Further oxidation of allylic hydroperoxides of PUFAs.

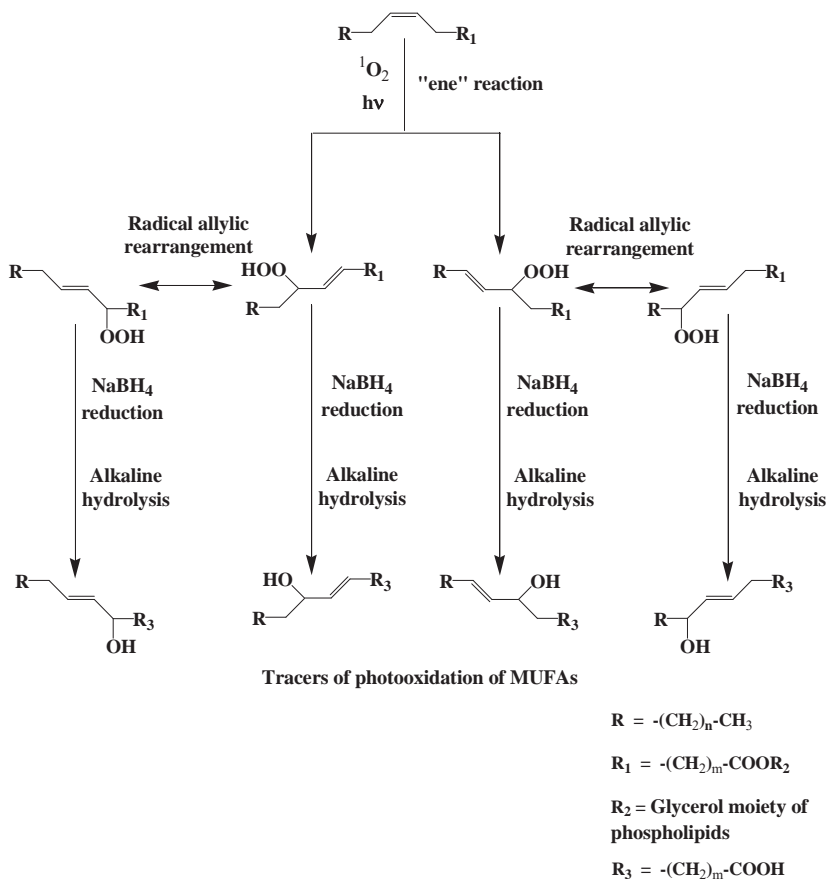


Figure 11. Type-II photosensitized oxidation of MUFA components of phospholipids, and subsequent $NaBH_4$ reduction and alkaline hydrolysis of the resulting hydroperoxides.

Type-II photosensitized oxidation of MUFA components of phospholipids involves the addition of 1O_2 to the two carbon atoms of their double bond and leads to the formation of two *trans* allylic hydroperoxides (Fig. 11; Frankel et al., 1979; Frankel, 1998). These hydroperoxides can subsequently undergo stereoselective radical allylic rearrangement (Fig. 6) affording two other isomers with a *trans* double bond (Fig. 11; Porter et al., 1995). *Trans* allylic hydroxy acids arising from $NaBH_4$ reduction and alkaline

hydrolysis of photooxidized MUFA-containing phospholipids (Fig. 11) are sufficiently stable for use as tracers of type-II photosensitized oxidation processes, but using them requires prior subtraction of the amounts of these compounds arising from autoxidation processes, which can be estimated (Marchand and Rontani, 2001) (see Chapter 10).

ω -Hydroxy monounsaturated fatty acids

The outer layer of the epidermal cells of primary plant tissues like leaves (cuticle) is composed of an insoluble polyester polymer (cuticular wax; Graça et al., 2002) that, when depolymerized, mainly affords C_{16} and C_{18} saturated and monounsaturated ω -hydroxycarboxylic acids (Kolattukudy, 1980). We previously demonstrated that in senescent plants, i.e. when rate of ^3Chl and $^1\text{O}_2$ formation exceeds the quenching capacity of the photoprotective system (Fig. 3), $^1\text{O}_2$ can migrate outside the chloroplasts and affect the unsaturated components of cuticular waxes, notably 18-hydroxyoctadec-9(*cis*)-enoic (18-hydroxyoleic) acid (Rontani et al., 2005a). Type-II photosensitized oxidation of this acid affords 9-hydroperoxy-18-hydroxyoctadec-10(*trans*)-enoic and 10-hydroperoxy-18-hydroxyoctadec-8(*trans*)-enoic acids (Fig. 12).

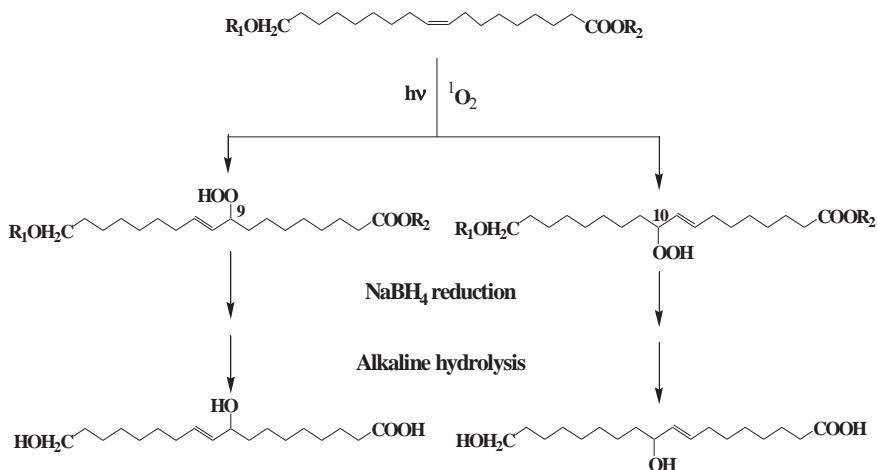


Figure 12. Type-II photosensitized oxidation of 18-hydroxyoleic acid in polymeric cuticular waxes. Adapted from Rontani et al. (2005a).

The corresponding alcohols resulting from the reduction of these hydroperoxides (Fig. 12) were proposed as indicators of photooxidation of the unsaturated components of higher plant cuticular waxes in the natural environment (Rontani et al., 2005a).

Sterols

Sterols are monohydroxy alcohols with a rigid tetracyclic structure or steroid nucleus and a short branched alkyl chain (Fig. 13), which are important membrane components of phototrophic organisms as they help structurally stabilize the phospholipid bilayers and regulate membrane fluidity and permeability (Piepho et al., 2012). In some plants, they have a specific function in cell proliferation, signal transduction, and modulation of the activity of some membrane-bound enzymes (Volkman, 2003). The main sterols are Δ^5 -sterols, but Δ^7 -sterols can also be found in small quantities (Martin-Creuzburg and Merkel, 2016). They may be free, esterified with a fatty acid or sulphuric acid, or etherified with a monosaccharide (glycosides) (Fig. 13).

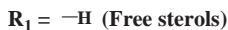
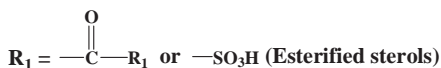
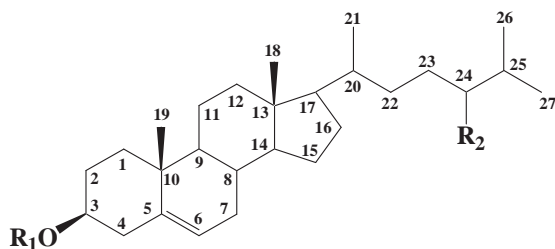


Figure 13. Generalized structure of Δ^5 -sterols (additional double bonds may be found at C-7, C-8, C-22, C-24(28) or C-25-27). Adapted from Volkman (2003).

$^1\text{O}_2$ attack on the Δ^5 double bond of these compounds mainly produces a $\Delta^6-5\alpha$ -hydroperoxide and to a lesser extent $\Delta^4-6\alpha/\beta$ -hydroperoxides (Kulig and Smith, 1973; Korytowski et al., 1992; Fig. 14).

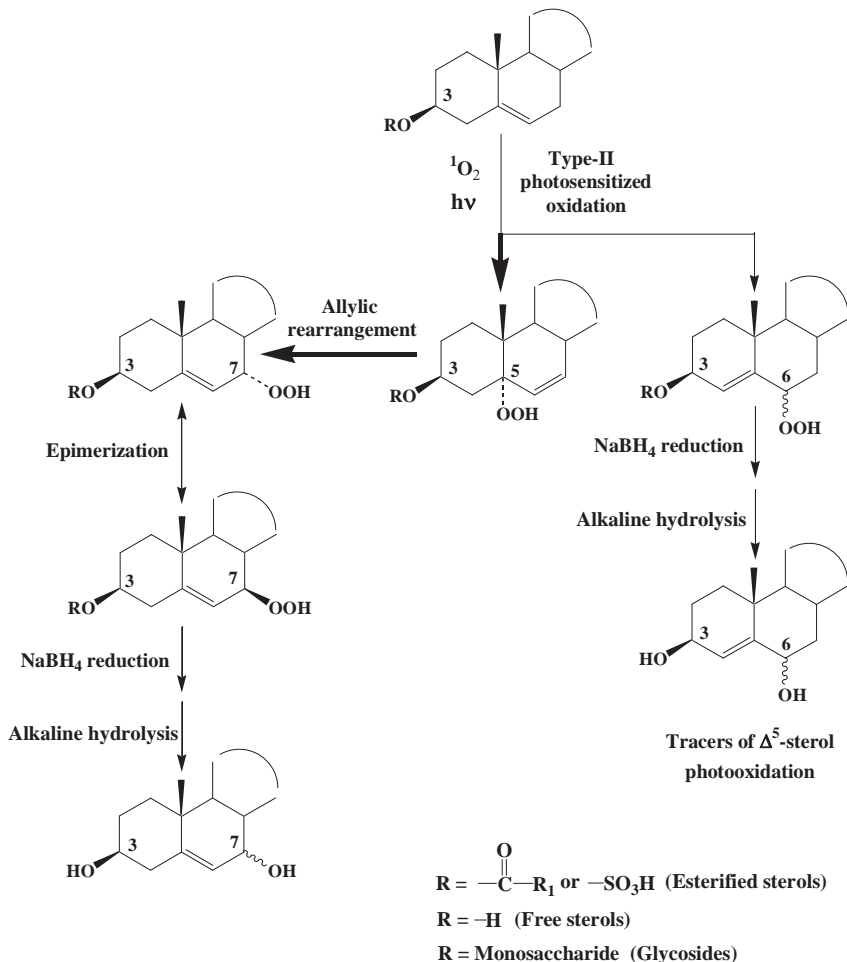


Figure 14. Type-II photosensitized oxidation of Δ^5 -sterols. Adapted from Rontani, (2008).

Although highly specific, $\Delta^6-5\alpha$ -hydroperoxides readily undergo allylic rearrangement to $\Delta^5-7\alpha$ -hydroperoxides, which in turn epimerize to the

corresponding 7 β -hydroperoxides (Fig. 14; Smith, 1981). These 7 α / β -hydroperoxysterols were ruled out as candidate markers of type-II photosensitized oxidation of Δ^5 -sterols due to their lack of specificity (See Chapter 10) and stability (Christodoulou et al., 2009; Rontani et al., 2009). Although produced in lower relative proportions compared to the Δ^6 -5 α -hydroperoxides, Δ^4 -6 α / β -hydroperoxides appear more environmentally stable. Indeed, β -scission of the alkoxy radicals resulting from homolytic cleavage of the peroxy bond of Δ^6 -5-hydroperoxysterols and Δ^5 -7 α -hydroperoxysterols affords radicals more stable than in the case of Δ^4 -6-hydroperoxysterols and is thus strongly favoured (Christodoulou et al., 2009). Δ^4 -Stera-3 β ,6 α / β -diols resulting from NaBH₄ reduction to the corresponding hydroperoxides (Fig. 14) have thus been proposed as reliable tracers of type-II photosensitized oxidation of Δ^5 -sterols (Christodoulou et al., 2009). The Δ^4 -6 α / β -hydroperoxides/ Δ^6 -5 α -hydroperoxides ratio (0.3) generally found in biological membranes (Korytowski et al., 1992) prompted the idea of estimating the extent of photooxidation (%) of the parent sterol using Eq. 5 (Christodoulou et al., 2009; Rontani et al., 2009).

$$\Delta^5\text{-sterol photooxidation \%} = \Delta^4\text{-6}\alpha/\beta\text{-hydroperoxides \%} \times (1+0.3)/0.3 \quad (5)$$

Even though trisubstituted double bonds react more quickly with ¹O₂ than disubstituted double bonds (Table 1), type-II photosensitized oxidation appeared to be slower for Δ^5 -sterols than MUFAs in solvents and in biological membranes (Rontani et al., 2011a). This weak reactivity was attributed to the rigid tetracyclic structure of sterols inducing steric hindrance during the ¹O₂ attack of the sterol Δ^5 double bond (Beutner et al., 2000).

Vitamin E

Vitamin E, an important constituent of photoprotective systems in cells, is capable of highly efficient ¹O₂ scavenging (Neely et al., 1988). The reaction of vitamin E with ¹O₂ mainly results in the formation of 8 α -hydroperoxytocopherone (Yamauchi and Matsushita, 1979; Clough et al., 1979; Fig. 15), which may subsequently be cleaved to different isoprenoid compounds after homolytic and heterolytic cleavages (Nassiry et al., 2009; Fig. 15).

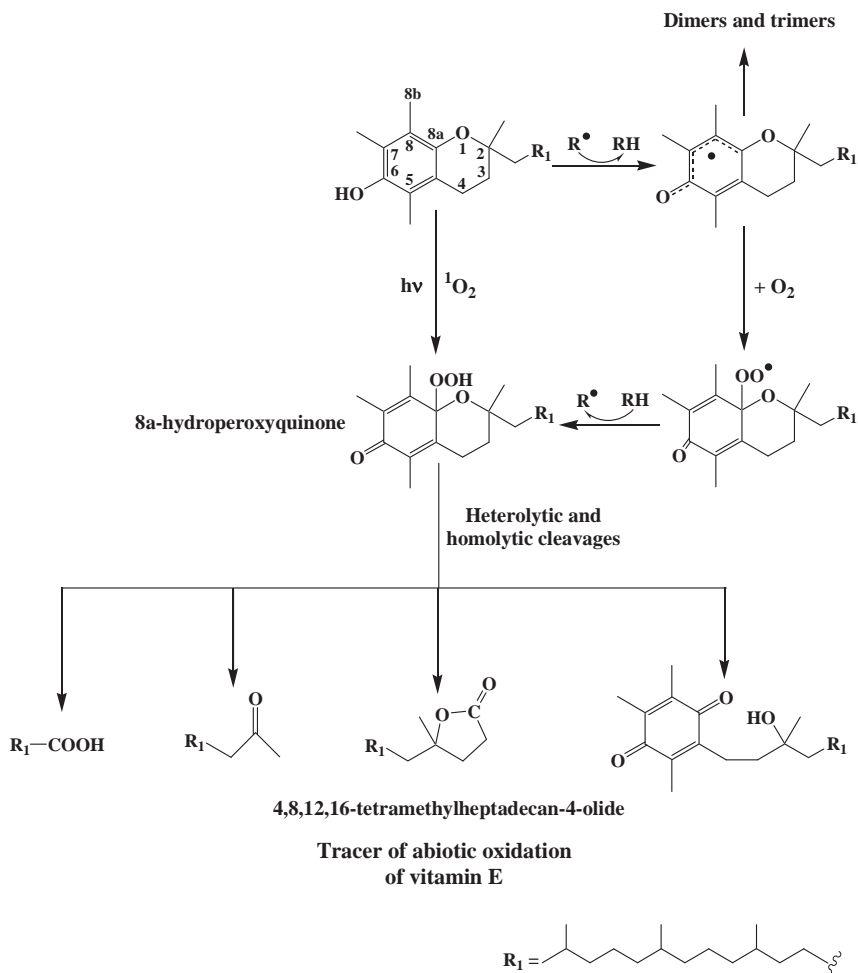


Figure 15. Type-II photosensitized and radical oxidation of vitamin E. Adapted from Rontani and Belt (2020).

Unfortunately, peroxy radicals also react with the 8a position of vitamin E, affording 8a-hydroperoxytocopherone (Liebler, 1994) (Fig. 15), which means that isoprenoid compounds resulting from homolytic and heterolytic cleavages of this compound cannot serve as specific tracers of type-II photosensitized oxidation of vitamin E. However, among them, 4,8,12,16-tetramethylheptadecan-4-olide appeared to be sufficiently stable

and specific to act as marker of abiotic oxidation of vitamin E, and so this lactone was proposed as a potential tracer of organic matter sedimentation under oxic conditions (Nassiry et al., 2009).

Pentacyclic triterpenes

Pentacyclic triterpenes and their derivatives, which can be divided into three main classes, i.e. lupane, oleanane and ursane, are all widely found in angiosperms (Jäger et al., 2009). These polycyclic structures can occur as free, esterified (with hydroxycinnamic acids for instance) or glycosylated forms, where glycosylated forms are called triterpenoid saponins (Furtado et al., 2017). There has been little investigation into the type-II photosensitized oxidation of these compounds, although there has been a recent study on betulin, α -amyrin and β -amyrin, which belong to the three main classes of pentacyclic triterpenoids and possess double bonds able to be attacked by $^1\text{O}_2$ (Fig. 16) (Galeron et al., 2016a; 2016b).

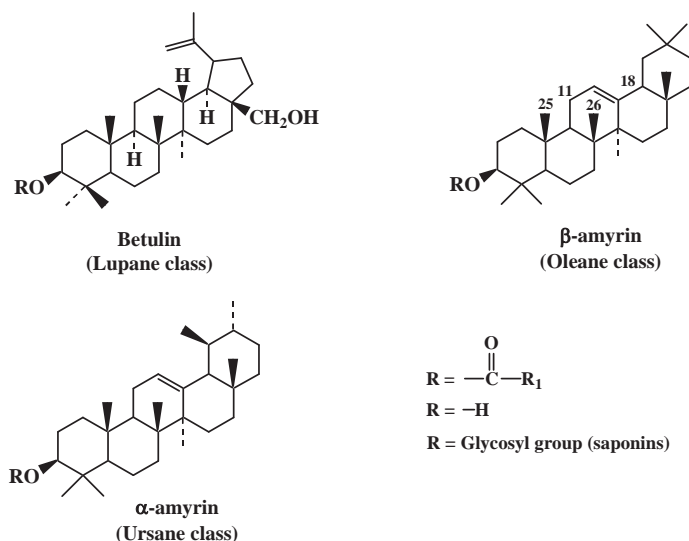


Figure 16. Structures of betulin, α -amyrin and β -amyrin.

Betulin was photodegraded in pyridine in the presence of hematoporphyrin as sensitizer (Galeron et al., 2016a), and its photodegradation rate appeared to be 17-fold slower than that of esterified cholesterol. This relatively low reactivity is consistent with the well-known increase in double-bond

reactivity to $^1\text{O}_2$ with increasing alkyl substitution (Table 1; Hurst et al., 1985). Type-II photooxidation of betulin specifically produces lup-20(30)-ene-3 β ,28-diol-29-hydroperoxide, which is quantifiable after NaBH_4 reduction in the form of lup-20(30)-ene-3 β ,28,29-triol (Fig. 17). The very high regioselectivity of betulin attack by $^1\text{O}_2$ is in good agreement with previous results on gem-disubstituted alkenes possessing a methyl and a bulky substituent. Indeed, in this case photooxygenation shows a strong preference for hydrogen abstraction from the methyl group that is geminal to the larger substituent of the alkene (Alberti and Orfanopoulos, 2006).

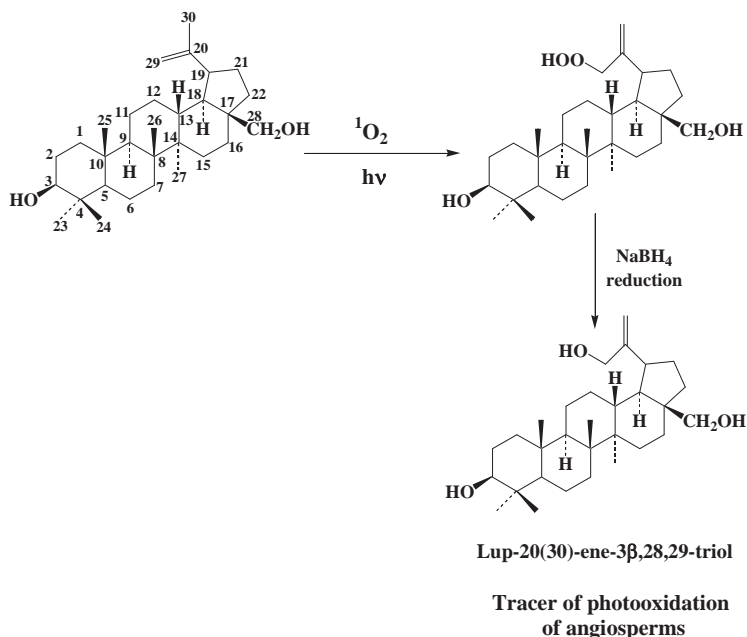


Figure 17. Type-II photosensitized oxidation of betulin. Adapted from Galeron et al. (2016a).

Lup-20(30)-ene-3 β ,28,29-triol, which is found in senescent leaves of *Quercus ilex* (Galeron et al., 2016a), was proposed as a marker of type-II photosensitized oxidation in angiosperms.

Despite the presence of trisubstituted Δ^{12} double bonds known to be reactive to $^1\text{O}_2$ (Table 1), α - and β -amyrins were totally unaffected during photodegradation experiments (Galeron et al., 2016b). This lack of reactivity was attributed to the involvement of steric hindrance when $^1\text{O}_2$

approaches the double bond. Indeed, during the ‘ene’ reaction, the presence of the bulky methyl groups 25 and 26 in the amyirin structures can potentially hinder the approach of the beta side of the Δ^{22} double bond and of the axial allylic hydrogen atoms carried by carbon-11 and -18 (Fig. 16).

Alkenones

Alkenones are a class of mono-, di-, tri-, tetra- and penta-unsaturated C_{35} – C_{40} methyl and ethyl ketones that are produced by some marine haptophytes and widespread in the oceans (Volkman et al., 1980, 1995; de Leeuw et al., 1980; Marlowe et al., 1984; Prahl et al., 2006; Jaraula et al., 2010). An unsaturation ratio of C_{37} alkenones (the $U_{37}^{K'}$ index defined in Eq. 6, where $[C_{37:2}]$ and $[C_{37:3}]$ are the concentrations of di- and tri-unsaturated C_{37} alkenones, respectively) is now widely used in paleoceanography to reconstruct past sea surface temperatures (SSTs) (e.g. Brassell et al., 1986; Prahl and Wakeham, 1987; Müller et al., 1998).

$$U_{37}^{K'} = [C_{37:2}] / ([C_{37:2}] + [C_{37:3}]) \quad (6)$$

Type-II photosensitized oxidation of these compounds was investigated in senescent haptophytes in order to determine whether these degradation processes could appreciably alter the $U_{37}^{K'}$ index by inducing a faster degradation of the $C_{37:3}$ alkenone relative to the $C_{37:2}$ (Rontani et al., 1997a; Mouzdahir et al., 2001; Christodoulou et al., 2010). Type-II photosensitized oxidation of alkenones appeared to be too slow to induce significant alteration of $U_{37}^{K'}$ index before the photosensitizing substances were destroyed. This lack of photodegradation was attributed to the *trans* configuration of alkenone double bonds (Rechka and Maxwell, 1988), which are known to be \approx 7-fold less reactive to 1O_2 than the *cis* configuration (Table 1), and to the separation of the double bonds by five carbon atoms in the alkenone structure instead of one in the very reactive PUFAs (Rontani et al., 1997a; Mouzdahir et al., 2001). The fact that alkenones are localized in cytoplasmic vesicles (Eltgroth et al., 2005) may also explain this poor reactivity by decreasing the likelihood of interaction between 1O_2 (produced in chloroplasts) and alkenone molecules.

It may be expected that if the configuration of their double bonds had been *cis*, then there would have been intensive selective photodegradation

of di- and tri-unsaturated alkenones during senescence of the haptophytes, thus confounding the use of $U_{37}^{K'}$ for paleotemperature estimation (Rontani et al., 2013a).

Long-chain *n*-alkenes

Some microalgae are able to biosynthesize long-chain alkenes (Volkman, 2018). This is notably the case of the Eustimatophyte *Nannochloropsis salina* that produces C₂₅, C₂₇ and C₂₉ mono- and poly-unsaturated *n*-alkenes (Gelin et al., 1997) and the Prymnesiophyceae *Emiliania huxleyi* (Volkman et al., 1980) that contains C₃₁, C₃₃, C₃₇ and C₃₈ *n*-alkenes with two, three and four double bonds. Type-II photosensitized oxidation of *n*-alkenes was investigated in senescent cells of *N. salina* and *E. huxleyi* (Mouzdahir et al., 2001).

In *N. salina*, there was strong photodegradation of C₂₅-C₂₉ poly-unsaturated *n*-alkenes, with degradation rates increasing logically with number of double bonds. In contrast, mono-unsaturated *n*-alkenes appeared to be unaffected (Mouzdahir et al., 2001). This lack of reactivity was attributed to the terminal position of the double bond in these compounds (Gelin et al., 1997), which is well-known to offer little reactivity to ¹O₂ (Table 1) (Kopecky and Reich, 1965).

In *E. huxleyi*, C₃₁ and C₃₃ *n*-alkenes possessing *cis* double bonds (Rieley et al., 1998) were strongly photodegraded, while major C₃₇ and C₃₈ *n*-alkenes possessing *trans* internal double bonds (Rieley et al., 1998) appeared particularly recalcitrant to ¹O₂ (Mouzdahir et al., 2001). Although, as in the case of alkenones (see above), we cannot rule out an effect of C₃₇ and C₃₈ *n*-alkene localization in cytoplasmic inclusions (Eltgroth et al., 2005) on their reactivity to ¹O₂, these results flag up the importance of lipid double-bond configuration during type-II photosensitized oxidation processes.

Highly branched isoprenoid (HBI) alkenes

Highly-branched isoprenoid (HBI) alkenes are produced by a relatively short list of marine and freshwater diatoms belonging to the *Berkeleya*, *Haslea*, *Navicula*, *Pleurosigma*, *Pseudosolenia* and *Rhizosolenia* genera (Belt and Müller, 2013; Belt, 2018). C₂₅ HBI alkenes (exhibiting 1-6 double bonds) are the most commonly reported in marine sediments (Rowland and Robson, 1990; Belt et al., 2000). Among these compounds, 3,9,13-trimethyl-6-(1,5-dimethylhexyl)-tetradec-1-ene (called IP₂₅) and 2,6,10,14-tetramethyl-7-(3-methylpent-4-enyl)-pentadec-6(17)-ene (called

IPSO₂₅; Fig. 18) have been proposed as proxies of past seasonal sea ice in the Arctic and Antarctic, respectively (Belt et al., 2016; Belt, 2018). 2,6,10,14-Tetramethyl-9-(3'-methylpent-4-enylidene)-pentadec-6(Z)-ene (HBI III; Fig. 18) has been identified as a potentially useful open-water counterpart to IP₂₅ (Belt, 2018).

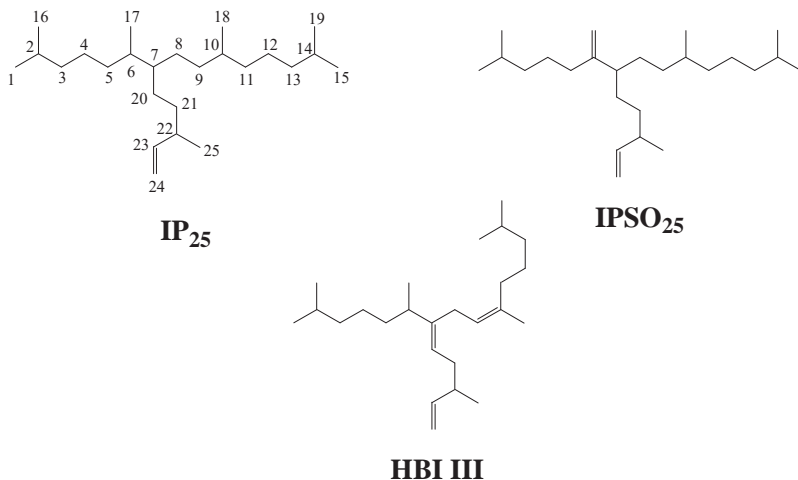


Figure 18. Structures and numbering of IP₂₅, IPSO₂₅ and HBI III.

Type-II photosensitized oxidation of several HBI alkenes was studied in solvents and in senescent diatoms (Rontani et al., 2011a; 2014b). In polyunsaturated HBI alkenes, attack by ¹O₂ occurs preferentially at the trisubstituted double bonds (Fig. 19), which are more reactive than the (6-17) methylidene group or the (23-24) terminal double bonds (Table 1) (Kopecky and Reich, 1965; Hurst et al., 1985).

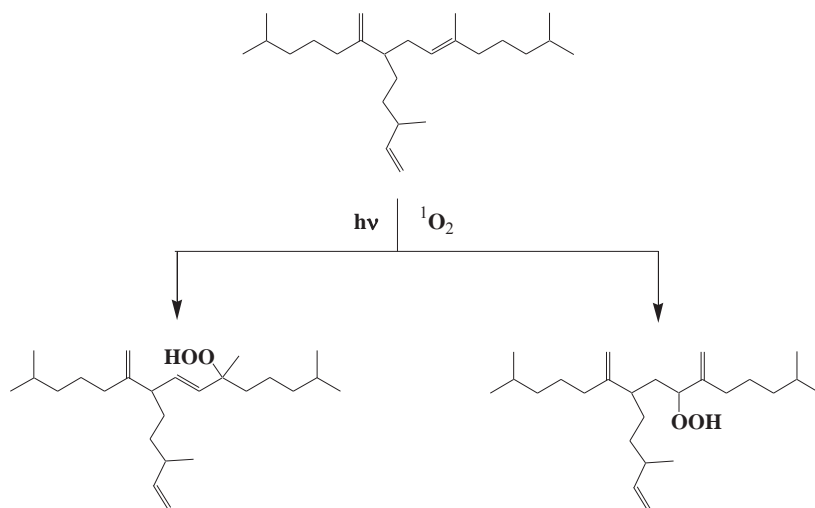


Figure 19. Type-II photosensitized oxidation of a triunsaturated HBI alkene possessing one trisubstituted double bond. Adapted from Rontani et al. (2011a).

Due to the very low 1O_2 reactivity of methyldene groups and terminal double bonds, the degradation rates of HBI alkenes increase with number of trisubstituted double bonds. HBI alkenes with one trisubstituted double bond are photooxidized 16-fold faster than phytol esters possessing a similar double bond (Rontani et al., 2011a). This results from electronic effects induced by the electron-accepting ester group in phytol esters that decrease the electron density of the double bond and thus its reactivity to 1O_2 (Griesbeck et al., 2003).

HBI alkenes with more than one trisubstituted double bond appeared to be photodegraded at similar or higher rates compared to PUFAs, vitamin E and chlorophyll (Rontani et al., 2011a; 2014b), which are known to be highly reactive to 1O_2 (Yamauchi and Matsushita, 1979; Clough et al., 1979; Nassiry et al., 2009). Unfortunately, the oxidation products of these HBI alkenes are not accumulate, due to the involvement of fast secondary oxidation reactions.

Summary of the results obtained

Table 2 below recaps the relative type-II photosensitized degradation rates of the main unsaturated lipid components of phototrophic organisms investigated to date.

Compound	Relative rates*
HBI alkenes with 3 trisubstituted double bonds	1.0
HBI alkenes with 2 trisubstituted double bonds	0.8
Carotenoids	0.7
Chlorophylls	0.7
Di-, tri-, tetra- and penta-unsaturated PUFAs	0.1-0.6
Vitamin E	0.5
HBI alkenes with 1 trisubstituted double bond	0.4
Di-, tri- and tetra-unsaturated <i>cis n</i> -alkenes	0.001-1.0
Chlorophyll phytol side-chain	0.13
MUFAs	0.06
Δ^5 -Sterols	0.02
Betulin	0.001
Di-, tri- and tetra-unsaturated alkenones	<0.001
Di- and tri-unsaturated <i>trans n</i> -alkenes	<0.001
Amyrins	0
IPSO ₂₅	0
IP ₂₅	0

* Estimated from: Nelson, 1993; Cuny et al., 1999; Rontani et al., 1995, 1997b, 1998, 2011a; Mouzdahir et al., 2001.

Table 2. Relative rates of type-II photosensitized oxidation of unsaturated lipids.

CHAPTER SIX

INDUCTION OF TYPE-II PHOTOSENSITIZED OXIDATION IN NON-PHOTOTROPHIC ORGANISMS

Type-II photosensitized oxidation in heterotrophic bacteria

Significant amounts of photooxidation products of *cis*-vaccenic acid arising from the “ene” reaction (i.e. 11-hydroperoxyoctadec-12(*trans*)-enoic and 12-hydroperoxyoctadec-10(*trans*)-enoic acids; Fig. 20) were previously detected in particulate matter and recent sediment samples collected in diverse zones of the oceans (Marchand and Rontani, 2001; Rontani et al., 2011b; 2012a). *cis*-Vaccenic acid, which is produced by many species of heterotrophic bacteria (Gillan and Sandstrom, 1985), is generally considered as a bacterial biomarker (Sicre et al., 1988; Keweloh and Heipieper, 1996). Given the lack of a chlorophyll photosensitizer in heterotrophic bacteria, this photooxidation appeared to be enigmatic.

Irradiation of axenic and non-axenic cultures of the diatom *Skeletonema costatum* allowed us to attribute this unexpected photooxidation of *cis*-vaccenic acid to a transfer of $^1\text{O}_2$ from senescent phytoplanktonic cells to their attached bacteria (Rontani et al., 2003a). Indeed, it was recently demonstrated that $^1\text{O}_2$ has a much larger intracellular sphere of activity than previously thought (Ogilby, 2010). The radius of this sphere of activity from the point of production was estimated to be between 155 and 340 nm (Baier et al., 2005; Ogilby, 2010; Skovsen et al., 2005), which is a large-enough distance to allow $^1\text{O}_2$ to cross the cellular membranes (Ogilby, 2010) and thus reach attached bacteria.

Due to the lack of efficient photoprotective and antioxidant systems in heterotrophic bacteria (Garcia-Pichel, 1994), $^1\text{O}_2$ can cause substantial damage in these microorganisms and affect not only MUFAs but also proteins (Davies, 2005) and nucleic acids (Dias Cavalcante et al., 2002). The deleterious effects of $^1\text{O}_2$ on bacteria are well known, and photodynamic

killing of bacteria using light and synthetic $^1\text{O}_2$ -producing photosensitizers to induce a phototoxic reaction (a strategy called photodynamic therapy, PDT) has even emerged as a viable treatment for several oncological and non-oncological indications (Jarvi et al., 2012).

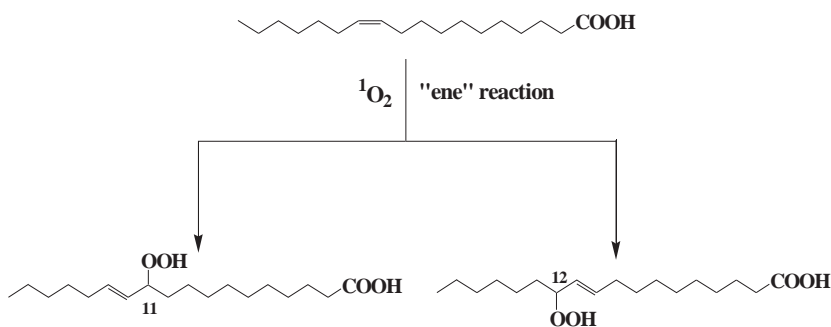


Figure 20. Type-II photosensitized oxidation of *cis*-vaccenic acid.

It is generally well accepted that marine bacteria colonize and contribute to the degradation of phytoplankton-derived particles (Fig. 21), but $^1\text{O}_2$ production in senescent phytoplanktonic cells can also induce oxidative damage in attached bacteria during their stay within the euphotic layer of the oceans (Petit et al., 2013). This oxidative-driven damage could limit bacterial growth and thus contribute to better preservation of algal organic matter during sedimentation.

Note, however, that the presence of a silica matrix (as in the case of highly-silicified diatoms) or high amounts of surrounding exopolymeric substances (EPS) (as in the case of ice algae) can inhibit the transfer of $^1\text{O}_2$ and thus limit the photooxidative alteration of attached bacteria (Petit et al, 2015a; Amiraux et al., 2017). In contrast, a carbonaceous matrix (as in the case of coccolithophorids) does not seem to inhibit $^1\text{O}_2$ transfer, probably due to the release of coccoliths upon cell death (Petit et al., 2015a). The limitation of $^1\text{O}_2$ transfer by a silica or EPS matrix could be attributed to the polar nature of silica or polysaccharides, respectively, which would decrease the lifetime of $^1\text{O}_2$ (Suwa et al., 1977), and/or to the presence of some components of the diatom frustule or EPS structure (e.g. mycosporine-like amino acids; Ingalls et al., 2010) acting as quenchers of $^1\text{O}_2$ (Suh et al., 2003). Petit et al. (2015a) could previously clearly demonstrate *in vitro* that the inhibition of the transfer of $^1\text{O}_2$ to the attached bacteria is directly linked to the concentration of biogenic silica

concentration in diatoms cells and could thus favour biodegradation of phytodetritus resulting from these organisms.

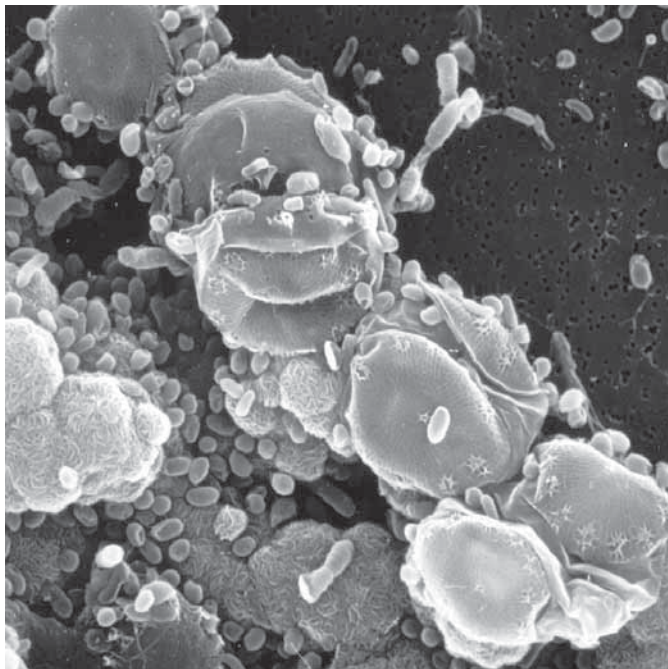
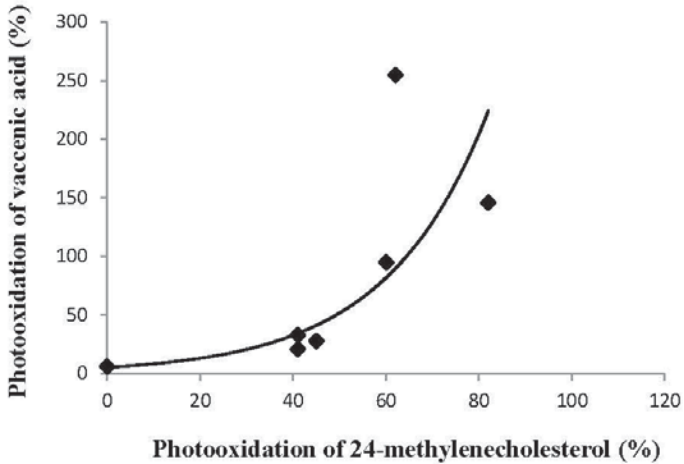


Figure 21. Scanning electron microscopy image of diatoms (*Skeletonema costatum*) contaminated by heterotrophic bacteria.

EPS concentrations in Arctic sea ice are typically an order of magnitude higher than for under-ice and open water environments (Krembs and Engel, 2001; Meiners et al., 2003). The lower production of EPS by open water phytoplankton thus favours $^1\text{O}_2$ transfer from phytodetritus to attached bacteria and, as a result, increases the susceptibility of the latter towards oxidative damage (Fig. 22)

A



B

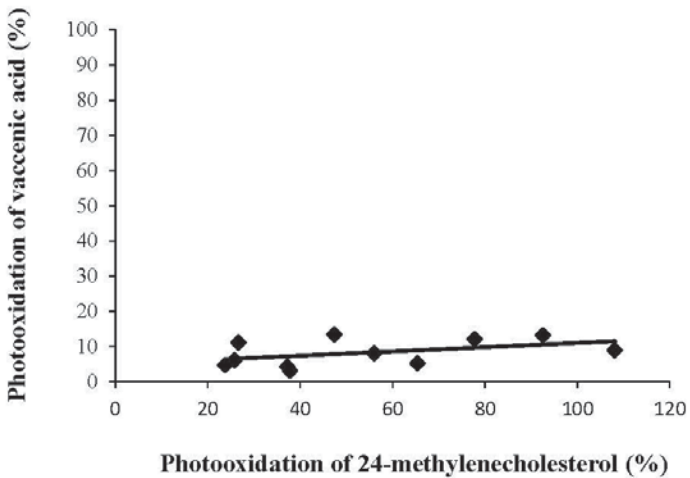
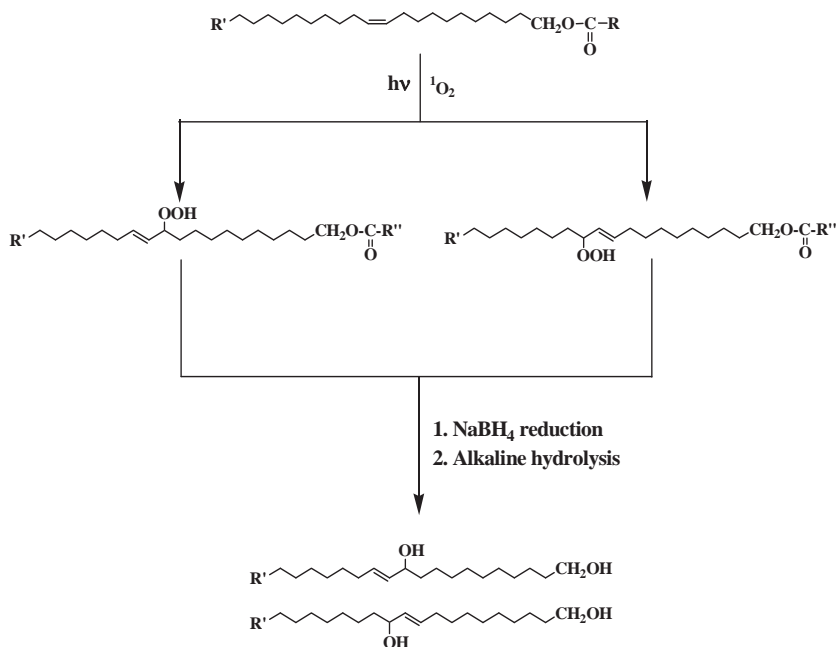


Figure 22. Cross-plot of % photooxidation of *cis*-vaccenic acid versus % photooxidation of 24-methylenecholesterol illustrating the variation of photooxidation of attached bacteria relative to that of the algae in the case of pelagic (A) and sympagic (B) diatoms. Adapted from Amiraux et al. (2017).

Type-II photosensitized oxidation in zooplanktonic material

Marine zooplankton count four main types of storage lipids: triacylglycerols, wax esters, phospholipids, and diacyl-glycerol ethers (Lee et al., 2006). Wax esters consisting of simple esters of long-chain primary alcohols and long-chain fatty acids are major storage lipids in high-latitude species (Lee et al., 2006).



R = Fatty acid alkyl chain

R' = $\text{CH}_3\text{-}$ or $\text{CH}_3\text{-(CH}_2\text{)}_2\text{-}$

R'' = Photooxidized fatty acid alkyl chain

Figure 23. Type-II photosensitized oxidation of $\text{C}_{20:\Delta 11}$ and $\text{C}_{22:\Delta 11}$ alkan-1-ol components of zooplanktonic wax esters. Adapted from Rontani et al. (2012).

In herbivorous copepods that undergo diapause, the most common alkan-1-ols of the wax esters are generally $\text{C}_{20:\Delta 11}$ and $\text{C}_{22:\Delta 11}$ (Albers et al., 1996). Photooxidation products of these two alcohols resulting from the

involvement of the “ene” reaction (Fig. 23) were recently observed after NaBH_4 reduction and alkaline hydrolysis of suspended particulate material collected in the Beaufort Sea (Canadian Arctic) (Rontani et al., 2012a).

This unexpected photooxidation of wax esters was attributed to the presence in these samples of copepod faecal pellets of both lipid droplets (rich in wax esters) (Najdek et al., 1994) and intact phytoplankton cells (containing undigested chlorophyll or phaeopigments; Turner, 2002). Indeed, the fact that phytoplanktonic cells are in close contact with lipid droplets in faecal pellets should favour the transfer of $^1\text{O}_2$ (produced from chlorophyll and phaeopigments in phytoplankton cells) to the double bonds of wax esters (Rontani et al., 2012a). Moreover, the apolar nature of lipid droplets should increase the lifetime and the diffusive distance of $^1\text{O}_2$ (Suwa et al., 1977).

CHAPTER SEVEN

EFFECT OF TEMPERATURE AND IRRADIANCE ON THE EFFICIENCY OF TYPE-II PHOTOSENSITIZED OXIDATION PROCESSES

Temperature dependence of type-II photosensitized oxidation processes

Surprisingly, previous analyses of particulate matter samples collected in both the Arctic (Rontani et al., 2012a) and Antarctic (Rontani et al., 2019a) showed that the efficiency of type-II photosensitized oxidation of phytoplanktonic lipids was considerably higher there than in equatorial zones (Rontani et al., 2011b). On the basis of the interesting work of Ehrenberg et al. (1998) showing that high temperatures increase the rates of $^1\text{O}_2$ diffusion outside cell membranes, an effect of temperature on these unexpected observations was suspected.

Recently, then, we studied type-II photosensitized oxidation of lipids (photodynamic effect) and chlorophyll photooxidation (sensitizer photobleaching) (Fig. 2) in dead cells of the centric diatom *Chaetoceros neogracilis* RCC2022 at different temperatures (Amiraux et al., 2016). The results showed a 3.0 ± 0.5 -fold increase in $k_{\text{camp}}/k_{\text{chl}}$ ratio (where k_{camp} and k_{chl} are the pseudo-first-order photodegradation rates of campesterol and chlorophyll, respectively) when temperature decreased from 17°C to 7°C. Low temperatures clearly favour the photodynamic effect at the expense of photobleaching, and thus make the type-II photosensitized oxidation of lipids more efficient (Fig. 24). These temperature effects could explain the higher photooxidation of phytoplanktonic lipids previously observed in polar zones (Rontani et al. 2012a, 2019a), although as we will see in the next subchapter, solar irradiance may also play a role.

Solar irradiance dependence of Type-II photosensitized oxidation processes

During the *in vitro* study of Amiraux et al. (2016) carried out on dead cells of *C. neogracilis* RCC2022, it was also observed that weak solar irradiances strongly enhance the efficiency of type-II photosensitized oxidation of lipids (Fig. 24). Indeed, $k_{\text{camp}}/k_{\text{chl}}$ ratio increased 4.2 ± 0.8 -fold when irradiance decreased from 2038 to 165 $\mu\text{mol photons m}^{-2}\text{s}^{-1}$. This enhanced efficiency of the photodynamic effect was attributed to relative preservation of the sensitizer (chlorophyll) at low irradiances resulting in a longer-lasting production of $^1\text{O}_2$ and thus more intense lipid damage (Amiraux et al., 2016).

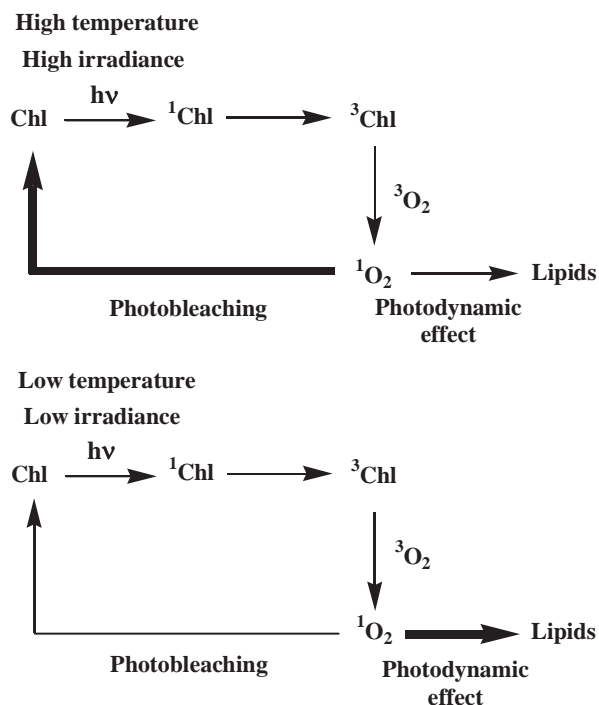


Figure 24. Effect of temperature and irradiance on efficiency of the photodynamic effect.

More recently, we compared the efficiency of the photodynamic effect in Arctic sinking particle samples collected in ice-covered and open water regions (Rontani et al., 2021b). The efficiency of the photodynamic effect was found to differ significantly between sinking particles collected under sea ice compared to open water ($k_{\text{bra}}/k_{\text{chl}} = 4.0 \pm 2.2$ at 30 m under the ice *versus* 0.5 ± 0.2 at 100 m in open water, where k_{bra} and k_{chl} are the pseudo-first-order photodegradation rates of brassicasterol and chlorophyll, respectively; Rontani et al., 2021b). This enhanced efficiency of the photodynamic effect in ice-covered zones was attributed to the weak solar irradiance intensity generally observed under ice. Indeed, in the Arctic, photosynthetically active radiation (PAR) irradiance is vastly higher in open water than in ice-covered zones (365 ± 62 *versus* 10.9 ± 2.7 $\mu\text{mol photons m}^{-2}\text{s}^{-1}$ in the surface mixed layer, respectively; Alou-Font et al., 2016).

CHAPTER EIGHT

FREE RADICAL OXIDATION (AUTOXIDATION) PROCESSES

Ground-state triplet molecular oxygen ($^3\text{O}_2$) is a paramagnetic bi-radical with two electrons occupying separate π^* orbitals with parallel spins. Spin restriction means that it has less oxidizing ability than $^1\text{O}_2$ in which the two electrons are paired with opposite spins (Krumova and Cosa, 2016). Indeed, the unpaired electrons of $^3\text{O}_2$ can only interact with unpaired electrons of transition metals or organic radicals, which in the latter case drives autoxidation reactions. Autoxidation involves free-radical-mediated oxidation chain reactions, which can be divided into three steps: chain initiation, propagation, and termination (Schaich, 2005).

Chain initiation

In order to proceed, the autoxidation process requires initiators or catalysts (able to produce radicals by removing an electron to the substrate molecule or breaking a covalent bond). The most common initiators are heat, light, metals, and certain enzymes.

High temperatures provide enough energy to break C-C or C-H covalent bonds in organic molecules and thus generate a huge variety of radicals (Nawar, 1969). However, this is not the case of the moderate temperatures generally found in the natural environment, which can only break weak bonds such as the O-O bond of hydroperoxides (which have a bond energy of only 34 kcal/mol) produced by other processes such as photosensitized oxidation (Girotti, 1998).

As seen in the Chapter 1, some chromophore-containing molecules can be directly excited in the UV and visible region of solar light, affording long-lived triplet states (Zafiriou et al., 1984). Some of these triplet states can abstract hydrogen atoms on other molecules and initiate type-I photosensitized oxidation processes (Fig. 1), which are in fact light-induced free-radical chain oxidation processes. This is notably the case for the excited triplet state of carbonyl compounds, which can form at

wavelengths < 350 nm (Schaich, 2005; Fig. 25). Solar UV radiation can also break weak covalent bonds such as the O-O peroxy bond (Schaich, 2005).

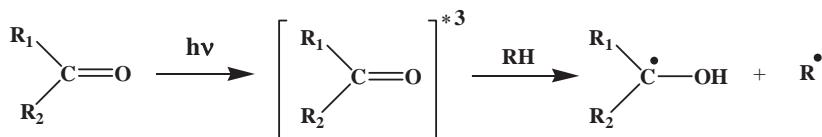


Figure 25. Light-induced free-radical chain oxidation in the case of carbonyl compounds.

Redox-active metal ions undergoing one-electron transfer (e.g. Fe^{2+} , Co^{2+} , Fe^{3+} , Cu^{2+} , Mn^{2+} , Zn^{2+} , Mg^{2+} , V^{2+}) are thought to be major initiators of lipid oxidation in biological systems (Pokorny, 1987). Indeed, they are ubiquitous, active in many forms, and highly efficient at even very low concentrations (Schaich, 2005). They can direct the cleavage of hydroperoxides through either alkoxy radicals (hydroperoxide reduction) (Eq. 7) or peroxy radicals (hydroperoxide oxidation) (Eq. 8). Note that hydroperoxide reduction proceeds much faster than hydroperoxide oxidation.



Certain enzymes such as lipoxygenases (LOXs) that produce radicals during their catalytic cycle can also catalyze the induction of free-radical oxidation chains (Fig. 26; Bhattacharjee, 2014; Fuchs and Spitteller, 2014). Moreover, the production of increasing amounts of free radicals may damage the active site of LOXs and release Fe^{2+} ions (Sato et al., 1992; Fuch and Spitteller, 2014) that can very efficiently catalyze the reduction of hydroperoxides to alkoxy radicals (Eq. 7).

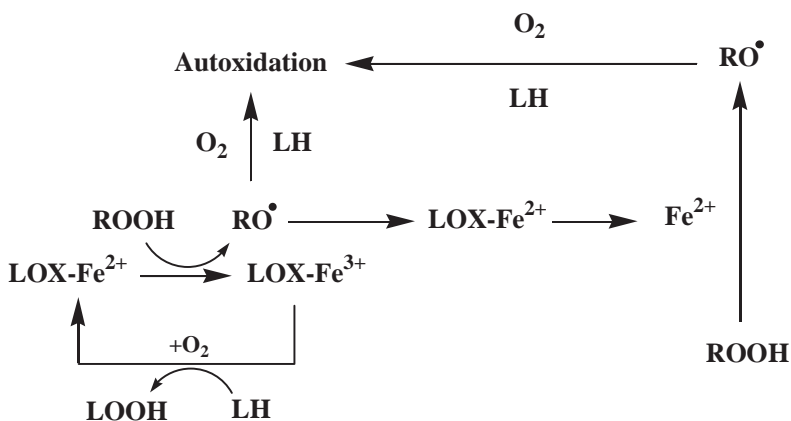


Figure 26. Induction of free-radical chain oxidation by lipoxygenases (LOX-Fe²⁺ = native ferrous lipoxygenase, LOX-Fe³⁺ = active ferric lipoxygenase, LH = lipid, LOOH and ROOH = hydroperoxides)

Propagation

The propagation step proceeds as a succession of reactions in which each radical produced in one reaction is consumed in the next (Fossey et al., 1995). It generally proceeds via hydrogen atom abstraction through a cyclic network of peroxy–hydroperoxide-mediated free-radical chain reactions (Yin et al., 2011; Fig. 27). Hydrogen atoms are generally abstracted from tertiary, allylic or α to oxygen positions, with doubly allylic hydrogen atoms being the most susceptible to abstraction. These radicals are then converted to hydroperoxides after the addition of molecular oxygen (Fig. 27).

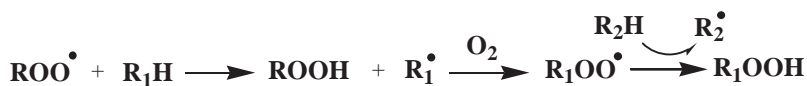


Figure 27. Hydrogen abstraction by peroxy radicals.

Interestingly, abstraction is not selective in the case of the hydroxyl radical (HO•), which is so electrophilic and reactive that it can abstract hydrogen atoms indiscriminately from all positions of alkyl chains (Schaich, 2005).

Peroxy radicals can also add to double bonds, affording di-peroxides after reaction with molecular oxygen or epoxides by fast intramolecular homolytic substitution (Fig. 28). However, hydrogen abstraction processes generally dominate the autoxidation of unsaturated compounds, and radical addition only becomes competitive when the double bond is conjugated, terminal, or 1,1-disubstituted (Hiatt and McCarrick, 1975). Conditions that favour addition generally develop during lipid oxidation, due to the increasing number of conjugated double bonds.

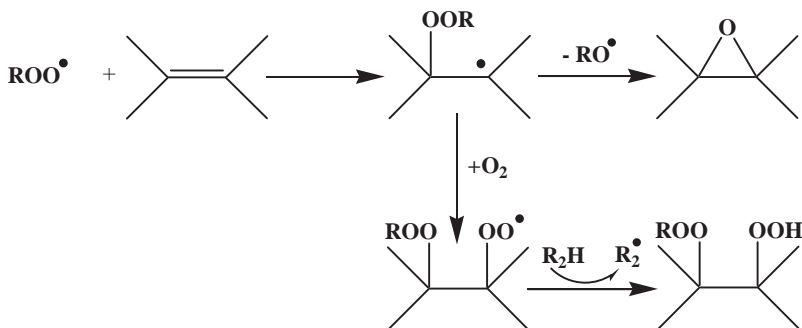


Figure 28. Addition of peroxy radicals to double bonds.

Termination

Termination reactions decrease the number of radicals and yield non-radical products such as alcohols and ketones (Schaich, 2005). They involve either (i) radical recombination (Figs. 29A and 29B), (ii) electron transfer (Fig. 29C), or (iii) radical elimination (Fig. 29D). Antioxidants, which play a key role during this step, can function as: (i) reducing agents (electron or hydrogen atom donors) or (ii) peroxy radical chain interrupters. Chain-breaking antioxidants react with peroxy radicals to yield stabilized radicals that are unable to further propagate the oxidative chain (Amorati et al., 2017).

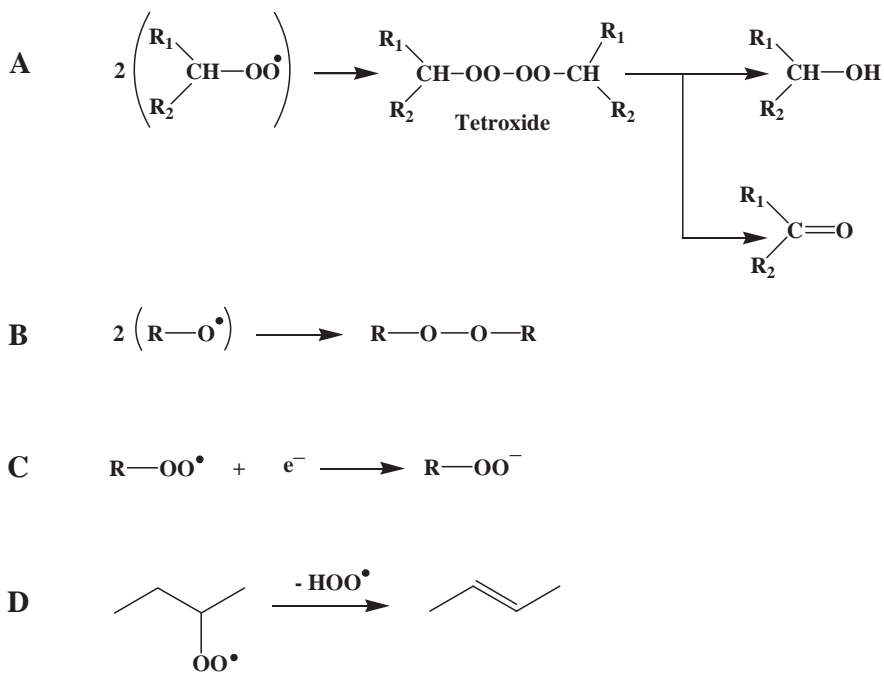


Figure 29. Disproportionation (radical self-recombination) of (A) peroxy and (B) alkoxy radicals, (C) peroxy radical reduction, and (D) hydroperoxy radical elimination.

CHAPTER NINE

INDUCTION OF AUTOXIDATION PROCESSES IN MEMBRANES OF PHOTOTROPHIC ORGANISMS

As in the case of type-II photosensitized oxidation, autoxidation processes should only be prevalent in phototrophic organisms when they senesce or undergo intense stresses, i.e. when ROS (including $^1\text{O}_2$) concentrations exceed the quenching capacities of the antioxidant defence system.

Induction of autoxidation processes during the senescence of phototrophic organisms

Autoxidation processes are generally thought to play a key role in the deleterious effects of senescence in plants (Leshem, 1988). Viral infection (Evans et al., 2006) and autocatalytic programmed cell death (Bidle and Falkowski, 2004) of phototrophic organisms can also lead to elevated production of ROS able to induce the autoxidation of cell components.

In senescent phototrophic cells, initiation of autoxidation processes mainly appears to result from the decomposition of hydroperoxides produced by the photodegradation of cellular components (Girotti, 1998; Rontani et al., 2003b). As seen in the previous chapter, heat, light, some redox-active metal ions, and certain enzymes can cleave these hydroperoxides to hydroxyl, peroxy and alkoxy radicals (Fig. 30). Even though photochemically-produced hydroperoxides present in the cells are a major driver of lipid autoxidation (Galeron et al., 2016c), it is important to note that the intensity of autoxidative processes also depends on conditions conducive to homolytic cleavage of these hydroperoxides (Sheldon and Kochi, 1976; Schaich, 2005; Fig. 30).

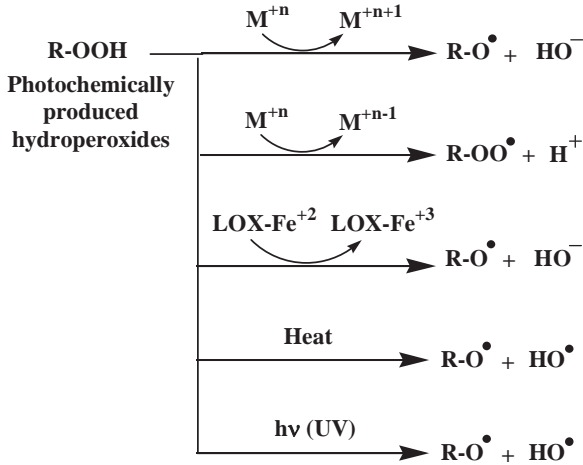


Figure 30. Initiation of autoxidation processes from photochemically-produced hydroperoxides. Adapted from Rontani and Belt (2020).

Induction of autoxidation processes under abiotic stresses

In the natural environment, plants are exposed to a number of abiotic stresses (salinity, drought, extreme temperature, metal toxicity, air pollutants, ultraviolet light, and high doses of pesticides; Choudhury et al., 2013; Xie et al., 2019) that can alter ROS metabolism and thus induce their accumulation (Chaki et al., 2020). Like during senescence, high concentrations of these reactive species can overwhelm the antioxidant defence system, thus leading to oxidative stress and, ultimately, to cell death.

Induction of autoxidation processes under natural environmental conditions

As the propagation of radical chain oxidation requires the presence of molecular oxygen (Fig. 27), autoxidation processes can operate in all the oxic environments. These processes will be particularly efficient when plant material experiences long residence times under oxic conditions, whether on land or in the oceanic water column. Note that in soils and sediments possessing a thick oxic layer, the contact of organic matter with oxygen may be relatively long (decades to centuries in the case of some Arctic sediments; Rontani et al., 2018a). In such particular environments,

even weakly reactive substrates such as terminal alkenes or branched hydrocarbons could be significantly affected by autoxidation processes (Rontani et al., 2018a).

CHAPTER TEN

AUTOXIDATION OF THE MAIN UNSATURATED LIPIDS OF AUTOTROPHIC ORGANISMS: SELECTION OF PROCESS SPECIFIC TRACERS

Chlorophyll

Autoxidation of the tetrapyrrolic core of chlorophyll *a* was studied *in vitro* in the presence of hydrogen peroxide (Walker et al., 2002). It mainly resulted in the formation of ^{13}C -hydroxychlorophyll *a* (Fig. 31). This compound and/or its Mg-lacking counterpart ^{13}C -hydroxyphaeophytin have been detected in senescent *Thalassiosira pseudonana* and *Closterium* sp. cultures (Louda et al., 1998; Franklin et al., 2012), in virally-infected cultures of *Emiliana huxleyi* (Bale et al. 2013) and *Ostreococcus Tauri* (Steele et al., 2018), and in several sediments (Villanueva et al., 1994; Stephens et al., 1997; Louda et al., 2000; Walker et al., 2002). Their relative stability to further oxidation (attributed to the lack of readily-abstractable hydrogen atoms at C- 13 ; Walker et al., 2002) served as rationale for using these oxidation products as potential markers of chlorophyll oxidation processes for paleoenvironmental assessment (Walker et al., 2002; Squier et al., 2005), and some authors suggested using these oxidized transformation products of chlorophyll as indicators of the oxicity of the depositional environment (Louda et al., 2000; Squier et al., 2002; Walker et al., 2002).

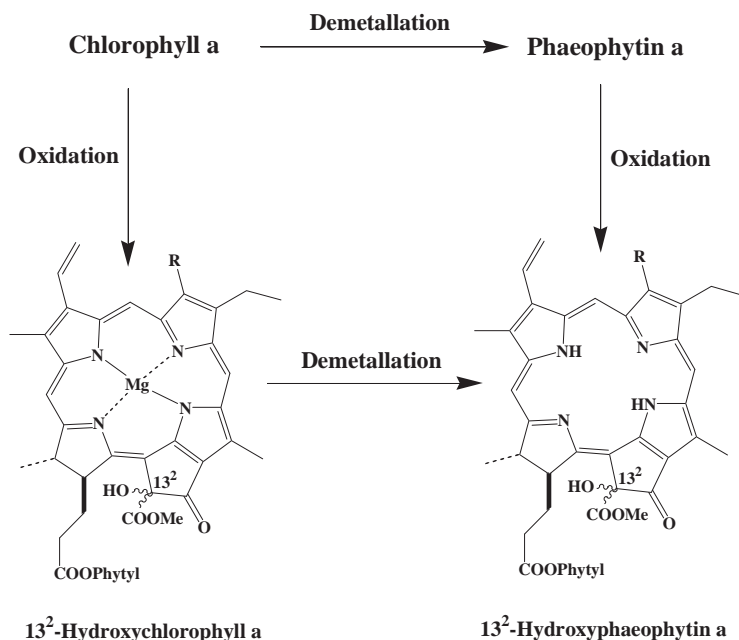
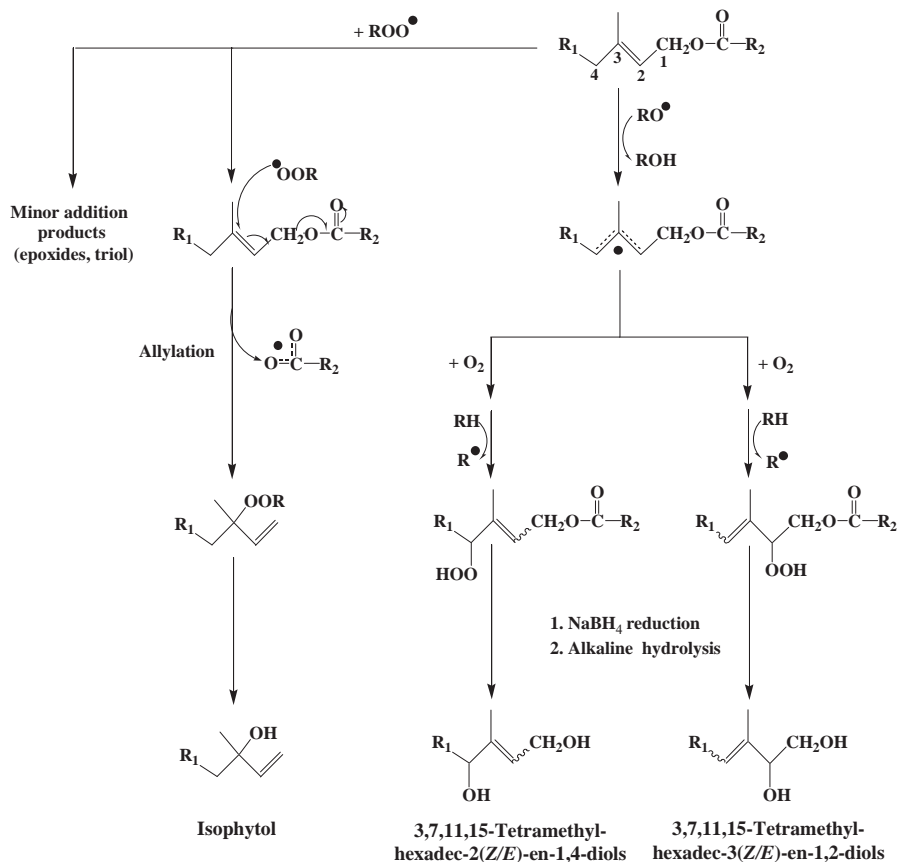


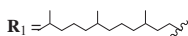
Figure 31. Pathways forming 13²-hydroxychlorophyll and 13²-hydroxyphaeophytin.

Chlorophyll phytyl side-chain autoxidation mainly involves allylic hydrogen atom abstraction. As the presence of an ester group on the carbon-1 of the phytyl chain strongly decreases the reactivity of hydrogen atoms to abstraction (Huyser and Johnson, 1968), these processes mainly act on the secondary allylic carbon-4. Subsequent oxidation of the allylic radicals thus formed yields four isomeric hydroperoxides which are converted (after NaBH₄ reduction and alkaline hydrolysis) to 3,7,11,15-tetramethylhexadec-3-en(*Z/E*)-1,2-diols and 3,7,11,15-tetramethyl-hexadec-2-en(*Z/E*)-1,4-diols (Rontani and Aubert, 2005; Fig. 32).

It was recently observed that autoxidation of the chlorophyll phytyl side chain also affords 3-peroxy-3,7,11,15-tetramethylhexadec-1-ene, which is converted to 3,7,11,15-tetramethylhexadec-1-en-3-ol (isophytol) after NaBH₄ reduction (Rontani and Galeron, 2016). The formation of this hydroperoxide was attributed to an allylation (Berkessel, 2014) of the chlorophyll phytyl side chain initiated by the addition of peroxy radical on the ethylenic carbon-3 of the molecule (Rontani et al., 2019a; Fig. 32).



Tracers of chlorophyll phytol side-chain autoxidation



Pyr = More or less oxidized tetrapyrrolic structure

RH = Hydrogen donor

Figure 32. Autoxidation of the chlorophyll phytol side chain. Adapted from Rontani and Belt (2020) and Rontani et al. (2019a).

This reaction appears to be driven by the formation of a highly stable acetoxyl radical. Peroxyl radicals also add on the ethylenic carbon-2, but

to a lesser extent, and only affording very minor oxidation products (mainly epoxides and a triol) (Rontani, 2012).

Consequently, isophytol, 3,7,11,15-tetramethylhexadec-3-en(*Z/E*)-1,2-diols and 3,7,11,15-tetramethyl-hexadec-2-en(*Z/E*)-1,4-diols have been proposed as specific tracers of chlorophyll phytyl side-chain autoxidation (Rontani and Aubert, 2005; Rontani and Galeron, 2016).

Carotenoids

Autoxidation of carotenoids results first in the production of epoxides, carbonyl compounds and uncharacterized oligomers (Boon et al., 2010). Further oxidation processes produce secondary short-chain carbonyl and carboxylic compounds (Mordi et al., 1993). Unfortunately, none of these oxidation products are sufficiently stable and specific to serve as tracers of carotenoid autoxidation.

Unsaturated fatty acids

PUFAs, which contain methylene-interrupted double bonds and thus *bis*-allylic hydrogen atoms that are particularly reactive to abstraction, are strongly affected by autoxidation processes (Frankel, 1998), and their oxidation rates logically increase with number of double bonds (Cosgrove et al., 1987). Unfortunately, as in the case of type-II photosensitized oxidation, the instability of the primary oxidation products formed precludes the use of these compounds as tracers of PUFA autoxidation in the natural environment.

Autoxidation of the MUFA components of phospholipids, which mainly involves allylic hydrogen abstraction and subsequent oxidation of the allylic radicals thus formed, affords six isomeric allylic hydroperoxides (Porter et al., 1995; Fig. 33). These compounds can be converted to the corresponding hydroxy acids after NaBH₄ reduction and alkaline hydrolysis (Fig. 33). The crucial factor here is that free radical oxidation of MUFAs affords *cis* and *trans* hydroxy acids whereas type-II photosensitized oxidation only gives *trans* hydroxy acids (Fig. 11), which means that *cis* hydroxy acids are specific tracers of autoxidation processes. These compounds proved valuable for distinguishing the proportion of *trans* hydroxy acids resulting from autoxidative processes from the proportion arising from photooxidative processes (Marchand and Rontani, 2001).

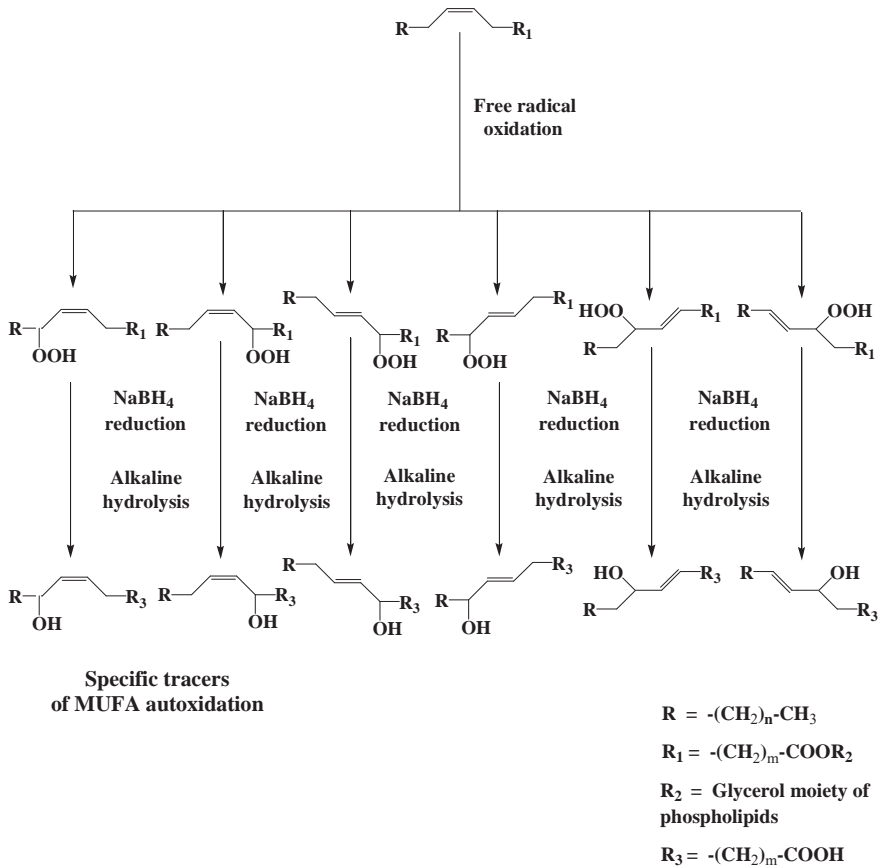


Figure 33. Autoxidation of the MUFA components of phospholipids and subsequent $NaBH_4$ reduction and alkaline hydrolysis of the resulting hydroperoxides. Adapted from Rontani (2012) and Rontani and Belt (2020).

Indeed, based on the proportions of *cis* hydroxy acids detected and the ambient temperature T ($^{\circ}C$), it is possible to estimate the proportion of *trans* hydroxy acids arising from autoxidation of MUFAs using different equations (see Eqs. 9-12 given for Δ^9 MUFAs) (Frankel 1998; Marchand and Rontani, 2001).

$$([8-cis] + [11-cis])/[9-trans] = -0.0138T + 1.502 \quad (9)$$

$$([8-cis] + [11-cis])/[10-trans] = -0.0144T + 1.553 \quad (10)$$

$$[8-cis]/([8-cis] + [8-trans]) = -0.0055T + 0.627 \quad (11)$$

$$[11-cis]/([11-cis] + [11-trans]) = -0.0055T + 0.627 \quad (12)$$

ω -Hydroxy monounsaturated fatty acids

Autoxidation of the unsaturated components of cuticular waxes such as 18-hydroxyoleic acid (Kolattukudy, 1980) and subsequent NaBH_4 reduction and alkaline depolymerisation afford six isomeric allylic dihydroxy acids (two *cis* and four *trans*) (Fig. 34). As in the case of MUFAs, the (autoxidation-specific) *cis* dihydroxy acids can be used to estimate the proportion of *trans* isomers resulting from autoxidation.

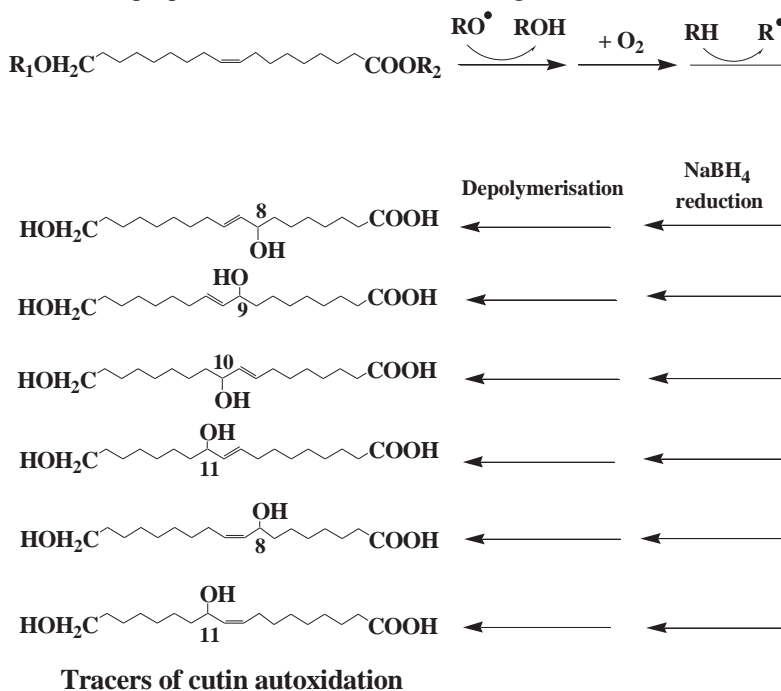
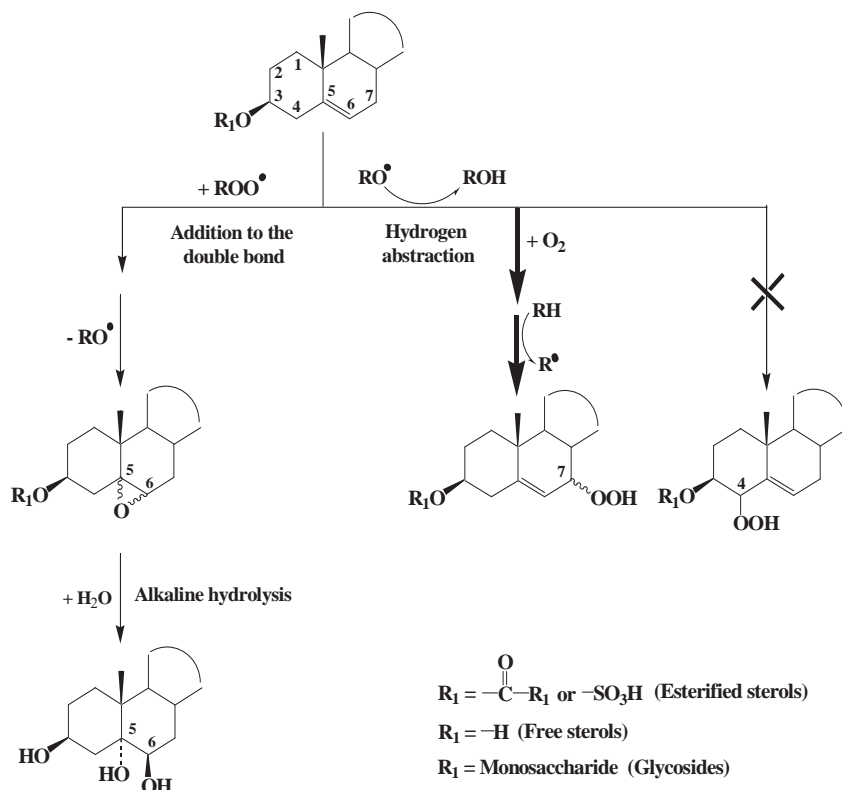


Figure 34. Autoxidation of 18-hydroxyoleic acid in polymeric cuticular waxes.

Δ^5 -sterols

Autoxidation of Δ^5 -sterol mainly involves hydrogen abstraction and, to a lesser extent, peroxy radical addition to the double bond (Smith, 1981; Morrissey and Kiely, 2006). Hydrogen abstraction focuses on the allylic carbon-7 of the steroid nucleus and does not act on the allylic carbon-4 (Fig. 35). This selectivity may be attributed to the fact that the dissociation energy of the carbon-hydrogen bond is weakest at this position (89.0 and 83.2 kcal/mol for C4-H and C7-H, respectively; Zielinski, 2021), which allows peroxy or alkoxy radicals to readily abstract these hydrogen atoms (Murphy and Johnson, 2008).



Tracer of sterol autoxidation

Figure 35. Autoxidation of Δ^5 -sterols. Adapted from Rontani and Belt (2020).

As seen in Chapter 5, $7\alpha/\beta$ -hydroperoxysterols resulting from hydrogen abstraction at carbon-7 (Fig. 35) can also be formed by allylic rearrangement of photochemically-produced 5α -hydroperoxysterols and then be easily homolytically cleaved. They are thus not sufficiently specific and stable to be used as tracers of Δ^5 -sterol autoxidation.

Addition of peroxy radicals to the double bond of Δ^5 -sterols affords isomeric $5\alpha,6\alpha$ - and $5\beta,6\beta$ -epoxysterols by fast intramolecular homolytic substitution (see chapter 8). These epoxides can be easily hydrolysed to the corresponding $3\beta,5\alpha,6\beta$ -trihydroxysterols by some enzymes (epoxide hydrolases; Aringer and Eneroth, 1974) and during alkaline hydrolysis classically employed during lipid analyses (Fig. 35). These triols were proposed as suitable tracers of sterol autoxidation in autotrophic organisms (Christodoulou et al., 2009; Rontani et al., 2009). The extent of sterol autoxidation can be estimated using Eq. 13 based on previously determined relative formation rate constants of epoxysterols and 7 -hydroperoxysterols (Morrissy and Kiely, 2006).

$$\text{Sterol autoxidation \%} = 3\beta,5\alpha,6\beta\text{-trihydroxysterol \%} \times 2.4 \quad (13)$$

Vitamin E

Autoxidation processes act intensively on vitamin E, but unfortunately afford the same products as type-II photosensitized oxidation (Liebler, 1994; Rontani et al., 2007b; Fig. 15). Among these compounds, only the lactone 4,8,12,16-tetramethylheptadecan-4-olide appeared sufficiently stable and specific to act as a marker of abiotic oxidation of vitamin E (Nassiry et al., 2009).

Pentacyclic triterpenes

Autoxidation of pentacyclic triterpenes of the lupane group (betulin, lupeol and betulinic acid) mainly involves peroxy radical addition to their 20-29 double bond (Galeron et al., 2016a; Fig. 36). Indeed, as seen in Chapter 8, terminal double bonds are conducive to these reactions (Schaich, 2005). In the case of betulin, they result in the formation of 20,29-epoxy-lupan-3 β ,28-diol (by fast intramolecular homolytic substitution) and a diperoxide that is strongly stabilized by intramolecular hydrogen bonding (Galeron et al., 2016a; Fig. 36).

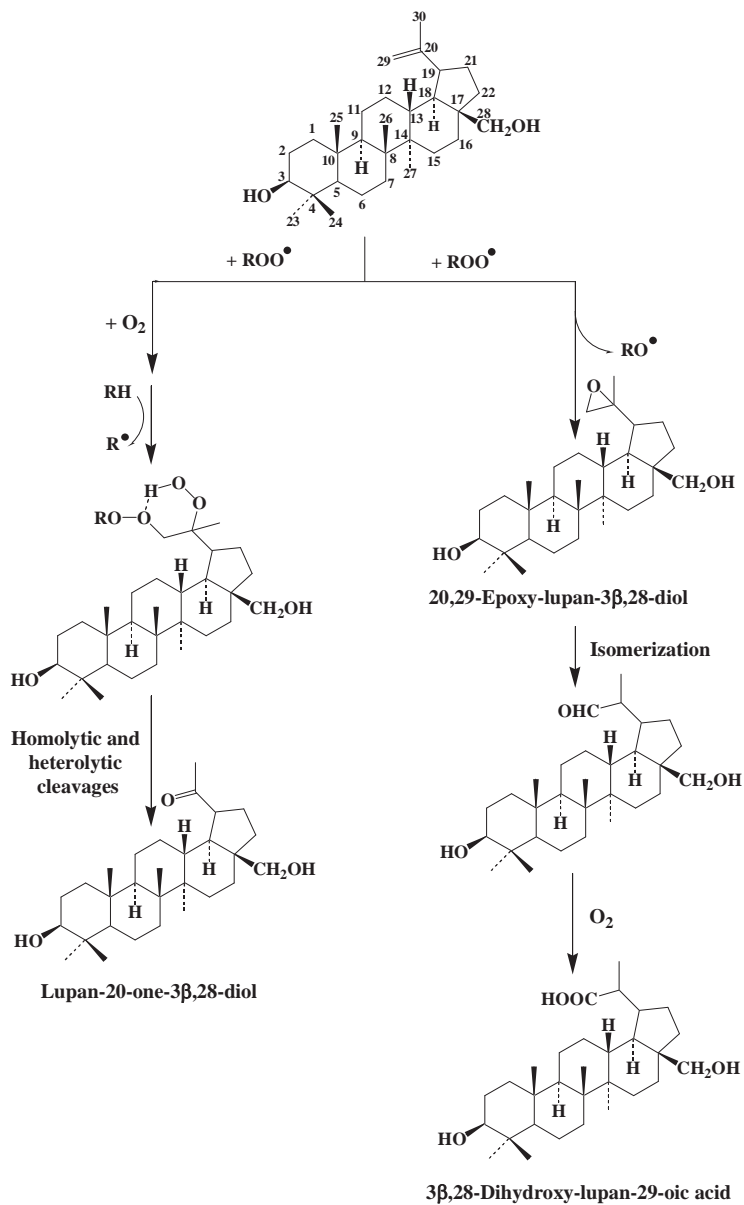


Figure 36. Autoxidation of betulin. Adapted from Galeron et al. (2016a).

Homolytic and heterolytic cleavages of this diperoxide result in the formation of the stable lupan-20-one-3 β ,28-diol (Fig. 36) while 20,29-epoxy-lupan-3 β ,28-diol rearranges to 3 β ,28-dihydroxy-lupanal (Tolstikov et al., 2005). In the presence of molecular oxygen, this aldehyde is then quickly oxidized to the corresponding acid (3 β ,28-dihydroxy-lupan-29-oic acid; Fig. 36). Lupan-20-one-3 β ,28-diol and 3 β ,28-dihydroxy-lupan-29-oic acid, which are detectable in riverine particles, have been proposed as tracers of betulin autoxidation (Galeron et al., 2016a).

In the case of pentacyclic triterpenes of the ursane and oleanane groups (e.g. α - and β -amyryns) possessing a trisubstituted Δ^{22} double bond instead of the terminal double bond of lupanes (Fig. 16), autoxidation processes mainly involve hydrogen abstraction and specifically produce 11 α -hydroperoxyamyryns (Galeron et al., 2016b; Fig. 37). This high regioselectivity (lack of hydrogen abstraction at the allylic carbon-18) was attributed to the presence of the methyl group 28 hindering the approach of peroxy radicals to the hydrogen atom carried by the allylic carbon-18 (Galeron et al., 2016b). Steric hindrance can also explain the high stereospecificity observed (methyl groups 25 and 26 hindering the approach of peroxy radicals to the β -side of the molecule; Fig. 37).

Homolytic cleavage of 11 α -hydroperoxyamyryns affords the corresponding ketones 3 β -hydroxy-urs-12-en-11-one and 3 β -hydroxy-olean-12-en-11-one (11-oxoamyryns) and to a lesser extent the corresponding alcohols (11 α -hydroxyamyryns; Galerón et al., 2016b; Fig. 37). Surprisingly, 11 α -hydroperoxyamyryns are unaffected by the NaBH₄-reduction often employed in the treatment of natural samples containing labile hydroperoxides. They are thus thermally cleaved to the corresponding 11-oxoamyryns during GC or GC-MS analyses using hot (splitless) injectors (Galerón et al., 2016b; Fig. 37).

11-oxoamyryns could be detected in dry *Smilax aspera* leaves (Galerón et al., 2016b). Moreover, incubation of this material in water containing Fe²⁺ ions (well-known initiators of autoxidative processes; see Chapter 8) was able to confirm the autoxidative production of these compounds from the respective amyryns under conditions closer to those of the natural environment (Galerón et al., 2016b). These compounds have consequently been proposed as specific tracers of amyryn autoxidation.

Oxidation products of pentacyclic triterpenes of the lupane, ursane and oleanane groups, such as lupan-20-one-3 β ,28-diol, 3 β ,28-dihydroxy-lupan-29-oic acid, 3 β -hydroxy-urs-12-en-11-one and 3 β -hydroxy-olean-12-en-11-one, all emerge as useful tracers of autoxidation in angiosperms.

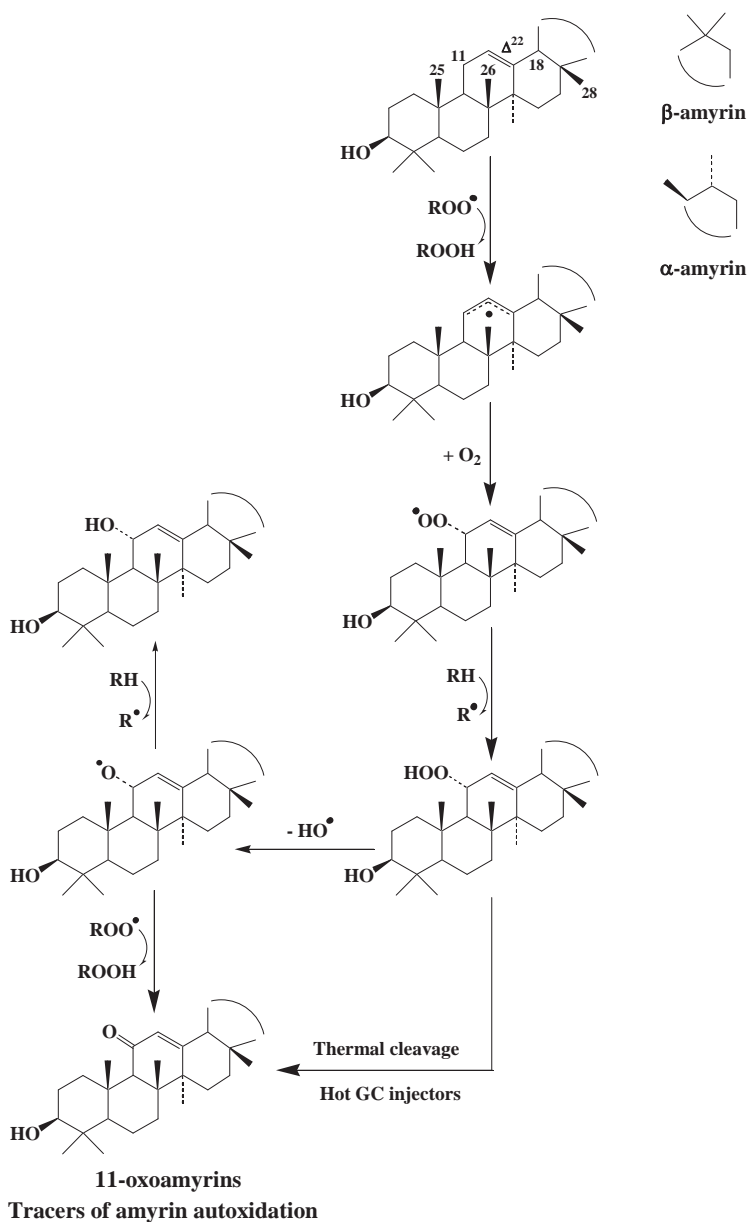


Figure 37. Autoxidation of amyryns. Adapted from Galeron et al. (2016b)

Dehydroabietic acid

Dehydroabietic acid (8,11,13-abietatrien-18-oic acid; DHAA), which is a component of fresh conifer resin, is often used as a tracer of gymnosperms (Brassell et al., 1983; Otto et al., 2005). The selectivity of this compound was recently challenged by Costa et al. (2015) who detected DHAA in several cyanobacteria. However, it seems that the environmental amounts of plant-origin DHAA are so much higher than environmental amounts of cyanobacterial-origin DHAA that this compound still makes a reliable tracer of gymnosperm autoxidation (Rontani et al., 2017).

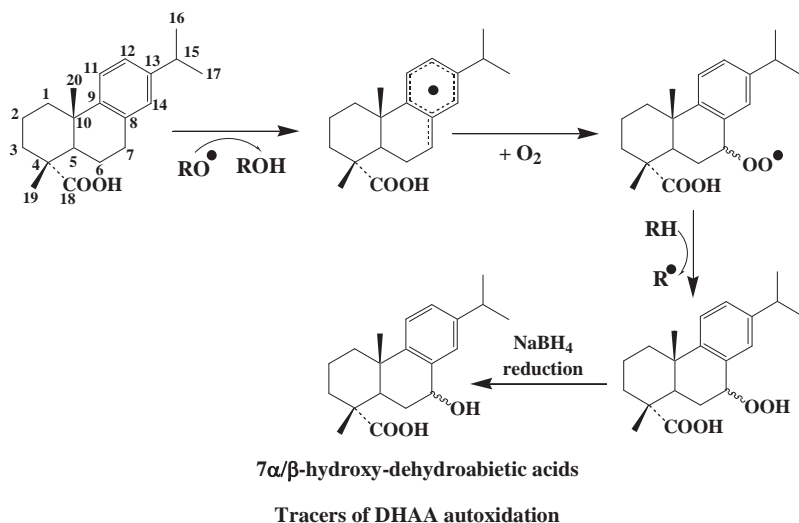


Figure 38. Autoxidation of dehydroabietic acid. Adapted from Rontani et al. (2015).

Autoxidation of DHAA mainly involves hydrogen atom abstraction at the benzylic (C-7) position (Fig. 38; Rontani et al., 2015) and results in the formation of $7\alpha/\beta$ -hydroperoxydehydroabietic acids. To be used as tracers of autoxidation of gymnosperms in the environment, these unstable hydroperoxides need to be reduced to the corresponding alcohols ($7\alpha/\beta$ -hydroxydehydroabietic acids; Fig. 38). Note that these hydroxy acids can also be produced during the metabolism of DHAA by some bacteria (e.g. Doménech-Carbó et al., 2006) (See Chapter 16), although the amounts of metabolites generally accumulated by bacteria are too small to rule out the

use of $7\alpha/\beta$ -hydroxydehydroabietic acids as tracers of gymnosperm autoxidation.

Alkenones

The autoxidative reactivity of alkenones has been studied *in vitro* (Rontani et al., 2006). These polyunsaturated ketones appeared to be more sensitive to oxidative free radical processes than esterified phytol, MUFAs and Δ^5 -sterols. It seems that the *trans* configuration of the double bonds of alkenones, which protects these compounds from type-II photosensitized oxidation (see Chapter 5), has no effect on autoxidation. Indeed, Waraho et al. (2011) observed no significant differences in lipid oxidation rates between *cis* and *trans* C_{18:1Δ9} acids. As in the case of PUFAs, oxidation rates of alkenones increase logically with number of double bonds, and this increasing reactivity with degree of unsaturation induces a significant increase of $U_{37}^{K'}$ index (up to 0.20; Rontani et al., 2006).

Free radical oxidation of each isolated 1,2-disubstituted double bond of alkenones (as in the case of MUFAs) mainly involves allylic hydrogen abstraction and results in the formation of six isomeric allylic hydroperoxides (four *trans* and two *cis*) (Rontani et al., 2006, 2013a; Fig. 39). Unfortunately, these hydroperoxyalkenones, which could be used as tracers of alkenone oxidation after NaBH₄ reduction to their corresponding diols (Fig. 39), are not accumulated. Indeed, due to the presence of other reactive double bonds, they undergo further oxidation reactions affording unstable polyhydroperoxyalkenones. Interestingly, diols resulting from the reduction of monohydroperoxyalkenones were detected in cultures of *E. huxleyi* strain CS-57 that exhibited anomalously high $U_{37}^{K'}$ values (Rontani et al., 2007a) and in surface sediments from SE Alaska (Rontani et al., 2013a). These tracers could therefore, in some cases, be used as qualitative indicators of autoxidative alteration of $U_{37}^{K'}$. In absence of these tracers, more stable lipid oxidation products (e.g. of Δ^5 -sterols) could be used to identify cases where there has been substantial autoxidation of organic matter, and thus by extension alkenones (Rontani et al., 2009) (see Chapter 14).

In some marine zones, autoxidation of alkenones can be significant enough to explain certain discrepancies between sea surface temperatures and alkenone-based temperature estimates observed in marine particulate matter (Freeman and Wakeham, 1992) and oxic sediment samples (Hoefs et al., 1998; Gong and Hollander, 1999; Prah et al., 2003).

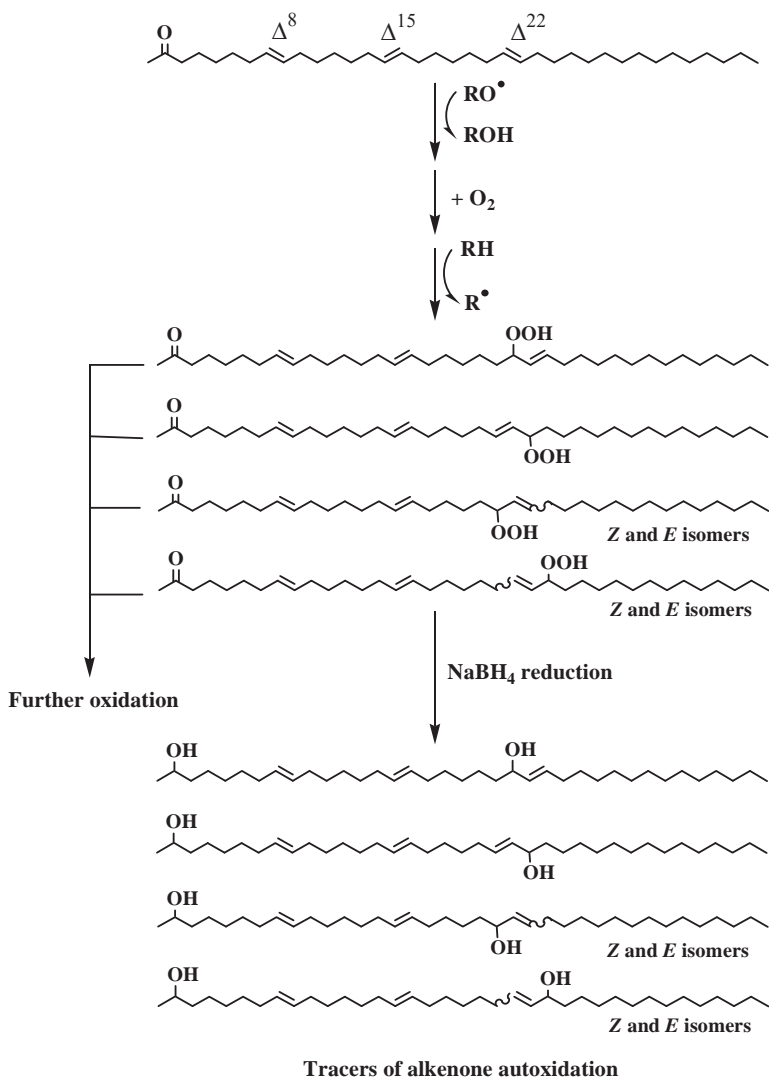


Figure 39. Autoxidation of $\text{C}_{37:3}$ alkenone (simplified scheme showing only the oxidation of the Δ^{22} double bond). Adapted from Rontani et al. (2013a).

Long-chain *n*-alkenes

Autoxidation of long-chain *n*-alkenes has never, to our knowledge, been studied. As in the case of alkenones (Fig. 39), free radical oxidation of isolated internal *cis* or *trans* double bonds of long-chain *n*-alkenes is expected to involve hydrogen atom abstraction and produce six allylic hydroperoxides. In contrast, in the case of terminal alkenes, peroxy radical addition should be strongly favoured (Schaich, 2005), resulting in the production of terminal epoxides after fast intramolecular homolytic substitution (Fig. 40).



Figure 40. Autoxidation of terminal long-chain alkenes.

Highly branched isoprenoid (HBI) alkenes

The sensitivity of HBI alkenes to autoxidation processes is strongly dependent on the number, degree of substitution and positions of their double bonds. Mono- and di-unsaturated HBI alkenes (such as IP₂₅ and IPSO₂₅) possessing only terminal or 1,1-disubstituted double bonds (Fig. 18) appeared to autoxidize very slowly (Rontani et al 2014b). While autoxidation rates of HBI alkenes logically increase with increasing number of double bonds, the more reactive HBI alkenes were found to be those possessing a bis-allylic position, which are degraded at similar rates as PUFAs (Rontani et al., 2014b). Indeed, it was previously demonstrated that hydrogen abstraction is 60 times higher at bis-allylic positions than in the case of mono-allylic counterparts (Ingold, 1969).

Autoxidation of HBI alkenes possessing a bis-allylic position (such as the widely-distributed HBI III; Fig. 18) thus mainly involves hydrogen atom abstraction at this position and affords two isomeric hydroperoxides with conjugated double bonds (Fig. 41). Unfortunately, these compounds, which are particularly prone to addition by peroxy radicals and readily undergo copolymerization with oxygen (Yin et al., 2011), are quickly converted to very polar and oligomeric secondary oxidation products. Moreover, they are not specific (also produced by type-II photosensitized oxidation of HBI III) (Rontani et al., 2014b).

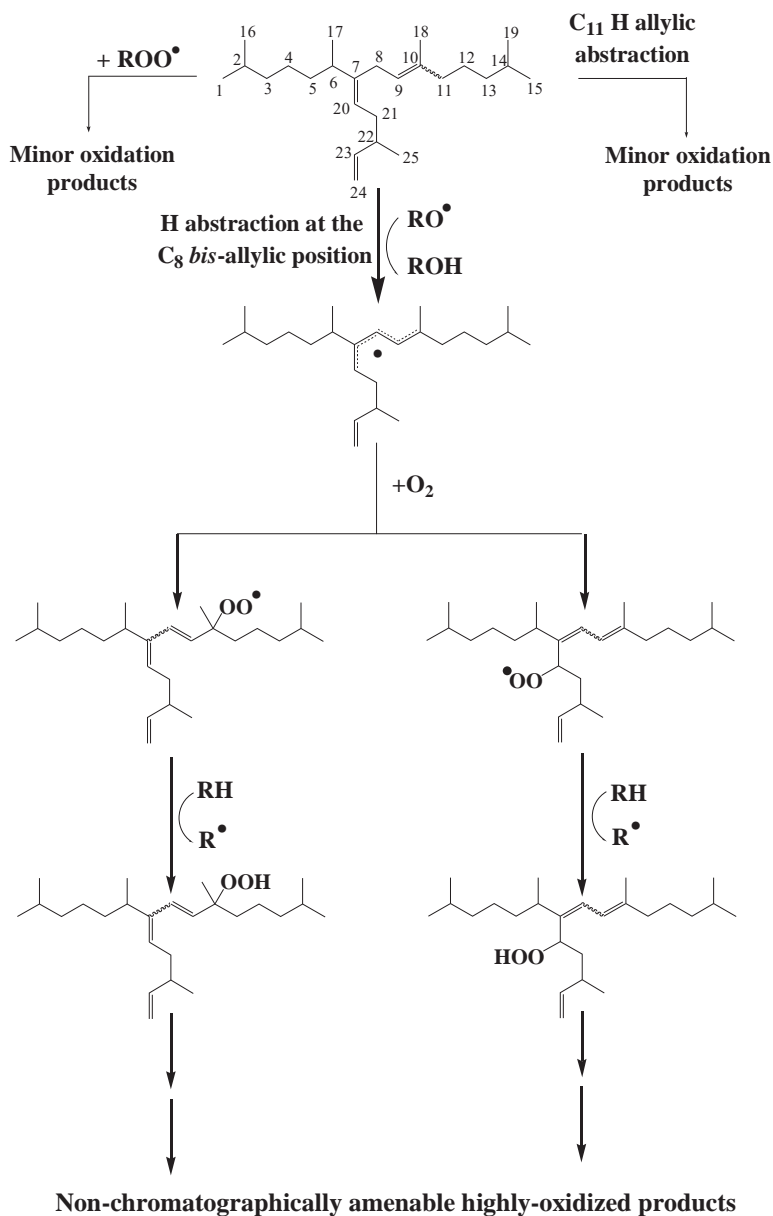


Figure 41. Autoxidation of HBI III. Adapted from Rontani et al. (2014b).

In contrast, the autoxidation of IP₂₅ is very slow and involves hydrogen atom abstraction at the tertiary allylic carbon-22 and the tertiary carbon-2, carbon-6, carbon-10 and carbon-14 and subsequent oxidation of the radicals thus formed, affording several hydroperoxides (Rontani et al., 2018a; Fig. 42).

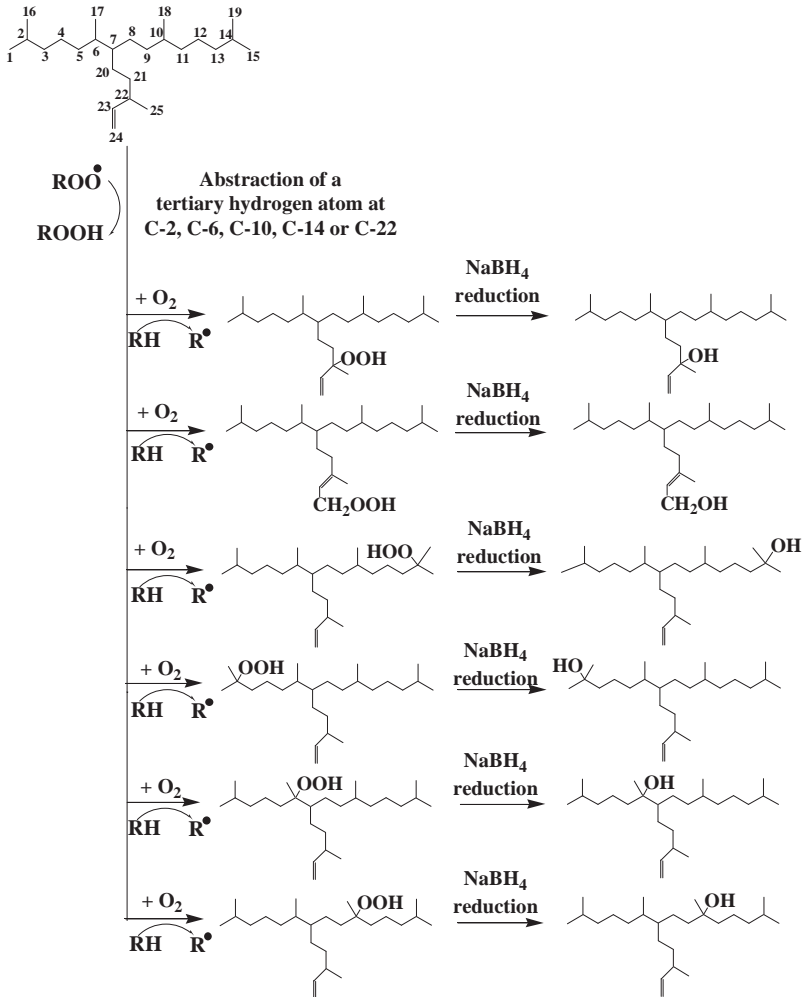


Figure 42. Autoxidation of IP₂₅. Adapted from Rontani et al. (2018a).

The corresponding alcohols (obtained after NaBH_4 reduction; Fig. 42) were recently detected in Arctic sediments (Rontani et al., 2018a), thus evidencing the autoxidative degradation of IPSO_{25} . It thus seems that autoxidation of very poorly-reactive compounds may be prevalent in the natural environment when organic material experiences long residence times under oxic conditions.

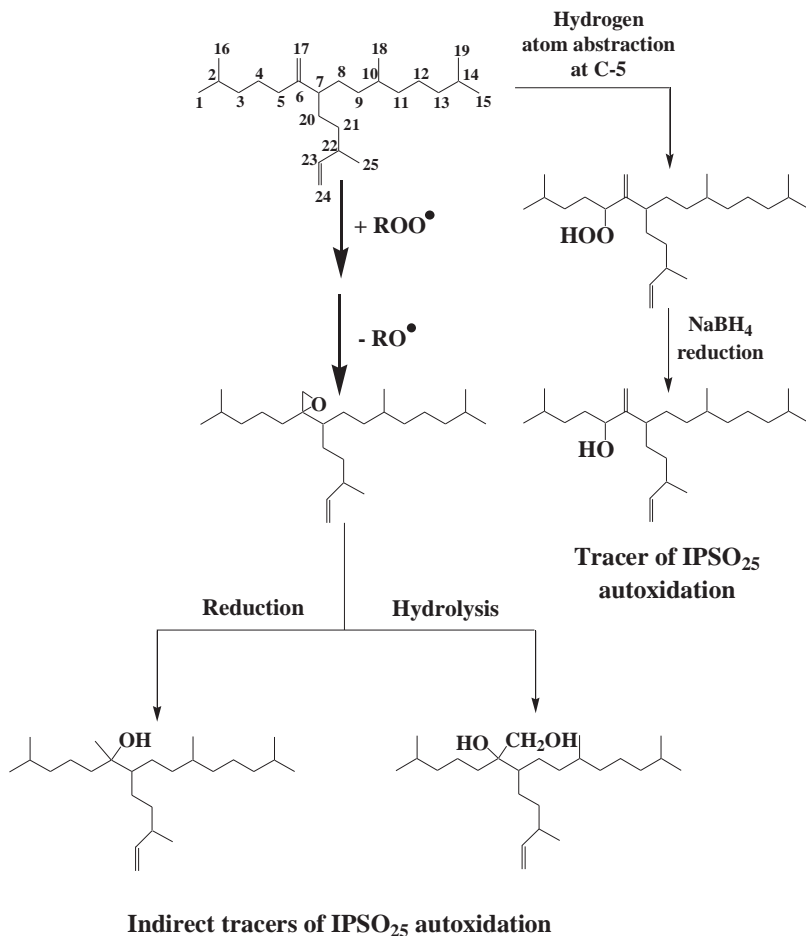


Figure 43. Autoxidation of IPSO_{25} and abiotic degradation of the foregoing epoxide. Adapted from Rontani et al. (2019b).

There appeared to be particularly efficient addition of peroxy radicals to the 1,1-disubstituted 6–17 double bond of IPSO₂₅, affording an epoxide after fast intramolecular homolytic substitution (Rontani et al., 2019b; Fig. 43). Unfortunately, this compound is not sufficiently stable in sediments to serve as a tracer of IPSO₂₅ autoxidation. Indeed, it is quickly hydrolysed to the corresponding diol or reduced to the corresponding tertiary alcohol (Fig. 43) (see Chapter 16). Note, however, that both these degradation products have been detected in Arctic sediments (Rontani et al., 2019b) and seem to be sufficiently stable and specific to serve as ‘indirect’ tracers of IPSO₂₅ autoxidation.

Less efficient hydrogen atom abstraction at C-5 and subsequent NaBH₄ reduction) affords 6-methylidene-2,10,14-trimethyl-7-(3-methylpent-4-enyl)-pentadecan-5-ol (Fig. 43), which is a well specific tracer of IPSO₂₅ autoxidation.

Summary of the results obtained

Compound	Relative autoxidation rates*
PUFAs	1.0
HBI alkenes with a bis-allylic position	0.61
Tetraunsaturated alkenones	0.32
Triunsaturated alkenones	0.20
Diunsaturated alkenones	0.11
HBI alkenes with four double bonds	0.10
Δ ⁵ -sterols	0.088
MUFAs	0.057
β-amyrin	0.055
HBI alkenes with three double bonds	0.046
DHAA	0.046
α-amyrin	0.038
Betulin	0.034
Chlorophyll phytyl side chain	0.032
IPSO ₂₅	0.006
IP ₂₅	0.002

*Estimated from Rontani et al., (2006, 2014b), Galeron et al., (2016a, 2016b).

Table 3. Relative rates of free radical oxidation of unsaturated lipids.

Table 3 recaps the relative free radical oxidation rates of the main unsaturated lipid components of phototrophic organisms investigated to date. Note that these values are only indicative of the relative reactivities

of the given compounds. Additional compartmentalisation effects can also play a role in heterogeneous microenvironments such as cells of phototrophs and the reactivity of lipids can thus also strongly depend on their localization in the cells. Moreover, it must keep in mind that even very weakly-reactive compounds (e.g. branched saturated hydrocarbons) could be affected by autoxidation processes when organic matter experiences long-enough residence times (decades to centuries) in the oxic layer of sediments (Rontani et al., 2018a).

CHAPTER ELEVEN

GAS CHROMATOGRAPHY-MASS SPECTROMETRY CHARACTERIZATION OF SELECTED TRACERS OF LIPID PHOTO- AND AUTOXIDATION

This chapter describes the main fragment ions employed for gas chromatography–mass spectrometry (GC-MS) characterization of silylated lipid oxidation products in natural samples. Trimethylsilylation is often used as derivatization procedure during GC-MS analyses (Pierce, 1982; Evershed, 1993). Trimethylsilyl (TMS) derivatives result from active proton displacement by a trimethylsilyl group. Numerous protic functional groups found in organic compounds (alcohols, acids, amines, thiols) can be converted to highly volatile yet thermally stable TMS derivatives that present outstanding gas chromatographic characteristics. Moreover, when used in GC-MS analyses, TMS groups increase the total ion current and, therefore, the sensitivity of detection (Halket and Zaikin, 2003). Electron ionization (EI) mass spectra of TMS derivatives generally exhibit a significant $[M-15]^+$ ion formed by loss of a methyl group bonded to silicon, which is especially useful for determining molecular mass. These mass spectra are also hugely informative for structural elucidations (Goad and Akihisa, 1997; Harvey and Vouros, 2020).

Accurate masses of the different fragment ions formed are given in this Chapter, which makes them amenable to use in very specific gas chromatography-electron ionization quadrupole time-of-flight mass spectrometry (GC-QTOF) analyses while the corresponding unit masses can still be used in classical or tandem GC-MS analyses.

Lipid oxidation products were previously formally identified (see the numerous references cited) by comparing their retention times and accurate mass and mass spectra against those of suitable standards (See Chapter 12).

Chlorophyll phytyl side chain

TOF mass spectra of the TMS derivatives of 3-methylidene-7,11,15-trimethylhexadecan-1,2-diol (phytyldiol, a tracer of chlorophyll phytyl side-chain photooxidation), 3,7,11,15-tetramethylhexadec-3-en(*Z/E*)-1,2-diols and 3,7,11,15-tetramethyl-hexadec-2-en(*Z/E*)-1,4-diols (tracers of chlorophyll phytyl side-chain autoxidation) are shown in Fig. 45. The mass spectra of phytyldiol and 3,7,11,15-tetramethylhexadec-3-en(*Z/E*)-1,2-diol TMS derivatives (Figs. 45A and 45B) exhibit interesting specific fragment ions at m/z 353.3235 that result from classical α -cleavage between the carbon atoms 1 and 2 bearing the two TMS ether groups (Rontani and Aubert, 2005; Fig. 44). In contrast, in the case of 3,7,11,15-tetramethyl-hexadec-2-en(*Z/E*)-1,4-diol TMS derivatives, α -cleavage acts between carbon atoms 4 and 5 affording a stable and specific fragment ion at m/z 245.1388 (Rontani and Aubert, 2005; Fig. 44).

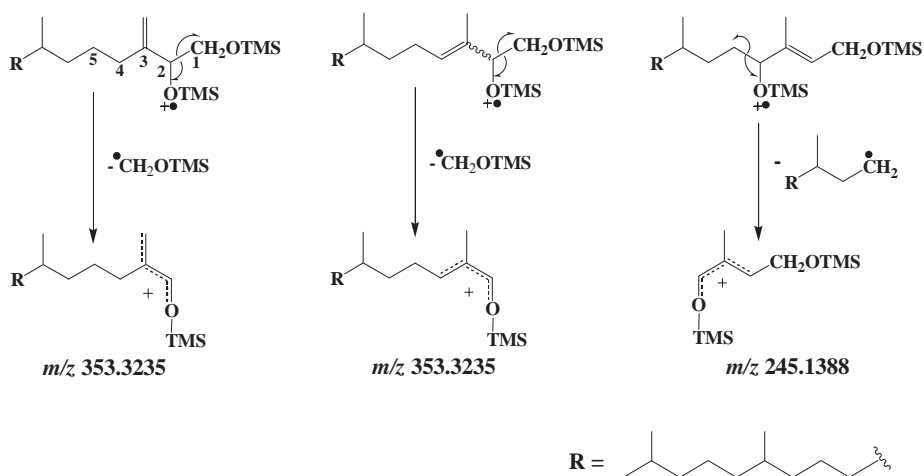


Figure 44. Main EI mass fragmentations of TMS derivatives of phytyldiol, 3,7,11,15-tetramethylhexadec-3-en(*Z/E*)-1,2-diols and 3,7,11,15-tetramethylhexadec-2-en(*Z/E*)-1,4-diols.

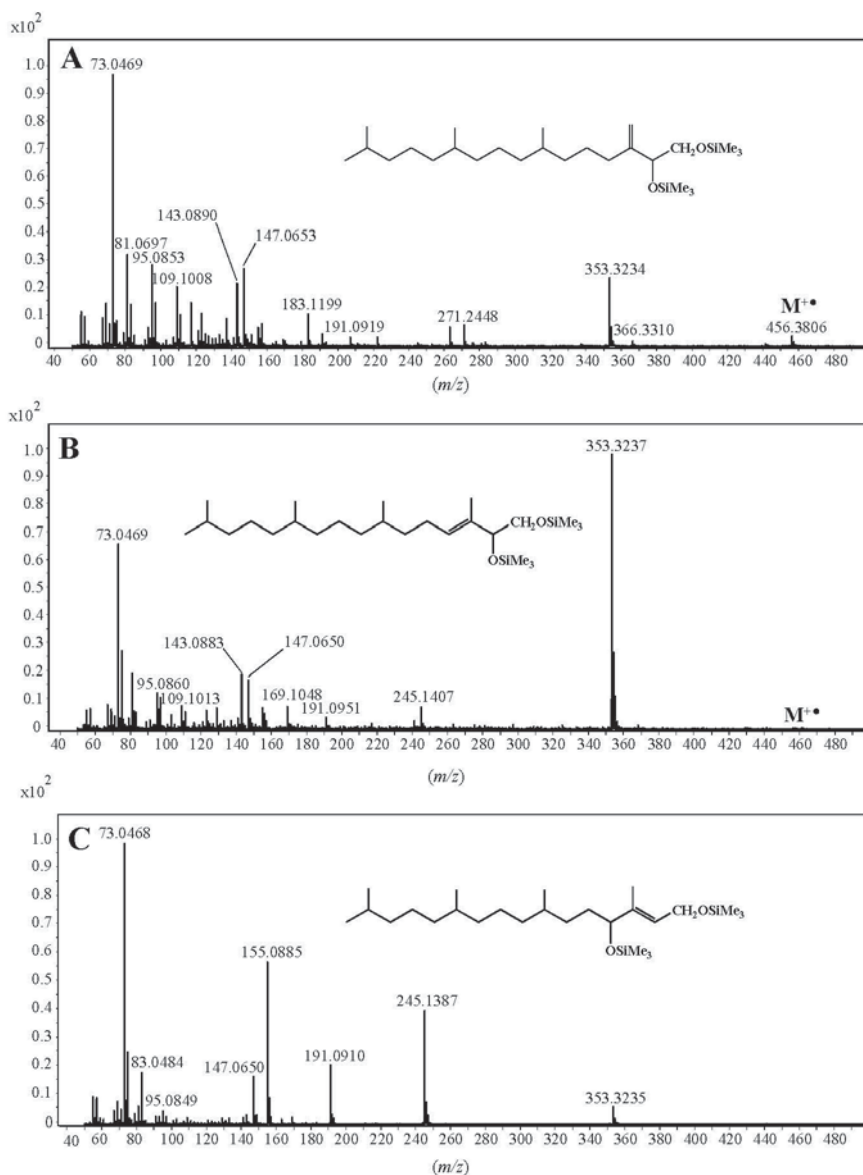


Figure 45. TOF mass spectra of TMS derivatives of phytyldiol (A), 3,7,11,15-tetramethylhexadec-3-en(*Z/E*)-1,2-diols (B) and 3,7,11,15-tetramethylhexadec-2-en(*Z/E*)-1,4-diols (C).

Interestingly, fragment ions at m/z 353.3235 (corresponding to the loss of a methyl radical by the molecular ion) are also found in low abundance in TOF mass spectra of TMS derivatives of phytol and isophytol. Tracking ions at m/z 353.3235 and 245.1388 thus allows easy characterization and quantification of phytol and its main oxidation products (isophytol, phytyldiol, 3,7,11,15-tetramethylhexadec-3-en(*Z/E*)-1,2-diols and 3,7,11,15-tetramethylhexadec-2-en(*Z/E*)-1,4-diols) in environmental samples. An example is given in Fig. 46.

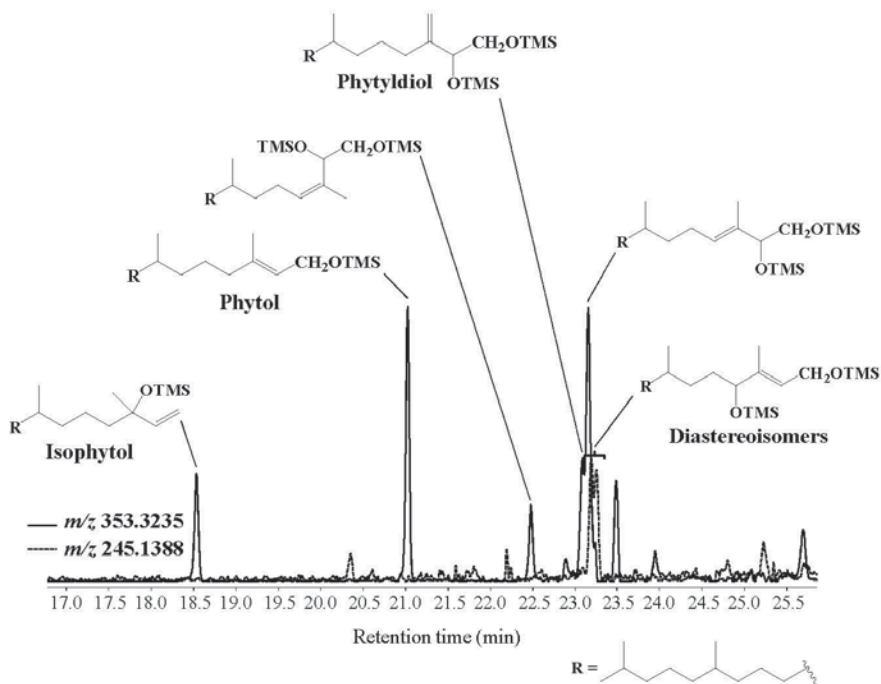


Figure 46. Partial ion chromatograms (m/z 353.3235 and 245.1388) showing the distribution of the chlorophyll phytyl side chain and its oxidation products in particulate matter collected in the Rhône River (France).

Monounsaturated fatty acids

EI fragmentation of TMS derivatives of isomeric allylic hydroxyacids resulting from photo- and autoxidation of MUFA and subsequent NaBH_4 reduction mainly involves α -cleavage at the TMS ether group. It acts on the saturated side of the molecule (as the vinylic position of the double

bond hinders cleavage on the other side) and affords stable and informative fragment ions. Fig. 47 describes EI fragmentation of TMS derivatives of oleic acid oxidation products as an illustrative example.

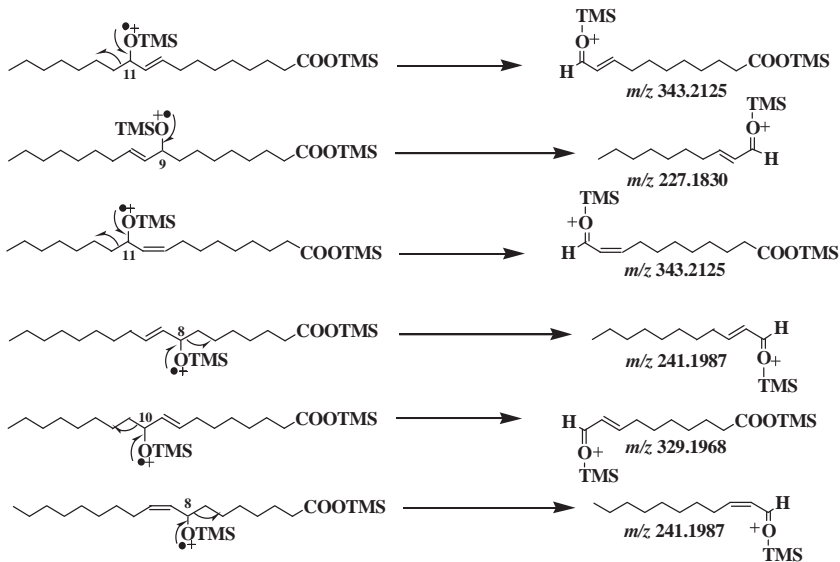


Figure 47. EI fragmentation of TMS derivatives of oleic acid oxidation products.

Different fragment ions are produced depending on the carbon atom number and double-bond position of the MUFAs. Table 4 recaps those resulting from α -cleavage of silylated oxidation products of the more common MUFAs.

Silylated oxidation products of some MUFAs often coelute with higher homologous fatty acid TMS derivatives found in high proportions in lipid extracts. Unfortunately, EI mass spectra of these silylated acids also exhibit some weak isobaric fragment ions that can complicate classical GC-MS characterization of MUFA oxidation products, which in practice makes it necessary to use GC-QTOF or triple quadrupole GC-MS (GC-MS/MS) for such analyses.

High-resolution accurate-mass GC-QTOF has been employed to successfully characterize TMS derivatives of MUFA oxidation products in natural samples (Amiriaux et al., 2016, 2017; Galeron et al., 2018; Rontani et al., 2018b, 2021a). This powerful technique allows clean characterization and quantification of these compounds in complex lipid extracts. An example of the technique in application is given in Fig. 48.

MUFAs	m/z	m/z	m/z	m/z
C ₁₆ :1Δ ₉	199.1518 ^a	213.1675 ^a	329.1968 ^b	343.2125 ^b
C ₁₆ :1Δ ₁₁	171.1206	185.1363	357.2280	371.2437
C ₁₆ :1Δ ₁₃	143.0748	157.1051	385.2592	399.2749
C ₁₈ :1Δ ₉	227.1830	241.1987	329.1968	343.2125
C ₁₈ :1Δ ₁₁	199.1518	213.1675	357.2280	371.2437
C ₁₈ :1Δ ₁₃	171.1206	185.1363	385.2592	399.2749
C ₂₀ :1Δ ₉	255.2139	269.2295	329.1968	343.2125
C ₂₀ :1Δ ₁₁	227.1830	241.1987	357.2280	371.2437
C ₂₀ :1Δ ₁₃	199.1518	213.1675	385.2592	399.2749
C ₂₂ :1Δ ₉	283.2451	297.2607	329.1968	343.2125
C ₂₂ :1Δ ₁₁	255.2139	269.2295	357.2280	371.2437
C ₂₂ :1Δ ₁₃	227.1830	241.1987	385.2592	399.2749

^a Fragments containing the terminal methyl group.

^b Fragments containing the trimethylsilyl ester group.

Table 4. Accurate masses of the main fragment ions produced during EI fragmentation of NaBH₄-reduced and silylated photo- and autoxidation products of the more common MUFAs.

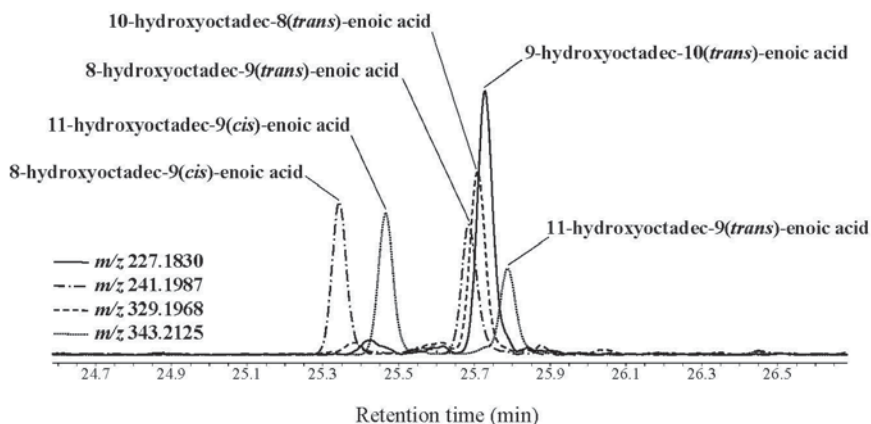


Figure 48. Partial ion chromatograms (m/z 227.1830, 241.1987, 329.1968 and 343.2125) showing the presence of oleic acid oxidation products in a particulate matter sample collected in the Chukchi Sea (Arctic).

Triple quadrupole mass spectrometers allow to carry out multiple-reaction monitoring (MRM) analyses, which are performed by isolating a precursor ion in the first quadrupole (Q1), fragmenting it within Q2, and monitoring the optimum fragment ions using Q3. The first step of MRM analyses consists in selecting intense and selective transitions from the precursor ions to the corresponding product ions. In the case of silylated MUFA oxidation products, the fragment ion at m/z 129 can be used as product ion for precursor ions containing the terminal methyl group, and ions resulting from two losses of trimethylsilanol (TMSOH) for the ions containing the TMS ester group (Fig. 49).

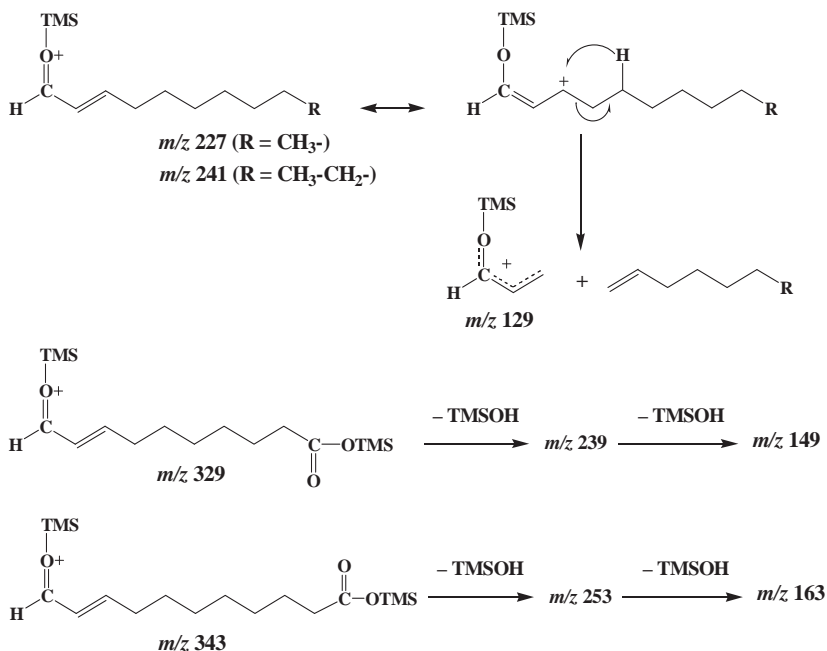


Figure 49. Formation of product ions employed in MRM analyses of silylated MUFA oxidation products: example of oleic acid.

MRM analyses using such transitions allow clean characterization and quantification of TMS derivatives of MUFA oxidation products in complex lipid extracts (Galeron et al., 2015). An example of the technique in application is given in Fig. 50.

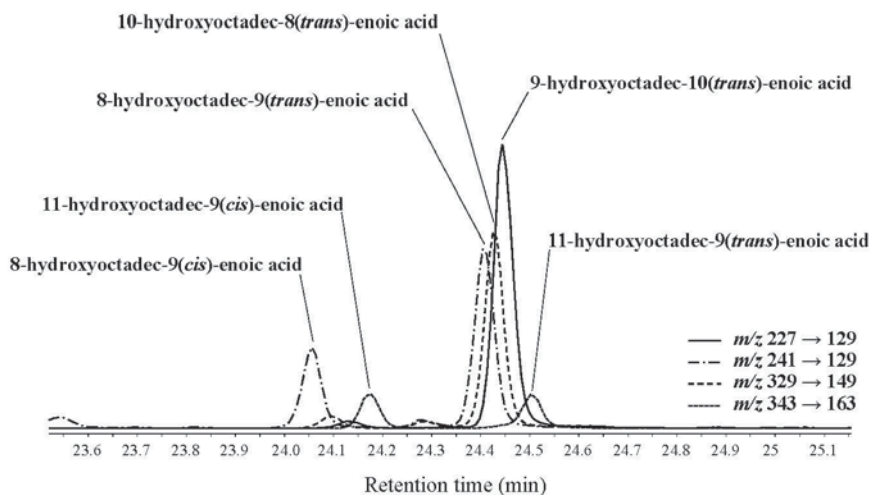


Figure 50. MRM chromatogram (m/z 199 \rightarrow 129, 213 \rightarrow 129, 329 \rightarrow 149 and 343 \rightarrow 163) showing the presence of oleic acid ($C_{18:\Delta 9}$) oxidation products in a particulate matter sample collected in the Rhône Estuary (Mediterranean Sea).

Δ^5 -sterols

EI fragmentation of TMS derivatives of Δ^4 -stera-3 β ,6 α / β -diols (proposed as tracers of type-II photosensitized oxidation of Δ^5 -sterols; see Chapter 5) was previously studied by Harvey and Vouros (1979). Elimination of TMSOH (m/z 90.0501) from $[M]^{+\bullet}$ led to abundant ions, which are often the base peaks of EI mass spectra of these compounds (Fig. 51). Harvey and Vouros (1979) posited a specific cleavage process involving double bond ionization and subsequent hydrogen migrations and cleavages of the C-1–C-10 and C-4–C-5 bonds (as shown in Fig. 52) to explain the formation of very interesting fragment ions at $[M - 143.0887]^+$. These specific ions proved to be very useful for monitoring Δ^4 -stera-3 β ,6 α / β -diol TMS derivatives and thus type-II photosensitized oxidation of the corresponding Δ^5 -sterol in natural samples. Accurate masses of the $[M - 143.0887]^+$ fragment ion of some common Δ^5 -sterols are given in Table 5.

Due to steric hindrance, the 3 β ,5 α ,6 β -trihydroxysterols proposed as tracers of Δ^5 -sterol autoxidation (see Chapter 10) are only silylated at their 3 and 6 positions by the reagents classically employed for trimethylsilylation (Rontani et al., 2014a). During EI fragmentation, these derivatives thus

readily leave a molecule of water and yield mass spectra that look very similar to those of the corresponding Δ^4 -stera-3 β ,6 β -diol TMS derivatives (Fig. 51A). Note that the relatively poor chromatographic properties of these only-partially-silylated derivatives can make them hard to detect, particularly at low concentrations. Research is in progress to develop a new method (using perfluoroanhydrides) capable of fully derivatizing these triols (Claude Aubert, Unpublished data, 2021).

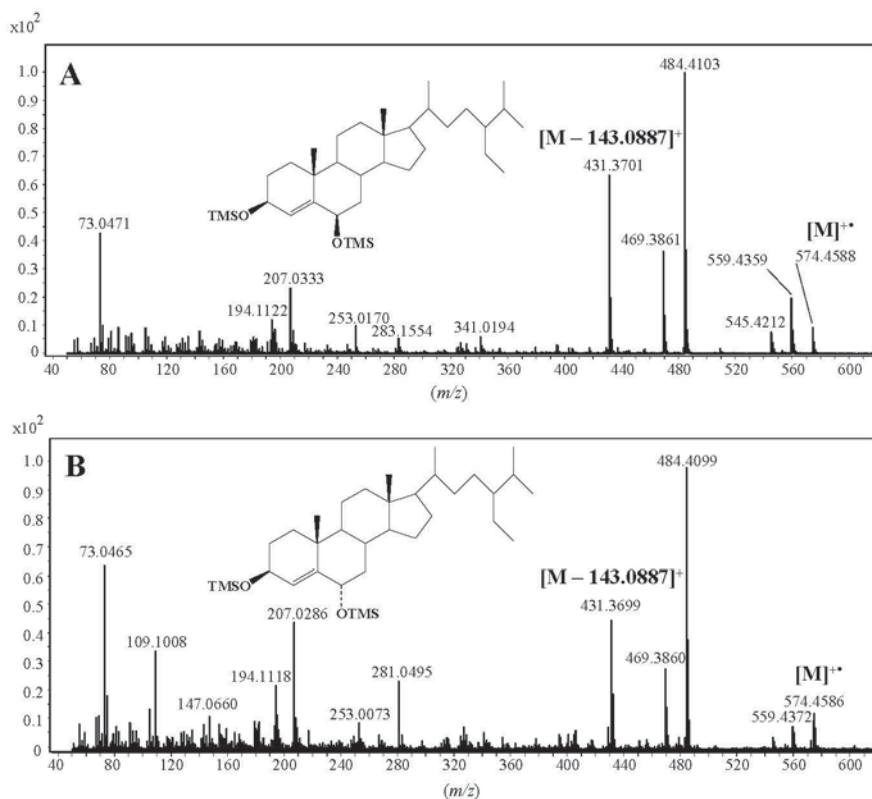


Figure 51. TOF mass spectra of TMS derivatives of 24-ethylcholest-4-en-3 β ,6 β -diol (A) and 24-ethylcholest-4-en-3 β ,6 α -diol.

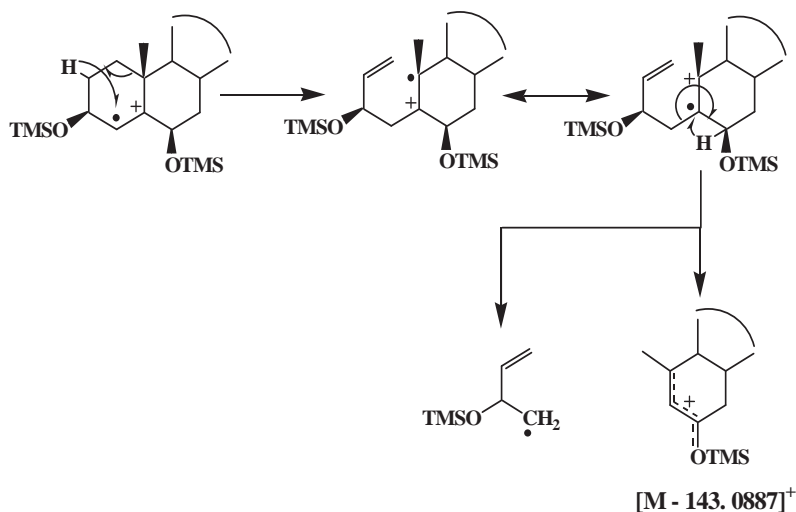


Figure 52. Pathways of fragment ion formation $[M - 143.0887]^+$ during EI fragmentation of Δ^4 -stera-3 β ,6 β -diols TMS derivatives. Adapted from Harvey and Vouros (1979).

Δ^5 -sterols	$[M - 143.0887]^+$
Cholesta-5,22-dien-3 β ,6 α / β -diols	401.3240
Cholesta-5,24-dien-3 β ,6 α / β -diols	401.3240
Cholest-5-en-3 β ,6 α / β -diols	403.3396
24-Methylcholest-5-en-3 β ,6 α / β -diols	417.3562
24-Methylcholesta-5,22-dien-3 β ,6 α / β -diols	415.3396
24-Methylcholesta-5,24/28-dien-3 β ,6 α / β -diols	415.3396
24-Ethylcholest-5-en-3 β ,6 α / β -diols	431.3710
24-Ethylcholesta-5,22-dien-3 β ,6 α / β -diols	429.3552

Table 5. Accurate masses of the $[M - 143.0887]^+$ fragment ion of some common Δ^5 -sterols.

The conversion of disilylated 3 β ,5 α ,6 β -trihydroxysterols to the corresponding 3 β ,6 β -diol TMS derivatives during EI ionization means that the fragment ion $[M - 143.0887]^+$ can be monitored to characterize and quantify both

photo- and autoxidation of Δ^5 -sterols in natural samples. An example is given in Fig. 53.

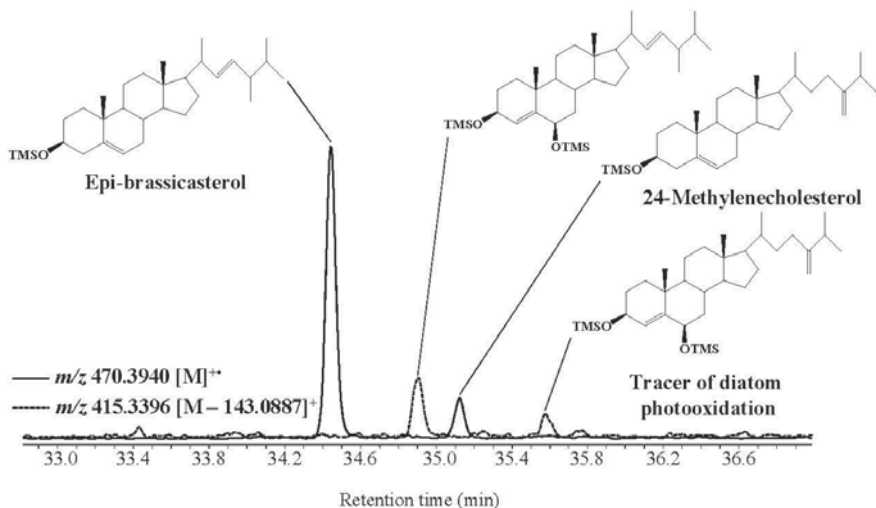


Figure 53. Partial ion chromatograms (m/z 431.3710) showing the presence of oxidation products of 24-ethylcholest-5-en-3 β -ol (sitosterol) in lipid extracts of dry *Smilax aspera* leaves.

Pentacyclic triterpenes

The TOF mass spectrum of lup-20(30)-ene-3 β ,28,29-triol TMS derivative proposed as a tracer of betulin photooxidation (see Chapter 5) exhibits a small molecular peak at m/z 674.4941 and several fragment ions at m/z 584.4440, 571.4360, 494.3824, 481.3860 and 391.3355 arising from successive losses of neutral TMSOH and CH_2OTMS radical (Fig. 54A). The relative intensity of the fragment ion at m/z 481.3860 makes it a good candidate for monitoring type-II photosensitized oxidation of betulin in environmental samples.

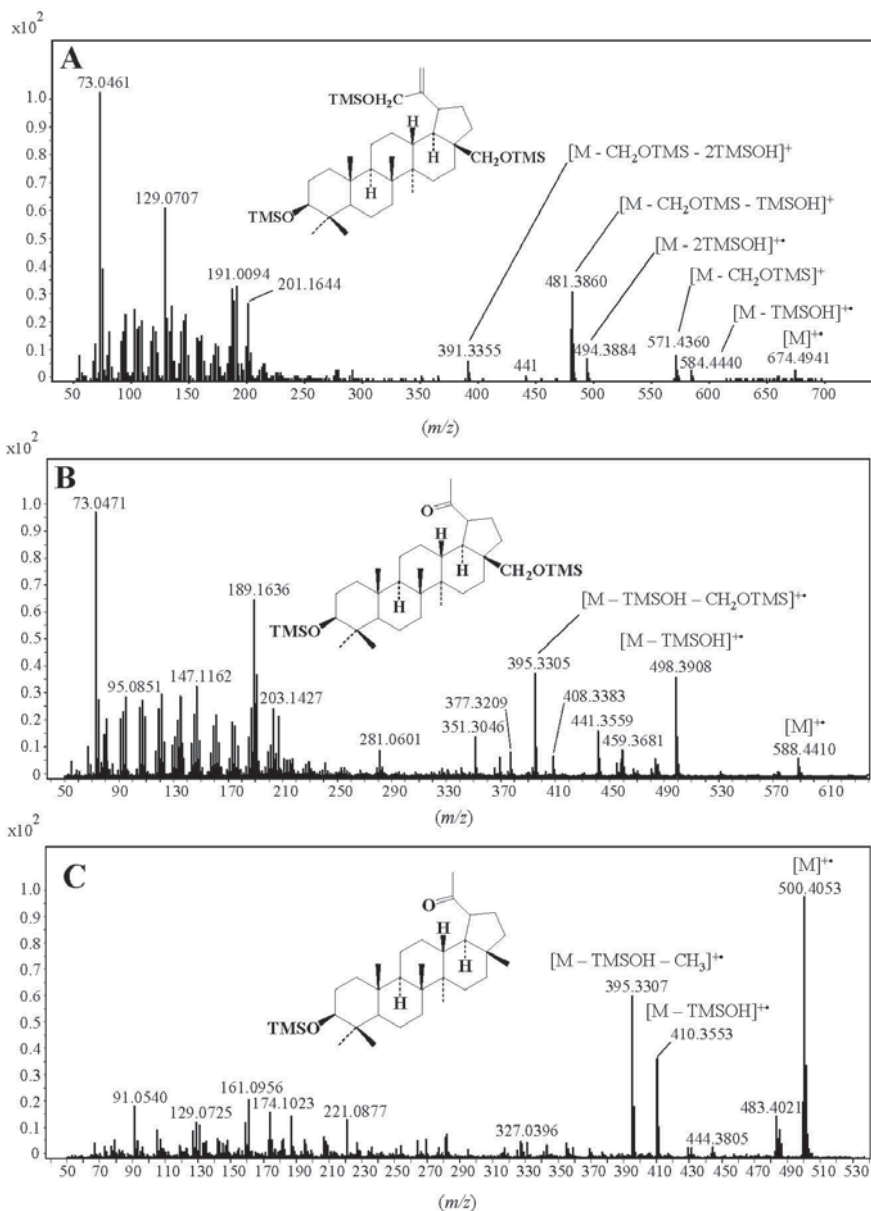


Figure 54. TOF mass spectra of lup-20(30)-ene-3 β ,28,29-triol (A), lupan-20-one-3 β ,28-diol (B) and lupan-20-one-3 β -ol (C) TMS derivatives.

Fig. 54 also gives the TOF mass spectra of lupan-20-one-3 β ,28-diol and lupan-20-one-3 β -ol resulting from the autoxidation of betulin and lupeol respectively (two of the main triterpenoids of the lupane group). The mass spectrum of lupan-20-one-3 β ,28-diol exhibits intense fragment ions at m/z 498.3908 and 395.3305 corresponding to $[M - \text{TMSOH}]^+$ and $[M - \text{TMSOH} - \text{CH}_2\text{OTMS}]^+$, respectively (Fig. 54B). The lack of a TMS ether group at carbon-28 means that the TMS derivative of lupan-20-one-3 β -ol only gets weakly fragmented during EI ionization. Its mass spectrum is thus dominated by the molecular peak at m/z 500.4053 and exhibits intense fragment ions at m/z 410.3553 and 395.3305 resulting from the successive losses of TMSOH and methyl radical (Fig. 54C).

Consequently, fragment ions at m/z 395.3305, 498.3908 and 500.4053 could be used for monitoring lupeol and betulin autoxidation in environmental samples. An example of application is given in Fig. 55.

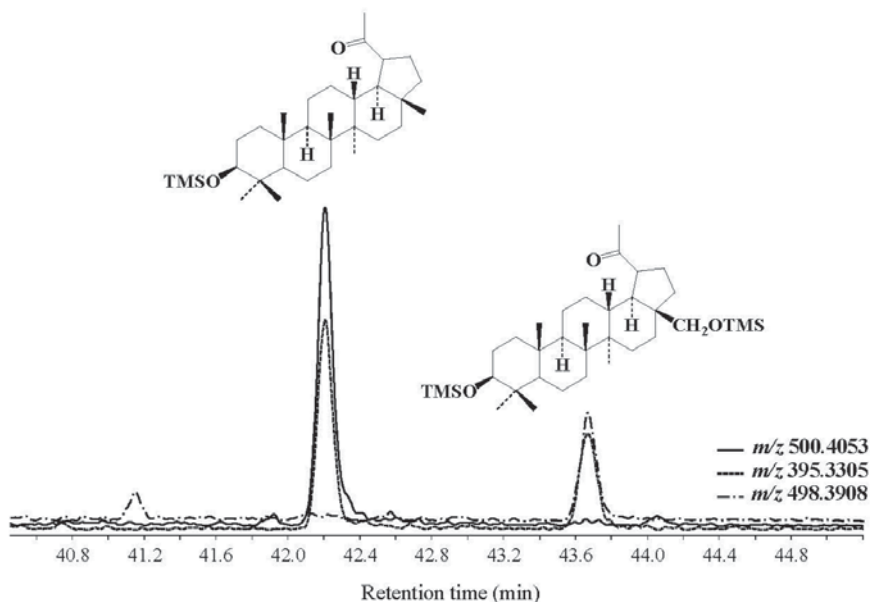


Figure 55. Partial ion chromatograms (m/z 395.3305, 498.3908 and 500.4053) showing the presence of oxidation products of lupeol and betulin in particulate matter collected in the Rhône Estuary (Mediterranean Sea).

TOF mass spectra of TMS derivatives of 3 β -hydroxy-urs-12-en-11-one and 3 β -hydroxyolean-12-en-11-one (resulting from α - and β -amyrin autoxidation, respectively; see Chapter 10) are given in Fig. 56.

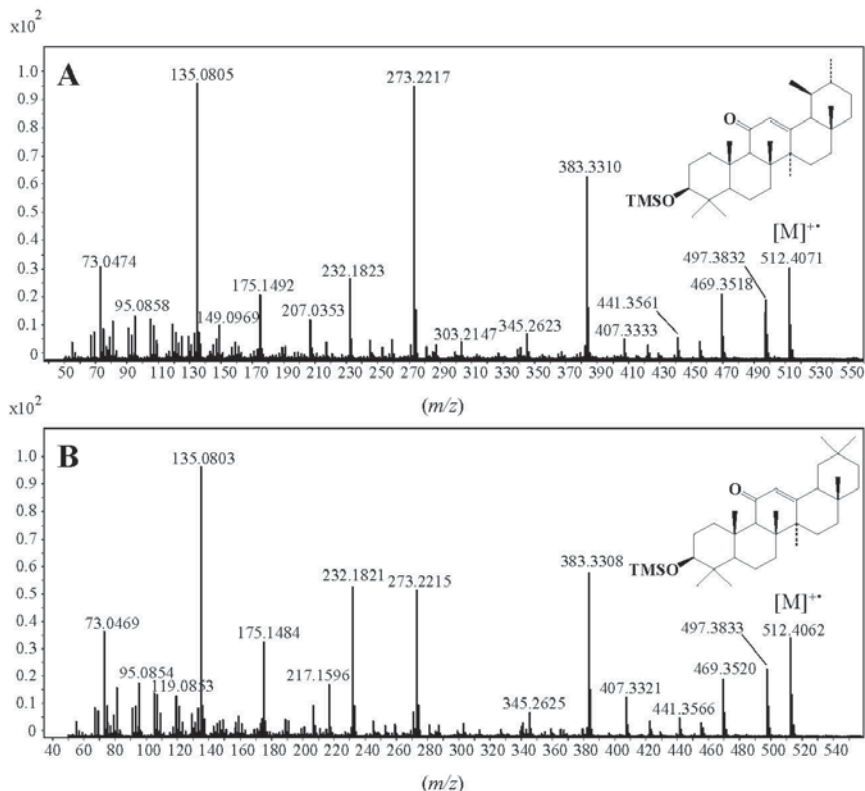
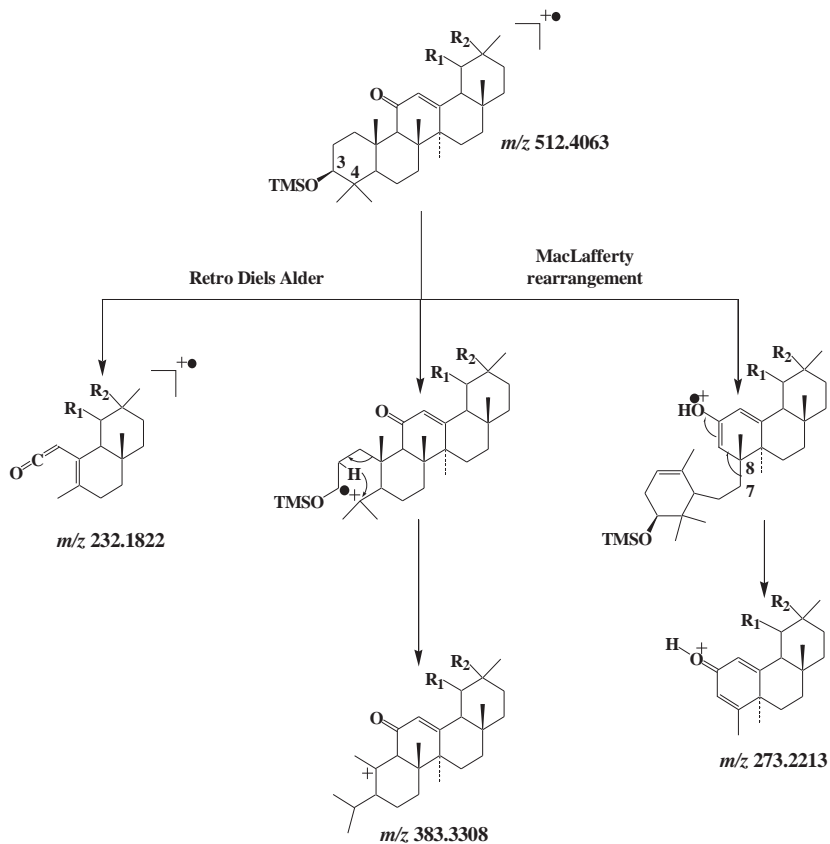


Figure 56. TOF mass spectra of 3 β -hydroxy-urs-12-en-11-one (A) and 3 β -hydroxyolean-12-en-11-one (B) TMS derivatives.

The EI fragmentation of these compounds was recently studied (Rontani et al., 2018c). The retro-Diels-Alder cleavage of the unsaturated ring C, which is a characteristic and diagnostically valuable feature in the mass spectra of most 12-oleanene and 12-ursene derivatives (Wahlberg and Enzell, 1971), leads to the formation of the fragment at m/z 232.1822 (Fig. 57), while γ -hydrogen rearrangement of the ionized 11-keto group (McLafferty rearrangement with charge retention) and subsequent cleavage of the 7–8 bond affords a well-stabilized fragment ion at m/z 273.2213 (Fig. 57). A fragmentation pathway involving loss of the TMS

group together with carbon-1, -2 and -3 of the A ring after initial cleavage of the 3–4 bond, similar to what is often observed with steroid structures possessing 4,4-dimethyl groups (Goad and Akihisa, 1997), was proposed to explain the formation of the fragment ion at m/z 383.3308 (Fig. 57).



3 β -hydroxy-urs-12-en-11-one: $R_1 = \text{CH}_3$ $R_2 = \text{H}$

3 β -hydroxy-olean-12-en-11-one: $R_1 = \text{H}$ $R_2 = \text{CH}_3$

Figure 57. EI fragmentation pathways of 3 β -hydroxy-urs-12-en-11-one and 3 β -hydroxyolean-12-en-11-one TMS derivatives.

The intense and specific fragment ions at m/z 512.4063 [M]⁺, 383.3308, 273.2213 and 232.1822 are useful for monitoring autoxidation products of α - and β -amyrins in environmental samples. An example of the technique in application is given in Fig. 58.

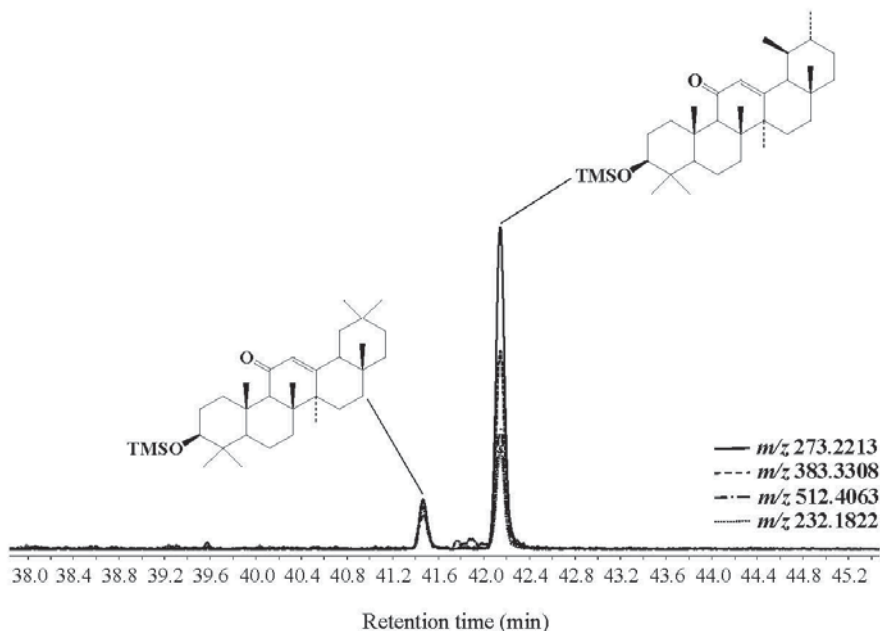


Figure 58. Ion chromatograms (m/z 232.1822, 273.2213, 383.3308 and 512.4063) showing the presence of autoxidation products of α - and β -amyrins in sediments collected in the Beaufort Sea (Canadian Arctic).

MRM analyses also showed promise for identifying and quantifying relatively low amounts of amyrin oxidation products in natural samples (Rontani et al., 2018c). The more selective and intense transitions m/z 273 \rightarrow 135 and m/z 232 \rightarrow 217 were selected for this purpose. The first transition results from the migration of methyl group 27 from carbon-14 to carbon-13 as previously proposed by Budzikiewicz et al. (1963) and concerted cleavage of the 13–18 and 15–16 bonds to afford a very well-stabilized ion at m/z 135 (Fig. 59). The second transition simply results from the loss of a methyl radical by the ion at m/z 232 resulting from retro-Diels-Alder cleavage of the molecular ion (Fig. 57).

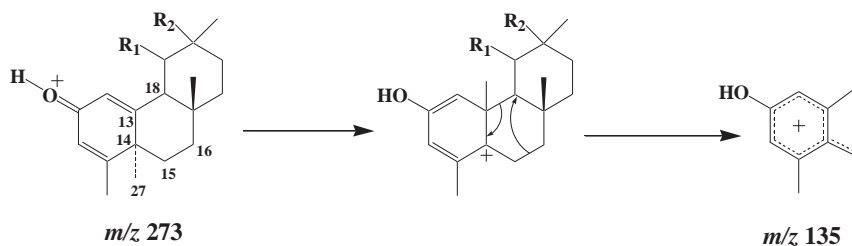


Figure 59. Proposed pathways for formation of the fragment ion at m/z 135. Adapted from Rontani et al. (2018c).

Dehydroabietic acid

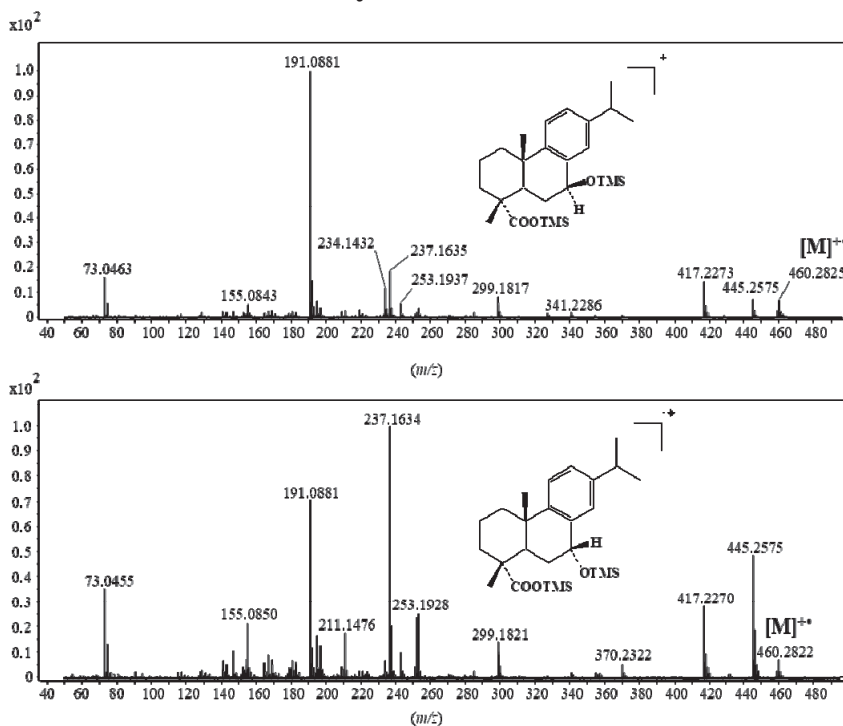


Figure 60. TOF mass spectra of 7β - (A) and 7α -hydroxydehydroabietic acid (B) TMS derivatives.

7α - and 7β -hydroxydehydroabietic acids were proposed as tracers of autoxidation in gymnosperms (see Chapter 10). Both TOF mass spectra of their TMS derivatives (given in Fig. 60) exhibit a significant molecular peak at m/z 460.2825 and fragment ions corresponding to the loss of methyl (m/z 445.2575) and isopropyl (m/z 417.2276) radicals. Other ions at m/z 191.0887, 234.1435 and 237.1638 are also observed, but their relative abundances differ strongly between the two isomers (Fig. 60).

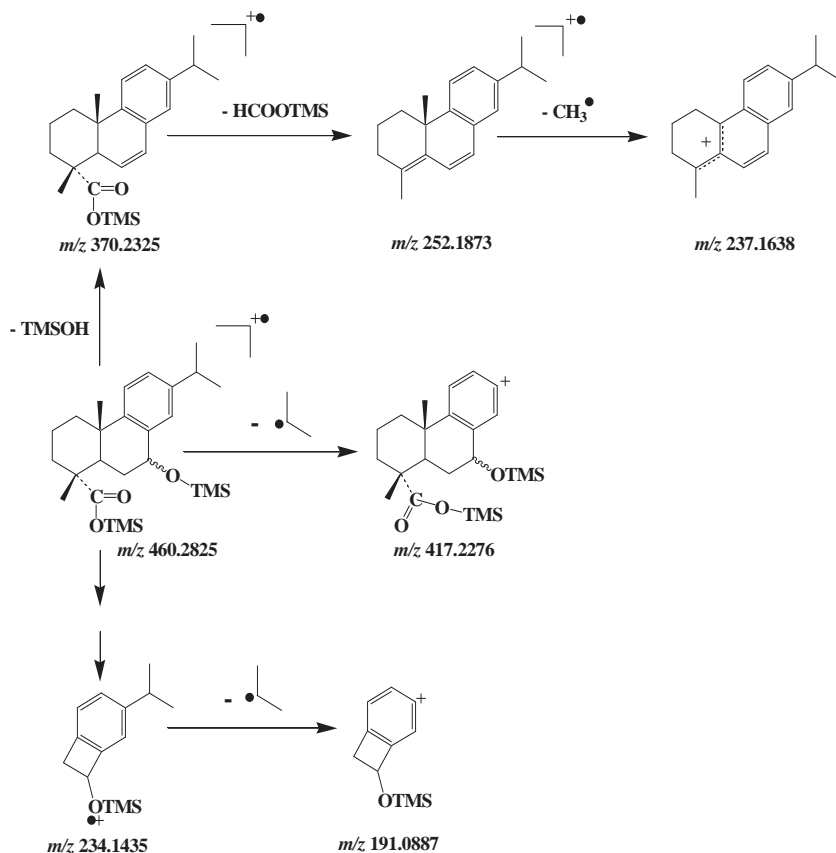


Figure 61. EI fragmentation pathways of $7\alpha/\beta$ -hydroxydehydroabietic acid TMS derivatives. Adapted from Rontani et al. (2015).

While formation of the ion at m/z 237.1638 results from classical successive losses of neutral TMS formate and methyl radical (Fig. 61), the formation of fragment ion at m/z 234.1435 involves relatively complex fragmentation pathways that were recently elucidated using deuterium labelling (Rontani et al., 2015) but cannot be detailed here. During these pathways, the 6-7 and 9-10 bonds are cleaved and a stable bicyclic ion is formed (Fig. 61) that can easily lose an isopropyl radical to give the stable fragment ion at m/z 191.0887.

Fragment ions at m/z 191.0887, 234.1435 and 237.1638 are sufficiently specific and intense for monitoring 7α - and 7β -hydroxydehydroabietic acids in natural samples. An example of the technique application is given in Fig. 62.

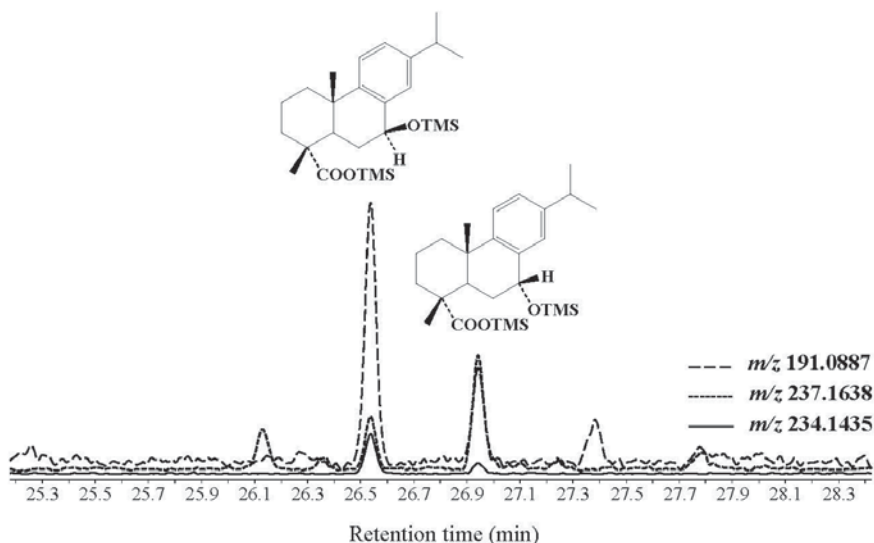


Figure 62. Ion chromatograms (m/z 191.0887, 234.1435 and 237.1638) showing the presence of autoxidation products of dehydroabietic acid in particulate matter collected in the Rhône Estuary (Mediterranean Sea).

Note that the transitions m/z 234 \rightarrow 191, m/z 252 \rightarrow 237 and m/z 460 \rightarrow 417 were successfully used for MRM-based identification and quantification of relatively low amounts of dehydroabietic acid autoxidation products in Arctic sea ice and sediment samples (Rontani et al., 2015).

Alkenones

As in the case of MUFA oxidation products (see above), EI fragmentation of TMS derivatives of isomeric diols resulting from alkenone autoxidation and subsequent NaBH₄ reduction mainly involves α -cleavage at the TMS ether group and acts on the saturated side of the molecule (Fig. 63).

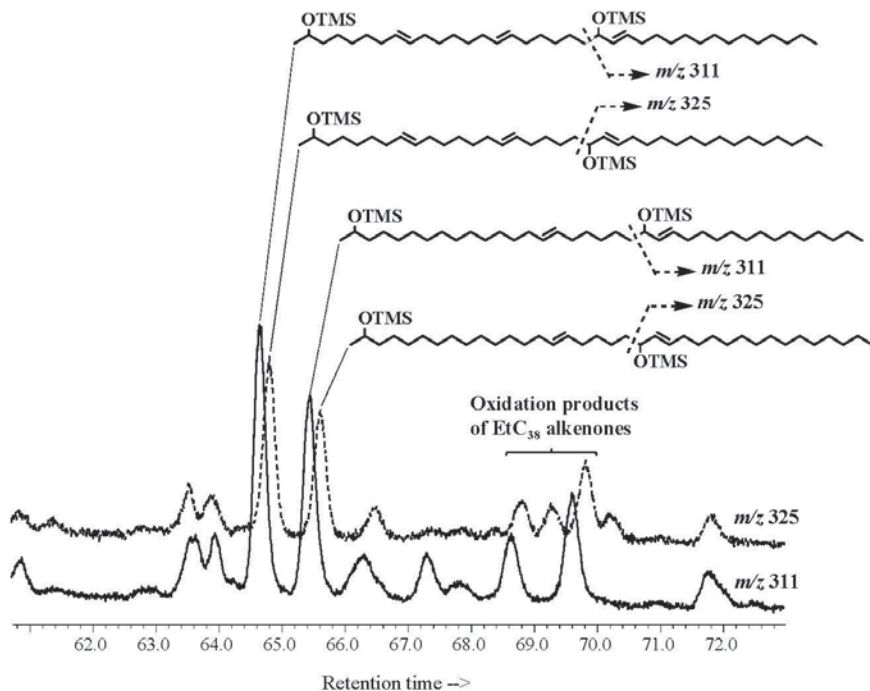


Figure 63. Partial m/z 311 and 325 chromatograms revealing the presence of silylated C₃₇ and C₃₈ alkenediols after NaBH₄ reduction and silylation of the total lipid fraction of *E. huxleyi* strain CS-57 that exhibited abnormally high $U_{37}^{K'}$ values. Adapted from Rontani et al. (2007a).

Oxidation products of the Δ^{22} double bond of alkenones afford (after NaBH₄ reduction and silylation) fragment ions containing the terminal methyl group of the molecule at m/z 311.2765 and 325.2922, which are sufficiently stable and specific to directly evidence alkenone autoxidation *in situ* (Rontani et al., 2013a). Unfortunately, as seen in Chapter 10, these

compounds are not accumulated and can therefore only give qualitative pointers on the autoxidative alteration of alkenones.

Highly branched isoprenoid (HBI) alkenes

The TOF mass spectra of IP₂₅ autoxidation-product TMS derivatives were recently reported (Rontani et al., 2018a). Fragment ions at *m/z* 131.0885, 143.0883 and 201.1670 (Fig. 64) appeared to be good candidates for monitoring these oxidation products in sediment samples (Rontani et al., 2018a).

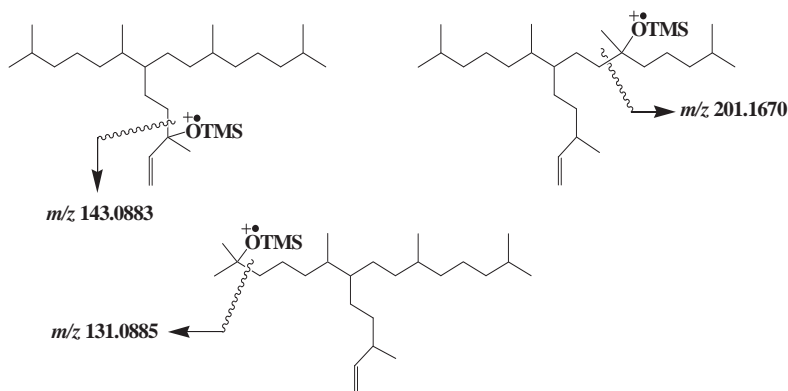


Figure 64. EI fragmentations of TMS derivatives of the main IP₂₅ autoxidation products.

TOF mass spectra of TMS derivatives of IP_{SO₂₅} oxidation products are also available in the literature (Rontani et al., 2019b). The TOF mass spectrum of the TMS derivative of 6-methylidene-2,10,14-trimethyl-7-(3-methylpent-4-enyl)-pentadecan-5-ol (a tracer of IP_{SO₂₅} autoxidation; Fig. 43) exhibits interesting specific fragment ions at *m/z* 365.3235 and 275.2742 (Fig. 65). The TOF mass spectrum of the TMS derivative of 2-(4-methylpentyl)-3-(3-methylpent-4-enyl)-6,10-dimethylundecane-1,2-diol (an indirect tracer of IP_{SO₂₅} autoxidation; Fig. 43) shows a notable molecular peak at *m/z* 526.4581 and an intense peak at *m/z* 333.3521 corresponding to [M – CH₂OTMS – TMSOH]⁺ (Fig. 65).

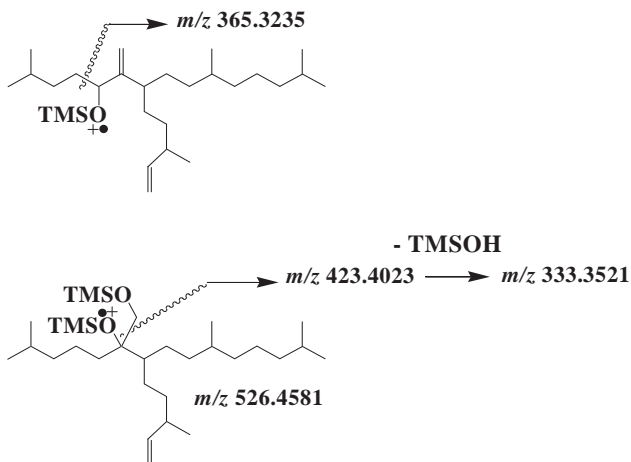


Figure 65. EI fragmentations of TMS derivatives of the main tracers of IPSO₂₅ autoxidation.

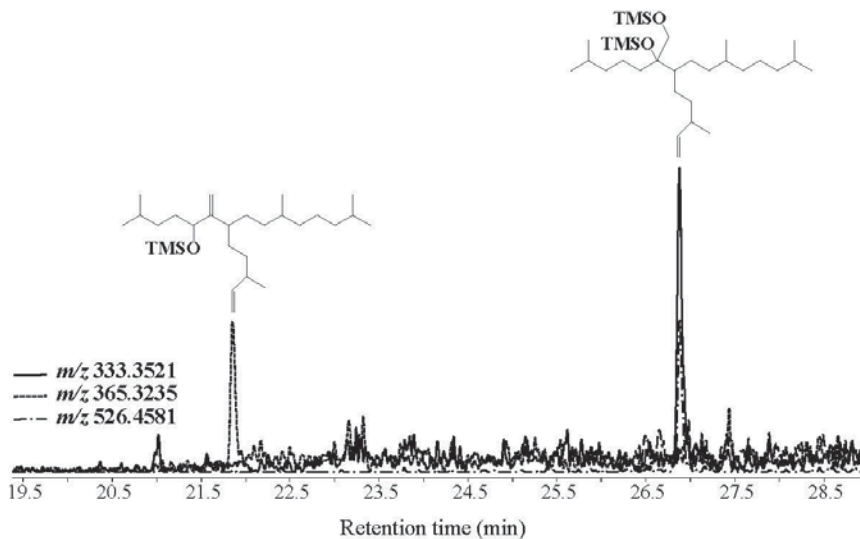


Figure 66. Ion chromatograms (m/z 333.3521, 365.3237 and 526.4581) showing the presence of IPSO₂₅ oxidation products in sediments from the Arctic.

These different fragment ions emerge as sufficiently stable and specific for monitoring IPSO₂₅ autoxidation in some sediments. An example in application is given in Fig. 66. Note, however, that sediments with a very low content of IPSO₂₅ and its oxidation products may require the use of MRM analyses (Rontani et al., 2019b).

The transitions m/z 213 \rightarrow 117, 213 \rightarrow 129 and 213 \rightarrow 143 (Fig. 67) appeared to be useful for the detection of isomeric 9-hydroxy-2,6,10,14-tetramethyl-7-(3-methylpent-1,4-dienyl)-pentadeca-7(20*E*),10(18)-diene and 9-hydroxy-2,6,10,14-tetramethyl-7-(3-methyl-pent-1,4-dienyl)-penta-deca-7(20*E*),10*E/Z*-diene TMS derivatives. These minor oxidation products result from hydrogen abstraction at carbon-11 of the HBI triene III (Fig. 41).

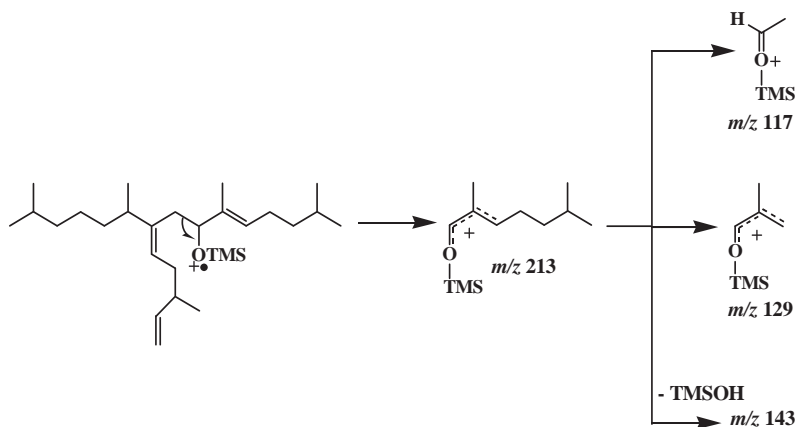


Figure 67. EI fragmentations of the 9-hydroxy-2,6,10,14-tetramethyl-7-(3-methyl-pent-1,4-dienyl)-pentadeca-7(20*E*),10*E*-diene TMS derivative. Adapted from Rontani et al. (2014d).

Indeed, MRM analyses using these transitions allowed to characterize these compounds in Arctic and Antarctic particulate matter samples (Rontani et al., 2014c; 2014d; 2019b). However, the instability of these primary oxidation products resulting from the further oxidation of the 7-20 trisubstituted double bond means that this information remains only qualitative. An example of application is given in Fig. 68.

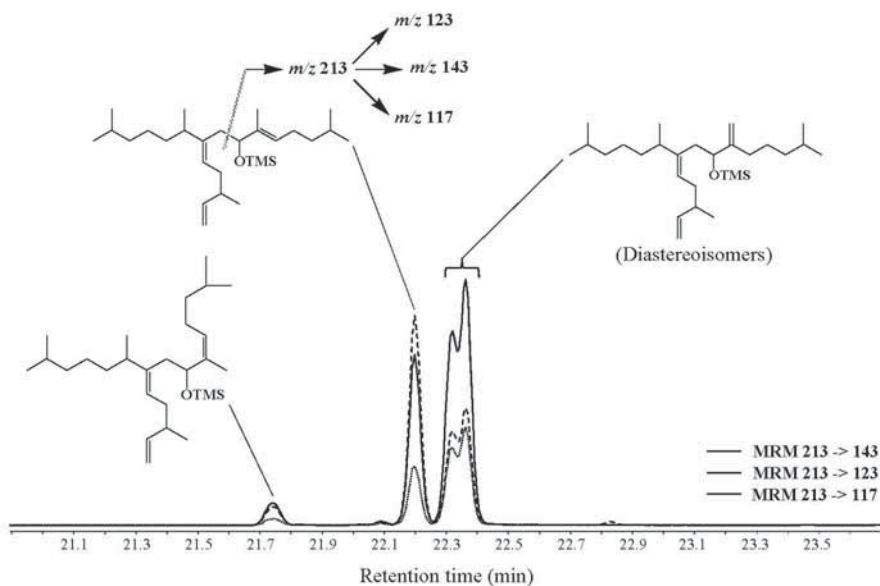


Figure 68. MRM chromatogram (m/z 213 \rightarrow 117, 213 \rightarrow 123 and 213 \rightarrow 143) showing the presence of 9-hydroxy-2,6,10,14-tetramethyl-7-(3-methylpent-1,4-dienyl)-pentadeca-7(20*E*),10(18)-diene and 9-hydroxy-2,6,10,14-tetramethyl-7-(3-methylpent-1,4-dienyl)-penta-deca-7(20*E*),10*E/Z*-diene TMS derivatives in a particulate matter sample from the Antarctic. Adapted from Rontani et al. (2014d).

CHAPTER TWELVE

QUANTIFICATION OF SELECTED TRACERS OF LIPID PHOTO- AND AUTOXIDATION IN ENVIRONMENTAL SAMPLES

Methodology

Lipid oxidation products	Origin	References or suppliers
Phytyldiol	S ^a	Rontani and Aubert, 2005
3,7,11,15-tetramethylhexadec-3-en(<i>Z/E</i>)-1,2-diols	S	Rontani and Aubert, 2005
3,7,11,15-tetramethylhexadec-2-en(<i>Z/E</i>)-1,4-diols	S	Rontani and Aubert, 2005
4,8,12,16-tetramethylheptadecan-4-olide	N ^b	Rufai et al., 2019
β -carotene-5,8-endoperoxide	S	Stratton et al., 1993
Isomeric MUFA oxidation products	S	Marchand and Rontani, 2001
3 β ,6 α / β -steradiols	C ^c	Maybridge Ltd
3 β ,5 α ,6 β -steratriols	S	Li and Li, 2013
Lup-20(30)-ene-3 β ,28,29-triol	S	Galeron et al., 2016a
Lupan-20-one-3 β ,28-diol	S	Galeron et al., 2016a
3 β -hydroxy-urs-12-en-11-one	S	Galeron et al., 2016b
3 β -hydroxyolean-12-en-11-one	S	Galeron et al., 2016b
7 α / β -hydroxydehydroabietic acids	S	Rontani et al., 2015
Allylic hydroxyalkenones	S	Rontani et al., 2007a
IPSO ₂₅ oxidation products	S	Rontani et al., 2019b

^a Synthetic

^b Natural extract

^c Commercially available

Table 6. Origin of the standard oxidation products employed as tracers of lipid photo- and autoxidation.

The quantification of each oxidation product involved extraction of specific fragment ions (see Chapter 11), peak integration, and determination

of individual response factors using external standards and adequate software. Most of the standards of lipid oxidation products are not commercially available and need to be synthesized. References describing the synthesis or isolation of these compounds (and the rare suppliers where available) are summarized in Table 6.

Quantification of lipid photo- and autoxidation in dead phytoplanktonic cells

The light-dependent degradation of unsaturated lipids in senescent or dead phytoplankton cells generally shows a good fit to apparent first-order kinetics (Rontani et al., 1998). The rate constants of these processes (k) can thus be easily determined from regression lines determined as $\ln(C/C_0) = -kD$ (where C is concentration at the time of sampling, C_0 is initial concentration, and D is cumulative light dose). The percentages of photodegradation of the main unsaturated lipids observed in dead cells of various phytoplanktonic strains are summarized in Table 7 and appeared to be very high.

Lipids	<i>Haslea Ostrearia</i> ^a	<i>Dunaliella sp.</i> ^b	<i>Phaeodactylum tricornutum</i> ^b	<i>E. huxleyi</i> ^d
Chlorophyll				100
Carotenoids				100
HBI triene	99			
Phytyl chain	72	88	95	96
C _{16:1} acid	70			79
C _{18:1} acid		88	88	72
C _{18:2} acid		100	99	
C _{18:3} acid		100		91
C _{20:5} acid	100			
Δ ⁵ -sterols	41	71	50	43

Table 7. Percent photodegradation of unsaturated lipids in dead phytoplanktonic cells. Summarized from Rontani et al. (1998)^a, (2011a)^b and Christodoulou et al. (2010)^c.

Autoxidation of unsaturated lipids was studied in diatoms collected in Antarctica and incubated in the presence of Fe²⁺ ions (Rontani et al., 2011a). The results obtained, which are summarized in Table 8, confirmed

the high autoxidative reactivity of HBI possessing *bis*-allylic positions (HBI III) and PUFAs.

Lipids	Autoxidation percentage
HBI triene III (<i>Z</i>)	42
HBI triene III (<i>E</i>)	44
C _{21:1} <i>n</i> -alkene	29
Phytyl chain	21
C _{16:1} acid	4
C _{20:5} acid	54
24-methylcholesta-5,22(<i>E</i>)-dien-3 β -ol	1
24-methylcholesta-5,24/28-dien-3 β -ol	3

Table 8. Percent autoxidation of lipid components of diatom cells collected from Commonwealth Bay (East Antarctica) and incubated in seawater in the presence of Fe²⁺ ions at 4°C under darkness. Adapted from Rontani et al. (2011a).

Quantification of lipid photo- and autoxidation in senescent leaves of terrestrial higher plants

Photodegradation of lipids was monitored in dry leaves of Mediterranean angiosperms (*Quercus ilex*, *Smilax aspera*, *Petroselinum sativum* and *Urtica dioica*; Rontani et al., 2014a; Rontani, 2019; Rontani, unpublished data, 2014). The results obtained are summarized in Table 9. The photodynamic effect appeared to be less efficient in these organisms than in phytoplankton (Table 8). The very fast photodegradation of chlorophyll during the senescence of temperate terrestrial higher plants appears to substantially limit its photosensitizing properties relative to the other cell lipid components and notably to 24-ethylcholest-5-en-3 β -ol (sitosterol), which is the major sterol of terrestrial vascular plants (Lütjohann, 2004).

Lipids	<i>Q. ilex</i> ^a	<i>S. aspera</i> ^a	<i>P. sativum</i> ^b	<i>U. dioica</i> ^c
Chlorophyll	100	100	100	100
Sitosterol	49	33	9	36
Betulin	6			

Table 9. Percent photodegradation of unsaturated lipids in dry leaves of Mediterranean angiosperms. Summarized from Rontani (2019)^a, Rontani et al. (2014a)^b and Rontani (unpublished data, 2014)^c.

Autoxidation also appeared to play a significant role in the senescence of the terrestrial higher plants investigated (Galeron et al., 2016a; 2016b; Fig. 53; Table 10) and is likely induced by homolytic cleavage of photochemically-produced hydroperoxides, which should be strongly favoured by the strong UV irradiance and relatively high temperatures found in Mediterranean zones.

Lipids	<i>Q. ilex</i>	<i>S. aspera</i>
Sitosterol		2
Betulin	5	
α -amyrin		35
β -amyrin		33

Table 10. Percent autoxidation of unsaturated lipids in dry leaves of Mediterranean angiosperms. Summarized from Galeron et al. (2016a) and (2016b).

Quantification of lipid photo- and autoxidation in detached leaves of seagrasses

Type-II photosensitized oxidation processes are more efficient in senescent seagrasses (marine angiosperms; Table 11) than in senescent terrestrial angiosperms (Table 9). This higher efficiency may be attributed to the relative persistence of chlorophyll in senescent seagrasses (Pellikaan, 1982; Auby, 1991) due to the lower temperatures and solar irradiance generally observed in the aquatic realm, which allows long periods of ¹O₂ production (see Chapter 7).

Lipids	<i>Posidonia oceanica</i>	<i>Zostera noltii</i>
Chlorophyll	20	50
Sitosterol	72	95
24-ethylcholesta-5,22(E)-dien-3β-ol	69	

Table 11. Percent photodegradation of unsaturated lipids in senescent leaves of Mediterranean seagrasses. Summarized from Rontani et al. (2014a) and Rontani (2019).

In contrast, autoxidation processes appear to remain limited in detached leaves of these organisms (Rontani, 2019). However, their high content of photochemically-produced hydroperoxides (Rontani et al., 2014a; Rontani, 2019) may induce the intense autoxidation of sitosterol (see Chapter 9) previously observed in the oxic layer of coastal and estuarine sediments colonized by marine seagrasses (Rontani et al., 2014a).

Quantification of lipid photooxidation in dead photo- and photoheterotrophic bacteria

Light-induced degradation processes were previously studied in the purple sulphur bacteria *Thiohalocapsa halophila* and *Halochromatium salexigens* (Marchand and Rontani, 2003). After complete degradation of the sensitizer (bacteriochlorophyll *a*), an intense degradation of the main MUFAs (C_{16:1Δ9} and C_{18:1Δ11}) of these phototrophic bacteria was observed (Table 12). This degradation mainly involves type-II photosensitized oxidation processes.

These processes have also been studied in some aerobic anoxygenic bacteria (AAPs) (*Erythrobacter* sp. NAP1 and *Roseobacter* sp. COL2P; Rontani et al., 2003a), which are well-known photoheterotrophic organisms employing bacteriochlorophyll-containing reaction centers (Shiba, 1991; Yurkov & Beatty, 1998). In this case, the degradation observed (Table 12) was clearly the result of radical-induced processes. The lack of phytyldiol (a specific product of chlorophyll phytyl side chain type-II photosensitized oxidation; Fig. 8) at the end of irradiation confirmed that ¹O₂ is not produced during the photodegradation of these photoheterotrophic bacteria (Rontani et al., 2003a). The radical nature of this degradation is also well

supported by the detection of epoxyacids resulting from the addition of peroxy radicals to MUFA double bonds.

Lipids	<i>T.</i> <i>halophila</i> ^a	<i>H.</i> <i>salexigens</i> ^a	<i>E.</i> Sp. NAP1 ^b	<i>R.</i> Sp. COL2P ^b
Bacteriochlorophyll	100	100	nq	nq
C _{16:1Δ9} acid	nq ^c	60		
C _{18:1Δ11} acid	nq	51	21	39
C _{16:2} acid			63	

^a Purple sulphur bacterium

^b Aerobic anoxygenic bacterium

^c Not quantified

Table 12. Percent photodegradation of unsaturated lipids in dead phototrophic and photoheterotrophic bacteria. Summarized from Marchand and Rontani (2003) and Rontani et al. (2003a).

Detection of lipid photo- and autoxidation in suspended and sinking particles

The lipid oxidation content of suspended and sinking particles collected at widely-contrasted latitudes (Arctic Ocean, East Antarctica, Mediterranean Sea, and equatorial Pacific Ocean) has been investigated (Marchand et al., 2005; Christodoulou et al., 2009; Rontani et al., 2011b; 2012a; 2014c; 2016; 2018b; 2019a). Suspended particles were collected with Niskin bottles or *in situ* multiple-unit large-volume filtration systems (MULVFS), while sinking particles were collected with floating or fixed mooring sediment traps. The results obtained during these different studies, which are summarized in Tables 13 and 14, show that the photodynamic effect is particularly enhanced in polar zones (Rontani et al., 2021b) (see Chapter 13).

Lipids	Mediterranean Sea ^a		Arctic Ocean ^b		Equatorial Pacific Ocean ^c	
	Auto	Photo	Auto	Photo	Auto	Photo
Chlorophyll		10-100%	Qual ^d	0-100%		50-90%
Δ^5 -sterols		0-30%	0-20%	0-50%	0-30%	0-10%
MUFAs	0-50%	0-10%	0-70%	0-100%	0-5%	0-15%

^a Marchand et al., 2005

^b Rontani et al., 2012a; 2016; 2018b

^c Rontani et al., 2011b

^d Only qualitative information

Table 13. Percent auto- and photooxidation of unsaturated lipids measured in sinking particle samples.

Lipids	Arctic Ocean ^a		East Antarctica ^b		Equatorial Pacific Ocean ^c	
	Auto	Photo	Auto	Photo	Auto	Photo
Chlorophyll	Qual	0-50%	Qual ^d	3-50%		20-70%
Δ^5 -sterols	10-85%	0-30%		0-30%	0-30%	0-10%
MUFAs	10-70%	5-50%	0-90%	0-85%	0-10%	0-15%
HBI III	Qual	Qual				

^a Rontani et al., 2014c

^b Rontani et al., 2019a

^c Rontani et al., 2011b

^d Only qualitative information

Table 14. Percent auto- and photooxidation of unsaturated lipids measured in suspended particle samples.

Detection of lipid photo- and autoxidation in surface sediments

Lipid oxidation was also monitored in several surface sediments collected at widely-contrasted latitudes (Arctic Ocean, equatorial Atlantic Ocean, and Atlantic coast of France; Rontani et al., 2012b; 2014a; 2017; 2018a; 2019b; Galeron et al., 2018). The results obtained during these different studies are summarized in Table 15. Note that isomeric C₃₇ and C₃₈ diols arising from alkenone autoxidation and subsequent NaBH₄ reduction (Fig. 38) were detected in surface sediments from South East Alaska (Rontani et al., 2013a). These qualitative results (not included in Table 15) provide the first direct evidence of alkenone autoxidation in situ.

The strong autoxidation of unsaturated lipids of terrestrial higher plants observed in Arctic and equatorial sediments (Table 15) was attributed to the high photooxidation state of Arctic higher plants and to high equatorial temperatures, respectively (Galeron et al., 2018).

Lipids	Arctic Ocean ^a		Atlantic Coast, France ^b		Equatorial Atlantic Ocean ^c	
	Auto	Photo	Auto	Photo	Auto	Photo
Δ ⁵ -sterols	0-60%	0-40%	0-100%	0-100%		
MUFAs	0-20%	0-20%				
IP ₂₅	0-9%					
IPSO ₂₅	0-1%					
α-amyrin	80-100%				90-95%	
β-amyrin	90-95%				70-80%	
Betulin	90-100%				90-95%	
DHAA	30-80%					

^a Rontani et al., 2012b; 2017 ; 2018a ; 2019b

^b Rontani et al., 2014a

^c Galeron et al., 2018

Table 15. Percent auto- and photooxidation of unsaturated lipids measured in surface sediment samples.

Detection of lipid photo- and autoxidation in sea ice

Sympagic diatoms (inhabiting the ice matrix) are concentrated at the ice-water interface within the skeletal layer of congelation ice (Fig. 69). These diatoms were recently shown to exhibit higher sensitivity to light-induced stress than pelagic diatoms (Kvernvik et al., 2020). Such differences in sensitivity were attributed to the gradually-changing low-amplitude irradiance typically experienced by algae in ice compared to open water (Hill et al., 2018).

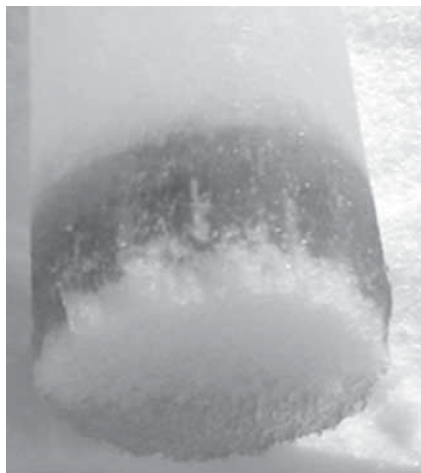


Figure 69. Typical sympagic algae layer at the underside of Arctic sea ice.

Previous research on the photo- and autoxidation of unsaturated lipid components of these organisms (Rontani et al., 2014c; 2018b) showed (Table 16) strong photobleaching of chlorophyll sensitizer and a weakly-efficient photodynamic effect in these organisms compared to pelagic phytoplankton (Table 7), which contrasts with their expected higher sensitivity to light-induced stress. This paradoxical observation may be attributed to PAR irradiance, which is considerably higher at the ice-water interface than in deeper open waters where pelagic algae live. Indeed, as seen in Chapter 7, high solar irradiances strongly weaken the efficiency of type-II photosensitized oxidation of algal lipids (Amiraux et al., 2016; Rontani et al., 2021b).

Lipids	Arctic sea ice	
	Autoxidation	Photooxidation
Chlorophyll ^a	Qual ^c	30-100%
Δ^5 -sterols ^a	0-50%	0-20%
MUFAs ^b	0-15%	0-10%
HBI III ^a	Qual	Qual

^a Rontani et al., 2014c

^b Rontani et al. 2018b

^c Only qualitative information

Table 16. Percent auto- and photooxidation of unsaturated lipids measured in Arctic sea ice samples.

Detection of lipid photo- and autoxidation in microbial mats

Microbial mats are complex communities of microorganisms that are usually organized into layers that can be seen with the naked eye (Fig. 70). In wet environments, the uppermost layers of microbial mats are generally dominated by aerobic photosynthesizing cyanobacteria (Des Marais, 2010). Type-II photosensitized oxidation processes can thus potentially intervene in these particular ecosystems. The photo- and autoxidation of unsaturated lipids were thus studied in microbial mat samples collected in the Camargue (France) which are dominated by *Microcoleus*-type cyanobacteria (Caumette et al., 2001; Marchand and Rontani, 2003). The results obtained are summarized in Table 17.

The very high solar irradiance measured at the surface of these mats ($3320 \mu\text{mol photons m}^{-2} \text{ s}^{-1}$ at 14 h in May; Wieland and Köhl, 2001) is almost certainly what drives the strong photobleaching of chlorophyll and the relatively weak efficiency of photodynamic effect observed (see Chapter 7). The production of high amounts of sulphides (well known to easily reduce hydroperoxides; Mihara and Tateba, 1986) by sulphate-reducing bacteria in the microbial mats (especially during the night) might explain the relatively weak intensity of autoxidative processes in these particular ecosystems.

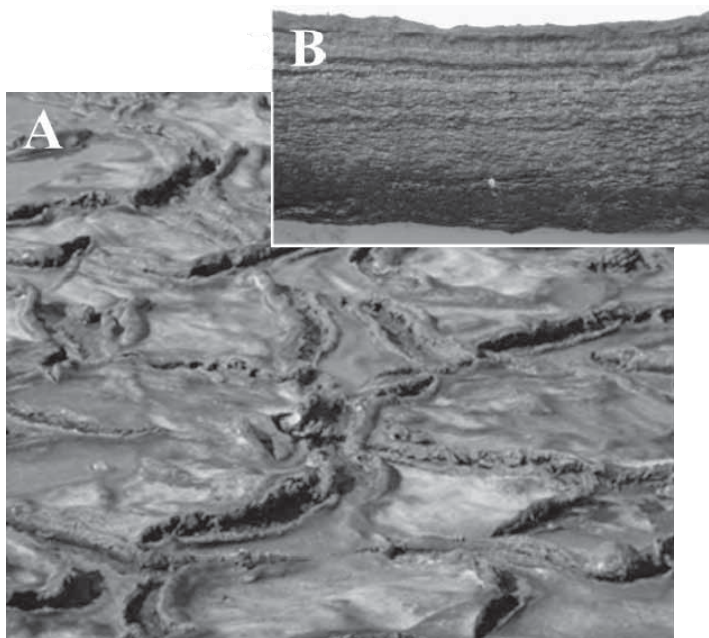


Figure 70. Macroscopic view of surface (A) and 0-10 cm cross section (B) of the microbial mats found in the Camargue (South of France).

Lipids	Camargue microbial mats ^a	
	Autoxidation	Photooxidation
Chlorophyll		80%
C _{16:1Δ9}	7%	8%
C _{18:1Δ9}	27%	30%
C _{18:1Δ11}	23%	14%

^a Marchand and Rontani, 2003

Table 17. Percent auto- and photooxidation of unsaturated lipids measured in Camargue microbial mats.

CHAPTER THIRTEEN

ENVIRONMENTAL HOTSPOTS OF PHOTO- AND AUTOXIDATION OF PHOTOTROPHIC ORGANISMS

Type-II photosensitized oxidation

As seen in Chapter 7, temperature and intensity of solar irradiance both strongly affect the efficiency of type-II photosensitized oxidation processes (i.e. ratio of photodynamic effect-to-sensitizer photobleaching; Fig. 3) in phototrophic organisms. The efficiency of type-II photosensitized oxidation was recently compared in phytoplankton collected at different latitudes (Rontani et al., 2021b). These investigations clearly showed enhanced photooxidation of lipids at the expense of chlorophyll photodegradation in polar regions compared to temperate and equatorial regions. This enhancement might result from lower temperatures in polar regions decreasing the diffusion rates of $^1\text{O}_2$ outside the membranes (Ehrenberg et al., 1998) and thus favouring oxidative damage. However, there were also strong differences in the efficiency of the photodynamic effect between particles collected under ice and in open water zones in both Arctic (Fig. 71) and Antarctic (Fig. 72) samples. These differences may stem from the respective contributions of sympagic (i.e. living within ice) vs. pelagic algae to the different samples. Indeed, as seen in Chapter 12, sympagic algae are more sensitive to light-induced stress than pelagic algae (Kvernvik et al., 2020). However, the lack of correlation observed between lipid photooxidation percentage and concentration of the sea ice lipid biomarker IP₂₅ (Belt and Müller, 2013) argues against this hypothesis (Rontani et al., 2021b). In fact, the intensity of solar irradiance, which is considerably lower under ice than in open water zones (Alou-Font et al., 2016), was found to be the key parameter in type-II photosensitized oxidation of lipids in senescent phytoplankton.

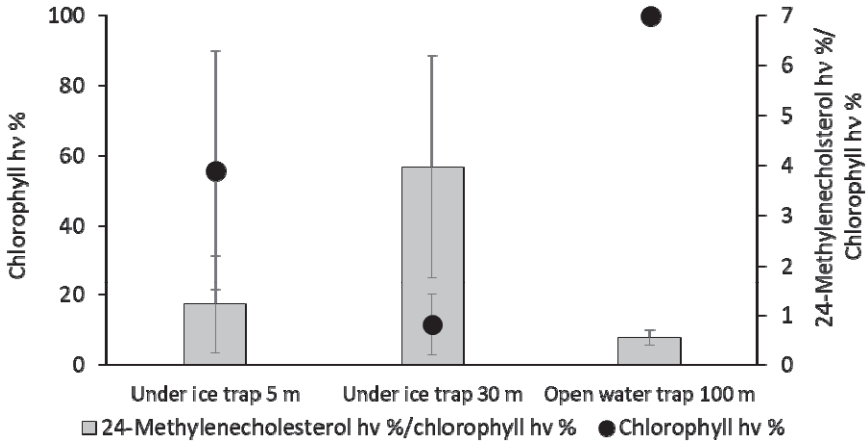


Figure 71. Values for the ratio of 24-methylenecholesterol photooxidation %-to-chlorophyll photooxidation % and chlorophyll photooxidation % in samples of sinking particulate matter collected in Arctic ice-covered and open-water zones. Adapted from Rontani et al. (2021b).

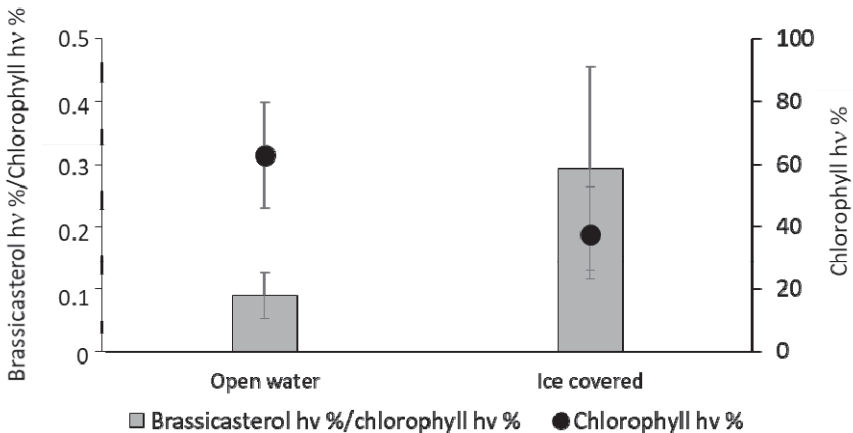


Figure 72. Values for the ratio of brassicasterol photooxidation %-to-chlorophyll photooxidation % and chlorophyll photooxidation % in samples of suspended particulate matter collected in open and ice-covered zones along a N-S transect terminating in the Amundsen Sea (Antarctica). Adapted from Rontani et al. (2021b).

The efficiency of type-II photosensitized oxidation processes is particularly high in strongly-aggregated sympagic algae due to the concentration of the less-metabolically-active sea ice algae in aggregates (Riebesell et al., 1991) sinking quickly to deep waters where light transmission is low (Rontani et al., 2016).

Paradoxically, in temperate and strongly light-irradiated equatorial regions (solar irradiance ranging from 100 to 250 W m⁻² in the Amazon Basin; Pinker and Laszlo, 1992), the short lifespan of the chlorophyll sensitizer coupled with the high diffusion rate of ¹O₂ means that only weakly-damaging type-II photoprocesses occur (Galeron et al., 2018).

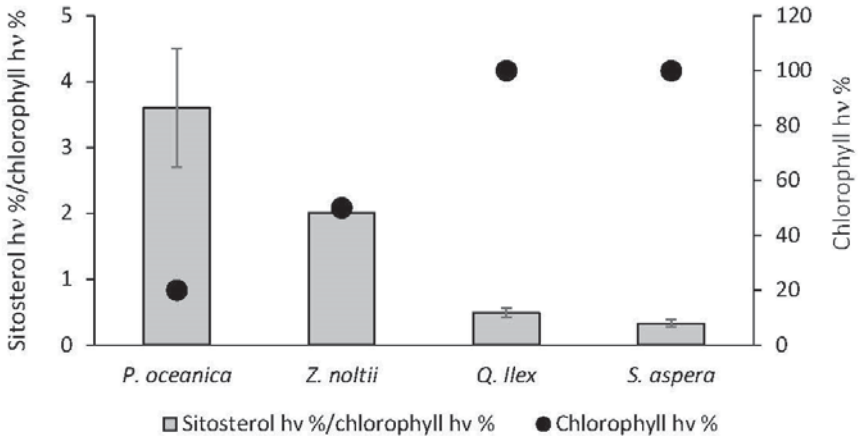


Figure 73. Values for the ratio of sitosterol photooxidation %-to-chlorophyll photooxidation % and chlorophyll photooxidation % in terrestrial and aquatic angiosperms. Adapted from Rontani et al. (2014a) and Rontani (2019).

Temperature and solar irradiance also induce contrasted patterns of efficiency of the photodynamic effect in terrestrial and aquatic higher plants (Fig. 73). Indeed, in temperate regions, these processes appear to be more intense in aquatic angiosperms such as *P. oceanica* and *Z. noltii* than in terrestrial angiosperms such as *Q. ilex* and *S. aspera*, likely due to the lower temperatures and solar irradiance generally observed in aquatic environments than on land.

Autoxidation

As seen above, high temperatures and solar irradiance intensities have a negative effect on the type-II photosensitized oxidation of lipid components of phototrophic organisms. The enhanced photooxidation that occurs during the senescence of Arctic terrestrial higher plants thus produces high proportions of hydroperoxides that, once homolytically cleaved, induce intense autoxidation (Fig. 74).

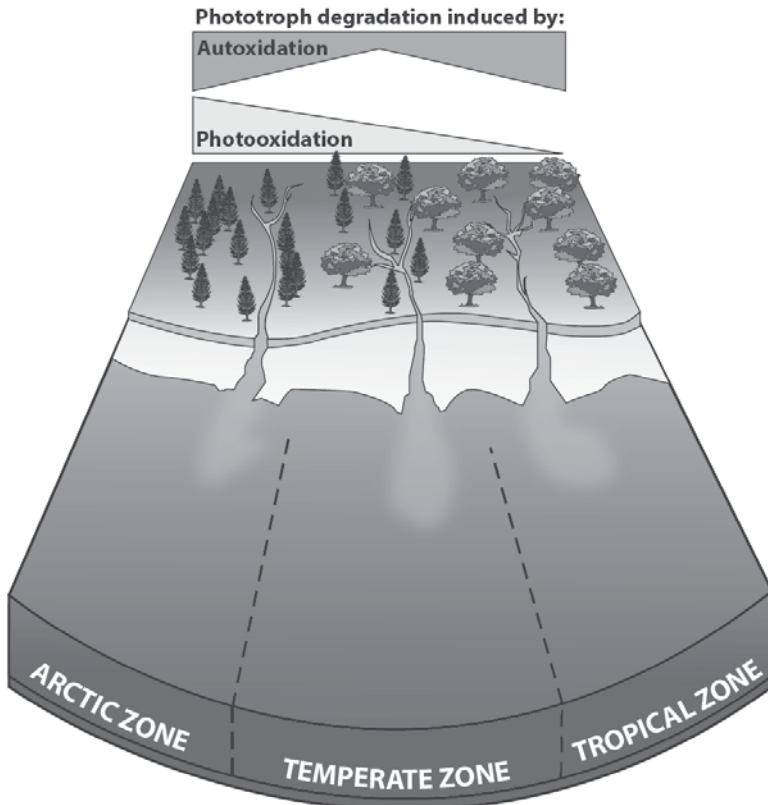


Figure 74. Abiotic degradation of phototrophs in Arctic, temperate and equatorial zones. Adapted from Galeron et al. (2018).

The amounts of photochemically-produced hydroperoxides are logically lower in equatorial and temperate regions than at higher latitudes (Galeron et al., 2018). However, in equatorial regions, the particularly high temperatures and solar irradiance intensities observed on land very efficiently cleave the small amounts of hydroperoxides resulting from photooxidation (see Chapter 8), which results in intense production of free radicals and thus strong autoxidation of the lipid components of equatorial higher plants (Fig. 74; Galerón et al., 2018). In contrast, in temperate regions, photooxidative damage and hydroperoxide cleavage, which are relatively limited, only induce moderate autoxidation of phototrophs (Fig. 74).

Analysis of samples of suspended particulate matter from different rivers and estuaries at different latitudes showed that autoxidative degradation of vascular plant-derived lipids is particularly intense in estuarine waters (Rontani et al., 2014c, Galerón et al., 2017; 2018). The induction of these processes seems linked to lipoxygenase activation, which increases with salinity (Mittova et al., 2002; Zhang et al., 2012). Indeed, the lipoxygenase catalytic cycle, through the generation of alkoxy radicals, may induce autoxidative damage (Fig. 26; Fuchs and Spiteller, 2014). The release of Fe^{2+} when the radicals generated cause damage at the active site of lipoxygenase itself (Sato et al., 1992; Fuchs and Spiteller, 2014) could be another mechanism that induces autoxidation in estuarine waters (Fig. 75). Activation of lipoxygenases involves the reaction of the ferrous enzyme with hydroperoxides, producing an active ferric enzyme and an alkoxy radical (Ivanov et al., 2005; Fig. 75). It is thus strongly favoured in vascular plant debris carried by Arctic and equatorial rivers containing high proportions of photooxidative and/or autoxidative-produced hydroperoxides (Galerón et al., 2018).

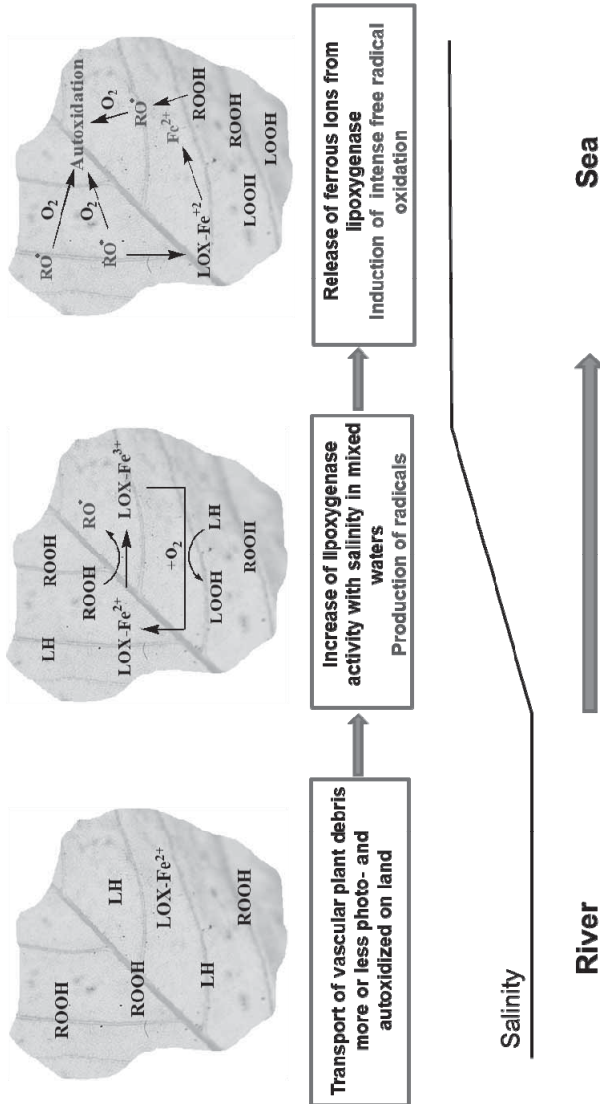


Figure 75. Proposed pathways for lipoxygenase-induced autoxidative degradation of terrestrial vascular plant material in estuaries. Adapted from Galeron et al. (2018). (LH = linoleic or linolenic acids; LOX-Fe²⁺ = inactive lipoxygenase; LOX-Fe³⁺ = active lipoxygenase)

CHAPTER FOURTEEN

POTENTIAL APPLICATIONS OF LIPID OXIDATION TRACERS

Use of lipid oxidation products as stress indicators of specific organisms

Type-II photosensitized oxidation and autoxidation products of lipid components of phototrophs are mainly produced during their senescence (see Chapters 2 and 9), which makes these compounds very useful indicators of environmental stress. In the case of unsaturated lipids which are far less prevalent in phototrophs and their associated heterotrophs (Table 18), their oxidation states can afford very instructive information on the stress state of specific organisms.

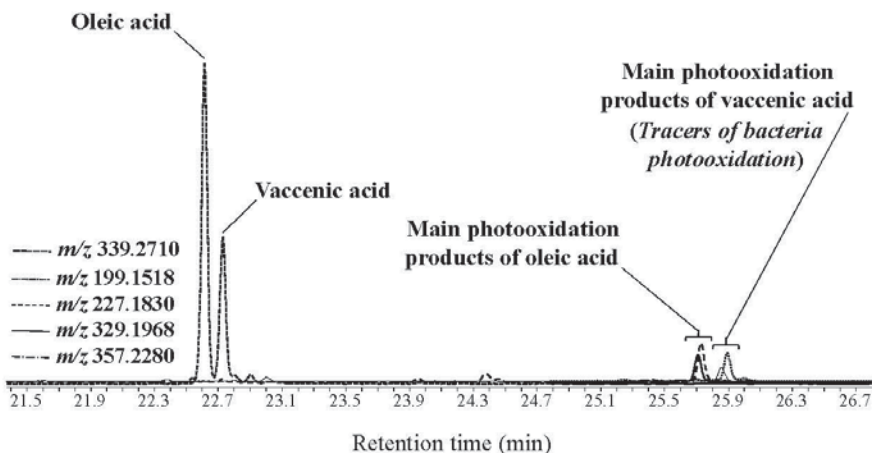


Figure 76. Ion chromatograms at m/z 339.2710 $[M - CH_3]^+$, 199.1518, 227.1830, 329.1968 and 357.2280 showing the presence of oleic and vaccenic acids and their photooxidation products in suspended particulate matter collected in Chukchi Sea (Arctic).

Lipid oxidation products afford information on the physiological state of terrestrial vascular plants, pelagic and sympagic diatoms, green algae, haptophytes and copepods (Table 18). Moreover, as seen in Chapter 6, type-II photosensitized oxidation processes can also significantly affect heterotrophic bacteria associated with phytoplankton. Oxidation products of specific bacterial MUFAs such as $C_{18:1\Delta 11}$ and $C_{16:1\Delta 11}$ (Sicre et al., 1988; Burot et al., 2021) could thus prove very useful for monitoring photooxidative stress in heterotrophic bacteria associated with phytoplanktonic cells (Fig. 76).

Lipids	Origin	References
α - and β -amyrins	Terrestrial angiosperms	Jäger et al., 2009
Betulin	Terrestrial angiosperms	Jäger et al., 2009
Lupeol	Terrestrial angiosperms	Jäger et al., 2009
Dehydroabietic acid	Gymnosperms	Otto et al., 2005
18-hydroxyoleic acid	Terrestrial angiosperms	Kolattukudy, 1980
24-methylenecholesterol	Diatoms	Volkman, 2003
24-norsterol	Diatoms	Rampen et al., 2007
Δ^7 -sterols	Green algae	Patterson, 1974
$C_{18:1\Delta 11}$ acid	Heterotrophic bacteria	Sicre et al., 1988
$C_{16:1\Delta 11}$ acid	Heterotrophic bacteria	Burot et al., 2021
$C_{16:1\Delta 9}$ acid	Diatoms	Liang and Mai, 2005
IP ₂₅	Sympagic diatoms	Belt and Müller, 2013
IPSO ₂₅	Sympagic diatoms	Belt et al., 2016
C_{37} and C_{38} alkenones	Haptophytes	Brassell et al., 1986
$C_{20:1}$ and $C_{22:1}$ <i>n</i> -alkenols	Herbivorous copepods	Lee et al., 2006
Myxoxanthophyll	Cyanophytes	Bianchi et al., 1993
Bacteriochlorophylls	Photosynthetic bacteria	Oren, 2011

Table 18. Main unsaturated lipids employed as biomarkers for assessing sources of organic matter in the environment. (This list is not exhaustive).

Monitoring on the photooxidation of 24-methylenecholesterol (mainly derived from diatoms; Volkman, 2003; Rampen et al., 2010) and epi-brassicasterol (arising from diatoms and/or prymnesiophytes; Volkman, 2003) in particulate matter samples clearly showed a strong efficiency of type-II photosensitized oxidation processes in diatoms (Rontani et al., 2012a; 2016; 2019a; Fig. 77). The less efficient photooxidation observed

in prymnesiophytes was attributed to their high content of mycosporine-like amino acids, which are known to protect cells against reactive oxygen species such as $^1\text{O}_2$ (Suh et al., 2003; Elliott et al., 2015).

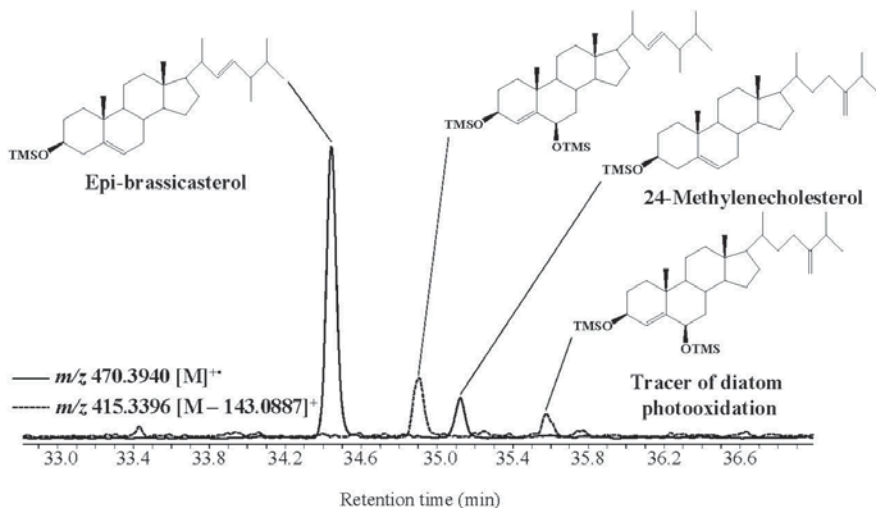
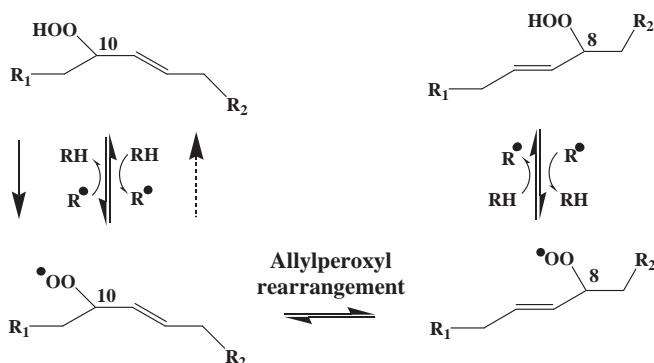


Figure 77. Ion chromatograms at m/z 470.3940 and 415.3396 showing the higher reactivity of diatoms to type-II photosensitized oxidation processes in suspended particles collected in East Antarctica.

Allylic rearrangement of hydroperoxides resulting from MUFA oxidation in biological membranes is very sensitive to the hydrogen atom donor properties of the surrounding molecules (Porter et al., 1994; 1995). In algal membranes containing a high proportion of intact and/or oxidized PUFAs, which are very good hydrogen atom donors (Porter et al., 1995), allylic rearrangement is logically relatively limited (Fig. 78). In contrast, bacterial periplasm containing only saturated fatty acids (SFAs) and MUFAs (both poor hydrogen atom donors) is conducive to allylic rearrangement. Fig. 79 presents a typical profile of MUFA autoxidation products observed in high-PUFA-content algae. This high sensitivity of allylic rearrangement to the hydrogen atom donor properties of surrounding molecules could be particularly useful when only oxidation products of non-source-specific MUFAs (such as oleic and palmitoleic acids) are present. In this case, the extent of allylic rearrangement of various hydroperoxides found in each sample may be indicative of the degree of unsaturation of initial membranes of the organisms (bacteria or algae) present in the sample.



Good hydrogen donor surrounding molecules (PUFAs) (dashed arrow)

Weak hydrogen donor surrounding molecules (SFAs or MUFAs) (full arrow)

Figure 78. Effect of the hydrogen atom donor properties of surrounding molecules on allylic rearrangement of MUFA oxidation products. The example given is the case of a 10-hydroperoxyacid.

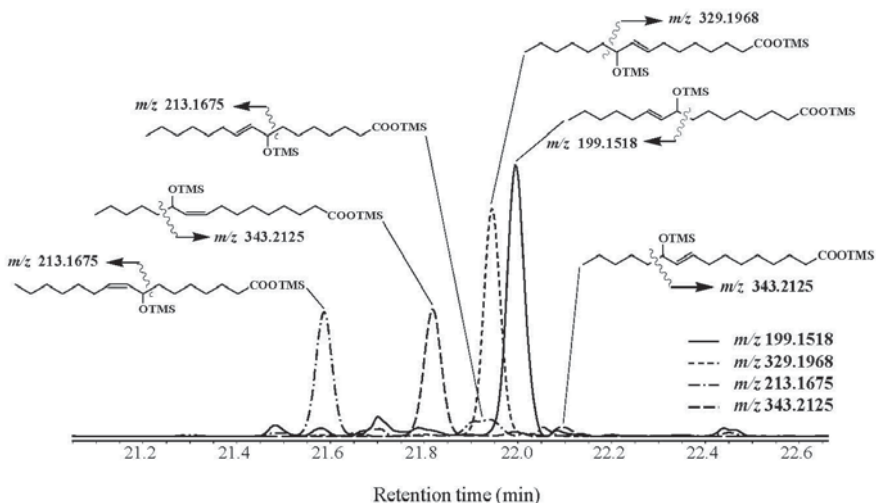


Figure 79. Partial ion chromatograms (m/z 199.118, 213.1675, 329.1968 and 343.2125) showing a very weak allylic rearrangement of palmitoleic acid oxidation products in a PUFA-rich particulate matter sample collected at 10 m under the ice in Baffin Bay (Arctic).

Use of lipid oxidation products as proxies of paleoenvironmental changes

Some lipid oxidation products surprisingly appeared to be relatively well preserved in sediment samples (Rontani et al., 1996b; Rontani and Marchand, 2000; Marchand and Rontani, 2001; Rontani et al., 2012b; 2017). Their preserved state was attributed to protection conferred by intact membranes of well silicified diatoms or higher plant debris. Indeed, the lipid oxidation products present in sediments are mainly in esterified or bound forms (Rontani and Marchand, 2000), which are mainly found in intact biological debris (Cranwell, 1978; Sun et al., 1993). Monitoring these oxidation products in sediments could thus give very useful information concerning past environmental changes.

Phytyldiol/phytol ratio (chlorophyll phytyl side-chain photooxidation index, CPPI; see Chapter 5) was previously proposed for monitoring past photodegradation of chlorophylls with a phytyl side chain in sediments (Rontani et al., 1996b). Indeed, it was observed that “esterified or bound” phytyldiol is degraded in recent sediments at a similar rate to “esterified or bound” unchanged chlorophyll phytyl side chain (Rontani and Grossi, 1995; Rontani et al., 1996b). This non-selective degradation together with detection of significant amounts of intact “esterified or bound” phytyldiol in sediments aged up to 2.5×10^4 years BP (Philippe Cuny, unpublished data, 1996) well supports the use of this ratio as paleotracer of chlorophyll photodegradation.

More recently, relatively high and variable proportions of autoxidation products of α - and β -amyrins were detected in sediments aged up to 800 years BP collected in the Beaufort Sea (Canadian Arctic) (Jean-François Rontani, unpublished data, 2010; Fig. 80). Interestingly, the lowest autoxidation percentages observed between 300 and 400 years BP correspond to a period when the Canadian Arctic was colder than now (Barry et al., 1977). As seen in Chapters 8 and 9, temperature plays a key role in the homolytic cleavage of photochemically-produced hydroperoxides and thus in the initiation of autoxidation reactions. The limitation of autoxidative damage observed at the lowest temperatures is thus perfectly logical. In future studies, it will be very instructive to compare the variations of these autoxidation percentages with those of classical proxies of paleotemperatures (alkenones, TEX₈₆ or foraminiferal assemblages; for a review, see Hertzberg and Schmidt, 2016).

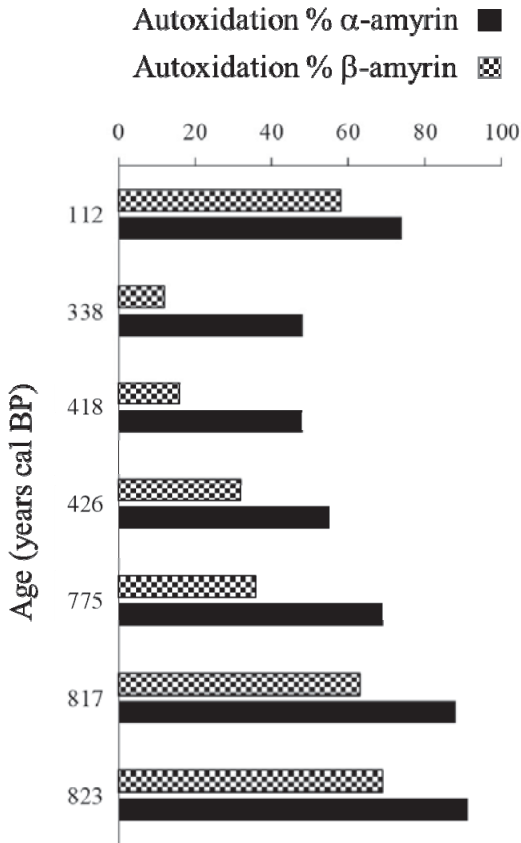


Figure 80. Variation of α - and β -amyrin autoxidation percentages in sediments collected in the Beaufort Sea near the Mackenzie Estuary (Malina Program, 2009).

Some lipid tracers are used to trace anoxic conditions in ancient water columns of lakes, inland seas and oceans (Brocks et al., 2005; Hebbing et al., 2006). For example, the carotenoids isorenieratene and okenone, which are only produced by phototrophic sulfur bacteria belonging to the Chromatiaceae and Chlorobiaceae (Schaeffer et al., 1997; Brocks and Pearson, 2005), are widely employed as indicators of hypoxia. Photooxidation and autoxidation of the lipid components of phytoplankton requires the presence of molecular oxygen, and so the distributions of lipid oxidation products in marine sediments would potentially make useful tools for determining the redox conditions of the bottom waters at the time of

deposition. The weak abiotic degradation of sterols (up to 5%) observed in the oxygen-deficient suboxic zone of the Black Sea (Rontani and Wakeham, 2008), which contrasts markedly with the strong autoxidation of sterols in the north-western Mediterranean (Fig. 81) where the entire water column is oxygenated (6 mL L⁻¹ O₂ in the mixed layer to 25 m depth and 4 mL L⁻¹ from 100 m down to 800 m depth; Rontani et al., 2009) well supports the argument that lipid oxidation products are suitable for use as indicators of oxic conditions during sedimentation.

Use of lipid oxidation products to detect abiotic alteration of paleoproxies

Lipid oxidation products could prove equally useful for monitoring abiotic alterations of some proxies under environmental conditions, and thus inform validity assessments on future paleoenvironmental studies (Rontani et al., 2013a). For example, high proportions of autoxidation products of IP₂₅ or IPSO₂₅ (see Chapter 10) in marine sediments could be indicative of a partial diagenetic degradation of these widely-employed sea-ice proxies (Belt and Müller, 2013; Belt et al., 2016) and thus of potential biases in reconstructions of Arctic and Antarctic sea ice ages.

The alkenone-based $U_{37}^{K'}$ index is now universally accepted as a robust proxy for reconstructing environmental temperatures (Brassell et al., 1986; Prahl and Wakeham, 1987; Müller et al., 1998). However, when working with the $U_{37}^{K'}$ temperature proxy, it is vital to keep in mind that selective autoxidative degradation of these compounds can introduce biases. Unfortunately, as seen in Chapter 10, autoxidation products of alkenones are too unstable to be used as direct tracers of this potential degradation in sediments. Homolytic and heterolytic cleavages (see Chapter 4) of hydroperoxides resulting from methyl C₃₇ alkenone autoxidation afford, after subsequent NaBH₄ reduction, a complex mixture composed of saturated *n*-alkan-1-ols and fatty acids ranging from C₁₃ to C₁₆ plus two series of C₁₃–C₁₆ (ω -1)-hydroxyacids and (1, ω -1)-diols (Rontani et al., 2007c). In the case of autoxidation products of ethyl C₃₈ alkenones, after reduction these cleavages afford C₁₄–C₁₇ (ω -2)-hydroxyacids and (1, ω -2)-diols, instead of C₁₃–C₁₆ (ω -1)-hydroxyacids and (1, ω -1)-diols (Rontani et al., 2007c). Among these different compounds, (ω -1)- and (ω -2)-hydroxyacids (obtained after reduction of the corresponding ketoacids) were selected as potential tracers of alkenone autoxidation. After NaBD₄ reduction to increase the selectivity of these tracers, silylated [12-²H]-12-hydroxytetradecanoic, [13-²H]-13-hydroxytetradecanoic, [14-²H]-14-hydroxyhexadecanoic and [15-²H]-15-hydroxyhexadecanoic acids were

detected in suspended particles collected in the Ligurian Sea, indicating a strong autoxidative alteration of alkenones in the samples analyzed (Rontani et al., 2007c). In the presence of a high proportion of these compounds (relative to alkenones), we can expect to see a “warming effect”, in which case caution is warranted before using the inferred temperature data.

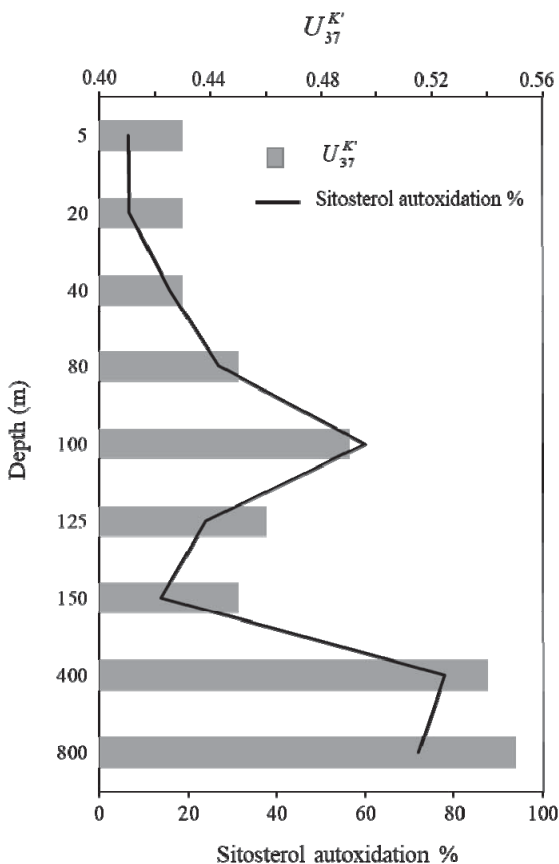


Figure 81. $U_{37}^{K'}$ index and percent sitosterol autoxidation measured in suspended particulate matter samples collected in the Ligurian Sea. Adapted from Rontani et al. (2009).

More stable oxidation products of other lipids can also be used to identify cases where autoxidation of organic matter, and by extension alkenones, has been significant enough to expect a shift in $U_{37}^{K'}$ values. Fig. 81 gives a nice example showing the variation of $U_{37}^{K'}$ index and percent autoxidation of sitosterol (a sterol present in some alkenone-producing Prymnesiophyceae; Marlowe et al., 1984) in suspended particulate matter collected at different depths in the Ligurian Sea (Rontani et al., 2009). The strong correlation observed ($R^2 = 0.94$, $n = 9$) provides a strong indication of autoxidative alteration of alkenones in the suspended particles investigated.

A link between autoxidation and the observed increase of $U_{37}^{K'}$ values in CO_2 -stressed *E. huxleyi* cells was previously demonstrated by plotting the variation of this index according to percent autoxidation of oleic acid ($R^2 = 0.97$; Rontani et al., 2007a). Unfortunately, assigning a magnitude to temperature bias due to autoxidation in environmental samples remains more problematic (Rontani et al., 2013a).

Use of lipid oxidation products for ozone depletion monitoring

Christodoulou et al. (2010) compared visible and UV light-induced degradation of lipid components of *E. huxleyi* and thus observed that UV exposure induced photosensitized stereomutation (*cis-trans* isomerization) of the double bonds of some MUFA oxidation products (Fig. 82). The resulting *cis*-hydroxyacids (e.g. 9-hydroxyoctadec-10(*cis*)-enoic and 10-hydroxyoctadec-8(*cis*)-enoic acids in the case of oleic acid autoxidation), which are only produced in trace amounts during visible light-induced degradation or autoxidation of MUFAs (Frankel, 1998; Porter et al., 1995), were proposed as tracers of UV-induced photodegradation (Christodoulou et al., 2010). Such compounds could provide new ways to gain information on current environmental problems related to ozone depletion. Indeed, although some recovery of stratospheric ozone seems evident in certain locations since the 1989 Montreal Protocol (Steinbrecht et al., 2009), the impacts of climate change on the future global UV environment and the resulting responses in plants are still not well understood (Watanabe et al., 2011; Andrady et al., 2012; Warjent and Jordan, 2013).

$R = -(CH_2)_6-CH_3$

$R' = -(CH_2)_6-COOH$

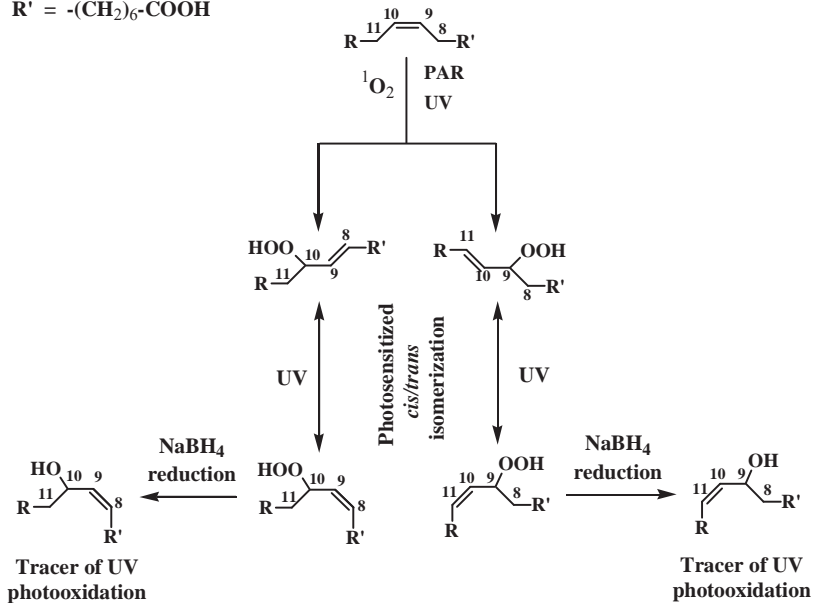


Figure 82. Simplified scheme showing visible and UV-induced photodegradation of oleic acid in senescent phytoplanktonic cells. Adapted from Christodoulou et al. (2010).

Use of lipid oxidation products in permafrost degradation monitoring

Permafrost, which is defined as subsurface earth materials remaining below $0^\circ C$ for two consecutive years, is widespread in the Arctic and boreal regions of the Northern Hemisphere (Zhang et al. 1999). Carbon dioxide and/or methane (greenhouse gas) released to the atmosphere as a result of destabilization and microbial decomposition of permafrost carbon have the potential to significantly accelerate global warming (Schuur et al., 2008). We cannot confidently predict the influence of global change on the delivery and preservation of permafrost over the Arctic shelves without a far more complete understanding of the fundamental processes that control the degradation and preservation of this material (Rontani et al., 2017).

As the organic carbon in permafrost originates mainly from plants (Schuur et al., 2008), it must also be affected by photo- and autoxidation processes, which are very intense in the Arctic (see Chapter 7) and can strongly affect permafrost mineralization. Indeed, there are very complex interactions between biotic and abiotic degradation processes, and previous abiotic alteration of phototrophic material can positively or negatively alter its bioavailability (see Chapter 15). These interactions are strongly dependent on: (i) the phototrophic organisms and bacteria in presence and (ii) certain environmental conditions (such as temperature and solar irradiance). Some authors assert that oxidative stress caused by photochemical ROS generation should be regarded as an environmental variable determining the abundance, activity, and phylotype composition of environmentally-relevant bacterial groups (Glaeser et al., 2010; 2014).

Consequently, in future studies of permafrost degradation, it will be very important to avoid over-focusing on bacterial degradation processes and also take into account photo- and autoxidation and the many complex interactions between all these processes. The different lipid oxidation products described in this book will be very useful for such purpose.

Use of oxidation products for determining the double bond position of MUFAs and monounsaturated *n*-alkenols

Due to the migration of their double bond during ionization, TMS derivatives of MUFAs afford very similar EI mass spectra. To determine the position of this double bond and avoid this migration problem, it is necessary to prepare specific derivatives that 'fix' the double bond. Numerous methods are employed that involve reactions with either the double bond or the carboxylic group. The main derivatization techniques acting directly with the double bond are osmium tetroxide oxidation (affording diols which are then silylated; McCloskey and McClelland, 1965) and dimethyl disulfide addition (affording dithioethers; Nichols et al., 1986). Reaction of the carboxylic group with nitrogen-containing compounds affords derivatives (i.e. *N*-acylpyrrolidides, picolinyl esters or 4,4-dimethyloxazoline (DMOX); Andersson and Holman, 1974; Harvey, 1982; Fay and Richli, 1991) that act as highly favourable charge sites during ionization and therefore minimize double bond ionization and migration (Dubois et al., 2009).

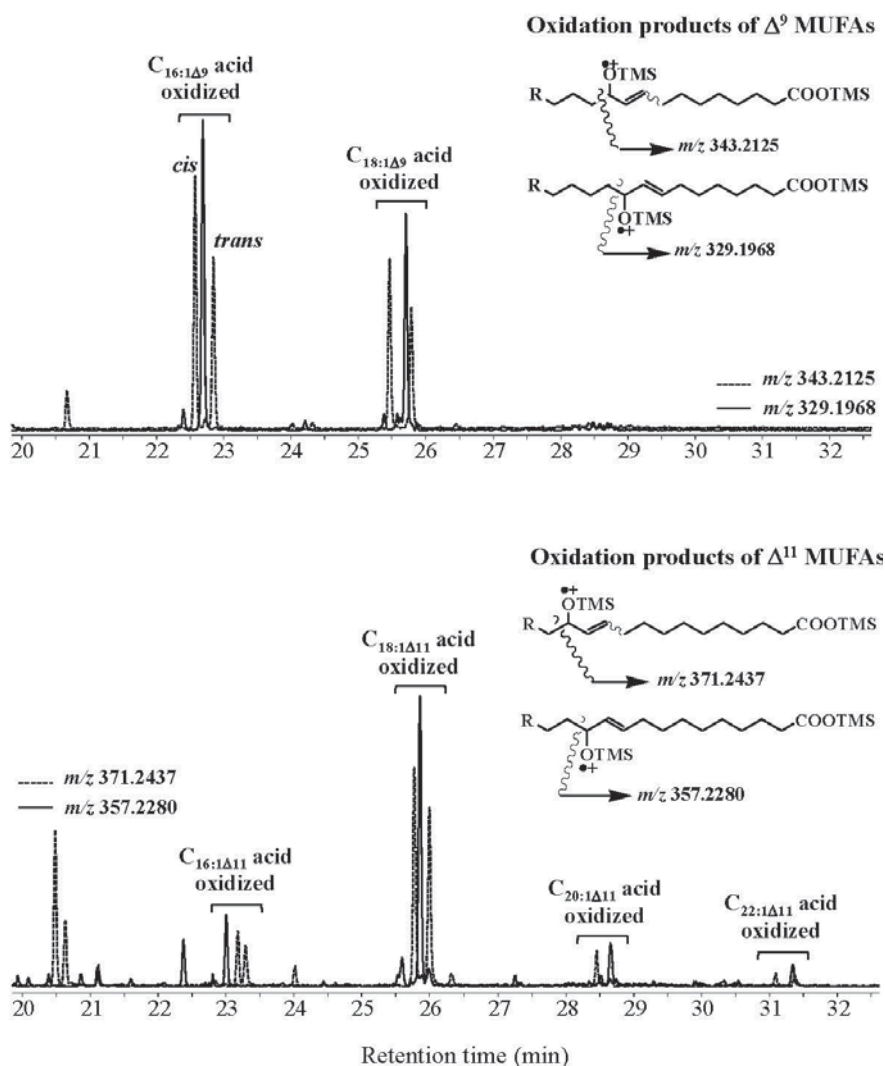


Figure 83. GC-QTOF determination of the double bond position of MUFAs with the TMS derivatives of their oxidation products in a suspended particulate matter sample collected in the Chukchi Sea (Arctic).

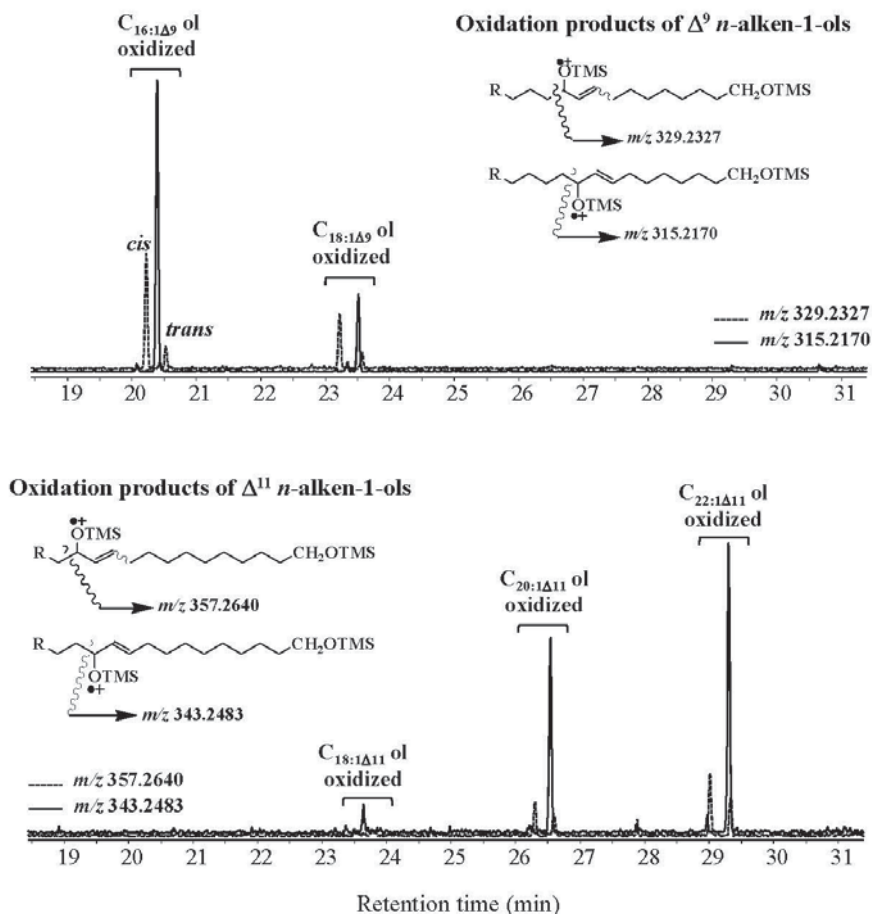


Figure 84. GC-QTOF determination of the double bond position of *n*-alken-1-ols with the TMS derivatives of their oxidation products in a sample of the bottommost layer (0–3 cm) of sea ice collected in Baffin Bay (Arctic).

GC-QTOF analyses of TMS derivatives of MUFA oxidation products, which are widespread in natural samples (see data given in Chapter 12), allow easy and unambiguous attribution of the position of the double bond of these compounds. An example of the technique in application is given in Fig. 83. Table 4 lists accurate masses of the fragment ions (containing the TMS ester group) employed for determining the double bond position

of the main MUFAs. Note that this attribution can also be carried out by classical GC-MS using unit masses.

This method of determining double bond position only requires adding a simple NaBH₄ reduction step (to reduce unstable hydroperoxyacids to the corresponding hydroxyacids; Marchand and Rontani, 2001) before the alkaline hydrolysis classically employed for the treatment of complex lipid extracts (Volkman, 2006). Note that this method can also be employed on monounsaturated *n*-alken-1-ols (resulting from the hydrolysis of zooplanktonic long-chain wax esters; Lee et al., 2006) by using the fragment ions of TMS derivatives of their oxidation products containing the two TMS ether functional groups (Rontani et al., 2021c; Fig. 84). However, this case demands the use of accurate masses (Table 19) as unit masses interfere with more stable isobaric fragment ions of TMS derivatives of MUFA oxidation products, which are present in environmental samples in higher proportions than those of monounsaturated *n*-alken-1-ols.

Parent <i>n</i> -alken-1-ol	<i>m/z</i>	<i>m/z</i>	<i>m/z</i>	<i>m/z</i>
C ₁₆ :1Δ ₉	199.1518 ^a	213.1675 ^a	315.2170 ^b	329.2327 ^b
C ₁₆ :1Δ ₁₁	171.1206	185.1363	343.2483	357.2640
C ₁₆ :1Δ ₁₃	143.0748	157.1051	371.2796	385.2953
C ₁₈ :1Δ ₉	227.1830	241.1987	315.2170	329.2327
C ₁₈ :1Δ ₁₁	199.1518	213.1675	343.2483	357.2640
C ₁₈ :1Δ ₁₃	171.1206	185.1363	371.2796	385.2953
C ₂₀ :1Δ ₉	255.2139	269.2295	315.2170	329.2327
C ₂₀ :1Δ ₁₁	227.1830	241.1987	343.2483	357.2640
C ₂₀ :1Δ ₁₃	199.1518	213.1675	371.2796	385.2953
C ₂₂ :1Δ ₉	283.2451	297.2607	315.2170	329.2327
C ₂₂ :1Δ ₁₁	255.2139	269.2295	343.2483	357.2640
C ₂₂ :1Δ ₁₃	227.1830	241.1987	371.2796	385.2953

^a Fragments containing the terminal methyl group.

^b Fragments containing the terminal trimethylsilyl ether group.

Table 19. Accurate masses of the main fragment ions produced during EI fragmentation of NaBH₄-reduced and silylated photo- and autoxidation products of the more common *n*-alken-1-ols.

CHAPTER FIFTEEN

INTERACTIONS BETWEEN BIOTIC AND ABIOTIC DEGRADATION PROCESSES

Biodegradative, autoxidative and photooxidative degradation processes at work in the environment cannot be considered separately. Indeed, these processes are inextricably linked, and an understanding of their interactions, although complex, is a fundamental step towards precisely identifying the balance between degradation and preservation of phototrophic organisms in the natural environment (Rontani et al., 2017; Rontani, 2019).

Interactions between photo- and autoxidation processes

As we saw in Chapter 9, homolytic cleavage of photochemically-produced hydroperoxides can initiate free radical oxidation chains and thus autoxidation (Girotti, 1998; Rontani et al., 2003b). Moreover, photooxidation processes can also degrade phenols (Opsahl and Benner, 1993), which are present at significant concentrations in higher plants (Zapata and MacMillan, 1979) and can inhibit autoxidation (due to their strong antioxidant properties; Foti, 2007).

Interactions between photooxidation and biodegradation processes

Photodegradation of the phenolic components of higher plants (Psahl and Benner, 1993), which are well-known for their antibacterial properties (Harrison, 1982; Cueva et al, 2020), can thus indirectly favour bacterial growth. Moreover, light-induced degradation can break down structural barriers in the leaves of higher plants and expose new microniches to bacterial colonization (Vähätalo et al., 1998; 2010), thus increasing the bioavailability of pieces of higher-plant detritus.

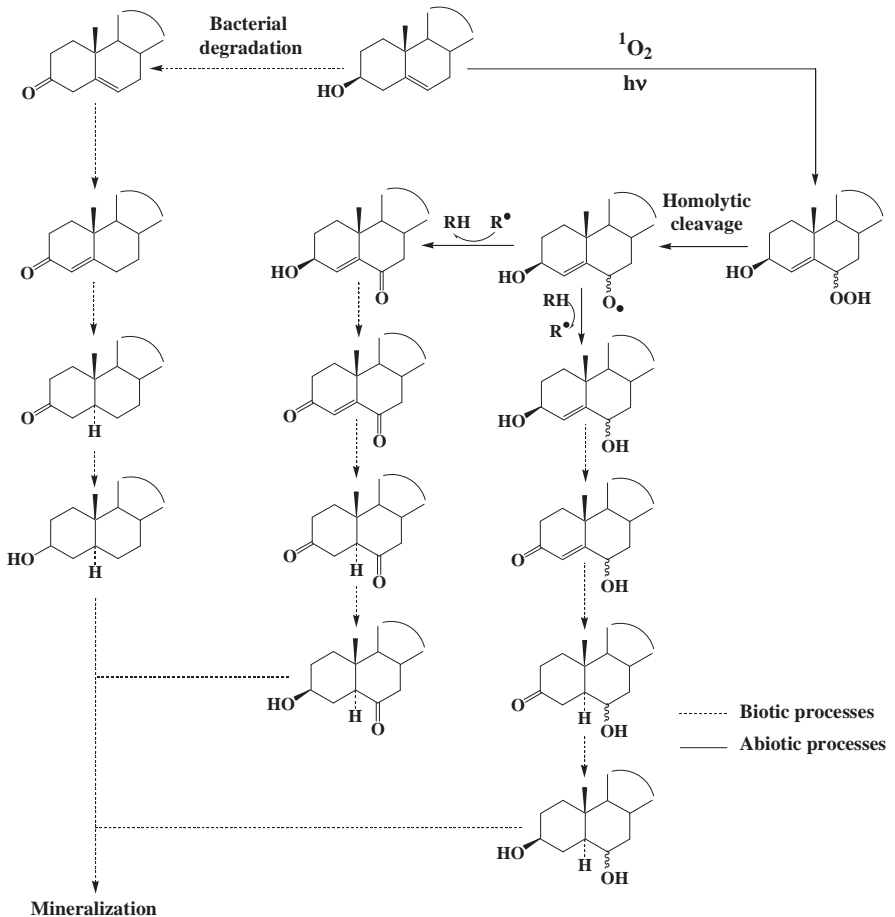


Figure 85. Biotic degradation of sitosterol and its photoproducts in senescent leaves of *P. oceanica*. Adapted from Rontani (2019).

In contrast, photooxidative hydroperoxides, which can be found in significant proportions in marine and terrestrial vascular plants and phytoplankton (Rontani, 2019; Rontani et al., 2014a; Petit et al., 2013), can exert detrimental effects on the invading microorganisms through their ability to induce damage of their protein and DNA (Farr and Kogoma, 1991). Several enzymatic processes avoiding accumulation of these toxic compounds can be employed by bacteria. These processes involve: (i) reduction to the corresponding hydroxyacids by lipoxygenases (Galliard

and Chan, 1980), (ii) conversion to oxoacids by lipohydroperoxidases (Kuehn et al., 1991), (iii) dehydration to allene oxides by hydroperoxide dehydrases and subsequent hydrolysis of these unstable intermediates (Hamberg, 1987), and (iv) direct cleavage of the hydroperoxides to aldehydes and oxoacids (Galliard et al., 1976).

Less toxic lipid photoproducts can be metabolized by bacteria at similar or higher rates than their parent lipids. A case in point was observed in senescent leaves of *P. oceanica*, where bacterial degradation processes act not only on sitosterol but also on its photooxidation products (6-keto- and hydroxysterols; Rontani, 2019; Fig. 85).

As seen in Chapter 6, during photooxidation of senescent phytoplanktonic cells, the sphere of activity of $^1\text{O}_2$ from its point of production has a wide enough radius to induce the degradation of associated heterotrophic bacteria (Rontani et al, 2003a; Petit et al., 2013). Transfer of $^1\text{O}_2$ from phytoplanktonic cells to their attached heterotrophic bacteria can cause substantial cell damage, as these microorganisms lack efficient photoprotective and antioxidant systems (Garcia-Pichel, 1994), and this damage can strongly affect their ability to degrade particulate organic matter. Rontani et al. (2011a) previously attributed the higher biodegradation observed in sinking particles than in suspended particles collected in equatorial Pacific to the abundance of charged mineral surfaces such as siliceous diatom frustules in sinking particles, whose presence reduces the lifetime of $^1\text{O}_2$ (see Chapter 6) and thus allows enhanced bacterial preservation.

Effects of singlet oxygen transfer on the diversity of bacteria attached to phytodetritus were previously investigated in a non-axenic culture of *E. huxleyi* in late-stationary phase (Petit et al., 2015b). In this culture, most of the attached bacteria ($91 \pm 3\%$) were dead and the residual living attached bacterial community appeared to be dominated by pigmented species (*Maribacter*, *Roseobacter*, *Roseovarius*...) whose resistance towards $^1\text{O}_2$ likely results from their high carotenoid content. Bacteria belonging to the family Rhodobacteraceae (Alphaproteobacteria) appear to be relatively insensitive to the reactive species of oxygen (Glaeser et al., 2010; Blanchet et al., 2016). Future research will need to determine whether the abundance of *Roseobacter* and other AAPs often observed during bloom termination (Pinhassi and Berman, 2003; Zhou et al., 2018) effectively results from their particular resistance to oxidative damage.

Shewanella oneidensis (strain MR1) has previously been used as a model organism to better understand attractive and/or repulsive effects of bacteria in response to specific chemical species such as $^1\text{O}_2$ (Petit et al., 2015b). This bacterium was selected on the basis of its high mobility (Sun

et al., 2014). The results obtained (Fig. 86) showed that *S. oneidensis* was unable to detect $^1\text{O}_2$ coming from dead *E. huxleyi* cells. This lack of repulsive effect was attributed to: (i) the very short diffusion distance (0.2 μm) of $^1\text{O}_2$ in water (Redmond and Kochevar, 2006; Ozog and Aebisher, 2018), (ii) the lack of sensors allowing $^1\text{O}_2$ detection by *S. oneidensis*, or (iii) an attractive effect of dead *E. huxleyi* cells outweighing the repulsive effect of $^1\text{O}_2$. Although these results cannot be extended to the whole bacteria, they strongly suggest that bacteria, which are strongly attracted by senescent phytoplanktonic cells, are unable to detect $^1\text{O}_2$ production. Consequently, they should accumulate on phytodetritus and be strongly affected by the $^1\text{O}_2$ transfer.

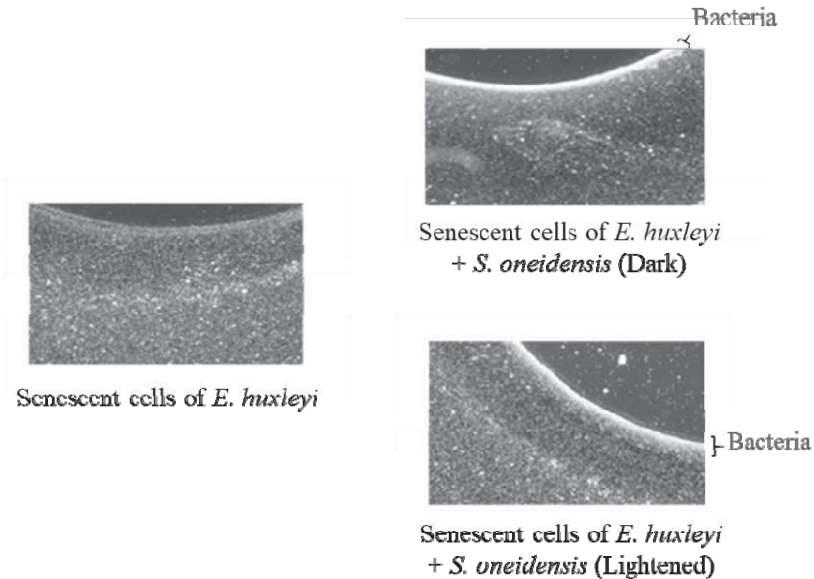


Figure 86. Chemotaxis of *S. oneidensis* in irradiated and non-irradiated cultures of *E. huxleyi*. Adapted from Petit et al. (2015b).

Interactions between autoxidation and biodegradation processes

Some epoxides (Swaving and de Bont, 1998), which may be produced after addition of peroxy radicals and subsequent fast intramolecular homolytic substitution (see Chapter 8), are relatively toxic and have to be removed in order for bacteria to survive. Removal involves glutathione

transferases (GSTs) (which catalyze the reduction of the epoxide ring to an alcohol; Kieslich et al., 1986) and epoxide hydrolases (which catalyze the hydrolysis of the epoxide ring to a vicinal diol; Michaels et al., 1980; Arand et al., 2005).

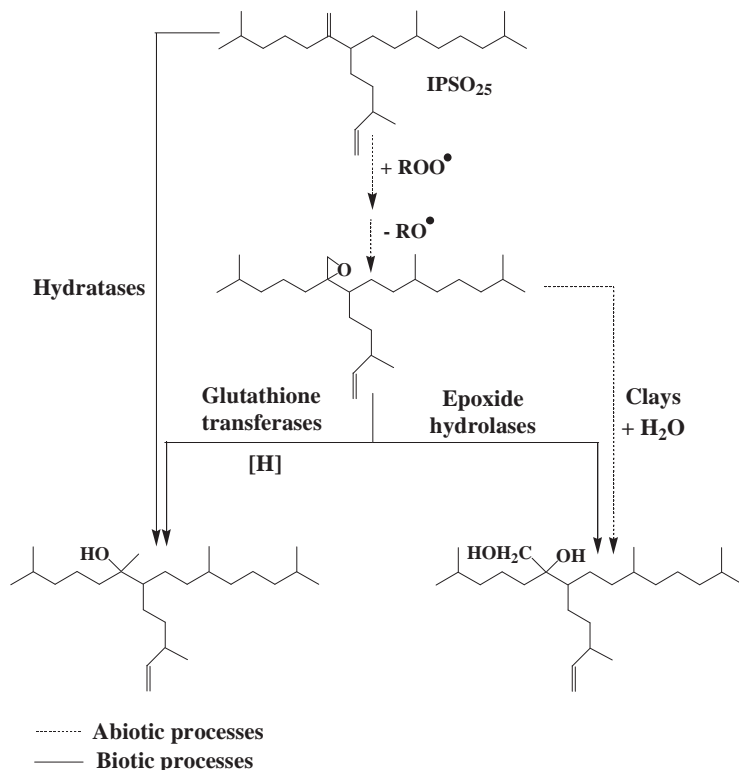


Figure 87. Interactions between biotic and abiotic degradation processes during the degradation of the HBI IPSO₂₅ in sediments. Adapted from Rontani et al. (2019b).

We recently observed that the epoxide 1,2-epoxy-2-(4-methylpentyl)-3-(3-methylpent-4-enyl)-6,10-dimethylundecane (the main autoxidation product of the HBI IPSO₂₅; Rontani et al., 2019b) is converted by sedimentary bacteria to the corresponding tertiary alcohol and diol (Fig. 87). This conversion of the epoxide to a tertiary alcohol was attributed to the involvement of glutathione transferases (Rontani et al., 2019b). However, direct conversion of IPSO₂₅ to this compound via a process

involving hydratases (well known to act on isoprenoid alkenes such as squalene, pristenes and phytene; Rontani et al., 2002, 2013b) cannot be totally excluded (Fig. 87). Hydrolysis of this epoxide to the corresponding diol was attributed to the involvement of epoxide hydrolases. However, epoxides can also be abiotically hydrolyzed in the presence of clays (Haag and Mill, 1988; Minerath et al., 2009).

Degradation of vitamin E by aerobic bacterial communities isolated from marine sediment and microbial mat samples appeared to be mainly carried out by strains belonging to the genera *Idiomarina* and *Bacillus* (Rontani et al., 2008). The detection of metabolites with a shortened side chain and opened chroman ring (indicative of the involvement of autoxidation processes) pointed to the fact that the aerobic degradation of vitamin E involves complex interactions between autoxidation and bacterial degradation processes (Fig. 88). The combination of these processes results in the utilization of the isoprenoid side chain of vitamin E as a carbon and energy source (production of 3 propionyl-CoA and 2 acetyl-CoA), leading to further metabolization of the residual 2,5,7,8-tetramethyl-2(20-carboxyethyl)-6-hydroxy-chroman (α -CEHC) and its opened oxidation products. Some of the detected metabolites of vitamin E resulting from the combination of autoxidation and aerobic biodegradation processes could potentially serve as specific tracers of oxic sedimentation conditions. However, aerobic biodegradation of vitamin E oxidation products is not limited to the isoprenoid side chain, and the opened chroman ring is also quickly consumed by bacteria. Consequently, it seems unlikely that these compounds preserve well in sediments.

It was also proposed previously that the formation of pristane (2,6,10,14-tetramethylpentadecane), which is an isoprenoid hydrocarbon widely distributed throughout the geosphere (Volkman and Maxwell, 1986), is driven by the anaerobic bacterial degradation of trimers resulting from autoxidation of α -tocopherol (see Chapters 5 and 10) initially produced within the water column during the senescence of phytoplankton organisms, and that seem to be well preserved in anoxic environments (Rontani et al., 2010). Biotic degradation of these trimeric oxidation products may involve either direct reductive cleavage to pristane similar to the reduction of epoxides to alcohols (Amate et al., 1991; Duetz et al., 2003; Fig. 89) or thermal formation and subsequent biohydrogenation of

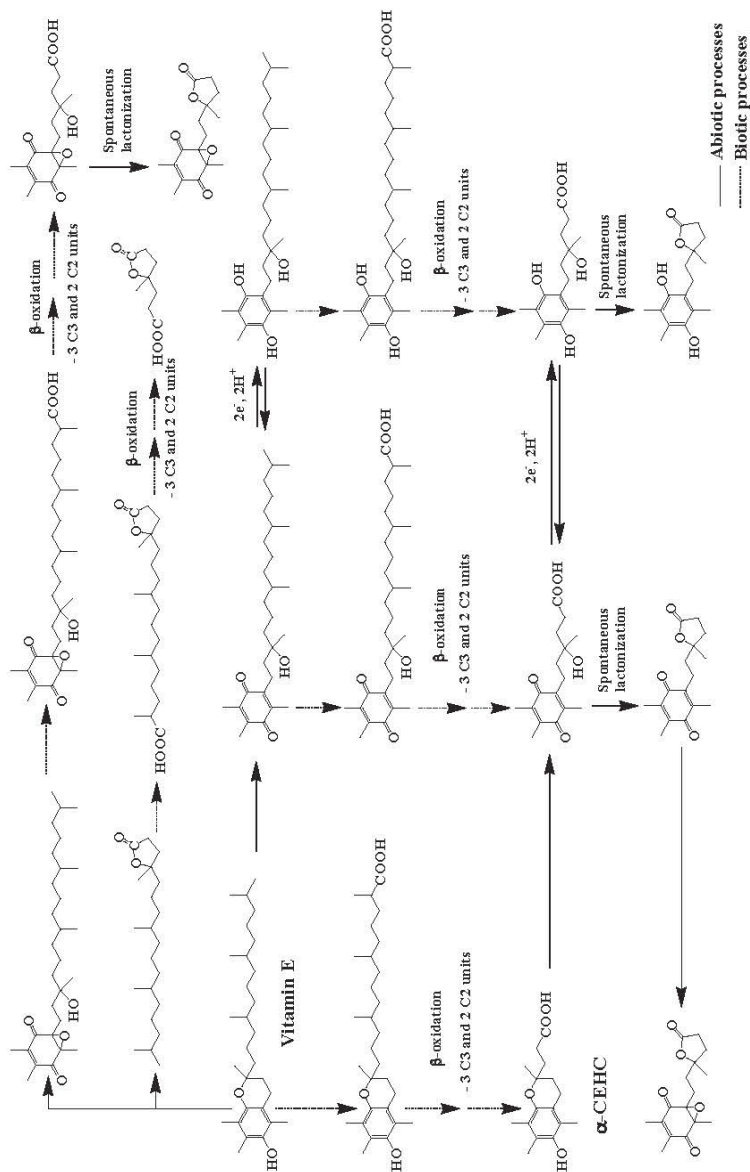


Figure 88. Interaction between aerobic bacterial degradation and autoxidation of vitamin E. Adapted from Rontani et al. (2008).

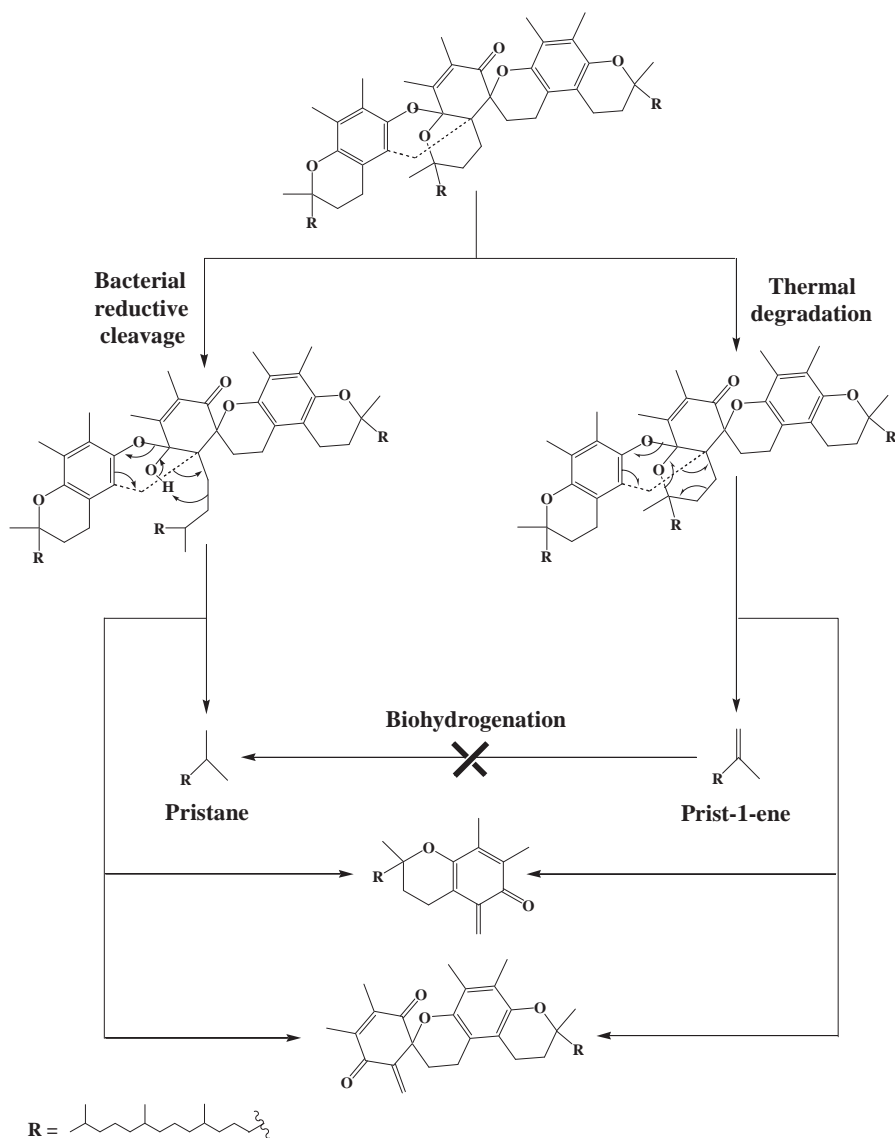


Figure 89. Proposed pathways for the biodegradation of trimeric oxidation products of α -tocopherol in anoxic sediments. Adapted from Rontani et al. (2010).

prist-1-ene to the corresponding alkane (Fig. 89). More recently, it was demonstrated that biohydrogenation has no significant action on the double bond of pristenes (Rontani et al., 2013b). This resistance was attributed to the lack of a binding polar group (or groups) to anchor the substrate to the enzyme and thus allow the double bond to reach the reductive catalytic site (Watts and Browse, 2000). This production of pristane from α -tocopherol autoxidation products does not support the use of pristane-to-phytane (2,6,10,14-tetramethylhexadecane) ratio as an indicator of oxic or anoxic stages of diagenesis (Brooks et al., 1969; Didyk et al., 1978), which was based on the assumption that both these compounds arise from degradation of the same precursor i.e; the chlorophyll phytol side chain.

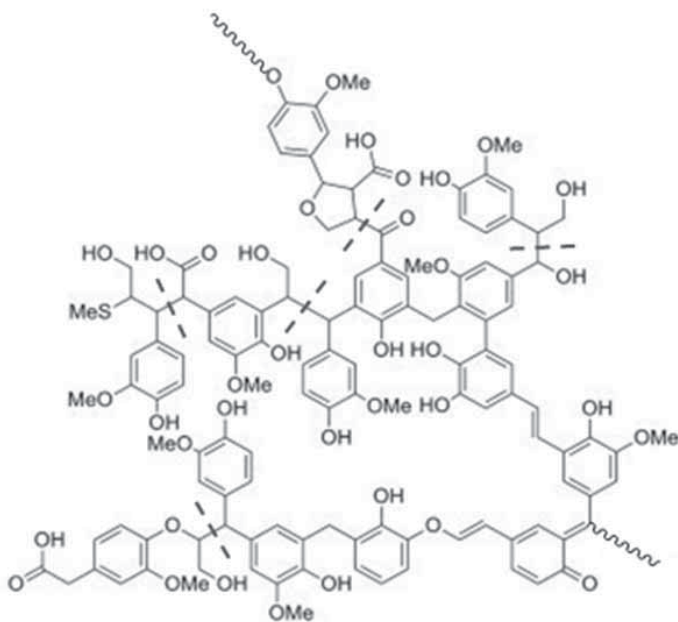


Figure 90. Partial structure of lignin with potential autoxidative cleavages in red. Adapted from Lange et al. (2013).

Note here that autoxidation processes can affect biopolymers (Schmid et al., 2007), lignin (Palmer et al., 1987; Waggoner et al., 2015) and kerogen (Fookes and Walters, 1990), inducing ring opening and chain cleavage (Fig. 90) which can then enhance the bacterial degradation of these

complex structures (Bianchi, 2011; Bianchi and Bauer, 2011; Bianchi et al., 2011). Such interactions could play an important role in the loss of lignin often observed during export of terrestrial organic matter in natural waters (Opsahl and Benner, 1997).

As seen in Chapter 8, some enzymes producing radical species during their catalytic cycle (such as lipoxygenases, peroxidases and laccases) can also initiate autoxidation reactions (Fuchs and Spiteller, 2014). The key role played by lipoxygenases in the induction of autoxidation of higher plant debris in estuaries (Galeron et al., 2018) was detailed in Chapter 13. The metabolism of lignin by some fungi (see next subchapter) offers another nice example of tight interactions between enzymes (peroxidases and laccases) and reactive oxygen species.

The particular case of the ‘enzymatic combustion’ of lignin

Lignin is an aromatic polymer that confers woody plant tissues with rigidity and resistance to biological attack. It represents approximately 20% of plant litter input into the soil (Datta et al., 2017). Due to the lack of hydrolyzable linkages in its complex tridimensional structure, lignin is very recalcitrant to biodegradation processes (Reid, 1995). Only some white-rot fungi (Basidiomycetes) are able to completely mineralize this polymer, which they achieve via a process involving ‘enzymatic combustion’ wherein enzymes generate reactive radical intermediates without direct control of the reactions leading to lignin breakdown (Kirk and Farrell, 1987; Reid, 1995). During this degradation of lignin, the white-rot fungi employ extracellular peroxidases and laccases. Peroxidases include lignin peroxidases (LiPs), Mn-dependent peroxidases (MnPs) and versatile peroxidases (VPs) (Hattaka and Hammel, 2010). LiPs oxidize non-phenolic lignin substructures by abstracting one electron and generating aryl cation radicals that then decompose chemically (Kirk and Farrell, 1987). MnPs oxidize Mn^{2+} to Mn^{3+} which then oxidizes phenolic rings to phenoxyl radicals, leading to the decomposition of the structures (Gold et al., 2000). VPs combine the molecular architecture and properties of LiPs and MnPs. Laccases use molecular oxygen as oxidant, and also oxidize phenolic rings to phenoxyl radicals (Thurston, 1994; Baldrian, 2006). The different aromatic radicals thus formed then evolve through different non-enzymatic reactions, including ether breakdown, aromatic ring cleavage, and demethoxylation. As ligninolytic enzymes are too big to penetrate the compact structure of wood tissues (Martinez et al., 2005), the initial stages of lignin degradation involve non-enzymatic reactions of low-molecular-

weight oxidants, and notably of ROS ($\text{HO}\cdot$, $\text{O}_2^{-\cdot}$, H_2O_2 , $\text{RO}\cdot$, $\text{ROO}\cdot$; Janusz et al. 2017). These different radical species resulting from enzymatic and Fenton (Eq. 14) reactions contribute to the oxidative depolymerization of lignin and its degradation products (Guillen et al. 2000).



CHAPTER SIXTEEN

ENZYMATIC OXIDATION: A POTENTIAL SOURCE OF BIASES IN LIPID OXIDATION ESTIMATES

Oxidation of MUFAs

Fatty acid dioxygenases catalyze the regiospecific and stereospecific insertion of two oxygen atoms into a fatty acid. They include lipoxygenases (LOXs), cyclooxygenases (COXs), heme-containing dioxygenases (DOXs) and α -dioxygenases (α -DOXs), and they produce fatty acid hydroperoxides or endoperoxides (Hamberg et al., 1994; Funk, 2001). Only DOXs have the potential to act on MUFAs and produce mid-chain hydroperoxides able to interfere with auto- and photooxidation products of these fatty acids (see Chapters 5 and 10).

Regiospecific enzymatic peroxidation of the allylic carbon 10 of *cis*-vaccenic acid was previously observed in some strains of AAPs (*Roseobacter* sp. strain BS110, *Roseobacter* sp. strain BS36 and *Erythrobacter* sp. strain MG3; Rontani et al., 2005b; Rontani and Kobližek, 2008) and in the purple sulphur bacterium *Thiohalocapsa halophila* incubated under aerobic conditions in the dark (Marchand et al., 2002). This enzymatic process was attributed to a DOX. The degradation of the 10-hydroperoxyoctadec-11(*cis*)-enoic acid thus formed mainly involves reduction to the corresponding hydroxyacid and cleavage to the corresponding oxoacid. 10-hydroxyoctadec-11(*cis*)-enoic acid likely arising from a similar enzymatic process and the subsequent NaBH₄-reduction of the corresponding hydroperoxyacid and oxoacid was also detected recently in lightened dead cells of *E. huxleyi* contaminated by the AAP *Dinoroseobacter shibae* (Fig. 91; Christopher Burot, unpublished data, 2021). The good correlation ($R^2 = 0.78$) between photooxidative damage in *D. shibae* and the enzymatic production of 10-hydroxyoctadec-11(*cis*)-enoic acid strongly suggests that this activity should play a role in this bacteria's resistance to oxidative stress. Note that in this case the strong dominance of the 10-*cis* isomer among the oxidation products of

cis-vaccenic acid (Fig. 91) clearly indicates its enzymatic origin, and thus serves to avoid overestimation of the abiotic degradation of this MUFA.

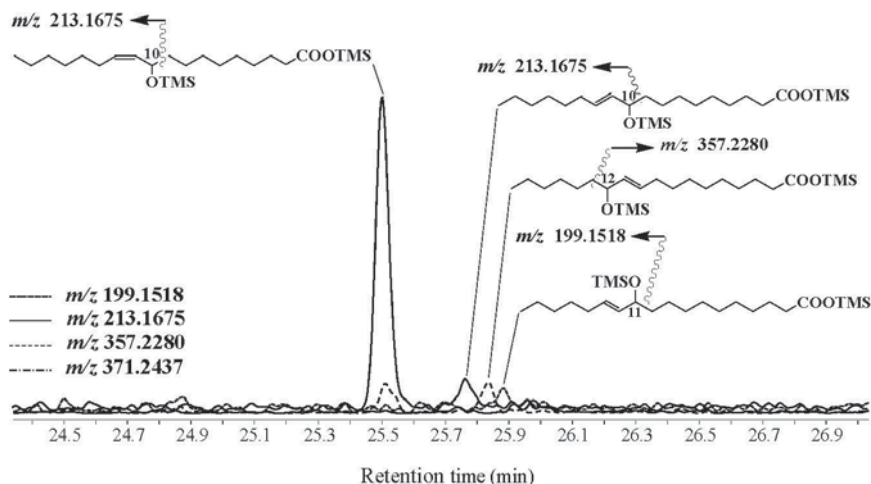


Figure 91. Partial ion chromatograms (m/z 199.1518, 213.1675, 357.2280 and 371.2437) showing the production of DOX and photooxidative oxidation products of *cis*-vaccenic acid in *D. shibae* associated to lightened dead *E. huxleyi* cells.

Type-II photosensitized oxidation and free radical-induced oxidation of Δ^9 MUFAs produce (after NaBH_4 -reduction of hydroperoxyacids) equal proportions of the major 9-*trans* and 10-*trans* isomeric allylic hydroxyacids (Frankel, 1998). However, a 10-hydroxyhexadec-8(*trans*)-enoic acid was previously found to strongly dominate among palmitoleic acid oxidation products observed in sea ice (Fig. 92) and in sinking particles in the Canadian Arctic (Amiriaux et al., 2017; Rontani et al., 2018b), in estuaries of diverse latitudes (Galeron et al., 2018), and also more recently in suspended particles collected in the English Channel (Rontani et al., 2021a).

This dominance was attributed to the involvement of a bacterial 10S-DOX enzyme capable of converting palmitoleic acid to 10(*S*)-hydroperoxyhexadec-8(*trans*)-enoic acid (reduced to the corresponding hydroxyacid during NaBH_4 -reduction). This enzyme was previously isolated from the bacteria *Pseudomonas aeruginosa* 42A2 (Guerrero et al., 1997; Busquets et al., 2004) but has recently also been found in other genera of marine bacteria, such as *Pseudoalteromonas*, *Shewanella* and *Aeromonas* (Shoja Chaghervand, 2019). This 10S-DOX activity seems to

be a detoxification strategy (Martinez et al., 2013; Rontani et al., 2021a) allowing bacteria to survive in the presence of the bactericidal free palmitoleic acid (Desbois et al., 2009; Desbois and Smith, 2010) released by diatoms as part of their well-known oxylipin-based chemical defence against copepods (Pohnert 2000; 2002).

Allylic rearrangement of 10-hydroperoxyhexadec-8(*trans*)-enoic and 9-hydroperoxyhexadec-10(*trans*)-enoic acids affords 8-*trans* and 11-*trans* isomers, respectively (Porter et al., 1995). 10*S*-DOX contribution to oxidation products of palmitoleic acid can thus be easily estimated from the difference between (10-*trans* + 8-*trans*) and (9-*trans* + 11-*trans*) oxidation products (Galeron et al., 2018; Rontani et al., 2018b).

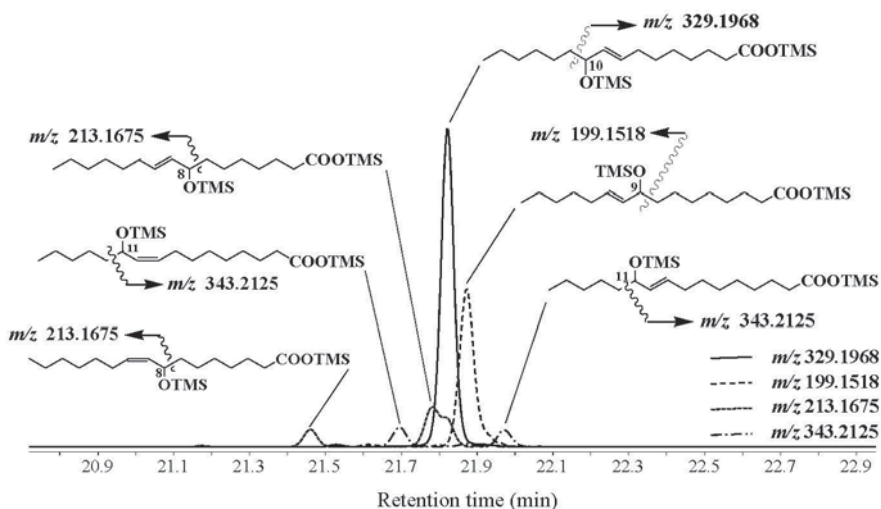


Figure 92. Partial ion chromatograms (*m/z* 199.1518, 213.1675, 329.1968 and 343.2125) showing the production of 10*S*-DOX, photo- and autoxidative oxidation products of palmitoleic acid in sea ice (0–3 cm) collected in Baffin Bay (Arctic) in Summer 2006.

Oxidation of HBI alkenes

Monoxygenases belonging to the cytochrome P450 superfamily can oxidize double bonds to epoxides and saturated carbon atoms to secondary alcohols (Guengerich, 2008). P450-dependent monoxygenases can produce epoxides from a broad range of lipophilic substrates including *n*-alkenes

(Soltani et al., 2004), terpenes (Duetz et al., 2003), unsaturated fatty acids (Ratledge, 1994) and alkenones (Zabeti et al., 2010).

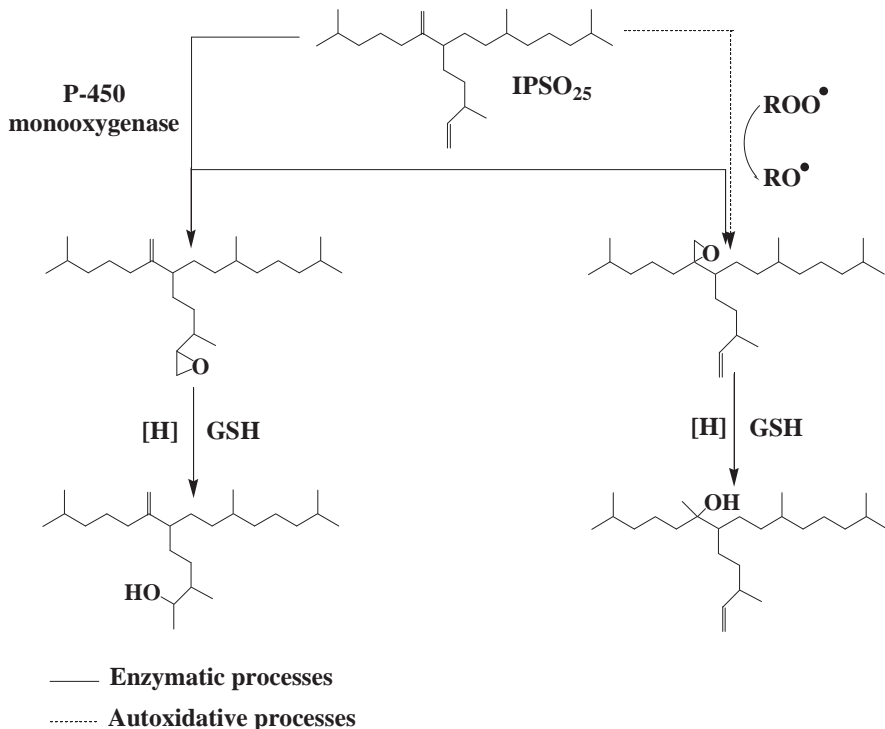


Figure 93. Expected enzymatic and autoxidative attacks of the double bonds of the HBI diene IPSO₂₅. Adapted from Rontani et al. (2019b).

These enzymes are thus able to produce 1,2-epoxy-2-(4-methylpentyl)-3-(3-methylpent-4-enyl)-6,10-dimethylundecane, which is the main autoxidation product of the HBI diene IPSO₂₅ (Fig. 93), and could introduce biases in estimates of the autoxidation of this HBI alkene. However, if bacterial epoxidation really affects IPSO₂₅, then it should act more intensively on the terminal 23–24 double bond (Fig. 93) due to the better proximity of the terminal double bond to the heme iron of cytochrome P450 (Andersen et al., 1997). As we saw in Chapter 15, in sediments, epoxides are quickly reduced to the corresponding alcohols by glutathione transferases (GSTs) (Fig. 93). The lack of the reduction product of the 23–24 epoxide in sediments (whereas the reduction product

of the 6-17 epoxide was present) points to the inefficiency of such bacterial processes on IPSO₂₅ (Rontani et al., 2019b).

Oxidation of dehydroabietic acid

Autoxidation of abietic acid mainly affords 7 α / β -hydroperoxydehydroabietic acids, which are reduced to the corresponding 7 α / β -hydroxyabietic acids after NaBH₄ reduction (see Chapter 10). These compounds were proposed as tracers of autoxidative alteration in gymnosperms (Rontani et al., 2015). Bacteria able to degrade dehydroabietic acid are widely distributed in the environment (Mohn, 1995; Martin et al., 1999; Luchnikova et al., 2019).

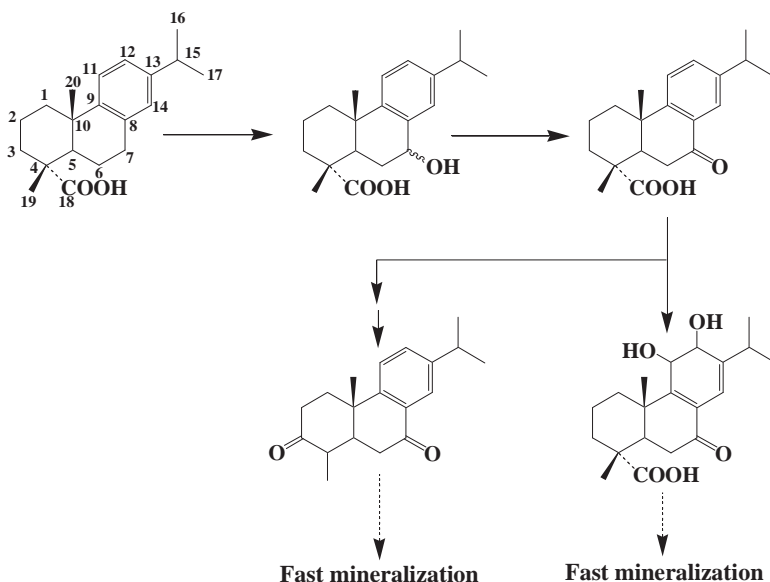


Figure 94. Bacterial metabolism of dehydroabietic acid.

Dehydroabietic acid is first oxidized by an unidentified enzyme at the C-7 position to yield 7-hydroxydehydroabietic acid and then 7-oxodehydroabietic acid (Fig. 94). After NaBH₄ reduction of environmental samples, these bacterial metabolites could thus interfere with dehydroabietic acid autoxidation estimates. However, it is important to note that these metabolites have often been isolated from culture media in the presence of

metabolic inhibitors or additional carbon and energy (e.g. *n*-hexadecane) sources. Without these additions, 7-hydroxydehydroabietic acid and 7-oxodehydroabietic acid are quickly metabolized via: (i) oxidation at C-3 and subsequent decarboxylation, or (ii) dioxygenation of the aromatic ring (Fig. 94; Mohn, 1995; Martin and Mohn, 2000). It thus seems very unlikely that these bacterial metabolites interfere with autoxidation products of dehydroabietic acid.

BIBLIOGRAPHY

- Afi, Latifa, Metzger, Pierre et al., 1996. Bacterial Degradation of Green Microalgae: Incubation of *Chlorella emersonii* and *Chlorella vulgaris* with *Pseudomonas oleovorans* and *Flavobacterium aquatile*. *Organic Geochemistry*, 25, 117-130. doi.org/10.1016/S0146-6380(96)00113-1
- Ahmad, Iqbal, Abbas, Syed H. et al., 2018. Stability-Indicating Photochemical Method for the Assay of Thiamine by Spectrophotometry. *Journal of Spectroscopy*, 2018, 178518. doi.org/10.1155/2018/3178518
- Albers, Carola S., Kattner, Gerhard, Hagen, Wilhem, 1996. The Compositions of Wax Esters, Triacylglycerols and Phospholipids in Arctic and Antarctic Copepods: Evidence of Energetic Adaptations. *Marine Chemistry*, 55, 347-358. doi.org/10.1016/S0304-4203(96)00059-X
- Alberti, Mariza N., Orfanopoulos, Michael, 2006. Stereoelectronic and Solvent Effects on the allylic Oxyfunctionalization of Alkenes with Singlet Oxygen. *Tetrahedron*, 62, 10660-10675. doi.org/10.1016/j.tet.2006.07.106
- Alberti, Mariza N., Vassilikogiannakis, Georgios, Orfanopoulos, Michael, 2008. Stereochemistry of the Singlet Oxygenation of Simple Alkenes: A Stereospecific Transformation. *Organic Letters*, 10, 3997-4000. doi.org/10.1021/ol801488w
- Alberti, Mariza N., Orfanopoulos, Michael, 2010. Recent Mechanistic Insights in the Singlet Oxygen Ene Reaction. *Synlett*, 7, 999-1026. doi: 10.1055/s-0029-1219790
- Alou-Font, Eva, Roy, Suzanne et al., 2016. Cell Viability, Pigments and Photosynthetic Performance of Arctic Phytoplankton in Contrasting Ice-Covered and Open-Water Conditions during the Spring-Summer Transition. *Marine Ecology Progress Series*, 543, 89-106. doi.org/10.3354/meps11562
- Amate Yolanda, Garcia-Granados Andr es et al., 1991. Biotransformation of 6 β -Eudesmanolides Functionalized at C-3 with *Curvularia lunata* and *Rhizopus nigricans* Cultures. *Tetrahedron*, 47, 5811-5818. doi.org/10.1016/S0040-4020(01)86531-5

- Amiraux, Rémi, Jeanthon, Christian et al., 2016. Paradoxical Effects of Temperature and Solar Irradiance on the Photodegradation State of Killed Phytoplankton. *Journal of Phycology*, 52, 475-485.
doi.org/10.1111/jpy.12410
- Amiraux, Rémi, Belt, Simon T. et al., 2017. Monitoring Photooxidative and Salinity-Induced Bacterial Stress in the Canadian Arctic Using Specific Lipid Tracers. *Marine Chemistry*, 194, 89-99.
doi.org/10.1016/j.marchem.2017.05.006
- Amorati, Riccardo, Baschieri, Andrea, Valgimigli, Luca, 2017. Measuring Antioxidant Activity in Bioorganic Samples by the Differential Oxygen Uptake Apparatus: Recent Advances. *Journal of Chemistry*, 6369358. doi.org/10.1155/2017/6369358
- Andersen, Melvin E., Eklund, Christopher R. et al., 1997. A Multicompartment Geometric Model of the Liver in Relation to Regional Induction of Cytochrome P450s. *Toxicology and Applied Pharmacology*, 144, 135-144. doi.org/10.1006/taap.1996.8066
- Andersson, Bengt A., Holman, Ralph T., 1974. Pyrrolidides for Mass Spectrometric Determination of the Position of the Double Bond in Monounsaturated Fatty Acids. *Lipids*, 9, 185-190.
doi.org/10.1007/BF02532690
- Andrady, Anthony L., Aucamp, Pieter J. et al., 2012. Environmental Effects of Ozone Depletion and its Interactions with Climate Change: Progress Report, 2011. *Photochemical and Photobiological Sciences*, 11, 13-27. doi.org/10.1039/c1pp90033a
- Arand, Michael, Cronin, Annette et al., 2005. Epoxide Hydrolases: Structure, Function, Mechanism, and Assay. *Methods in Enzymology*, 400, 569-588. doi.org/10.1016/S0076-6879(05)00032-7
- Aringer, Leif, Eneroth, Peter, 1974. Formation and Metabolism In Vitro of 5,6-Epoxides of Cholesterol and β -Sitosterol. *Journal of Lipid Research*, 15, 389-398. doi.org/10.1016/S0022-2275(20)36787-0
- Auby, Isabelle, 1991. Contribution à l'Etude des Herbiers de *Zostera noltii* du Bassin d'Arcachon : Dynamique, Production et Dégradation, Macrofaune Associée. PhD diss., Université de Bordeaux I.
- Baier, Jürgen, Maier, Max et al., 2005. Time-Resolved Investigations of Singlet Oxygen Luminescence in Water, in Phosphatidylcholine, and in Aqueous Suspensions of Phosphatidylcholine or HT29 Cells. *Journal of Physical Chemistry B*, 109, 3041-3046.
doi.org/10.1021/jp0455531
- Baldrian, Petr, 2006. Fungal Laccases – Occurrence and Properties. *FEMS Microbiology Reviews*, 30, 215-242.
doi.org/10.1111/j.1574-4976.2005.00010.x

- Bale, Nicole J., Airs, Ruth L. et al., 2013. Transformation of Chlorophyll a during Viral Infection of *Emiliania huxleyi*. *Aquatic Microbial Ecology*, 69, 205-210. doi.org/10.3354/ame01640
- Barry, Roger G., Arundale, Wendy H. et al., 1977. Environmental Change and Cultural Change in the Eastern Canadian Arctic during the Last 5000 Years. *Arctic and Alpine Research*, 9, 193-210. doi.10.1080/00040851.1977.12003914
- Belt, Simon T., Allard, W. Guy et al., 2000. Highly Branched Isoprenoids (HBIs): Identification of the Most Common and Abundant Sedimentary Isomers. *Geochimica et Cosmochimica Acta*, 64, 3839-3851. doi.org/10.1016/S0016-7037(00)00464-6
- Belt, Simon T., Müller, Juliane, 2013. The Arctic Sea Ice Biomarker IP₂₅: a Review of Current Understanding, Recommendations for Future Research and Applications in Palaeo Sea Ice Reconstructions. *Quaternary Science Reviews*, 79, 9-25. doi.org/10.1016/j.quascirev.2012.12.001
- Belt, Simon T., Smik, Lukas et al., 2016. Source Identification and Distribution Reveals the Potential of the Geochemical Antarctic Sea Ice Proxy IPSO₂₅. *Nature Communications*, 7, 12655. doi: 10.1038/ncomms12655
- Belt, Simon T., 2018. Source-Specific Biomarkers as Proxies for Arctic and Antarctic Sea Ice. *Organic Geochemistry*, 125, 277-298. doi.org/10.1016/j.orggeochem.2018.10.002
- Berkessel, Albrecht, 2014. "Science of Synthesis: Houben-Weyl Methods of Molecular Transformations". In *Peroxides*, edited by Thieme, Georg, 75. Stuttgart: Springer Verlag.
- Beutner, Stephan, Bloedorn, Britta et al., 2000. Synthetic Singlet Oxygen Quenchers. *Methods in Enzymology*, 329, 226-241. doi.org/10.1016/S0076-6879(00)19024-X
- Bhattacharjee, Soumen, 2014. Membrane Lipid Peroxidation and its Conflict of Interest: the Two Faces of Oxidative Stress. *Current Science*, 107, 1811-1823.
- Bianchi, Thomas S., Findlay, Stuart, Dawson, Rodger, 1993. Organic Matter Sources in the Water Column and Sediments of the Hudson River Estuary: the Use of Plant Pigments as Tracers. *Estuarine Coastal and Shelf Research*, 36, 359-376. doi.org/10.1006/ecss.1993.1022
- Bianchi, Thomas S., 2011. The Role of Terrestrially Derived Organic Carbon in the Coastal Ocean: A Changing Paradigm and the Priming Effect. *PNAS*, 108, 19473-19481. doi.org/10.1073/pnas.1017982108
- Bianchi Thomas S., Bauer, James E., 2011. « Particulate Organic Carbon Cycling and Transformation ». In *Treatise on Estuarine and Coastal*

- Science*, edited by E. Wolanski and D. S. MacLusky, 69–117. Waltham: Academic Press. doi. 10.1016/B978-0-12-374711-2.00503-9
- Bianchi, Thomas S., Wizocki, Laura A. et al., 2011. Sources of Terrestrial Organic Carbon in the Mississippi Plume Region: Evidence for the Importance of Coastal Marsh Inputs. *Aquatic Geochemistry*, 17, 431-456. doi.org/10.1007/s10498-010-9110-3
- Bidle, Kay D., Falkowski, Paul G., 2004. Cell Death in Planktonic, Photosynthetic Microorganisms. *Nature Reviews Microbiology*, 2, 643–655. doi.org/10.1038/nrmicro956
- Blanchet, Marine, Fernandez, Camila, Joux, Fabien, 2016. Photoreactivity of Riverine and Phytoplanktonic Dissolved Organic Matter and its Effects on the Dynamics of a Bacterial Community from the Coastal Mediterranean Sea. *Progress in Oceanography*, 163, 82-93. doi.org/10.1016/j.pocean.2017.03.003
- Boon, Caitlyn S., McClements, D. Julian et al., 2010. Factors Influencing the Chemical Stability of Carotenoids in Foods. *Critical Reviews in Food Science and Nutrition*, 50, 515-532. doi.org/10.1080/10408390802565889
- Brassell, Simon C., Eglinton, Geoffrey, Maxwell, James R., 1983. The Geochemistry of Terpenoids and Steroids. *Biochemical Society Transactions*, 1, 575-586. doi.org/10.1042/bst0110575
- Brassell, Simon C., Eglinton, Geoffrey et al., 1986. Molecular Stratigraphy: a New Tool for Climatic Assessment. *Nature*, 320, 129-133. doi.org/10.1038/320129a0
- Britton, George, 1995. Structure and Properties of Carotenoids in Relation to Function. *The FASEB Journal*, 9, 1551-1558. doi.org/10.1096/fasebj.9.15.8529834
- Brocks, Jochen J., Logan, Graham A. et al., 1999. Archean Molecular Fossils and the Early Rise of Eukaryotes. *Science*, 285, 1033-1036. doi.org/10.1126/science.285.5430.1033
- Brocks, Jochen J., Pearson, Ann, 2005. Building the Biomarker Tree of Life. *Reviews in Mineralogy and Geochemistry*, 59, 233-258. doi.org/10.2138/rmg.2005.59.10
- Brocks, Jochen J., Love, Gordon D. et al., 2005. Biomarker Evidence for Green and Purple Sulphur Bacteria in a Stratified Palaeoproterozoic Sea. *Nature*, 437, 866–870. doi.org/10.1038/nature04068
- Brooks, James D., Gould, Kenneth A., Smith, John W., 1969. Isoprenoid Hydrocarbons in Coal and Petroleum. *Nature*, 222, 257-259. doi.org/10.1038/222257a0

- Budzikiewicz, Herbert, Wilson, James M., Djerassi, Carl, 1963. Mass Spectrometry in Structural and Stereochemical Problems. XXXII.1 Pentacyclic Triterpenes. *Journal of the American Chemical Society*, 85, 3688-3699. doi.org/10.1021/ja00905a036
- Burot, Christopher, Amiraux, Rémi et al., 2021. Viability and Stress State of Bacteria Associated with Primary Production or Zooplankton-Derived Suspended Particulate Matter in Summer along a Transect in Baffin Bay (Arctic Ocean). *Science of the Total Environment*, 770, 145252. doi.org/10.1016/j.scitotenv.2021.145252
- Busquets, Montserrat, Deroncelé, Victor et al., 2004. Isolation and Characterization of a Lipoyxygenase from *Pseudomonas* 42A2 Responsible for the Biotransformation of Oleic Acid into (S)-(E)-10-hydroxy-8-octadecenoic acid. *Antonie van Leeuwenhoek*, 85, 129–139. doi.org/10.1023/B:ANTO.0000020152.15440.65
- Cadenas, Enrique, 1989. Biochemistry of Oxygen Toxicity. *Annual Review of Biochemistry*, 58, 79-110. doi.org/10.1146/annurev.bi.58.070189.000455
- Caumette, Pierre, Salvado, Juan-Carlos, 2001. Characterization of the Sampling Sites and Description of the Microbial Mats Investigated. First Scientific Progress Report of the MATBIOPOL European Project (Contract EVK3-CT-1999- 11800010), pp. 12–16.
- Chaki, Mounira, Begara-Morales, Juan C., Barroso, Juan B., 2020. Oxidative Stress in Plants. *Antioxidants*, 9, 481. doi.org/10.3390/antiox9060481
- Choudhury, Shuvasish, Panda, Piyalee et al., 2013. Reactive Oxygen Species Signaling in Plants under Abiotic Stress. *Plant Signaling & behavior*, 8, e23681. doi.org/10.4161/psb.23681
- Christodoulou, Stéphane, Marty, Jean-Claude et al., 2009. Use of Lipids and their Degradation Products as Biomarkers for Carbon Cycling in the Northwestern Mediterranean Sea. *Marine Chemistry*, 113, 25-40. doi.org/10.1016/j.marchem.2008.11.003
- Christodoulou, Stéphane, Joux, Fabien et al., 2010. Comparative Study of UV and Visible Light Induced Degradation of Lipids in Non-Axenic Senescent Cells of *Emiliania huxleyi*. *Marine Chemistry*, 119, 139-152. doi.org/10.1016/j.marchem.2010.01.007
- Clennan, Edward L., 1991. Synthetic and Mechanistic Aspects of 1,3-Diene Photooxidation. *Tetrahedron*, 47, 1343-1382. doi.org/10.1016/S0040-4020(01)86413-9
- Clough, Roger, L., Yee, B. G., Foote, Christopher S., 1979. Chemistry of Singlet oxygen. 30. The Unstable Primary Product of Tocopherol

- Photooxidation. *Journal of the American Chemical Society*, 101, 683-686. doi.org/10.1021/ja00497a033
- Collins, James R., Fredericks, Helen F. et al., 2018. The Molecular Products and Biogeochemical Significance of Lipid Photooxidation in West Antarctic Surface Waters. *Geochimica et Cosmochimica Acta*, 232, 234-244. doi.org/10.1016/j.gca.2018.04.030
- Cosgrove, John P., Church, Daniel F., Pryor, William A., 1987. The Kinetics of the Autoxidation of Polyunsaturated Fatty Acids. *Lipids*, 22, 299-304. doi.org/10.1007/BF02533996
- Costa, Maria Sofia, Rego, Adriana et al., 2015. The Conifer Biomarkers Dehydroabietic and Abietic Acids are Widespread in Cyanobacteria. *Scientific Reports*, 6, 23436. doi.10.1038/srep23436.
- Cranwell, Peter A., 1978. Extractable and Bound Lipid Components in a Freshwater Sediment. *Geochimica and Cosmochimica Acta*, 10, 1523-1532. doi.org/10.1016/0016-7037(78)90023-6
- Cueva, Carolina, Silva, Mariana et al., 2020. Interplay between Dietary Polyphenols and Oral and Gut Microbiota in the Development of Colorectal Cancer. *Nutrients*, 12, 65. doi.org/10.3390/nu12030625
- Cuny, Philippe, Rontani, Jean-François, 1999. On the Widespread Occurrence of 3-Methylidene-7,11,15-trimethylhexadecan-1,2-diol in the Marine Environment: a Specific Isoprenoid Marker of Chlorophyll Photodegradation. *Marine Chemistry*, 65, 155-165. doi.org/10.1016/S0304-4203(98)00093-0
- Cuny, Philippe, Romano, Jean-Claude et al., 1999. Comparison of the Photodegradation Rates of Chlorophyll Chlorin Ring and Phytol Side Chain in Phytodetritus: is the Phytyldiol Versus Phytol Ratio (CPPI) a New Biogeochemical Index? *Journal of Experimental Marine Biology and Ecology*, 237, 271-290. doi.org/10.1016/S0022-0981(99)00010-6
- Datta, Rahul, Kelkar, Aditi et al., 2017. Enzymatic Degradation of Lignin in Soil: A Review. *Sustainability*, 9, 1163. doi.org/10.3390/su9071163
- Davies, Michael J., 2005. The Oxidative Environment and Protein Damage. *Biochimica et Biophysica Acta (BBA) - Proteins and Proteomics*, 1703, 93-109. doi.org/10.1016/j.bbapap.2004.08.007
- De Leeuw, Jan W., Van der Meer, Francine W. et al., 1980. On the Occurrence and Structural Identification of Long Chain Unsaturated Ketones and Hydrocarbons in Sediments. *Physics and Chemistry of the Earth*, 12, 211-217. doi.org/10.1016/0079-1946(79)90105-8
- Desbois, Andrew P., Mearns-Sragg, Andrew, Smith, Valerie J., 2009. A Fatty Acid from the Diatom *Phaeodactylum tricornutum* is Antibacterial against Diverse Bacteria Including Multi-resistant *Staphylococcus aureus* (MRSA). *Marine Biotechnology*, 11, 45-52.

- doi.org/10.1007/s10126-008-9118-5
- Desbois, Andrew P., Smith, Valerie J., 2010. Antibacterial Free Fatty Acids: Activities, Mechanisms of Action and Biotechnological Potential. *Applied Microbiology and Biotechnology*, 85, 1629–1642. doi.org/10.1007/s00253-009-2355-3
- Des Marais, David J., 2010. “Marine Hypersaline *Microcoleus*-Dominated Cyanobacterial Mats in the Saltern at Guerrero Negro, Baja California Sur, Mexico: A System-Level Perspective”. In *Microbial Mats*, edited by Joseph Seckbach and Aharon Ore, 401-420. Dordrecht: Springer.
- Devasagayam, Thomas P. A., Kamat, Jayashree P., 2002. Biological Significance of Singlet Oxygen. *Indian Journal of Experimental Biology*, 40, 680–692.
- Dias Cavalcante, Ana K., Martinez, Glauca R. et al., 2002. Cytotoxicity and Mutagenesis Induced by Singlet Oxygen in Wild Type and DNA Repair Deficient *Escherichia coli* Strains. *DNA Repair*, 1, 1051-1056. doi.org/10.1016/S1568-7864(02)00164-7
- Didyk, Borys M., Simoneit Bernd R. T. et al., 1978. Organic Geochemical Indicators of Palaeoenvironmental Conditions of Sedimentation. *Nature*, 272, 216-222. doi.org/10.1038/272216a0
- Dmitrieva, Valeriya, Tyutereva, Elena V., Voitsekhovskaja, Olga V., 2020. Singlet Oxygen in Plants: Generation, Detection, and Signaling Roles. *International Journal of Molecular Sciences*, 21, 3237. doi.org/10.3390/ijms21093237
- Doménech-Carbò, Maria Teresa, Kuckova, Stepanka et al., 2006. Study of the Influencing Effect of Pigments on the Photoageing of Terpenoid Resins Used as Pictorial Media. *Journal of Chromatography A*, 1121, 248-258. doi.org/10.1016/j.chroma.2006.04.005
- Dubois, Nolween, Barnathan, Gilles et al., 2009. Gas chromatographic Behavior of Fatty Acid Derivatives for Mass Spectrometry on Low-Polarity Capillary Columns. *European Journal of Lipid Science and Technology*, 111, 688-697. doi.org/10.1002/ejlt.200800148
- Duetz Wouter A., Bouwmeester Harro, et al., 2003. Biotransformation of Limonene by Bacteria, Fungi, Yeasts and Plants. *Applied Microbiology and Biotechnology*, 61, 269-277. doi.org/10.1007/s00253-003-1221-y
- Ehrenberg, Benjamin, Anderson, Jamey L., Foote, Christopher S., 1998. Kinetics and Yield of Singlet Oxygen Photosensitized by Hypericin in Organic and Biologic Media. *Photochemistry and Photobiology*, 68, 135-140. doi.org/10.1111/j.1751-1097.1998.tb02479.x
- Elliott, Ashley, Mundy, Christopher J. et al., 2015. Spring Production of Mycosporine-Like Amino Acids and other UV-Absorbing Compounds

- in Sea Ice-Associated Algae Communities in the Canadian Arctic. *Marine Ecology Progress Series*, 541, 91-104.
doi.org/10.3354/meps11540
- Eltgroth, Matthew L., Watwood, Robin L., Wolfe, Gordon V., 2005. Production and Cellular Localization of Neutral Long-Chain Lipids in the Haptophyte Algae *Isochrysis galbana* and *Emiliania huxleyi*. *Journal of Phycology*, 41, 1000-1009.
doi.org/10.1111/j.1529-8817.2005.00128.x
- Engel, Norbert, Jenny, Titus A. et al., 1991. Chlorophyll Catabolism in *Chlorella protothecoides* Isolation and Structure Elucidation of a Red Bilin Derivative. *FEBS Letters*, 293, 131-133. doi.org/10.1016/0014-5793(91)81168-8
- Evershed, Richard, 1993. Biomolecular Archaeology and Lipids. *World Archaeology*, 25, 74-93. doi.org/10.1080/00438243.1993.9980229
- Farr, Spencer B., Kogoma, Tokio, 1991. Oxidative Stress Responses in *Escherichia coli* and *Salmonella typhimurium*. *Microbiology and Molecular Biology Reviews*, 55, 561-585.
- Fay, Laurent, Richli, Urs, 1991. Location of Double Bonds in Polyunsaturated Fatty Acids by Gas chromatography-Mass Spectrometry after 4,4-Dimethylloxazoline Derivatization. *Journal of Chromatography A*, 541, 9-98.
doi.org/10.1016/S0021-9673(01)95986-2
- Fiedor, Joanna, Fiedor, Leszec et al., 2005. Cyclic Endoperoxides of β -Carotene, Potential Pro-oxidants, as Products of Chemical Quenching of Singlet Oxygen. *Biochimica et Biophysica Acta – Bioenergetics*, 1709, 1-4. doi.org/10.1016/j.bbabi.2005.05.008
- Fischer, Beat B., Krieger-Liszkay, Anja et al., 2007. Role of Singlet Oxygen in Chloroplast to Nucleus Retrograde Signaling in *Chlamydomonas reinhardtii*. *FEBS Letters*, 581, 5555–5560.
doi.org/10.1016/j.febslet.2007.11.003
- Fookes, Christopher J. R., Walters, Cherie K., 1990. A Chemical Investigation of Shale Oil Ageing. *Fuel*, 69, 1105-1108.
doi.org/10.1016/0016-2361(90)90063-V
- Foote, Christopher S., 1976. "Photosensitized Oxidation and Singlet Oxygen: Consequences in Biological Systems". In *Free Radicals in Biology*, edited by William A. Pryor, 85-133. New York: Academic Press.
- Fossey, Jacques, Lefort, Daniel, Sorba, Jeanine, 1995. *Free Radicals in Organic Chemistry*. Paris: Masson.
- Foti, Mario C., 2007. Antioxidant Properties of Phenols. *Journal of Pharmacy and Pharmacology*, 59, 1673-1685.

- doi.org/10.1211/jpp.59.12.0010
- Frankel, Edwin N., Neff, William E., Bessler, Terry R., 1979. Analysis of Autoxidized Fats by Gas Chromatography-Mass Spectrometry: V. Photosensitized Oxidation. *Lipids*, 14, 961–967. doi.org/10.1007/BF02533431
- Frankel, Edwin N., 1984. Lipid Oxidation: Mechanisms, Products and Biological Significance. *Journal of the American Oil Chemist's Society*, 61, 1908-1917. doi.org/10.1007/BF02540830
- Frankel, Edwin N., 1998. *Lipid oxidation*. Dundee: The Oily Press.
- Franklin, Daniel J., Airs, Ruth L. et al., 2012. Identification of Senescence and Death in *Emiliania huxleyi* and *Thalassiosira pseudonana*: Cell Staining, Chlorophyll Alterations, and Dimethylsulfoniopropionate (DMSP) Metabolism. *Limnology and Oceanography*, 57, 305-317. doi.org/10.4319/lo.2012.57.1.0305
- Freeman, Katherine H., Wakeham, Stuart G., 1992. Variations in the Distributions and Isotopic Composition of Alkenones in Black Sea Particles and Sediments. *Organic Geochemistry*, 19, 277-285. doi.org/10.1016/0146-6380(92)90043-W
- Frimer, Aryeh A., 1979. The Reaction of Singlet Oxygen with Olefins: the Question of Mechanism. *Chemical Review*, 79, 359-387. doi.org/10.1021/cr60321a001
- Fuchs, Claus, Spiteller, Gerhard, 2014. Iron Release from the Active Site of Lipoxygenase. *Zeitschrift für Naturforschung C*, 55, 643-648.
- Funk, Colin D., 2001. Prostaglandins and Leukotrienes: Advances in Eicosanoid Biology. *Science*, 294, 1871-1875. doi.org/10.1126/science.294.5548.1871
- Furtado, Nije A. J. C., Pirson, Laeticia et al., 2017. Pentacyclic Triterpene Bioavailability: An Overview of In Vitro and In Vivo Studies. *Molecules*, 22, 400. doi.org/10.3390/molecules22030400
- Galeron, Marie-Aimée, Amiraux, Rémi et al., 2015. Seasonal Survey of the Composition and Degradation State of Particulate Organic Matter in the Rhône River Using Lipid Tracers *Biogeosciences*, 12, 1431-1446. doi.org/10.5194/bg-12-1431-2015
- Galeron, Marie-Aimée, Volkman, John K., Rontani, Jean-François, 2016a. Oxidation Products of Betulin: New Tracers of Abiotic Degradation of Higher Plant Material in the Environment. *Organic Geochemistry*, 91, 31-42. doi.org/10.1016/j.orggeochem.2015.10.010
- Galeron, Marie-Aimée, Vaultier, Frédéric, Rontani, Jean-François, 2016b. Oxidation Products of α - and β -Amyrins: Potential Tracers of Abiotic Degradation of Vascular-Plant Organic Matter in Aquatic Environments. *Environmental Chemistry*, 15237.

- doi.org/10.1071/EN15237
- Galeron Marie-Aimée, Radakovitch Olivier et al., 2016c. Metal Ions and Hydroperoxide Content: Main Drivers of Lipid Autoxidation in River Suspended Particulate Matter and Higher Plant Debris? *Journal of Marine Science and Engineering*, 4, 50. doi:10.3390/jmse4030050
- Galeron, Marie-Aimée, Radakovitch, Olivier et al., 2017. Autoxidation as a Major Player in the Fate of Terrestrial Particulate Organic Matter in Seawater. *JGR Biogeosciences*, 122, 1203-1215. doi.org/10.1002/2016JG003708
- Galeron Marie-Aimée, Radakovitch Olivier et al., 2018. Lipoyxygenase-Induced Autoxidative Degradation of Terrestrial Particulate Organic Matter in Estuaries: A Widespread Process Enhanced at High and Low Latitude. *Organic Geochemistry*, 115, 78-92. doi.org/10.1016/j.orggeochem.2017.10.013
- Galliard, Terence, Phillips, David R., Reynolds, John, 1976. The Formation of Cis-3-Nonenal, Trans-2-Nonenal and Hexanal from Linoleic Acid Hydroperoxide Isomers by a Hydroperoxide Cleavage Enzyme System in Cucumber (*Cucumis sativus*) Fruits. *Biochimica et Biophysica Acta*, 441, 181-192. doi.org/10.1016/0005-2760(76)90161-2
- Galliard, Terence, Chan, Henry W.-S., 1980. "Lipoyxygenases". In *The Biochemistry of Plants: a Comprehensive Treatise*, edited by P. K. Stumpf, 131-161. New York: Academic Press. doi.org/10.1016/B978-0-12-675404-9.50011-4
- Garcia-Pichel, Ferran, 1994. A Model for Internal Self-Shading in Planktonic Organisms and its Implications for the Usefulness of Ultraviolet Sunscreens. *Limnology and Oceanography*, 39, 1704-1717. doi.org/10.4319/lo.1994.39.7.1704
- Gelin, François, Boogers, Ilco et al., 1997. Resistant Biomacromolecules in Marine Microalgae of the Classes Eustigmatophyceae and Chlorophyceae: Geochemical Implications. *Organic Geochemistry*, 26, 659-675. doi.org/10.1016/S0146-6380(97)00035-1
- Giese, Arthur C., 1980. Photosensitization of Organisms, with Special Reference to Natural Photosensitizers. *Lasers in Biology and Medicine*, 299-314. doi.org/10.1007/978-1-4684-8550-9_19
- Gillan, Franck T., Sandstrom, Mark W., 1985. Microbial Lipids from a Nearshore Sediment from Bowling Green Bay, North Queensland: The Fatty Acid Composition of Intact Lipid Fractions. *Organic Geochemistry*, 8, 321-328. doi.org/10.1016/0146-6380(85)90011-7

- Girotti, Albert W., 1998. Lipid Hydroperoxide Generation, Turnover, and Effector Action in Biological Systems. *Journal of Lipid Research*, 39, 1529-1542. doi.org/10.1016/S0022-2275(20)32182-9
- Glaeser, Stefanie P., Grossart, Hans-Peter, Glaeser, Jens, 2012. Singlet Oxygen, a Neglected but Important Environmental Factor: Short-Term and Long-Term Effects on Bacterioplankton Composition in a Humic Lake. *Environmental Microbiology*, 12, 3124-3136. doi.org/10.1111/j.1462-2920.2010.02285.x
- Glaeser, Stefanie P., Berghoff, Bork A. et al., 2014. Contrasting Effects of Singlet Oxygen and Hydrogen Peroxide on Bacterial Community Composition in a Humic Lake. *Plos One*, 9, e2518. doi.org/10.1371/journal.pone.0092518
- Goad, L. John, Akihisa, Toshihiro, 1997. "Mass Spectrometry of Sterols". In *Analysis of Sterols*, edited by L. John Goad and Toshihiro Akihisa, 152-196. Dordrecht: Springer.
- Golbach, Jennifer L., Ricke, Steven C. et al., 2014. Riboflavin in Nutrition, Food Processing, and Analysis - A Review. *Journal of Food research*, 3, 23-35. doi: 10.5539/jfr.v3n6p23
- Gold, Michael H., Youngs, Heather L., Sollewijn Gelpke, Maarten D., 2000. "Manganese Peroxidases". In *Metal Ions in Biological Systems*, edited by Helmut Sigel, 558-586. Boca Raton: CRC Press. doi.org/10.1201/9781482289893
- Gollnick, Klaus, 1968. Type II Photooxygenation Reactions in Solution. *Advances in Photochemistry*, 6, 1.
- Gong, Changrui, Hollander, David J., 1999. Evidence for Differential Degradation of Alkenones under Contrasting Bottom Water Oxygen Conditions: Implication for Paleotemperature Reconstruction. *Geochimica et Cosmochimica Acta*, 63, 405-411. doi.org/10.1016/S0016-7037(98)00283-X
- Graça, José, Schreiber, Lukas, 2002. Glycerol and Glyceryl Esters of ω-Hydroxyacids in Cutins. *Phytochemistry*, 61, 205-215. doi.org/10.1016/S0031-9422(02)00212-1
- Griesbeck, Axel G., Adam, Waldemar et al., 2003. Photooxygenation of Allylic Alcohols: Kinetic Comparison of Unfunctionalized alkenes with Prenol-Type Allylic Alcohols, Ethers and Acetates. *Photochemistry Photobiology Sciences*, 2, 877-881. doi.org/10.1039/B302255B
- Guengerich, F. Peter, 2008. Cytochrome P450 and Chemical Toxicology. *Chemical Research in Toxicology*, 21, 70-83. doi.org/10.1021/tx700079z

- Guerrero, Angel, Casals, Isidre et al., 1997. Oxydation of Oleic Acid to (*E*)-10-hydroperoxy-8-octadecenoic and (*E*)-10-hydroxy-8-octadecenoic acids by *Pseudomonas* sp. 42A2. *Biochimica et Biophysica Acta (BBA) - Lipids and Lipid Metabolism*, 1347, 75-81. doi.org/10.1016/S0005-2760(97)00056-8
- Guillén, Francisco, Gómez-Toribio, Víctor et al., 2000. Production of Hydroxyl Radical by the Synergistic Action of Fungal Laccase and Aryl Alcohol Oxidase. *Archives of Biochemistry and Biophysics*, 383, 142-147. doi.org/10.1006/abbi.2000.2053
- Guo, Jingjing, Glendell, Miriam et al., 2020. Assessing Branched Tetraether Lipids as Tracers of Soil Organic Carbon Transport through the Carminowe Creek Catchment (Southwest England). *Biogeosciences*, 17, 3183-3201. doi.org/10.5194/bg-17-3183-2020
- Haag, Werner R., Mill, Theodore, 1988. Effect of a Subsurface Sediment on Hydrolysis of Haloalkanes and Epoxides. *Environmental Science and Technology*, 22, 658-663. doi.org/10.1021/es00171a007
- Halket, John M., Zaikin, Vladimir G., 2003. Review: Derivatization in Mass Spectrometry—1. Silylation. *European Journal of Mass Spectrometry*, 9, 1-21. doi.10.1255/ejms.527
- Halliwell, Barry, 1987. Oxidative Damage, Lipid Peroxidation and Antioxidant Protection in Chloroplasts. *Chemistry and Physics of lipids*, 44, 327-340. doi.org/10.1016/0009-3084(87)90056-9
- Hamberg, Mats, Zhang, Lian-Ying et al., 1994. Sequential Oxygenation of Linoleic Acid in the Fungus *Gaeumannomyces graminis*: Stereochemistry of Dioxygenase and Hydroperoxide Isomerase Reactions. *Archives of Biochemistry and Biophysics*, 309, 77-80. doi.org/10.1006/abbi.1994.1087
- Harbour, John R., Bolton, James R., 1978. The Involvement of the Hydroxyl Radical in the Destructive Photooxidation of Chlorophylls In Vivo and In Vitro. *Photochemistry and Photobiology*, 28, 231-234. doi.org/10.1111/j.1751-1097.1978.tb07700.x
- Harrison, Paul G., 1982. Control of Microbial Growth and of Amphipod Grazing by Water-Soluble Compounds from Leaves of *Zostera marina*. *Marine Biology*, 67, 225-230. doi.org/10.1007/BF00401288
- Harvey, David J., Vouros, Paul, 1979. Influence of the 6-Trimethylsilyl Group on the Fragmentation of the Trimethylsilyl Derivatives of some 6-Hydroxy- and 3,6-Dihydroxy-steroids and Related Compounds. *Biomedical Mass Spectrometry*, 6, 135-143. doi.org/10.1002/bms.1200060402

- Harvey, David J., 1982. Picolinyl Esters as Derivatives for the Structural Determination of Long Chain Branched and Unsaturated Fatty acids. *Biomedical Mass Spectrometry*, 9, 33-38. doi.org/10.1002/bms.1200090107
- Harvey, David J., Vouros, Paul, 2020. Mass Spectrometric Fragmentation of Trimethylsilyl and Related Alkylsilyl Derivatives. *Mass Spectrometry Reviews*, 39, 105-211. doi.org/10.1002/mas.21590
- Harwood, John L., Russell, Nicholas J., 1984. *Lipids in Plants and Microbes*. Dordrecht: Springer. doi.org/10.1007/978-94-011-5989-0_2
- Hattaka, Annele, Hammel, Kenneth E., 2010. "Fungal Biodegradation of Lignocelluloses". In *Industrial Applications. The Mycota (A Comprehensive Treatise on Fungi as Experimental Systems for Basic and Applied Research)*, edited by M. Hofrichter, 319-340. Berlin, Heidelberg: Springer. doi.org/10.1007/978-3-642-11458-8_15
- He, Yu-Ying, Häder, Donat-P., 2002. Reactive Oxygen Species and UV-B: Effect on Cyanobacteria. *Photochemistry Photobiology Sciences*, 1, 729-736. doi.org/10.1039/B110365M
- Hebting, Yanek, Schaeffer, Philippe et al., 2006. Biomarker Evidence for a Major Preservation Pathway of Sedimentary Organic Carbon. *Science*, 312, 1627-1631. doi.10.1126/science.1126372
- Hertzberg, Jennifer E., Schmidt, Matthew W., 2016. "Paleotemperatures". In *Encyclopedia of Geochemistry*, edited by William M. White, 1-8. Dordrecht: Springer International Publishing.
- Hiatt, Richard R., McCarrick, Thomas, 1975. Bimolecular Initiation by Hydroperoxides. *Journal of the American Chemical Society*, 97, 5234-5237. doi.org/10.1021/ja00851a035
- Hill, Victoria G., Light, Bonnie et al., 2018. Light Availability and Phytoplankton Growth beneath Arctic Sea Ice: Integrating Observations and Modeling, *JGR Oceans*, 123, 3651-3667. doi.org/10.1029/2017JC013617
- Hoefs, Marcel J. L., Versteegh, Gerard J. M. et al., 1998. Postdepositional Oxidic Degradation of Alkenones: Implications for the Measurement of Palaeo Sea Surface Temperatures. *Paleoceanography and Paleoclimatology*, 13, 42-49. doi.org/10.1029/97PA02893
- Houk, Kendal N., Williams, John C. et al., 1981. Conformational Control of Reactivity and Regioselectivity in Singlet Oxygen Ene Reactions: Relationship to the Rotational Barriers of Acyclic Alkylethylenes. *Journal of the American Chemical Society*, 103, 949-951. doi.org/10.1021/ja00394a044

- Huang, Yongsong, Lockheart, Matthew J. et al., 1995. Molecular and Isotopic Biogeochemistry of the Miocene Clarkia Formation: Hydrocarbons and Alcohols. *Organic Geochemistry*, 23, 785-801. doi.org/10.1016/0146-6380(95)80001-8
- Huang, Yongsong, Shuman, Bryan et al., 2004. Hydrogen Isotope Ratios of Individual Lipids in Lake Sediments as Novel Tracers of Climatic and Environmental Change: a Surface Sediment Test. *Journal of Paleolimnology*, 31, 363-375. doi.org/10.1023/B:JOPL.0000021855.80535.13
- Hurst, John R., Wilson, Stephen L., Schuster, Gary B., 1985. The Ene Reaction of Singlet Oxygen: Kinetic and Product Evidence in Support of a Peroxide Intermediate. *Tetrahedron*, 41, 2191-2197. doi.org/10.1016/S0040-4020(01)96592-5
- Huysen, Earl S., Johnson, Kenneth L., 1968. Nature of the Polar Effect in Hydrogen Atom Abstractions from Alcohols, Ethers, and Esters. *The Journal of Organic Chemistry*, 33, 3972-3974. doi.org/10.1021/jo01274a073
- Ingalls, Anitra E., Whitehead, Kenia, Bridoux, Maxime C., 2010. Tinted Windows: The Presence of the UV Absorbing Compounds Called Mycosporine-Like Amino Acids Embedded in the Frustules of Marine Diatoms. *Geochimica and Cosmochimica Acta*, 74, 104-115. doi.org/10.1016/j.gca.2009.09.012
- Ingold, Keith U., 1969. Peroxy Radicals. *Accounts of Chemical Research*, 2, 1-9. doi.org/10.1021/ar50013a001
- Iturraspe, José, Engel, Norbert, Gossauer, Albert, 1994. Chlorophyll Catabolism. Isolation and Structure Elucidation of Chlorophyll b Catabolites in *Chlorella protothecoides*. *Phytochemistry*, 35, 1387-1390. doi.org/10.1016/S0031-9422(00)86861-2
- Ivanov, Igor, Kuhn, Hartmut, Heydeck, Dagmar, 2005. Structural and Functional Biology of Arachidonic Acid 15-Lipoxygenase-1 (ALOX15). *Gene*, 573, 1-32. doi.org/10.1016/j.gene.2015.07.073
- Jäger, Sebastian, Trojan, Holger et al., 2009. Pentacyclic Triterpene Distribution in Various Plants – Rich Sources for a New Group of Multi-Potent Plant Extracts. *Molecules*, 14, 2016-2031. doi.org/10.3390/molecules14062016
- Janusz, Grzegorz, Pawlik, Anna et al., 2017. Lignin Degradation: Microorganisms, Enzymes Involved, Genomes Analysis and Evolution. *FEMS Microbiology Reviews*, 41, 941-962. doi.org/10.1093/femsre/fux049
- Jaraula, Caroline M.B., Brassell, Simon C. et al., 2010. Origin and Tentative Identification of Tri- to Penta-unsaturated Ketones in

- Sediments from Lake Fryxell, East Antarctica. *Organic Geochemistry*, 41, 386-397. doi.org/10.1016/j.orggeochem.2009.12.004
- Jarvi, Mark T., Patterson, Michael S., Wilson, Brian C., 2012. Insights into Photodynamic Therapy Dosimetry: Simultaneous Singlet Oxygen Luminescence and Photosensitizer Photobleaching Measurements. *Biophysical Journal*, 102, 661-671. doi.org/10.1016/j.bpj.2011.12.043
- Jónasdóttir, Sigrún H., 2019. Fatty Acid Profiles and Production in Marine Phytoplankton. *Marine Drugs*, 17, 151. doi.org/10.3390/md17030151
- Kasche Volker, Lindqvist Lars, 1964. Reactions between the Triplet State of Fluorescein and Oxygen. *The Journal of Physical Chemistry*, 68, 817-823. doi.org/10.1021/j100786a019
- Keweloh, Heribert, Heipieper, Hermann J., 1996. *Trans* Unsaturated Fatty Acids in Bacteria. *Lipids*, 31, 129-137. doi.org/10.1007/BF02522611
- Kieslich, Klaus, Abraham, Wolf-Rainer et al., 1986. "Transformation of Terpenoids". In *Progress in Essential Oil Research*, edited by E. J. Brunke, 368-394. Berlin: Walter de Gruyter and Co.
- Kirk, T. Kent, Farrell, Roberta, L., 1987. Enzymatic "Combustion": the Microbial Degradation of Lignin. *Annual Review of Microbiology*, 41, 465-501. doi.org/10.1146/annurev.mi.41.100187.002341
- Knox, J. Paul, Dodge, Alan D., 1985. Singlet Oxygen and Plants. *Phytochemistry*, 24, 889-896. doi.org/10.1016/S0031-9422(00)83147-7
- Koek, Maud M., Jellema, Renger H. et al., 2011. Quantitative Metabolomics Based on Gas Chromatography Mass Spectrometry: Status and Perspectives. *Metabolomics*, 7, 307-328. doi 10.1007/s11306-010-0254-3
- Kolattukudy, Pappachan, 1980. Biopolyester Membranes of Plants: Cutin and Suberin. *Science*, 208, 990-1000. doi: 10.1126/science.208.4447.990
- Kopercky, Karl R., Reich, Hans J., 1965. Reactivities in Photosensitized Olefin Oxidations. *Canadian Journal of Chemistry*, 43, 2265-2270. doi.org/10.1139/v65-306
- Korytowski, Witold, Bachowski, Gary J., Girotti, Albert W., 1992. Photoperoxidation of Cholesterol in Homogeneous Solution, Isolated Membranes, and Cells: Comparison of the 5 α - and 6 β -Hydroperoxides as Indicators of Singlet Oxygen Intermediacy. *Photochemistry and Photobiology*, 56, 1-8. doi.org/10.1111/j.1751-1097.1992.tb09594.x
- Krasnovsky, Arkady A., 1998. Singlet Molecular Oxygen in Photobiochemical Systems: IR Phosphorescence Studies. *Membrane & cell Biology*, 12, 665-690.
- Krembs, Christopher, Engel, Anja, 2001. Abundance and Variability of Microorganisms and Transparent Exopolymer Particles across the Ice-

- Water Interface of Melting First-Year Sea Ice in the Laptev Sea (Arctic). *Marine Biology*, 138, 173–185.
doi.org/10.1007/s002270000396
- Krumova, Katerina, Cosa, Gonzalo, 2016. “Overview of Reactive Oxygen Species”. In *Singlet Oxygen: Applications in Biosciences and Nanosciences*, edited by Nonell Santi and Flors Cristina, 1-21. The Royal Society of Chemistry’s. doi. 10.1039/9781782622208-00001
- Kuehn, Hartmut, Eggert, Lutz et al., 1991. Keto Fatty Acids not Containing Doubly Allylic Methylenes are Lipxygenase Substrates. *Biochemistry*, 30, 10269–10273. doi.org/10.1021/bi00106a026
- Kulig, Martin J., Smith, Leland L., 1973. Sterol Metabolism. XXV. Cholesterol Oxidation by Singlet Molecular Oxygen. *Journal of Organic Chemistry*, 38, 3639–3642. doi.org/10.1021/jo00960a050
- Kvernvik, Ane C., Rokitta, Sebastian D. et al., 2020. Higher Sensitivity towards Light Stress and Ocean Acidification in an Arctic Sea-Ice-Associated Diatom Compared to a Pelagic Diatom. *New Phytologist*, 226, 1708-1724. doi.org/10.1111/nph.16501
- Lange, Heiko, Decina, Sylvia, Crestini, Claudia, 2015. Oxidative Upgrade of Lignin – Recent Routes Reviewed. *European Polymer Journal*, 49, 1151-1173. doi.org/10.1016/j.eurpolymj.2013.03.002
- Lee, Richard F., Hagen, Wilhelm, Kattner, Gerhard, 2006. Lipid Storage in Marine Zooplankton. *Marine Ecology Progress Series*, 307, 273-306. doi:10.3354/meps307273
- Leshem, Ya’acov Y., 1988. Plant Senescence Processes and Free Radicals. *Free Radical in Biology and Medicine*, 5, 39–49.
doi.org/10.1016/0891-5849(88)90060-3
- Li, Tao, Li, Chunbao, 2013. Quantitative and Stereospecific Dihydroxylations of Δ^5 -Steroids: A Green Synthesis of Plant Growth Hormone Intermediates. *Journal of Agricultural and Food Chemistry*, 61, 12522-12530. doi.org/10.1021/jf404633y
- Liang, Ying, Mai, Kangsen, 2005. Effect of Growth Phase on the Fatty Acid Compositions of Four Species of Marine Diatoms. *Journal of Ocean University of China*, 4, 157-162. doi.org/10.1007/s11802-005-0010-x
- Liebler, Daniel C., 1994. Tocopherone and Epoxytocopherone Products of Vitamin E Oxidation. *Methods in Enzymology*, 234, 310-316.
doi.org/10.1016/0076-6879(94)34098-6
- Louda, J. William, Li, Jie et al., 1998. Chlorophyll-a Degradation during Cellular Senescence and Death. *Organic Geochemistry*, 29, 1233-1251. doi.org/10.1016/S0146-6380(98)00186-7

- Louda, J. William, Loitz, Joseph W. et al., 2000. Early Diagenetic Alteration of Chlorophyll-a and Bacteriochlorophyll-a in a Contemporaneous Marl Ecosystem; Florida Bay. *Organic Geochemistry*, 31, 1561-1580.
doi.org/10.1016/S0146-6380(00)00071-1
- Luchnikova, Natalia A., Ivanova, Kseniya M. et al., 2019. Microbial Conversion of Toxic Resin Acids. *Molecules*, 24, 4121.
doi.org/10.3390/molecules24224121
- Lütjohann, Dieter, 2004. Sterol Autoxidation: from Phytosterols to Oxyphytosterols. *British Journal of Nutrition*, 91, 3-4.
doi.org/10.1079/BJN20031048
- MacCloskey, James A., MacClelland, Martha J., 1965. Mass Spectra of O-Isopropylidene Derivatives of Unsaturated Fatty Esters. *Journal of the American Chemical Society*, 87, 5090-5093.
doi.org/10.1021/ja00950a019
- Mäkinen, Katja, Elfving, Michael et al., 2017. Fatty Acid Composition and Lipid Content in the Copepod *Limnocalanus macrurus* during Summer in the Southern Bothnian Sea. *Helgoland Marine Research*, 71, 11. doi.org/10.1186/s10152-017-0491-1
- Mansy, Sheref, S., 2010. "Membrane Transport in Primitive Cells". In *Additional Perspectives on The Origins of Life*, edited by David Deamer and Jack W. Szostak, 1-14. Cold Spring Harbor Laboratory Press.
- Marchand, Daphné, Rontani, Jean-François, 2001. Characterisation of Photo-oxidation and Autoxidation Products of Phytoplanktonic Monounsaturated Fatty Acids in Marine Particulate Matter and Recent Sediments. *Organic Geochemistry*, 32, 287-304.
doi.org/10.1016/S0146-6380(00)00175-3
- Marchand, Daphné, Grossi, Vincent et al., 2002. Regiospecific Enzymatic Oxygenation of *Cis*-Vaccenic Acid during Aerobic Senescence of the Halophilic Purple Sulfur Bacterium *Thiohalocapsa halophila*. *Lipids*, 37, 541-548. doi.org/10.1007/s11745-002-0930-2
- Marchand, Daphné, Rontani, Jean-François, 2003. Visible Light-Induced Oxidation of Lipid Components of Purple Sulfur Bacteria: a Significant Process in Microbial Mats. *Organic Geochemistry*, 34, 61-79. doi.org/10.1016/S0146-6380(02)00192-4
- Marchand, Daphné, Marty, Jean-Claude et al., 2005. Lipids and their Oxidation Products as Biomarkers for Carbon Cycling in the North-western Mediterranean Sea: Results from a Sediment Trap Study. *Marine Chemistry*, 95, 129-147.
doi.org/10.1016/j.marchem.2004.09.001

- Marlowe, I.T., Green, John C. et al., 1984. Long Chain (n -C₃₇–C₃₉) Alkenones in the Prymnesiophyceae. Distribution of Alkenones and other Lipids and their Taxonomic Significance. *British Phycological Journal*, 19, 203–216. doi.org/10.1080/00071618400650221
- Martin, Vincent J. J., Yu, Zhongtang, Mohn, William W., 1999. Recent Advances in Understanding Resin Acid Biodegradation: Microbial Diversity and Metabolism. *Archives of Microbiology*, 172, 131–138. doi.org/10.1007/s002030050752
- Martin, Vincent, Mohn, William W., 2000. Genetic Investigation of the Catabolic Pathway for Degradation of Abietane Diterpenoids by *Pseudomonas abietaniphila* BKME-9. *Journal of Bacteriology*, 182, 3784–3793. doi: 10.1128/jb.182.13.3784-3793.2000
- Martin-Creuzburg, Dominik, Merkel, Petra, 2016. Sterols of Freshwater Microalgae: Potential Implications for Zooplankton Nutrition. *Journal of Plankton Research*, 38, 865–877. doi.org/10.1093/plankt/fbw034
- Martinez, Angel T., Speranza, Mariela et al., 2005. Biodegradation of Lignocellulosics: Microbial, Chemical, and Enzymatic Aspects of the Fungal Attack of Lignin. *International Microbiology*, 8, 195–204. doi. 10.13039/501100003339
- Martínez, Eriel, Estupiñán, Mónica, et al., 2013. Functional Characterization of ExFadLO, an Outer Membrane Protein Required for Exporting Oxygenated Long-Chain Fatty acids in *Pseudomonas aeruginosa*. *Biochimie*, 95, 290–298. doi.org/10.1016/j.biochi.2012.09.032
- Meiners, Klaus, Gradinger, Rolf et al., 2003. Vertical Distribution of Exopolymer Particles in Sea Ice of the Fram Strait (Arctic) during Autumn. *Marine Ecology Progress Series*, 248, 1–13. doi:10.3354/meps248001
- Merzlyak, Mark N., Hendry, George A.F., 1994. Free Radical Metabolism, Pigment Degradation and Lipid Peroxidation in Leaves during Senescence. *Proceedings of the Royal Society of Edinburgh*, 102B, 459–471. doi.org/10.1017/S0269727000014482
- Michaels, Brooks C., Ruettinger, Richard T., Fulco, Armand J., 1980. Hydration of 9,10-Epoxy palmitic Acid by a Soluble Enzyme from *Bacillus megaterium*. *Biochemical and Biophysical Research Communications*, 92, 1189–1195. doi.org/10.1016/0006-291X(80)90412-X
- Mihara, Satoru, Tateba, Hideki, 1986. Photosensitized Oxygenation Reactions of Phytol and its Derivatives. *Journal of Organic Chemistry*. 51, 1142–1144. doi.org/10.1021/jo00357a043

- Min, David B., Boff, Jeffrey M., 2002. Chemistry and Reaction of Singlet Oxygen in Foods. *Comprehensive Reviews in Food Science and Food Safety*, 1, 58-72. doi.org/10.1111/j.1541-4337.2002.tb00007.x
- Minerath, Emily C., Schultz, Madeline P., Elrod, Matthew J., 2009. Kinetics of the Reactions of Isoprene-Derived Epoxides in Model Tropospheric Aerosol Solutions. *Environmental Science and Technology*, 43, 8133-8139. doi.org/10.1021/es902304p
- Mittova, Valentina, Tal, Moshe et al., 2002. Salt Stress Induces Up-Regulation of an Efficient Chloroplast Antioxidant System in the Salt-Tolerant Wild Tomato Species *Lycopersicon pennellii* but not in the Cultivated Species. *Physiologia Plantarum*, 115, 393-400. doi.org/10.1034/j.1399-3054.2002.1150309.x
- Mohn, William W., 1995. Bacteria Obtained from a Sequencing Batch Reactor that are Capable of Growth on Dehydroabiatic Acid. *Applied and Environmental Microbiology*, 61, 2145-2150. doi: 10.1128/aem.61.6.2145-2150.1995
- Morales, Javier, Günther, Germán et al., 2012. Singlet Oxygen Reactions with Flavonoids. A Theoretical - Experimental Study. *Plos One*, 7, e40548. doi:10.1371/journal.pone.0040548.g001
- Mordi, Raphael C., 1993. Mechanism of β -Carotene Degradation. *Biochemical Journal*, 292, 310-312. doi.org/10.1042/bj2920310
- Morrissey, Patrick A., Kiely, Mairead, 2006. Oxysterols: Formation and Biological Function. *Advanced Dairy Chemistry*, 2, 641-674. doi.org/10.1007/0-387-28813-9_18
- Mouzdahir, Abdelkrim, Grossi, Vincent et al., 2001. Visible Light-Dependent Degradation of Long-Chain Alkenes in Killed Cells of *Emiliania huxleyi* and *Nannochloropsis salina*. *Phytochemistry*, 6, 677-684. doi.org/10.1016/S0031-9422(00)00468-4
- Müller, Peter J., Kirst, Georg et al., 1998. Calibration of the Alkenone Paleotemperature Index U_{37}^K Based on Core-Tops from the Eastern South Atlantic and the Global Ocean (60°N-60°S). *Geochimica et Cosmochimica Acta*, 62, 1757-1772. doi.org/10.1016/S0016-7037(98)00097-0
- Murphy, Robert C., Johnson, Kyle M., 2008. Cholesterol, Reactive Oxygen Species, and the Formation of Biologically Active Mediators. *Journal of Biological Chemistry*, 283, 15521-15525. doi: 10.1074/jbc.R700049200
- Najdek, Mirjana, Puškarić, Staša, Bohdansky, Alexander B., 1994. Contribution of Zooplankton Lipids to the Flux of Organic Matter in the Northern Adriatic Sea. *Marine Ecology Progress Series*, 111, 241-249. doi:10.3354/meps111241

- Nassiry, Mina, Aubert, Claude et al., 2009. Generation of Isoprenoid Compounds, Notably prist-1-ene, via Photo- and Autoxidative Degradation of Vitamin E. *Organic Geochemistry*, 40, 38-50.
doi.org/10.1016/j.orggeochem.2008.09.009
- Nawar, Wassef W., 1969. Thermal Degradation of Lipids. *Journal of Agricultural and Food Chemistry*, 17, 18-21.
doi.org/10.1021/jf60161a012
- Nawkar, Ganesh M., Maibam, Punyakishore et al., 2013. UV-Induced Cell Death in Plants. *International Journal of Molecular Sciences*, 14, 1618-1628. doi:10.3390/ijms14011608
- Neely, William C., Martin, John M., Barker, Steven A., 1988. Products and Relative Reaction Rates of the Oxidation of Tocopherols with Singlet Molecular Oxygen. *Photochemistry and Photobiology*, 48, 423-428. doi.org/10.1111/j.1751-1097.1988.tb02840.x
- Neff, William E., Frankel, Edwin N., Fujimoto, Kenshiro, 1988. Autoxidative Dimerization of Methyl Linolenate and its Monohydroperoxides, Hydroperoxy Epidioxides and Dihydroperoxides. *Journal of the American Oil Chemist's Society*, 65, 616-623.
doi.org/10.1007/BF02540690
- Nelson, James R., 1993. Rates and Possible Mechanism of Light-Dependent Degradation of Pigments in Detritus Derived from Phytoplankton. *Journal of Marine Research*, 51, 155-179.
doi.org/10.1357/0022240933223837
- Nguyen Tu, Thanh Thuy, Egasse, Céline et al., 2017. Leaf Lipid Degradation in Soils and Surface Sediments: a Litterbag Experiment. *Organic Geochemistry*, 104, 35-41.
doi.org/10.1016/j.orggeochem.2016.12.001
- Nichols, Peter D., Guckert, James B., White, David C., 1986. Determination of Monosaturated Fatty Acid Double-Bond Position and Geometry for Microbial Monocultures and Complex Consortia by Capillary GC-MS of their Dimethyl Disulphide Adducts. *Journal of Microbiological Methods*, 5, 49-55.
doi.org/10.1016/0167-7012(86)90023-0
- Nilson, Rune, Merkel, Paul B., Kearns, David R., 1972. Unambiguous Evidence for the Participation of Singlet Oxygen in Photodynamic Oxidation of Amino Acids. *Photochemistry and Photobiology*, 16, 117-124. doi.org/10.1111/j.1751-1097.1972.tb07343.x
- Ogilby, Peter R., 2010. Singlet Oxygen: There is Indeed Something New under the Sun. *Chemical Society Reviews*, 8, 3181-3209.
doi.org/10.1039/B926014P.

- Opsahl, Stephen, Benner, Ronald, 1993. Decomposition of Senescent Blades of the Seagrass *Halodule wrightii* in a Subtropical Lagoon. *Marine Ecology Progress Series*, 94, 191-205. doi:10.3354/MEPS094191
- Orefice, Ida, Gerecht, Andreas et al., 2015. Determination of Lipid Hydroperoxides in Marine Diatoms by the FOX2 Assay. *Marine Drugs*, 13, 5767-5783. doi:10.3390/md13095767
- Oren, Aharon, 2011. 12 - Characterization of Pigments of Prokaryotes and their Use in Taxonomy and Classification. *Methods in Enzymology*, 38, 261-282. doi.org/10.1016/B978-0-12-387730-7.00012-7
- Otto, Angelika, Simoneit, Bernd R. T., Rember, William C., 2005. Conifer and Angiosperm Biomarkers in Clay Sediments and Fossil Plants from the Miocene Clarkia Formation, Idaho, USA. *Organic Geochemistry*, 36, 907-922. doi.org/10.1016/j.orggeochem.2004.12.004
- Ozog, Lukasz, Aebisher, David, 2018. Singlet Oxygen Lifetime and Diffusion Measurements. *European Journal of Clinical and Experimental Medicine*, 16, 123-126. 2544-2406. doi:10.15584/ejcem.2018.2.7
- Palmer, John M., Harvey, Patricia J., Schoemaker, Hans E., 1987. The role of Peroxidases, Radical Cations and Oxygen in the Degradation of Lignin. *Philosophical Transactions of the Royal Society of London*, 321, 495-505. doi.org/10.1098/rsta.1987.0027
- Parrish, Christopher C., Ackman, Robert G., 1983. Chromarod Separations for the Analysis of Marine Lipid Classes by Iatrosan Chromatography-Flame Ionization Detection. *Journal of Chromatography A*, 262, 103-112. doi.org/10.1016/S0021-9673(01)88091-2
- Parrish, Christopher C., 2013. Lipids in Marine Ecosystems. *International Scholarly Research Notices*, 604045. doi.org/10.5402/2013/604045
- Patterson, Glen W., 1974. Sterols of some Green Algae. *Comparative Biochemistry and Physiology Part B: Comparative Biochemistry*, 47, 453-457. doi.org/10.1016/0305-0491(74)90075-3
- Pattison, David I., Rahmanto, Aldwin S., Davies, Michael J., 2012. Photooxidation of Proteins. *Photochemical and Photobiological Sciences*, 11, 38-53. doi:10.1039/C1PP05164D
- Pellikaan, G. C., 1982. Decomposition processes of eelgrass *Zostera marina* L. *Hydrobiological Bulletin*, 16, 83-92. doi.org/10.1007/BF02255416
- Petit, Morgan, Sempéré, Richard et al., 2013. Transfer of Photooxidative Processes from Senescent Phytoplankton Cells to Attached Bacteria: Formation and Behaviour of *Cis*-Vaccenic Photoproducts. *Journal of Molecular Sciences*, 14, 11795-11815. doi: 10.3390/ijms140611795

- Petit, Morgan, Suroy, Maxime et al., 2015a. Transfer of Singlet Oxygen from Senescent Irradiated Phytoplankton Cells to Attached Heterotrophic Bacteria: Effect of Silica and Carbonaceous Matrices. *Marine Chemistry*, 171, 87-95.
doi.org/10.1016/j.marchem.2015.02.007
- Petit, Morgan, Bonin, Patricia et al., 2015b. Dynamic of Bacterial Communities Attached to Lightened Phytodetritus. *Environmental Science and Pollution Research*, 22, 13681-13692.
doi.org/10.1007/s11356-015-4209-0
- Pham, Thu Wong, Zaeem, Muhammad et al., 2019. Targeting Modified Lipids during Routine Lipidomics Analysis using HILIC and C30 Reverse Phase Liquid Chromatography coupled to Mass Spectrometry. *Scientific Reports*, 9, 5048. doi.org/10.1038/s41598-019-41556-9
- Piepho, Maike, Martin-Creuzburg, Dominik, Wacker, Alexander, 2012. Phytoplankton Sterol Contents Vary with Temperature, Phosphorus and Silicate Supply: a Study on Three Freshwater Species. *European Journal of Phycology*, 47, 138-145.
doi.org/10.1080/09670262.2012.665484
- Pierce, Alan E., 1982. *Silylation of Organic Compounds*. Rockford Illinois: Pierce Chemical Company.
- Pignitter, Mark, Somoza, Veronika, 2012. Critical Evaluation of Methods for the Measurement of Oxidative Rancidity in Vegetable Oils. *Journal of Food and Drug Analysis*, 20, 772-777.
doi:10.6227/jfda.2012200305
- Pinhassi, Jarone, Berman, Tom, 2003. Differential Growth Response of Colony-Forming α - and γ -Proteobacteria in Dilution Culture and Nutrient Addition Experiments from Lake Kinneret (Israel), the Eastern Mediterranean Sea, and the Gulf of Eilat. *Applied and Environmental Microbiology*, 69, 199-211.
doi.10.1128/AEM.69.1.199-211.2003
- Pinker, Rachel T., Laszlo Imre, 1992. Modelling Surface Solar Irradiance for Satellite Applications on a Global Scale. *Journal of Applied Meteorology and Climatology*, 31, 194-211.
doi.org/10.1175/1520-0450(1992)031<0194:MSSIFS>2.0.CO;2
- Pinnola, Alberta, Bassi, Roberto, 2018. Molecular Mechanisms Involved in Plant Photoprotection. *Biochemical Society Transactions*, 46, 467-482. doi.org/10.1042/BST20170307
- Pohnert, Georg, 2000. Wound-Activated Chemical Defense in Unicellular Planktonic Algae. *Angewandte Chemie*, 39, 4352-4354.
doi.org/10.1002/1521-3773(20001201)39:23<4352::AIDANIE4352>3.0.CO;2-U

- Pohnert, Georg, 2002. Phospholipase A2 Activity Triggers the Wound-Activated Chemical Defense in the Diatom *Thalassiosira rotula*. *Plant Physiology*, 129, 102-111. doi.org/10.1104/pp.010974
- Pokorny, Jan, 1987. "Major Factors Affecting the Autoxidation of Lipids. In: *Autoxidation of Unsaturated Lipids*, edited by Chan, Henry W.-S. (Ed.), 141-206. London: Academic Press.
- Porter, Ned A., Mills, Karen A., Carter, Randall L., 1994. A Mechanistic Study of Oleate Autoxidation: Competing Peroxyl H-Atom Abstraction and Rearrangement. *Journal of the American Chemical Society*, 116, 6690-6696. doi.org/10.1021/ja00094a026
- Porter, Ned A., Caldwell, Sarah E., Mills, Karen A., 1995. Mechanisms of Free Radical Oxidation of Unsaturated Lipids. *Lipids*, 30, 277-290. doi.org/10.1007/BF02536034
- Porter, Ned A., 2013. A Perspective on Free Radical Autoxidation: The Physical Organic Chemistry of Polyunsaturated Fatty Acid and Sterol Peroxidation. *Journal of Organic Chemistry*, 78, 3511-3524. doi.org/10.1021/jo4001433
- Prahl, Fredrick G., Wakeham, Stuart G., 1987. Calibration of Unsaturation Patterns in Long-Chain Ketone Compositions for Palaeotemperature Assessment. *Nature*, 330, 367-369. doi.org/10.1038/330367a0
- Prahl, Fredrick G., Cowie Gregory L. et al., 2003. Selective Organic Matter Preservation in "Burn-Down" Turbidites on the Madeira Abyssal Plain. *Paleoceanography*, 18, 1052. doi:10.1029/2002PA000853
- Prahl, Fredrick G., Mix, Alan C., Sparrow, Margaret A., 2006. Alkenone Paleothermometry: Biological Lessons from Marine Sediment Records off Western South America. *Geochimica et Cosmochimica Acta*, 70, 101-117. doi.org/10.1016/j.gca.2005.08.023
- Ramel, Fanny, Birtic, Simona et al., 2012. Chemical Quenching of Singlet Oxygen by Carotenoids in Plants. *Plant Physiology*, 158, 1267-127. doi.org/10.1104/pp.111.182394
- Rampen, Sebastiaan W., Schouten, Stefan et al., 2007. On the Origin of 24-Norcholestanes and their Use as Age-Diagnostic Biomarkers. *Geology*, 35, 419-422. doi.org/10.1130/G23358A.1
- Rampen, Sebastiaan W., Abbas, Ben A. et al., 2010. A Comprehensive Study of Sterols in Marine Diatoms (Bacillariophyta): Implications for their Use as Tracers for Diatom Productivity. *Limnology and Oceanography*, 55, 91-105. doi.org/10.4319/lo.2010.55.1.0091
- Ratledge, Colin, 1994. "Biodegradation of Oils, Fats and Fatty Acids". In *Biochemistry of Microbial Degradation*, edited by Colin Ratledge, 89-141. Dordrecht: Springer. doi.org/10.1007/978-94-011-1687-9_4

- Rechka J.A., Maxwell, James R., 1988. Characterisation of Alkenone Temperature Indicators in Sediments and Organisms. *Organic Geochemistry*, 13, 727-734. doi.org/10.1016/0146-6380(88)90094-0
- Redmond Robert W., Kochevar Irene E., 2006. Spatially Resolved Cellular Responses to Singlet Oxygen. *Photochemistry and Photobiology*, 82, 1178-1186. doi.org/10.1562/2006-04-14-IR-874
- Reid, Ian D., 1995. Biodegradation of Lignin. *Canadian Journal of Botany*, 73, 1011-1018. doi.org/10.1139/b95-351
- Riebesell Ulf, Schloss, Irene, Smetacek, Victor, 1991. Aggregation of Algae Released from Melting Sea Ice: Implications for Seeding and Sedimentation. *Polar Biology*, 11, 239-248. doi.org/10.1007/BF00238457
- Rieley, Gareth, Teece, Mark A. et al., 1998. Long-Chain Alkenes of the Haptophytes *Isochrysis galbana* and *Emiliania huxleyi*. *Lipids*, 33, 617-625. doi.org/10.1007/s11745-998-0248-0
- Roces, Carla B., Kastner, Elisabeth et al., 2016. Rapid Quantification and Validation of Lipid Concentrations within Liposomes. *Pharmaceutics*, 8, 29. doi:10.3390/pharmaceutics8030029
- Rontani, Jean-François, Grossi, Vincent et al., 1994. "Bound" 3-Methylidene-7,11,15-trimethylhexadecan-1,2-diol: a New Isoprenoid Marker for the Photodegradation of Chlorophyll-a in Seawater. *Organic Geochemistry*, 21, 135-142. doi.org/10.1016/0146-6380(94)90150-3
- Rontani, Jean-François, Grossi, Vincent, 1995. Abiotic Degradation of Intact and Photooxidized Chlorophyll Phytyl Chain under Simulated Geological Conditions. *Organic Geochemistry*, 23, 355-366. doi.org/10.1016/0146-6380(94)00129-O
- Rontani, Jean-François, Beker, Beatrix et al., 1995. Photodegradation of Chlorophyll Phytyl Chain in Dead Phytoplanktonic Cells. *Journal of Photochemistry and Photobiology A: Chemistry*, 85, 137-142. doi.org/10.1016/1010-6030(94)03891-W
- Rontani, Jean-François, Cuny, Philippe, Grossi, Vincent, 1996a. Photodegradation of Chlorophyll Phytyl Chain in Senescent Leaves of Higher Plants. *Phytochemistry*, 42, 347-351. doi.org/10.1016/0031-9422(95)00872-1
- Rontani, Jean-François, Raphel, Danielle, Cuny, Philippe, 1996b. Early Diagenesis of the Intact and Photooxidized Chlorophyll Phytyl Chain in a Recent Temperate Sediment. *Organic Geochemistry*, 24, 825-832. doi.org/10.1016/S0146-6380(96)00076-9
- Rontani, Jean-François, Cuny, Philippe et al., 1997a. Stability of Long-chain Alkenones in Senescing Cells of *Emiliania huxleyi*: Effect of

- Photochemical and Aerobic Microbial Degradation on the Alkenone Unsaturation Ratio ($U_{37}^{K'}$). *Organic Geochemistry*, 26, 503-509. doi.org/10.1016/S0146-6380(97)00023-5
- Rontani, Jean-François, Cuny, Philippe, Aubert, Claude, 1997b. Rates and Mechanism of Light-Dependent Degradation of Sterols in Senescent Cells of Phytoplankton. *Journal of Photochemistry and Photobiology, A: Chemistry*, 111, 139-144. doi.org/10.1016/S1010-6030(97)00221-9
- Rontani, Jean-François, 1998. Photodegradation of Unsaturated Fatty Acids in Senescent Cells of Phytoplankton: Photoproduct Structural Identification and Mechanistic Aspects. *Journal of Photochemistry and Photobiology, A: Chemistry*, 114, 37-44. doi.org/10.1016/S1010-6030(98)00201-9
- Rontani, Jean-François, Cuny, Philippe, Grossi, Vincent, 1998. Identification of a "Pool" of Lipid Photoproducts in Senescent Phytoplanktonic Cells. *Organic Geochemistry*, 29, 1215-1225. doi.org/10.1016/S0146-6380(98)00073-4
- Rontani, Jean-François, Marchand, Daphné, 2000. Δ^5 -Stenol Photoproducts of Phytoplanktonic Origin: a Potential Source of Hydroperoxides in Marine Sediments? *Organic Geochemistry*, 31, 169-180. doi.org/10.1016/S0146-6380(99)00156-4
- Rontani, Jean-François, Mouzdahir, Abdelkrim et al., 2002. Aerobic and Anaerobic Metabolism of Squalene by a Denitrifying Bacterium Isolated from Marine Sediment. *Archives of Microbiology*, 178, 279-287. doi.10.1007/s00203-002-0457-8
- Rontani, Jean-François, Koblížek, Michal et al., 2003a. On the Origin of *Cis*-Vaccenic Acid Photodegradation Products in the Marine Environment. *Lipids*, 38, 1085-1092. doi.org/10.1007/s11745-006-1164-z
- Rontani, Jean-François, Rabourdin, Adélaïde et al., 2003b. Photochemical Oxidation and Autoxidation of Chlorophyll Phytyl Side Chain in Senescent Phytoplanktonic Cells: Potential Sources of Several Acyclic Isoprenoid Compounds in the Marine Environment. *Lipids*, 38, 241-254. doi.org/10.1007/s11745-003-1057-1
- Rontani, Jean-François, Aubert, Claude, 2005. Characterization of Isomeric Allylic Diols Resulting from Chlorophyll Phytyl Side-Chain Photo- and Autoxidation by Electron Ionization Gas Chromatography/Mass Spectrometry. *Rapid Communications in Mass Spectrometry*, 19, 637-646. doi.org/10.1002/rcm.1835
- Rontani, Jean-François, Rabourdin, Adélaïde et al., 2005a. Visible Light-Induced Oxidation of Unsaturated Components of Cutins: a Significant

- Process during the Senescence of Higher Plants. *Phytochemistry*, 66, 313-321. doi.org/10.1016/j.phytochem.2004.12.015
- Rontani, Jean-François, Christodoulou, Stéphane, Koblížek, Michal, 2005b. GC-MS Structural Characterization of Fatty Acids from Marine Aerobic Anoxygenic Phototrophic Bacteria. *Lipids*, 40, 97-108. doi.org/10.1007/s11745-005-1364-6
- Rontani, Jean-François, Marty, Jean-Claude et al., 2006. Free Radical Oxidation (Autoxidation) of Alkenones and Other Microalgal Lipids in Seawater. *Organic Geochemistry*, 37, 354-368. doi.org/10.1016/j.orggeochem.2005.10.007
- Rontani, Jean-François, Jameson, Ian et al., 2007a. Free Radical Oxidation (Autoxidation) of Alkenones and Other Lipids in Cells of *Emiliania huxleyi*. *Phytochemistry*, 68, 913-924. doi.org/10.1016/j.phytochem.2006.12.013
- Rontani, Jean-François, Nassiry, Mina, Mouzdahir, Abdelkrim, 2007b. Free Radical Oxidation (Autoxidation) of α -Tocopherol (Vitamin E): A Potential Source of 4,8,12,16-Tetramethylheptadecan-4-olide in the Environment. *Organic Geochemistry*, 38, 37-47. doi.org/10.1016/j.orggeochem.2006.09.004
- Rontani, Jean-François, Harji, Ranjita, Volkman, John K., 2007c. Biomarkers Derived from Heterolytic and Homolytic cleavage of Allylic Hydroperoxides Resulting from Alkenone Autoxidation. *Marine Chemistry*, 107, 230-243. doi:10.1016/j.marchem.2007.07.006
- Rontani, Jean-François, 2008. "Photooxidative and Autoxidative Degradation of Lipid Components during the Senescence of Phototrophic Organisms". In *Phytochemistry Research Progress*, edited by Takumi Matsumoto, 115-154. New York: Nova Science Publishers.
- Rontani, Jean-François, Koblížek, Michal, 2008. Regiospecific Enzymatic Oxygenation of *Cis*-Vaccenic Acid in the Marine Phototrophic Bacterium *Erythrobacter* sp. strain MG3. *Lipids*, 43, 1065-1074. doi.org/10.1007/s11745-008-3237-7
- Rontani, Jean-François, Wakeham, Stuart G., 2008. Alteration of Alkenone Unsaturation Ratio with Depth in the Black Sea: Potential Roles of Stereomutation and Aerobic Biodegradation. *Organic Geochemistry*, 39, 1259-1268. doi.org/10.1016/j.orggeochem.2008.06.002
- Rontani, Jean-François, Nassiry, Mina et al., 2008. Aerobic Metabolism of Vitamin E by Marine Bacteria: Interaction with Free Radical Oxidation (Autoxidation) Processes. *Organic Geochemistry*, 39, 676-688. doi.org/10.1016/j.orggeochem.2008.02.018

- Rontani, Jean-François, Zabeti, Nathalie, Wakeham, Stuart G., 2009. The Fate of Marine Lipids: Biotic vs. Abiotic Degradation of Particulate Sterols and Alkenones in the Northwestern Mediterranean Sea. *Marine Chemistry*, 113, 9-18. doi.org/10.1016/j.marchem.2008.11.001
- Rontani, Jean-François, Nassiry, Mina et al., 2010. Formation of Pristane from α -Tocopherol under Simulated Anoxic Sedimentary Conditions: A Combination of Biotic and Abiotic Degradative Processes. *Geochimica and Cosmochimica Acta*, 74, 252-263. doi.org/10.1016/j.gca.2009.09.028
- Rontani, Jean-François, Belt, Simon T. et al., 2011a. Visible Light Induced Photo-oxidation of Highly Branched Isoprenoid (HBI) Alkenes: Significant Dependence on the Number and Nature of Double Bonds. *Organic Geochemistry*, 42, 812-822. doi.org/10.1016/j.orggeochem.2011.04.013
- Rontani, Jean-François, Zabeti, Nathalie, Wakeham, Stuart G., 2011b. Degradation of Particulate Organic Matter in the Equatorial Pacific Ocean: Biotic or Abiotic? *Limnology and Oceanography*, 56, 333-349. doi.org/10.4319/lo.2011.56.1.0333
- Rontani, Jean-François, 2012. "Photo- and Free Radical-Mediated Oxidation of Lipid Components during the Senescence of Phototrophic Organisms". In *Senescence*, edited by Nagata Tetsuji, 3-31. Rijeka: Intech.
- Rontani, Jean-François, Charrière, Bruno et al., 2012a. Intense Photooxidative Degradation of Planktonic and Bacterial Lipids in Sinking Particles Collected with Sediment Traps across the Canadian Beaufort Shelf (Arctic Ocean). *Biogeosciences*, 9, 4787-4802. doi.org/10.5194/bg-9-4787-2012
- Rontani, Jean-François, Charrière, Bruno et al., 2012b. Degradation State of Organic Matter in Surface Sediments from the Southern Beaufort Sea: a Lipid Approach. *Biogeosciences*, 9, 3513-3530. doi.org/10.5194/bg-9-3513-2012
- Rontani, Jean-François, Volkman, John K., et al., 2013a. Biotic and Abiotic Degradation of Alkenones and Implications for U_{37}^K Paleoproxy Applications: a Review. *Organic Geochemistry*, 59, 95-113. doi.org/10.1016/j.orggeochem.2013.04.005
- Rontani, Jean-François, Bonin, Patricia et al., 2013b. Anaerobic Bacterial Degradation of Pristenes and Phytanes in Marine Sediments Does not Lead to Pristane and Phytane during Early Diagenesis. *Organic Geochemistry*, 58, 43-55. doi.org/10.1016/j.orggeochem.2013.02.001
- Rontani, Jean-François, Vaultier, Frédéric, Bonin, P., 2014a. Biotic and Abiotic Degradation of Marine and Terrestrial Higher Plant Material in

- Intertidal Surface Sediments from Arcachon Bay (France): a Lipid Approach. *Marine Chemistry*, 158, 69-79.
doi.org/10.1016/j.marchem.2013.11.005
- Rontani, Jean-François, Belt, Simon T. et al., 2014b. Autoxidative and Photooxidative Reactivity of Highly Branched Isoprenoid (HBI) Alkenes. *Lipids*, 49, 481-494. doi.org/10.1007/s11745-014-3891-x
- Rontani, Jean-François, Belt, Simon T. et al., 2014c. Sequential Photo- and Autoxidation of Diatom Lipids in Arctic Sea Ice. *Organic Geochemistry*, 77, 59-71. doi.org/10.1016/j.orggeochem.2014.09.009
- Rontani, Jean-François, Belt, Simon T. et al., 2014d. Electron Ionization Mass Spectrometry Fragmentation Pathways of Trimethylsilyl Derivatives of Isomeric Allylic Alcohols Derived from HBI Alkene Oxidation. *Rapid Communications in Mass Spectrometry*, 28, 1937-1947. Doi.10.1002/rcm.6974
- Rontani, Jean-François, Aubert, Claude, Belt, Simon T., 2015. EIMS Fragmentation Pathways and MRM Quantification of 7 α / β -Hydroxy-Dehydroabiatic Acid TMS Derivatives. *Rapid Communications in Mass Spectrometry*, 26, 1606-1616. doi.org/10.1021/jasms.8b05097
- Rontani, Jean-François, Galeron, Marie-aimée, 2016. Autoxidation of Chlorophyll Phytol Side Chain in Senescent Phototrophic Organisms: A Potential Source of Isophytol in the Environment. *Organic Geochemistry*, 97, 35-40. doi.org/10.1016/j.orggeochem.2016.03.008
- Rontani, Jean-François, Belt, Simon T. et al., 2016. Monitoring Abiotic Degradation in Sinking Versus Suspended Arctic Sea Ice Algae during a Spring Ice Melt using Specific Lipid Oxidation Tracers. *Organic Geochemistry*, 98, 82-97. doi.org/10.1016/j.orggeochem.2016.05.016
- Rontani Jean-François, Galeron, Marie-Aimée et al., 2017. Identification of Di- and Triterpenoid Lipid Tracers Confirms the Significant Role of Autoxidation in the Degradation of Terrestrial Vascular Plant material in the Canadian Arctic. *Organic Geochemistry*, 108, 43-50.
doi.org/10.1016/j.orggeochem.2017.03.011
- Rontani, Jean-François, Belt, Simon T., Amiraux, Rémi, 2018a. Biotic and Abiotic Degradation of the Sea Ice Diatom Biomarker IP₂₅ and Selected Algal Sterols in Near-Surface Arctic Sediments. *Organic Geochemistry*, 118, 73-88. doi.org/10.1016/j.orggeochem.2018.01.003
- Rontani, Jean-François, Amiraux, Rémi et al., 2018b. Use of Palmitoleic Acid and its Oxidation Products for Monitoring the Degradation of Ice Algae in Arctic Waters and Bottom Sediments. *Organic Geochemistry*, 129, 88-102. doi.org/10.1016/j.orggeochem.2018.06.002
- Rontani, Jean-François, Charriere, Bruno et al., 2018c. Electron Ionization Mass Spectrometry Fragmentation and Multiple Reaction Monitoring

- Quantification of Autoxidation Products of α - and β -Amyrins in Natural Samples. *Rapid Communications in Mass Spectrometry*, 32, 1599-1607. doi.10.1002/rcm.8213
- Rontani, Jean-François, 2019. Biotic and Abiotic Degradation of Δ^5 -Sterols in Senescent Mediterranean Marine and Terrestrial angiosperms. *Phytochemistry*, 167, 112097. doi.org/10.1016/j.phytochem.2019.112097
- Rontani, Jean-François, Smik, Lukas et al., 2019a. Abiotic Degradation of Highly Branched Isoprenoid Alkenes and Other Lipids in the Water Column off East Antarctica. *Marine Chemistry*, 210, 34-47. doi.org/10.1016/j.marchem.2019.02.004
- Rontani, Jean-François, Smik, Lukas, Belt, Simon T., 2019b. Autoxidation of the Sea Ice Biomarker Proxy IPSO₂₅ in the Near-Surface Oxidation Layers of Arctic and Antarctic Sediments. *Organic Geochemistry*, 129, 63-76. doi.org/10.1016/j.orggeochem.2019.02.002
- Rontani, Jean-François, Belt, Simon T., 2020. Photo- and Autoxidation of Unsaturated Algal Lipids in the Marine Environment: An Overview of Processes, their Potential Tracers, and Limitations. *Organic Geochemistry*, 139, 103941. doi.org/10.1016/j.orggeochem.2019.103941
- Rontani, Jean-François, Smik, Lukas et al., 2021a. Seasonal Monitoring of Biotic and Abiotic Degradation of Suspended Particulate Lipids in the Western English Channel Suggests a Link between Bacterial 10S-DOX Activity and Production of Free Fatty Acids by Phytoplankton. *Marine Chemistry*, 230, 103928. doi.org/10.1016/j.marchem.2021.103928
- Rontani, Jean-François, Amiraux, Rémi et al., 2021b. Type II Photo-sensitized Oxidation in Senescent Microalgal Cells at Different Latitudes: Does Low Under-Ice Irradiance in Polar Regions Enhance Efficiency? *Science of the Total Environment*, 779, 146363. doi.org/10.1016/j.scitotenv.2021.146363
- Rontani, Jean-François, Smik, Lukas et al., 2021c. Biotic and Abiotic Degradation of Suspended Particulate Lipids along a Transect in the Chukchi Sea. *Organic Geochemistry*, (In preparation).
- Rowland, Steven J., Robson, John N., 1990. The Widespread Occurrence of Highly Branched Acyclic C₂₀, C₂₅ and C₃₀ Hydrocarbons in Recent Sediments and Biota - a Review. *Marine Environmental Research*, 30, 191-216. doi.org/10.1016/0141-1136(90)90019-K
- Rufai, Yakubu, Basar, Norazah, Sani, Ali Mohamedi, 2019. Optimization and Isolation of 4,8,12,16-Tetramethylheptadecan-4-olide from *Deinbollia pinnata*. *Asian Journal of Chemistry*, 11, 2503-2511. doi.org/10.14233/ajchem.2019.22165

- Saito, Isao, Inoue, Kenzo, Matsuura, Teruo, 1975. Occurrence of the Singlet Oxygen Mechanism in Photodynamic Oxidations of Guanosine. *Photochemistry and Photobiology*, 21, 27-30. doi.org/10.1111/j.1751-1097.1975.tb06625.x
- Sato Keizo, Akaike Takaaki et al., 1992. Hydroxyl Radical Production by H₂O₂ plus Cu, Zn- Superoxide Dismutase Reflects the Activity of Free Copper Released from the Oxidatively damaged Enzyme. *Journal of Biological Chemistry*, 267, 25371-25377. doi.org/10.1016/S0021-9258(19)74050-2
- Schaeffer, Philippe, Adam, Pierre et al., 1997. Novel Aromatic Carotenoid Derivatives from Sulfur Photosynthetic Bacteria in Sediments. *Tetrahedron Letters*, 38, 8413-8416. doi.org/10.1016/S0040-4039(97)10235-0
- Schaich, Karen M., 2005. Lipid Oxidation: Theoretical Aspects. In. *Bailey's Industrial Oil and Fat Products*, edited by Fereidoun Shahidi, 269–355. Chichester: John Wiley & Sons.
- Schenck, Günther O., Koch, Erhard, 1960. Zwischenreaktionen bei photosensibilisierten Prozessen in Lösungen. *Berichte der Bunsengesellschaft für physikalische Chemie*, 64, 170-177.
- Schmid, Manfred, Ritter, Axel et al., 2007. Autoxidation of Medium Chain Length Polyhydroxyalkanoate. *Biomacromolecules*, 8, 579-584. doi.org/10.1021/bm060785m
- Schuur, Edward A. G., Bockheim, James et al., 2008. Vulnerability of Permafrost Carbon to Climate Change: Implications for the Global Carbon Cycle. *Bioscience*, 58, 701-714. doi.org/10.1641/B580807
- Sheldon, Roger A., Kochi, Jay K., 1975. Metal-Catalyzed Oxidations of Organic Compounds in the Liquid Phase: A Mechanistic Approach. *Advances in Catalysis*, 25, 272-413. doi.org/10.1016/S0360-0564(08)60316-8
- Sheppard, April N., Acevedo, Orlando, 2009. Multidimensional Exploration of Valley–Ridge Inflection Points on Potential-Energy Surfaces. *Journal of the American Chemical Society*, 131, 2530-2540. doi.org/10.1021/ja803879k
- Shiba, Tsuneo, 1991. *Roseobacter litoralis* gen. nov., sp. nov., and *Roseobacter denitrificans* sp. nov., Aerobic Pink-Pigmented Bacteria which Contain Bacteriochlorophyll a. *Systematic and Applied Microbiology*, 14, 140-145. doi.org/10.1016/S0723-2020(11)80292-4
- Shoja Chaghervand, Shirin, 2019. “Characterization of the Enzymes Involved in the Diolsynthase Pathway in *Pseudomonas aeruginosa*”. PhD diss., Universitat de Barcelona.

- Shukla, Vivek, Kandeepan, Gurunathan, et al., 2016. Anthocyanins Based Indicator Sensor for Intelligent Packaging Application. *Agricultural Research*, 5, 205-209. doi.org/10.1007/s40003-016-0211-0
- Sicre, Marie-Alexandrine, Lepaillasseur, Jean-Louis et al., 1988. Characterization of Seawater Samples using Chemometric Methods Applied to Biomarker Fatty Acids. *Organic Geochemistry*, 12, 281-288. doi.org/10.1016/0146-6380(88)90265-3
- Skovsen, Esben, Snyder, John W. et al., 2005. Lifetime and Diffusion of Singlet Oxygen in a Cell. *The Journal of Physical Chemistry B*, 109, 8570–8573. doi.org/10.1021/jp051163i
- Smith, Leland L., 1981. Cholesterol Autoxidation 1981–1986. *Chemistry and Physics of Lipids*, 44, 87-125. doi.org/10.1016/0009-3084(87)90046-6
- Sokolov, Valerij S., Pohl, Peter, 2009. Membrane Transport of Singlet Oxygen Monitored by Dipole Potential Measurements. *Biophysical Journal*, 96, 77-85. doi.org/10.1529/biophysj.108.135145
- Soltani, Mohamed, Metzger, Pierre, Largeau, Claude, 2004. Effects of Hydrocarbon Structure on Fatty Acid, Fatty Alcohol, and β -Hydroxy Acid Composition in the Hydrocarbon-degrading bacterium *Marinobacter hydrocarbonoclasticus*. *Lipids*, 39, 491-505. doi.org/10.1007/s11745-004-1256-9
- Squier, Angela H., Hogson, Dominic A., Keely, Brendan J., 2005. Evidence of Late Quaternary Environmental Change in a Continental East Antarctic Lake from Lacustrine sedimentary pigment Distributions. *Antarctic Science*, 17, 361-376. doi. 10.1017/S0954102005002804
- Steele, Deborah J., Kimmance, Susan A. et al., 2018. Occurrence of Chlorophyll Allomers during Virus-Induced Mortality and Population Decline in the Ubiquitous Picoeukaryote *Ostreococcus tauri*. *Environmental Microbiology*, 20, 588-601. doi.org/10.1111/1462-2920.13980
- Steinbrecht, Wolfgang, Claude, Hans et al., 2009. Ozone and Temperature Trends in the Upper Stratosphere at Five Stations of the Network for the Detection of Atmospheric Composition Change. *International Journal of Remote Sensing*, 30, 1989-2009. doi.org/10.1080/01431160902821841
- Stephen, Mark P., Kadko, David C. et al., 1997. Chlorophyll-a and Pheopigments as Tracers of Labile Organic Carbon at the Central Equatorial Pacific Seafloor. *Geochimica et Cosmochimica Acta*, 61, 4605-4619. doi.org/10.1016/S0016-7037(97)00358-X

- Stratakis, Manolis, Orfanopoulos, Michael, 1997. Regioselectivity in the Ene Reaction of Singlet Oxygen with Alkenes. *Tetrahedron*, 56, 1595-1615. doi.org/10.1016/S0040-4039(96)02469-0
- Stratton, Steven P., Schaefer, William H., Liebler, Daniel C., 1993. Isolation and identification of singlet oxygen oxidation products of β -carotene. *Chemical Research in Toxicology*, 6, 542-547. doi.org/10.1021/tx00034a024
- Suh, Hwa-Jin, Lee, Hyun-Woo, Jung, Jin, 2003. Mycosporine Glycine Protects Biological Systems against Photodynamic Damage by Quenching Singlet Oxygen with a High Efficiency. *Photochemistry and Photobiology*, 78, 109-113. doi.org/10.1562/0031-8655(2003)0780109MGPBSA2.0.CO2
- Sun, Ming-Yi, Lee, Cindy, Aller, Robert C., 1993. Anoxic and Oxidative Degradation of ^{14}C -Labeled Chloropigments and a ^{14}C -Labeled Diatom in Long Island Sound Sediments. *Limnology and Oceanography*, 38, 1438-1451. doi.org/10.4319/lo.1993.38.7.1438
- Sun, Ming-Yi, Aller, Robert C. et al., 1999. Enhanced Degradation of Algal Lipids by Benthic Macrofaunal Activity: Effect of *Yoldia limatula*. *Journal of Marine Research*, 57, 775-804. doi.org/10.1357/002224099321560573
- Sun, Linlin, Dong, Yangyang et al., 2014. Two Residues Predominantly Dictate Functional Difference in Motility between *Shewanella oneidensis* Flagellins FlaA and FlaB. *Journal of Biological Chemistry*, 289, 14547-14559. doi.org/10.1074/jbc.M114.552000
- Suwa, Kunihiko, Kimura, Tokuji, Schaap, A. Paul, 1977. Reactivity of Singlet Molecular Oxygen with Cholesterol in a Phospholipid Membrane Matrix. A Model for Oxidative Damage of Membranes. *Biochemical and Biophysical Research Communications*, 75, 785-792. doi.org/10.1016/0006-291X(77)91541-8
- Swaving, Jelto, de Bont, Jan A. M., 1998. Microbial Transformation of Epoxides. *Enzyme and Microbial Technology*, 22, 19-26. doi.org/10.1016/S0141-0229(97)00097-5
- Thurston, Christopher F., 1994. The Structure and Function of Fungal Laccases. *Microbiology*, 140, 19-26.
- Tolstikov, Genrich A., Flekhter, Oxana B. et al., 2005. Betulin and its Derivatives. Chemistry and Biological Activity. *Chemistry for Sustainable Development*, 13, 1-29.
- Triantaphylides, Christian, Krischke et al. 2008. Singlet Oxygen is the Major Reactive Oxygen Species Involved in Photooxidative Damage to Plants. *Plant Physiology* 148, 960-968. doi/10.1104/pp.108.125690

- Turner, James A., Herz, Werner, 1977. Unusual Effect of Epoxidic Oxygen on the Ease of Base-Catalyzed Decomposition of Epidioxides. *Journal of Organic Chemistry*, 42, 2006-2008.
doi.org/10.1021/jo00431a038
- Turner, Jefferson T., 2002. Zooplankton Fecal Pellets, Marine Snow and Sinking Phytoplankton Blooms. *Aquatic Microbial Ecology*, 27, 57-102. doi.10.3354/ame027057
- Vähätalo, Anssi V., Sondergaard, Morten et al., 1998. Impact of Solar Radiation on the Decomposition of Detrital Leaves of Eelgrass *Zostera marina*. *Marine Ecology Progress Series*, 170, 107-117. doi.10.3354/meps170107
- Vähätalo, Anssi V., 2009. "Light, Photolytic Reactivity and Chemical Products". In *Biochemistry of Inland Waters*, edited by Gene E. Likens, 37-49. Amsterdam: Elsevier Academic Press.
- Villanueva, Joan, Grimalt, Joan O. et al., 1994. Chlorophyll and Carotenoid Pigments in Solar Saltern Microbial Mats. *Geochimica et Cosmochimica Acta*, 58, 4703-4715.
doi.org/10.1016/0016-7037(94)90202-X
- Volkman, John K., Eglinton, Geoffrey et al., 1980. Long-Chain Alkenes and Alkenones in the Marine Coccolithophorid *Emiliania huxleyi*. *Phytochemistry*, 19, 2619-2622.
doi.org/10.1016/S0031-9422(00)83930-8
- Volkman, John K., Maxwell James R., 1986. Acyclic Isoprenoids as Biological Markers. *Methods in Geochemistry and Geophysics*, 24, 1-42.
- Volkman, John K., Allen, David I. et al., 1986. Bacterial and Algal Hydrocarbons in Sediments from a Saline Antarctic Lake, Ace Lake. *Organic Geochemistry*, 10, 671-681.
doi.org/10.1016/S0146-6380(86)80003-1
- Volkman, John K., Barrett, Stephanie M. et al., 1995. Alkenones in *Gephyrocapsa oceanica*: Implications for Studies of Paleoclimate. *Geochimica et Cosmochimica Acta*, 59, 513-520.
doi.org/10.1016/0016-7037(95)00325-T
- Volkman, John K., 2003. Sterols in Microorganisms. *Applied Microbiology and Biotechnology*, 60, 495-506.
doi.org/10.1007/s00253-002-1172-8
- Volkman, John K., 2006. Lipid Markers for Marine Organic Matter. *The Handbook of Environmental Chemistry*, 2, 27-70.
doi.org/10.1007/698_2_002

- Volkman, John K., 2018. "Lipids of Geochemical Interest in Microalgae". In *Hydrocarbons, Oils and Lipids: Diversity, Origin, Chemistry and Fate*, edited by Heinz Wilkes, 159-191. Springer Verlag. doi.org/10.1007/978-3-319-90569-3
- Waggoner, Derek C., Chen, Hongmei et al., 2015. Formation of Black Carbon-Like and Alicyclic Aliphatic Compounds by Hydroxyl Radical Initiated Degradation of Lignin. *Organic Geochemistry*, 82, 69-76. doi.org/10.1016/j.orggeochem.2015.02.007
- Wahlberg, Inger, Enzell, Curt R., 1971. 3-Oxo-6 β -hydroxyolean-12-en-28-oic acid, a New Triterpenoid from Commercial Tolu Balsam. *Acta Chemica Scandinavica*, 25, 70-76.
- Walker, J. Stuart, Squier, Angela H. et al., 2002. Origin and Significance of 13²-Hydroxychlorophyll Derivatives in Sediments. *Organic Geochemistry*, 33, 1667-1674. doi.org/10.1016/S0146-6380(02)00178-X
- Waraho, Thaddao, McClements, D. Julian, Decker, Eric A., 2011. Impact of Free Fatty Acid Concentration and Structure on Lipid Oxidation in Oil-in-Water Emulsions. *Food Chemistry*, 129, 854-859. doi.org/10.1016/j.foodchem.2011.05.034
- Warjent, Jason J., Jordan, Brian R., 2013. From Ozone Depletion to Agriculture: Understanding the Role of UV Radiation in Sustainable Crop Production. *New Phytologist*, 197, 1058-1076. doi.org/10.1111/nph.12132
- Watanabe, Shingo, Sudo, Kengo et al., 2011. Future Projections of Surface UV-B in a Changing Climate. *Journal of Geophysical Research*, 116, D16118. doi.org/10.1029/2011JD015749
- Waterson, Elisabeth J., Canuel, Elisabeth A., 2008. Sources of Sedimentary Organic Matter in the Mississippi River and Adjacent Gulf of Mexico as Revealed by Lipid Biomarker and $\delta^{13}\text{C}$ TOC Analyses. *Organic Geochemistry*, 39, 422-439. doi.org/10.1016/j.orggeochem.2008.01.011
- Watt, Jennifer L., Browse, John, 2000. A Palmitoyl-CoA-Specific $\Delta 9$ Fatty Acid Desaturase from *Caenorhabditis elegans*. *Biochemical and Biophysical Research Communications*, 272, 263-269. doi.org/10.1006/bbrc.2000.2772
- Wieland, Andreas, Kuhl, Michael, 2001. Oxygen Cycling in Microbial Mats from Camargue (France), Ebro delta (Spain) and Mesocosms (Eilat, Israel). First Scientific Progress Report of the MATBIOPOL European Project (Contract EVK3-CT- 1691999-00010), pp. 25-42.
- Xia, Wei, Budge, Suzanne M., 2017. Techniques for the Analysis of Minor Lipid Oxidation Products Derived from Triacylglycerols:

- Epoxides, Alcohols, and Ketones. *Comprehensive Reviews in Food Science and Food Safety*, 16, 735-758.
doi.org/10.1111/1541-4337.12276
- Xie, Zhouli, Nolan, Trevor M. et al., 2019. AP2/ERF Transcription Factor Regulatory Networks in Hormone and Abiotic Stress Responses in *Arabidopsis*. *Frontiers in Plant Sciences*, 10, 228.
doi.org/10.3389/fpls.2019.00228
- Yamauchi, Ryo, Matsushita, Setsuro, 1979. Light-Induced Lipid Peroxidation in Isolated Chloroplasts and Role of α -Tocopherol. *Agricultural and Biological Chemistry*, 43, 2157-2161.
doi.org/10.1271/bbb1961.43.2157
- Yamauchi, Ryo, Miyake, Nobuyuki et al., 1993. Products Formed by Peroxyl Radical Oxidation of β -carotene. *Journal of Agricultural Food Chemistry*, 41, 708–713. doi.org/10.1021/jf00029a005
- Yin, Huiyong, Xu, Libin, Porter, Ned A., 2011. Free Radical Lipid Peroxidation: Mechanisms and Analysis. *Chemical Reviews*, 111, 5944-5972. doi.org/10.1021/cr200084z
- Yurkov, Vladimir V., Beatty, J. Thomas, 1998. Aerobic Anoxygenic Phototrophic Bacteria. *Microbiology and Molecular Biology Reviews*, 62, 695-724. doi.10.1128/MMBR.62.3.695-724.1998
- Zabeti, Nathalie, Bonin, Patricia et al., 2010. Potential Alteration of $U_{37}^{K'}$ Paleothermometer due to Selective Degradation of Alkenones by Marine Bacteria Isolated from the Haptophyte *Emiliania huxleyi*. *FEMS Microbiology Ecology*, 73, 83–94. doi.org/10.1111/j.1574-6941.2010.00885.x
- Zafirou, Oliver C., Jousset-Dubien, Jacques et al., 1984. Photochemistry in Natural Waters. *Environmental Science and Technology*, 18, 358A-370A. doi.org/10.1021/es00130a001
- Zapata, Olga, MacMillan, Calvin, 1979. Phenolic Acids in Seagrasses. *Aquatic Botany*, 7, 307-317. doi.org/10.1016/0304-3770(79)90032-9
- Zhang, Tianjin, Barry, Roger G. et al., 1999. Statistics and Characteristics of Permafrost and Ground-Ice Distribution in the Northern Hemisphere. *Polar Geography*, 23, 132-154.
doi.org/10.1080/10889379909377670
- Zhang, Lei, Zhang, Guowei et al., 2012. Effect of Soil Salinity on Physiological Characteristics of Functional Leaves of Cotton Plants. *Journal of Plant Research*, 126, 293-304. doi.org/10.1007/s10265-012-0533-3
- Zhou, Jin, Richlen, Mindy L. et al., 2018. Microbial Community Structure and Associations during a Marine Dinoflagellate Bloom. *Frontiers in Microbiology*, 9, 1201. doi.10.3389/fmicb.2018.01201

- Zielinski, Zosia A. M., 2021. Cholesterol Autoxidation Revisited and Mechanistic Insights into Hydrogen Atom Transfer Reactions to Peroxyl Radicals. PhD Diss., University of Ottawa.
- Zolla, Lello, Rinalducci, Sara, 2002. Involvement of Active Oxygen Species in Degradation of Light-Harvesting Proteins under Light Stresses. *Biochemistry*, 41, 14391-14402. doi.org/10.1021/bi0265776